AD-A241 378

CHEMICAL
RESEARCH,
DEVELOPMENT &
ENGINEERING
CENTER

(2)

CRDEC-SP-038

PROCEEDINGS OF THE WORKSHOP ON PROBLEMS OF ROTATING LIQUIDS

Miles C. Miller
RESEARCH DIRECTORATE

Daniel D. Joseph
UNIVERSITY OF MINNESOTA
Minneapolis, MN 55455

July 1991

U.S. ARMY
ARMAMENT
MUNITIONS
CHEMICAL COMMAND

Aberdeen Proving Ground, Maryland 21010-5423

REPORT DOCUMENTATION PAGE

Form Approved
OMB No 0704-0188

1. AGENCY USE ONLY (Leave blank)	2. REPORT DATE	3. REPORT TYPE AND DATES COVERED
	1991 July	Final, 91 Apr - 91 Apr

4. TITLE AND SUBTITLE

Proceedings of the Workshop on Problems of Rotating Liquids

5. FUNDING NUMBERS

PR-FI-1-1Z1RA-NMCL

6. AUTHOR(S)

Miles C. Miller (CRDEC) (sponsor)
Daniel D. Joseph (University of Minnesota) (sponsor)

7. PERFORMING ORGANIZATION NAME(S) AND ADDRESS(ES)

CDR, CRDEC, ATTN: SMCCR-RSP-A, APG, MD 21010-5423
Department of Aerospace Engineering & Mechanics
University of Minnesota
Minneapolis, MN 55455

8. PERFORMING ORGANIZATION REPORT NUMBER

CRDEC-SP-038

9. SPONSORING/MONITORING AGENCY NAME(S) AND ADDRESS(ES)

10. SPONSORING/MONITORING AGENCY REPORT NUMBER

11. SUPPLEMENTARY NOTES

12a. DISTRIBUTION/AVAILABILITY STATEMENT

Approved for public release; distribution is unlimited.

12b. DISTRIBUTION CODE

13. ABSTRACT (Maximum 200 words)

A "Workshop on Problems of Rotating Fluids" was held at the U.S. Army High Performance Computing Research Center on 22-23 of April 1991. This meeting was co-sponsored by M. Miller, CRDEC and D. Joseph, University of Minnesota. The purpose of the workshop was to review the status of technology related to rotating fluid dynamics with special emphasis on liquid-filled projectiles. Sixteen technical papers were presented by individuals from the government and academia.

14. SUBJECT TERMS

Projectile   Fluid dynamics
Liquid-fill   Flight stability

15. NUMBER OF PAGES

340

16. PRICE CODE

17. SECURITY CLASSIFICATION OF REPORT	18. SECURITY CLASSIFICATION OF THIS PAGE	19. SECURITY CLASSIFICATION OF ABSTRACT	20. LIMITATION OF ABSTRACT
UNCLASSIFIED	UNCLASSIFIED	UNCLASSIFIED	UL

Blank

FORWARD

The "Workshop on Problems of Rotating Liquids" was held at the Army High Performance Computing Research Center (AHPCRC) in Minneapolis, MN on 22-23 April 1991. The two day meeting was co-sponsored by Professor Daniel Joseph, University of Minnesota and Miles Miller, U.S. Army Chemical Research, Development and Engineering Center (CRDEC). Dr. Joseph is engaged in fluid dynamic research under an Army Research Office (ARO) contract and Mr. Miller is the Scientific Coordinator for the Fluid Dynamics Area of the CRDEC Basic Research Program.

The "Workshop" primarily dealt with the subject of liquid-filled projectile flight instabilities. The meeting location was selected to reflect the critical use of Computational Fluid Dynamics (CFD) and high performance computers in support of this technology area and was the first "Workshop" hosted by the AHPCRC. Those invited to attend had all contributed to the technical aspects of this topic. The list of attendees is contained on page 337.

The two general goals of the "Workshop" were to:

* Help resolve an important problem in the nation's interest.

* Move the general subject of fluid dynamics forward.

More specific objectives of the "Workshop" were to assess the progress made in this technology and recommend research activities to address particular needs.

The "Workshop" agenda is shown on pages 339 and 340. The first day was devoted to overviews, tours, and special presentations. The second day's activities were concerned with various "work in progress" sponsored or performed by either the U.S. Army Ballistic Research Laboratory (BRL) or the CRDEC. The papers presented by individuals from the Ohio State University represent work performed under a research contract funded by the CRDEC. These proceedings contain copies of the viewgraphs shown by each presenter.

The last time a special meeting on this subject was held was at the "Roundtable On Liquid-Filled Shell" held in September of 1984. That meeting had charted the course of study in this area for the past seven years and it seemed timely that we should reassess our progress at this point. During the "Wrap-Up" session of the "Workshop", the recommendations of the previous "Roundtable" were reviewed by the attendees and an updated list of new topics and future directions for research in this area was formulated. These results are summarized in the last section of these proceedings.

PREFACE

The Workshop on Problems of Rotating Liquids was held 22-23 April 1991 at the U.S. Army High Performance Computing Research Center (AHPCRC), Minneapolis, MN, and was authorized under Project No. FI-1-1Z1RA-NMCL.

The use of trade names or manufacturers' names in this report does not constitute an official endorsement of any commercial products. This report may not be cited for purposes of advertisement.

Acknowledgments

Special thanks is given to Dr. Sell and his staff at the AHPCRC for making the various lodging and meeting arrangements.

Blank

CONTENTS

Blank

ROTATING FLUIDS WORKSHOP

OVERVIEW OF CRDEC RESEARCH PROGRAM FOR LIQUID-FILLED PROJECTILES

Miles C. Miller

U.S. Army, Chemical Research, Development and Engineering Center
Research Dir, Physics Div, Aerodynamics Research
and Concepts Assistance Branch

22-23 April 1991

Army High Performance Computing Research Center
University of Minnesota

OVERVIEW OF CRDEC RESEARCH PROGRAM
FOR LIQUID-FILLED PROJECTILES

In the short time I have this morning, I want to indicate the reasons why the CRDEC was interested in holding this workshop; what our main technical interests are; and provide a brief review of the background, current efforts, and future directions in this area.

The main area of "Rotating Liquids" of interest to the CRDEC has to do with the flight stability of liquid-filled projectiles. The CRDEC is the development agency for chemical weapons which include antipersonnel, antimateriel, flame & incendiary and smoke & obscurants. Most of these weapons involve spinning projectiles which contain liquid or non-rigid payloads. This would include artillery shells, mortars, grenades, small arms, missiles, etc.

At the previous "Roundtable on Liquid-Filled Projectiles", held in September 1984, a relatively detailed history of this technology was presented. For the benefit of those of you who are new to this topic, I would like to briefly review certain highlights.

This viewgraph depicts a historical perspective of the significant events in this area. While the CRDEC has been interested in this problem since World War I, until the late 1970's, their effort was limited primarily to experimental studies in direct support of developmental munitions. The bulk of the scientific research was accomplished by the BRL. The Stewartson-Wedemeyer Theory appeared to adequately address the liquid-fills of interest at that time. Consequently, the BRL effort concentrated on experimental activities such as free gyroscope and yaw sonde investigations.

The research activities at the CRDEC started in 1977 as a consequence of a flight stability problem with XM761; a 155mm, artillery projectile which had a partial solid/partial liquid payload composition. The result of this effort was the evolution of the Test Fixture For Non-Rigid Payloads. This experimental apparatus forces a full sized payload container to assume the simultaneous spinning and coning motion of a projectile in flight. The test fixture was used to eliminate the XM761 problem culminating in the M825 projectile. It was subsequently employed to discover and characterize the destabilizing influence of highly viscous liquid-fills.

The real beginnings of the CRDEC research effort took place in 1982 with the establishment of the Fluid Dynamics Work Area of the CRDEC Basic Research Program. At the same time, the Laboratory Test Fixture For Non-Rigid Payloads was extensively modified to increase its performance, automate the data acquisition and reduction, and facilitate experimental operations. It is currently being employed for basic research studies as well as for various developmental munition programs. Examples of both uses will be presented as part of the "Work In Progress" portion of this meeting.

The significant point of this viewgraph is the extensive amount of work put into this technical area by the army during the last ten years and the complimentary efforts of the many different individuals and organizations involved. Their combined efforts have caused the technology associated with this problem to progress considerably as illustrated in the next viewgraphs.

The destabilizing moment produced by a Liquid-fill in a spinning and coning cylinder can be depicted as a function of the fluid characteristics (i.e., Reynolds number) and the projectile motion (i.e., non-dimensional coning rate). Fifteen years ago, the theory, and in fact the knowledge of liquid-filled projectiles was limited to very low viscosity liquid-fills. These could be predicted quite nicely by the Stewartson-Wedemeyer Theory. Ten years ago, we were aware, through laboratory experiments, of a new form of instability at the higher viscosities, but had no predictive theory. Within the last decade, we have developed theoretical methods to handle the entire range of liquid viscosities. Murphy has extended the Stewartson-Wedemeyer theory for the high Reynolds numbers and computerized its use. Hall, Sedney and Gerber and Herbert and Li have both developed theoretical methods which cover the low Reynolds number range. The general capabilities of the various analytical methods are summarized in the next viewgraph.

The CRDEC Basic Research Program has followed a three pronged approach as illustrated in this viewgraph. The theoretical and numerical studies are completed under research contracts through academic institutions with the CRDEC performing primarily experimental investigations using their Laboratory Test Fixture for Non-Rigid Payloads. The following series of viewgraphs summarizes the significant accomplishments achieved through the CRDEC sponsored program. The next viewgraphs list the publications related to this area which were sponsored by the CRDEC. This work has been complimented by research at the BRL and various ARO

funded research. CRDEC and BRL personnel meet every two months to review their respective activities.
The CRDEC effort has concentrated on, but not been limited to, highly viscous liquids. The goal has been to understand, predict and prevent flight instabilities due to any liquid-fill. A comprehensive summary of papers on the year's research findings are presented each year at the CRDEC Scientific Conference on Chemical Defense Research. A review of the Fluid dynamics progress is held for the ARO each spring at the CRDEC. The following is an abbreviated version of this year's CRDEC/ARO review which took place in early April 1991.

The overall objective of the Fluid Dynamics Work Area of the CRDEC Basic Research Program is shown in this viewgraph. While the area of antipersonnel, chemical munitions has been reduced, it has been replaced with the other areas as shown. While efforts still continue to understand and predict flight instabilities, the current emphasis is on determining ways to reduce or eliminate them.

The Fluid Dynamics Area involves two areas of emphasis: Fluid-Filled Projectile Flight Instabilities and Fluid Rheology. The latter topic is important not only for this area, but for other CRDEC programs as well. The Fluid-Filled Projectile work receives the major portion of the funding for the reasons shown in this viewgraph: problem unique to CRDEC; CRDEC possesses special experimental facilities; and new chemical munition fills must be addressed. As indicated in this viewgraph, the CRDEC in-house effort deals mainly with experimental studies which support theoretical studies performed under contract by universities

This viewgraph contains selected accomplishments during FY91 in the theoretical/numerical area achieved by Dr. Herbert, Dr. Li and Mr. Selmi, researchers at the Ohio State University under a CRDEC research contract. The next two viewgraphs highlight the computer graphics techniques and the two, immiscible fluid analysis being pursued. In particular, the two fluid analysis includes the case of very small amounts of the lower viscosity fluid which is the basis for the additive approach to reducing the destabilizing moment due to the higher viscosity fluid.

FY91 experimental accomplishments at the CRDEC are summarized in the next viewgraph. The next three viewgraphs include additional details for these items. Detailed studies were conducted on the CRDEC test fixture to assess the effect of relative viscosity, density and amount of additive. These data can be compared with the theoretical results shown previously. Test Fixture experiments showed that the payload container inner surface roughness has no influence on the flight stability. The CRDEC Test Fixture was used to evaluate an artillery projectile containing a viscoelastic fill for a special Operation Desert Storm application. The ability to measure the despin moment due to an arbitrary non-rigid payload on the Test Fixture and then to compute the associated destabilizing yawing moment, with confidence, was established through the basic research program on liquid-filled projectiles.

Additional accomplishments are listed in the next viewgraph followed by four viewgraphs illustrating the basic results of the instrumented flight test program. These illustrate that the partial-fill condition produces the same instability as the fully-filled condition; the shear thinning, viscoelastic fill provides a stable flight; and the immiscible, low viscosity additive does eliminate flight instabilities, but transient effects must be considered. The classic "Epicyclic Theory" of projectile motion has been modified to include the effects of a liquid-fill; indicating the combination of the internal payload and external aerodynamic effects on the projectile flight flight stability.

Future Directions in this CRDEC research area are shown in the next viewgraph. Work will continue to assess the use of immiscible, low viscosity additives to reduce or eliminate viscous, liquid-fill flight instabilities, especially considering launch transient effects. The potential use of longitudinal baffles as a means of eliminating flight instabilities will also be evaluated. Previous Test Fixture data, depicted in the next viewgraph, indicate that they may be effective under certain conditions. Two, three and four section baffles will be investigated on the Laboratory Test Fixture for Non-Rigid Payloads. The influence of viscoelastic effects on creating very large despins at relatively low spin rates as shown in this viewgraph will also be studied. Other non-Newtonian fluids will also be investigated.

SIGNIFICANT EVENTS IN LIQUID-FILLED PROJECTILE FLIGHT STABILITY TECHNOLOGY

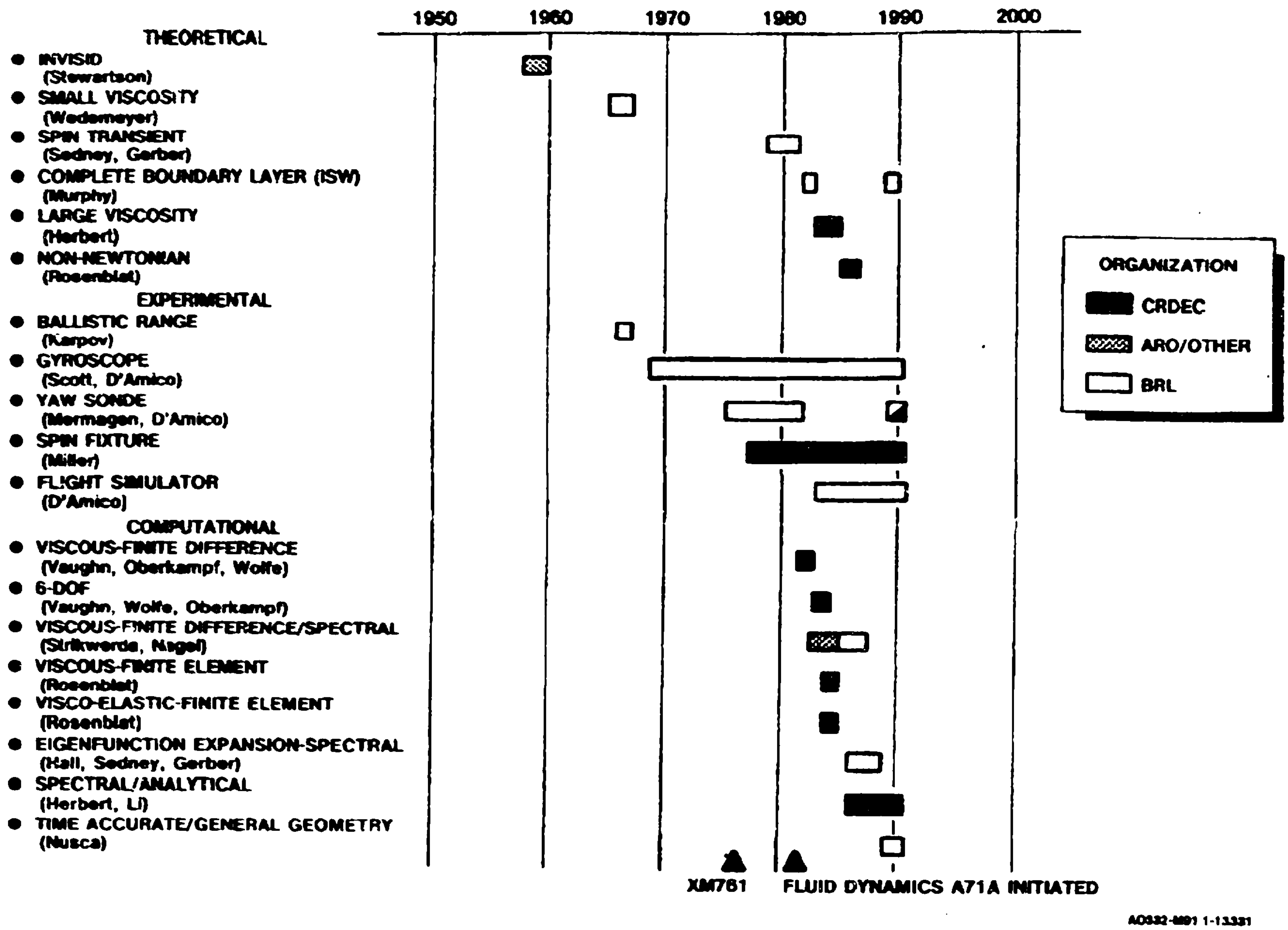

GENERAL TYPES OF LIQUID-FILL INDUCED DESTABILIZING MECHANISMS

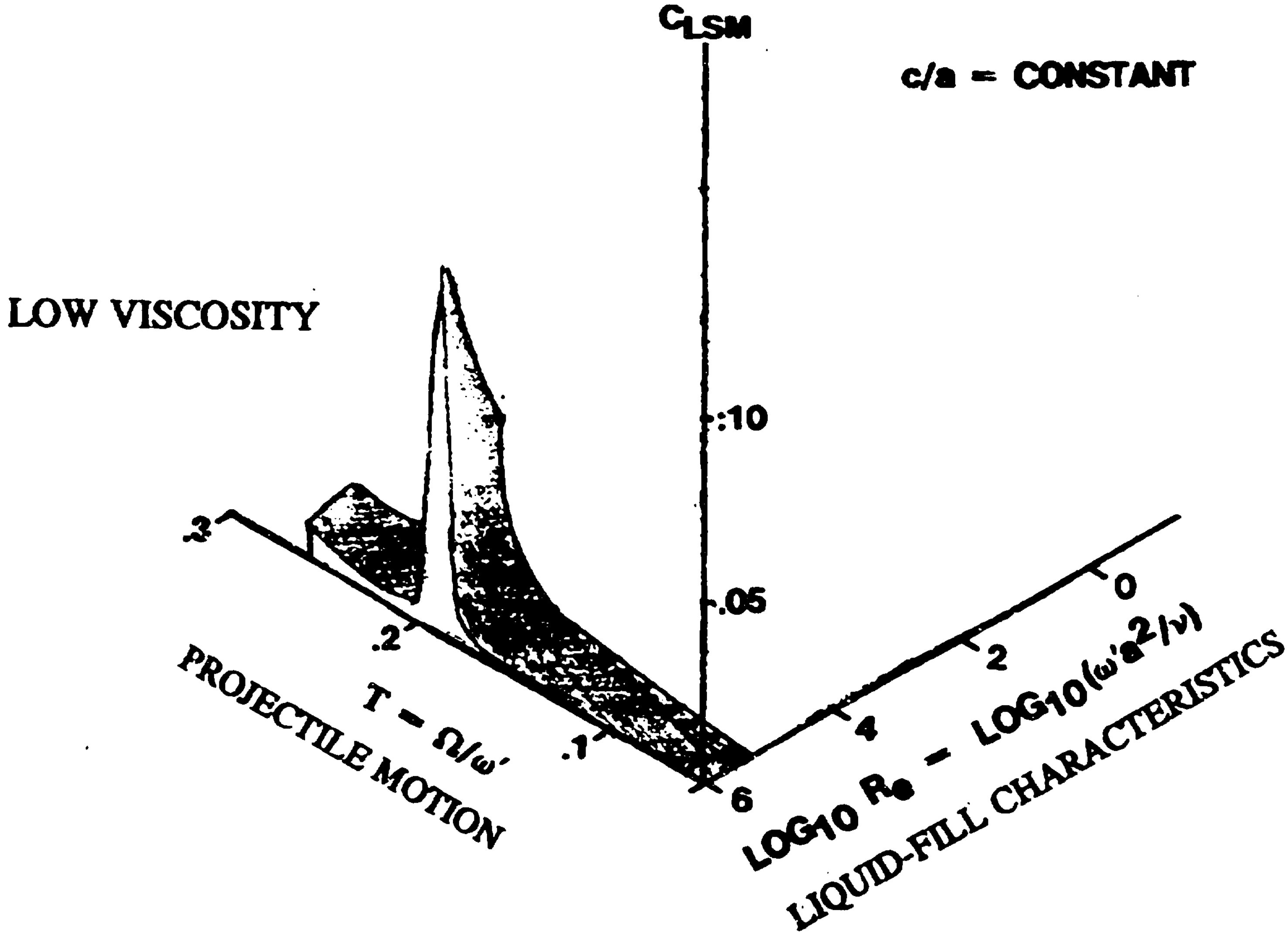

GENERAL TYPES OF LIQUID-FILL INDUCED DESTABILIZING MECHANISMS

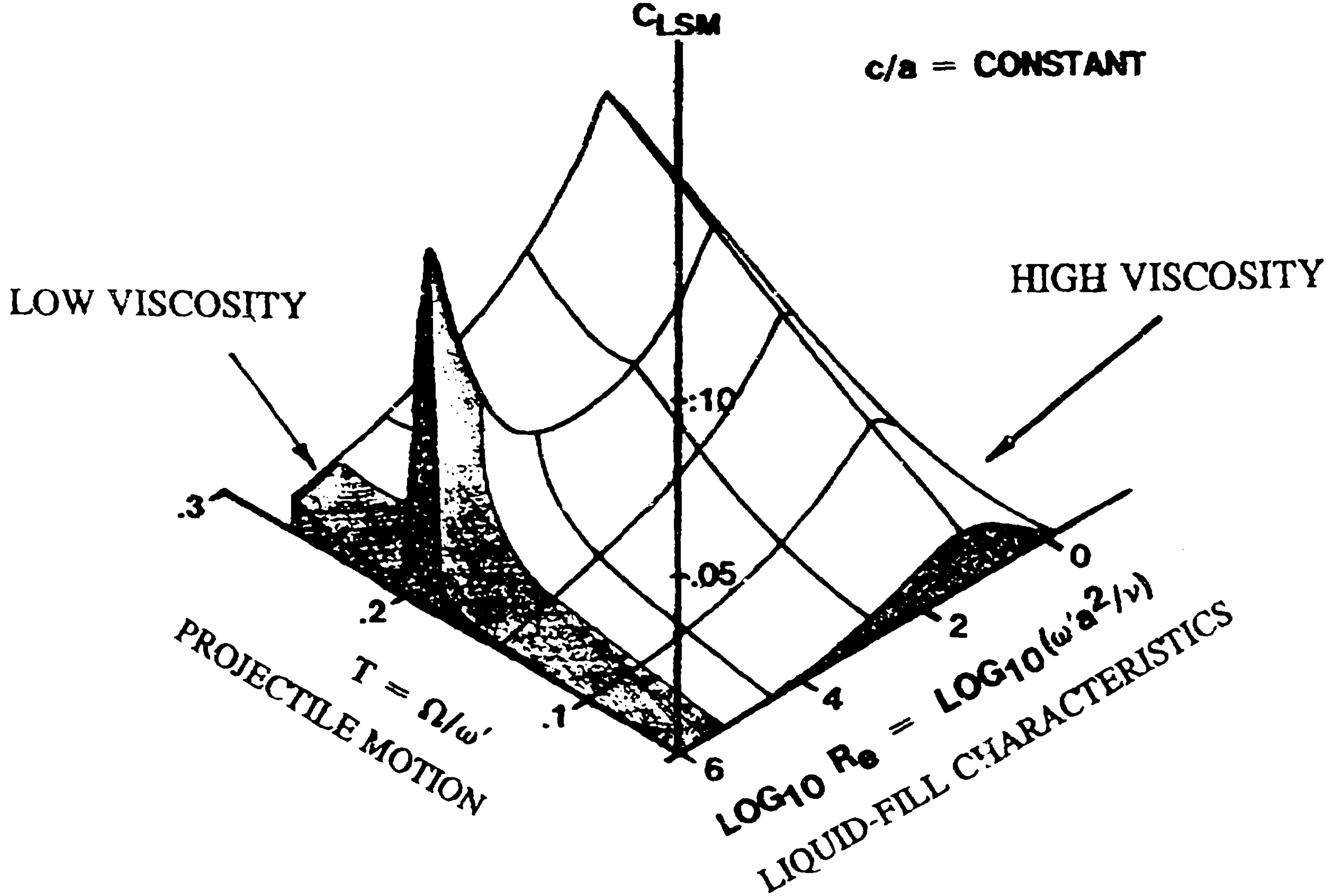

DESTABILIZING LIQUID MOMENT COEFFICIENT

THEORETICAL METHODS

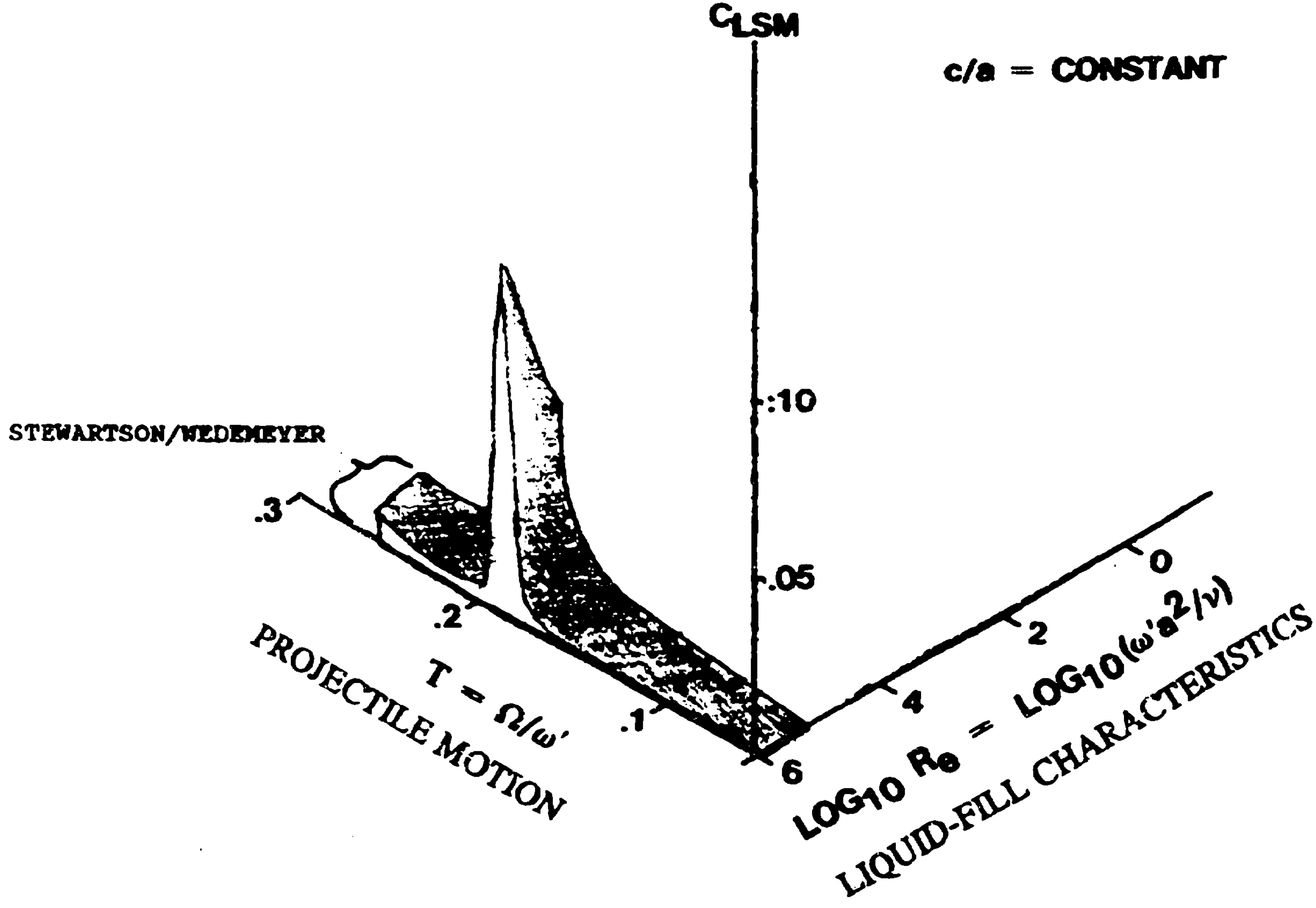

DESTABILIZING LIQUID MOMENT COEFFICIENT

THEORETICAL METHODS

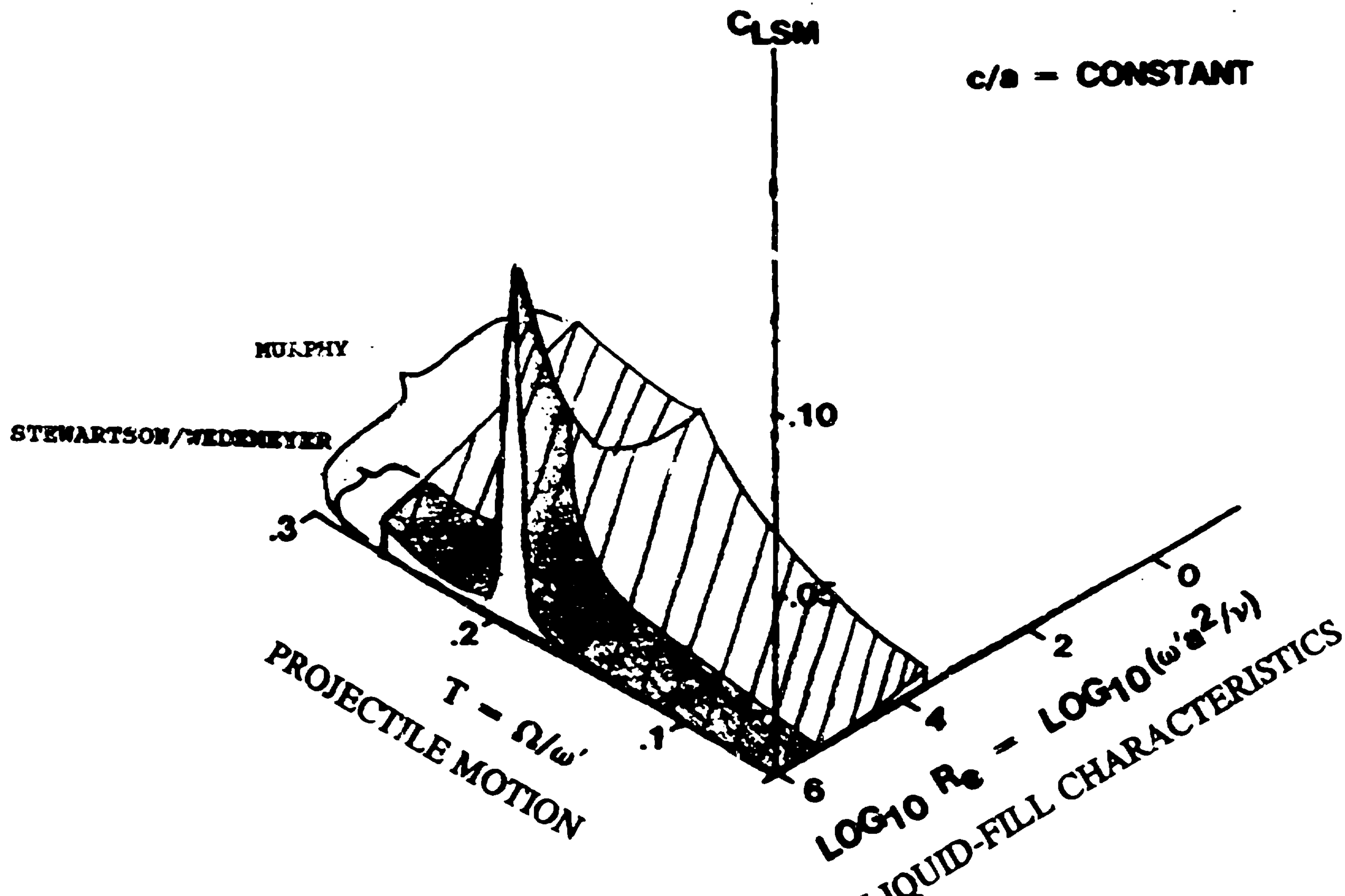

DESTABILIZING LIQUID MOMENT COEFFICIENT

THEORETICAL METHODS

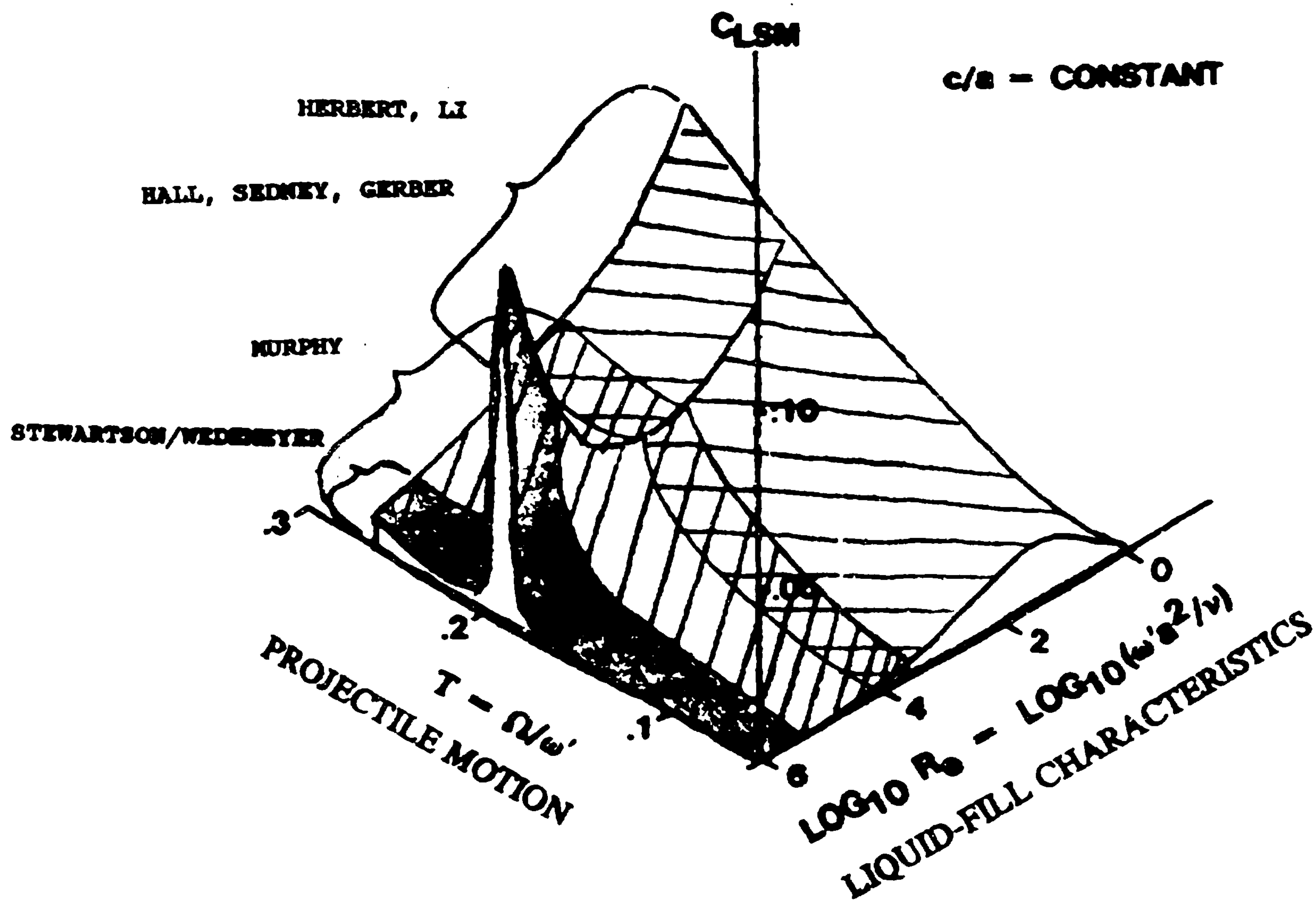

LIQUID FILLED PROJECTILE FLIGHT INSTABILITIES
THEORETICAL ANALYSES

THEORY	YEAR	FLUID		REYNOLDS NUMBER			CYLINDER ASPECT RATIO		DATA			
		NEWTONIAN	NON-NEWTONIAN	HIGH	MEDIUM	LOW	INFINITE	FINITE	FREQUENCIES	FLOW FIELD	ROLLING MOMENT	YAW/PITCH MOMENT
STEWARTSON	1959	★		★				★	★			
WEDEMEYER	1966	★		★				★	★			
MURPHY	1983	★		★	★			★	★		★	★
HERBERT	1985	★			★	★	★			★	★	
ROSENBLAT	1986		★		★	★	★			★	★	
HALL, SEDNEY, GERBER	1987	★			★	★		★		★	★	★
HERBERT, LI	1988	★			★	★		★	★	★	★	★
HERBERT, LI SELMI	1991	★		★	★	★		★	★	★	★	★

AO332-8891 1133-01

SIGNIFICANT ACCOMPLISHMENTS OF CRDEC RESEARCH IN LIQUID-FILLED PROJECTILES

1977 - CRDEC Laboratory Test Fixture built and used to solve liquid-fill flight stability problem of developmental smoke projectile.

1978 - Discovery of new type of flight instabilty created by highly viscous liquid-fills from laboratory fixture experiments at the CRDEC.

1979 - Extensive experimental investigation of viscous liquid-fills using CRDEC test fixture.

1981 - Flow visualization studies conducted for internal flow inside spinning/coning cylinder using CRDEC test fixture.

1982 - Fluid Dynamics Work Area established in CRDEC Basic Research Program.

1983 - Direct laboratory measurement of the destabilizing yawing moment due to a highly viscous liquid-fill using the CRDEC test fixture.

1983 - Computational Fluid Dynamic (CFD) analysis of the viscous liquid-fill situation by Sandia Laboratories supported by the CRDEC.

1984 - "Roundtable on Liquid-Filled Shell" co-sponsored by CRDEC.

1984 - Theoretical analysis of viscous liquid-fill problem by Herbert (VPI) including use of volume integral to compute liquid-induced moments supported by the CRDEC.

1985 - Six Degree-of-Freedom flight motion/trajectory program for liquid-filled projectiles evolved by Sandia Laboratories supported by the CRDEC.

1985 - Finite element CFD analysis completed for viscous liquid-fill problem by Rosenblat (Fluid Dynamics International) supported by the CRDEC.

1985 - Development of general relationship between liquid rolling and liquid yawing moments by Rosenblat supported by the CRDEC.

1985 - Formualtion of a three-dimensional graph to depict the entire liquid-filled projectile flight stability problem by CRDEC researchers.

1986 - CFD analysis conducted for viscoealstic fluid-filled projectile by Rosenblat supported by the CRDEC.

1986 - Laboratory measurement of the influence of a viscoelastic fluid-fill in creating projectile flight instabilities using the CRDEC test fixture.

1986 - Formulation of the theoretical relationship between the liquid-fill induced rolling and yawing moments by Rosenblat supported by the CRDEC.

1987 - Detailed experiments to validate the linear and generalized liquid moment coeffients using the CRDEC test fixture.

1987 - Fully spectral CFD code developed by Herbert (Ohio State Univ) for viscous liquid-fill problem supported by the CRDEC.

1988 - Purely analytical method developed to compute liquid-fill moments at any Reynolds number by Herbert and Li supported by the CRDEC.

1989 - Laboratory measurements of the effect of partial-fill case with a viscous liquid-fill using the CRDEC test fixture.

1989 - Laboratory demonstration of the use of an immiscible, low viscosity additive to eliminate viscous liquid-fill flight instabilities. Concept evolved in collaboration with Joseph (University of Minnesota).

1990 - Experimental evaluation of effect of internal surface texture of payload container on creation of viscous liquid-fill, flight instabilities.

1990 - Detailed experimental evaluation performed on influence of various immiscible, low viscosity additives using CRDEC test fixture.

1991 - Theoretical analysis completed to predict effect of two immiscible fluids covering entire range of viscosity, density and relative volumes by Selmi (Ohio State Univ) supported by CRDEC.

1991 - Instrumented flight tests conducted to validate viscoelastic fluid, partial-fill case, and immiscible additives.

1991 - Enhanced computer graphic techniques evolved to facilitate visualization and intrpretat[illegible] of internal fluid dynamics of spinning/coning cyinder by Herbert supported by CRDEC.

BIBLIOGRAPHY OF LIQUID-FILLED PROJECTILE PUBLICATIONS SPONSORED BY CRDEC BASIC RESEARCH PROGRAM

Miller, M. C.; "Flight Instability Test Fixture for Non-Rigid Payloads", Proceedings of 1977 CSL Technical Conference, May 1978.

D'Amico, W. P. and Miller, M. C.; "Flight Instability Produced by a Rapidly Spinning, Highly Viscous Liquid", Journal of Spacecraft and Rockets, Vol 16, No. 1, January-February 1979.

Miller, M. C.; "Flight Instabilities of Spinning Projectiles Having Non-Rigid Payloads", AIAA 19th Aerospace Sciences Meeting, Paper No. AIAA-81-0225, January 1981.

Miller, M. C.; "Void Characteristics of Liquid-Filled Cylinder Undergoing Spinning and Coning Motion", Journal of Spacecraft and Rockets, Vol 18, No. 3, May-June 1981.

Miller, M. C.; "Flight Instabilities of Spinning Projectiles Having Non-Rigid Payloads", Journal of Guidance, Control and Dynamics, Vol 5, No. 2, March-April 1982.

Miller, M. C.; "Flight Instabilities of Spinning Projectiles Having Non-Rigid Payloads", Proceedings of 1982 Army Science Conference, June 1982.

Miller, M. C.; "A New Flight Instability Affecting Spinning Projectiles Having Non-Rigid Payloads", 28th Conference of Army Mathematicians, Army Research Office Report No. 83-1, February 1983.

Herbert, T.; "Fluid Motion in a Rotating and Nutating Container", CRDC-CR-84087, July 1984.

Miller, M. C.; "Laboratory Measurements of Despin and Yawing Moments Produced by a Viscous Liquid in a Spinning/Nutating Container", Proceedings of the 1983 CRDC Scientific Conference on Chemical Defense Research, CRDC-SP-84014, October 1984.

Herbert, T.; "The Flow of a Highly Viscous Fluid in a Spinning and Nutating Cylinder", Proceedings of the 1983 CRDC Scientific Conference on Chemical Defense Research, CRDC-SP-84014, October 1984.

Vaughn, H. L., Oberkampf, W. L. and Wolfe, W. P.; "Numerical Solution to the Navier-Stokes Equations for Spinning and Nutating Fluid Payloads", Proceedings of the 1983 CRDC Scientific Conference on Chemical Defense Research, CRDC-SP-84014, October 1984.

Miller, M. C.; "Measurement of Despin and Yawing Moments Produced by a Viscous Liquid", Journal of Guidance, Control and Dynamics, Vol 6, No. 2, March-April 1985.

Herbert, T.; "Instability of the Viscous Flow in a Spinning and Nutating Cylinder", Proceedings of the 1984 CRDC Scientific Conference on Chemical Defense Research, CRDC-SP-85006, June 1985.

Vaughn, H. L., Wolfe, W. P. and Oberkampf, W. L.; "Six Degree-of-Freedom Simulation of M483 Fluid Payload Projectile Using Numerically Computed Fluid Moments", Proceedings of the 1984 CRDC Scientific Conference on Chemical Defense Research, CRDC-SP-85006, June 1985.

Miller, M. C.; "Visualization Studies of Viscous Liquid Flow in a Spinning and Coning Cylinder", Proceedings of the 1984 CRDC Scientific Conference on Chemical Defense Research, CRDC-SP-85006, June 1985.

Vaughn, H. R., Oberkampf, W. L. and Wolfe, W. P.; "Fluid Motion Inside a Spinning, Nutating Cylinder", Journal of Fluid Mechanics, Vol 150, January 1985.

Vaughn, H. R., Wolfe, W. P., and Oberkampf, W. L.; "Six Degree-of-Freedom Simulation of Fluid Payload Projectiles Using Numerically Computed Fluid Moments", Sandia National Laboratories Report SAND 85-1166, July 1985.

Herbert, T.; "Viscous Fluid Motion in a Spinning and Nutating Cylinder", CRDC-CR-86004, November 1985.

Miller, M. C.; "Liqu d-Filled Projectiles - New Problems, New Solutions", Proceedings of the 9th American Defense Preparedness Association International Ballistics Conference, Vol 2, May 1986.

Herbert, T.; "Fluid Motion in Liquid-Filled Shells", 4th Army Applied Mathematics and Computating Conference, May 1986.

Miller, M. C.; "Liquid-Filled Projectile - New Problems, New Solutions", Proceedings of the 9th American Defense Preparedness Association International Ballistics Conference, Vol 2, May 1986.

Herbert, T.; "Fluid Motion in Liquid-Filled Shells", 4th Army Applied Mathematics and Computing Conference, May 1986.

Herbert, T.; "On the Fluid Motion in Liquid-Filled Shells", Proceedings of the 1985 CRDC Scientific Conference on Chemical Defense Research, CRDC-SP-86007, June 1986.

Rosenblat, S.; "Viscoelastic Fluid Flow in a Spinning and Nutating Cylinder", Proceedings of the 1985 CRDC Scientific Conference on Chemical Defense Research, CRDC-SP-86007, June 1986.

Miller, M. C. and Weber, D. J.; "Liquid-Filled Projectile Flight Instabilities, a Unified Picture", Proceedings of the 1985 CRDC Scientific Conference on Chemical Defense Research, CRDC-SP-86007, June 1986.

Rosenblat, S.; "Finite Element Calculations of Viscoelastic Fluid Flow in a Spinning and Nutating Cylinder", CRDEC-CR-87021, December 1986.

Miller, M. C.; "Liquid-Filled Projectiles - New Problems, New Solutions", Army R D and A Magazine, November-December 1986.

Herbert, T.; "Viscous Fluid Motion in a Spinning and Nutating Cylinder", Journal of Fluid Mechanics, Vol 167, 1986.

Miller, M. C. and Weber, D. J.; "Measurement of Despin Moment Produced by a Viscoelastic Fluid in a Spinning and Coning Cylinder", Proceedings of the 1986 CRDEC Scientific Conference on Chemical Defense Research, CRDEC-SP-87008, June 1987.

Rosenblat, S.; "Non-Newtonian Fluid in a Spinning and Coning Cylinder", Proceedings of the 1986 CRDEC Scientific Conference on Chemical Defense Research, CRDEC-SP-87008, June 1987.

Herbert, T.; "A Spectral Navier-Stokes Solver for the Flow in a Spinning and Coning Cylinder", Proceedings of the 1986 CRDEC Scientific Conference on Chemical Defense Research, CRDEC-SP-87008, June 1987.

Herbert, T.; "Numerical Study of the Flow in a Spinning and Nutating Cylinder", AIAA 19th Fluid Dynamics, Plasma Dynamics and Laser Conference, Paper AIAA-87-1445, June 1987.

Weber, D. J. and Miller, M. C.; "Despin Moment Measurements for Viscous Liquids in a Spinning and Coning Cylinder", Proceedings of the 1987 CRDEC Scientific Conference on Chemical Defense Research, CRDEC-SP-88013, June 1988.

Herbert, T.; "Flight Simulation for Liquid Filled Projectiles", Proceedings of the 1987 CRDEC Scientific Conference on Chemical Defense Research, CRDEC-SP-88013, June 1988.

Miller, M. C. and Weber, D. J.; "Destabilizing Moments Produced by a Viscoelastic Fluid in a Spinning and Coning

Cylinder", Proceedings of the 1988 Army Science Conference, October 1988.

Weber, D. J. and Miller, M. C.; "Liquid Induced Rolling and Yawing Moment Coefficients for Viscous Newtonian Fluids in a Spinning and Coning Cylinder", Proceedings of the 1988 CRDEC Scientific Conference on Chemical Defense Research, CRDEC-SP-013, August 1989.

Miller, M. C.; "Laboratory Test Fixture for Non-Rigid Payloads", Proceedings of the International Congress of Instrumentation in Aerospace Simulation Facilities (ICIASF'89), September 1989.

Herbert, T.; "Interior Fluid Dynamics of Liquid-Filled Projectiles", CRDEC-CR-058, December 1989.

Herbert, T. and Selmi, M.; "Two Fluid Flows in a Spinning and Nutating Cylinder", Proceedings of the 1989 CRDEC Scientific Conference on Chemical Defense Research, CRDEC-SP-024, August 1990.

Weber, D. J. and Miller, M. C.; "Effect of Partial-Fill Condition on the Destabilizing Moment Produced by a Viscous Liquid in a Spinning and Coning Cylinder", Proceedings of the 1989 CRDEC Scientific Conference on Chemical Defense Research, CRDEC-SP-024, August 1990.

Miller, M. C.; "Reduction of Viscous Liquid-Fill Flight Instability by Addition of Immiscible, Low Viscosity Liquid", Proceedings of the 1989 CRDEC Scientific Conference on Chemical Defense Research, CRDEC-SP-024, August 1990.

Li, R. and Herbert, T.; "Computational Study of the Flow in Spinning and Nutating Cylinders", AIAA Journal, Vol 28, No. 9, September 1990.

Miller, M. C.; "Experimental Studies of Low Viscosity, Immiscible Additives to Reduce the Destabilizing Moment Produced by a Viscous Liquid", Proceedings of the 1990 CRDEC Scientific Conference on Chemical Defense Research, CRDEC-SP-034, August 1991.

Weber, D. J.; "Effect of Surface Roughness on the Creation of Viscous Liquid-Fill Flight Instabilities", Proceedings of the 1990 CRDEC Scientific Conference on Chemical Defense Research, CRDEC-SP-034, August 1991.

Selmi, M. and Herbert, T.; "Two-Fluid Flow in Spinning and Nutating Cylinders", Proceedings of the 1990 CRDEC Scientific Conference on Chemical Defense Research, CRDEC-SP-034, August 1991.

Herbert, T.; "Computer Visualization of Flows", Proceedings of the 1990 CRDEC Scientific Conference on Chemical Defense Research, CRDEC-SP-034, August 1991.

Li, R. and Herbert, T.; "Numerical Study of Unsteady, 3D Flows in a Spinning and Nutating Cylinder", Proceedings of the 1990 CRDEC Scientific Conference on Chemical Defense Research, CRDEC-SP-034, August 1991.

Miller, M. C.; "Elimination of Viscous Liquid-Fill Flight Instability by Means of Lower Viscosity, Immiscible, Liquid Additive", AIAA 29th Aerospace Sciences Meeting, Paper No. AIAA-91-0679, January 1991.

CRDEC BASIC RESEARCH IN FLUID DYNAMICS

OBJECTIVE

CONDUCT EXPERIMENTAL AND THEORETICAL INVESTIGATIONS OF PHYSICAL PROPERTIES, DYNAMIC CHARACTERSTICS, AND NEW PHENOMENA RELATED TO THE DELIVERY OF CHEMICAL PAYLOADS ASSOCIATED WITH ANTIMATERIEL, SMOKE & OBSCURATION AND FLAME & INCENDIARY APPLICATIONS.

METHODOLOGY

* UNDERSTAND PHYSICS OF EFFECT
* ESTABLISH PREDICTIVE CAPABILITY
* DETERMINE MEANS TO CONTROL EFFECT

FLUID DYNAMICS

TASK	OBJECTIVE
1. Fluid-Filled Projectile Flight Instabilities	Perform experimental and theoretical studies to understand, predict and control flight instabilities of liquid-filled projectiles for chemical munitions.
2. Fluid Rheology	Perform experimental and theoretical studies to establish improved techniques for techniques for determining rheological properties and dynamic behavior of chemical compositions.

CRDEC EMPHASIS ON LIQUID-FILLED PROJECTILE RESEARCH

- Problem unique to CRDEC -- Not encountered by Air Force, Navy, or other Army developers
- CRDEC possesses special experimental facility (Laboratory Test Fixture for Non-Rigid Payloads)
- New and unconventional chemical payload compostions being evolved by CRDEC -- Including anti-materiel; smoke & obscurant and flame & incendiary munitions

A0332-0103-L91 1-13327

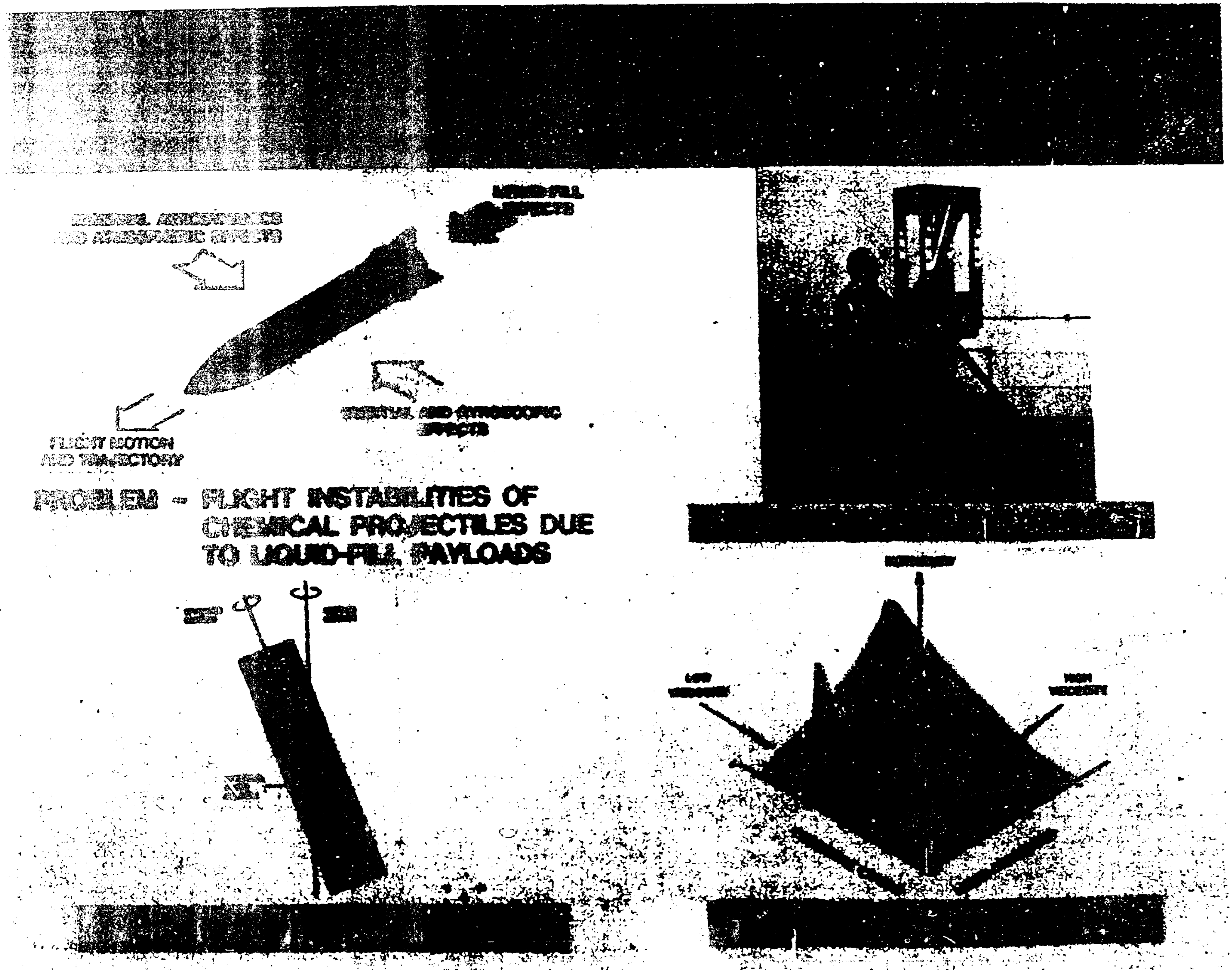
FLIGHT MOTION AND TRAJECTORY
PROBLEM - FLIGHT INSTABILITIES OF CHEMICAL PROJECTILES DUE TO LIQUID-FILL PAYLOADS

FLUID DYNAMICS
(FY91 ACCOMPLISHMENTS)

TITLE: FLUID-FILLED PROJECTILE FLIGHT INSTABILITIES

* Theoretical: (CRDEC research contract with The Ohio State University)

  * Developed advanced computer graphics techniques to illustrate, interpret and validate internal flow - includes still and animated displays (Anatomy of Liquid-Filled Projectiles).

  * Analysis performed for two immiscible fluids with large differences in viscosity with the lower viscosity fluid present in small amounts.

  * Evaluated effects of transient conditions on creation of liquid-fill induced flight instabilities and compared with experimental results.

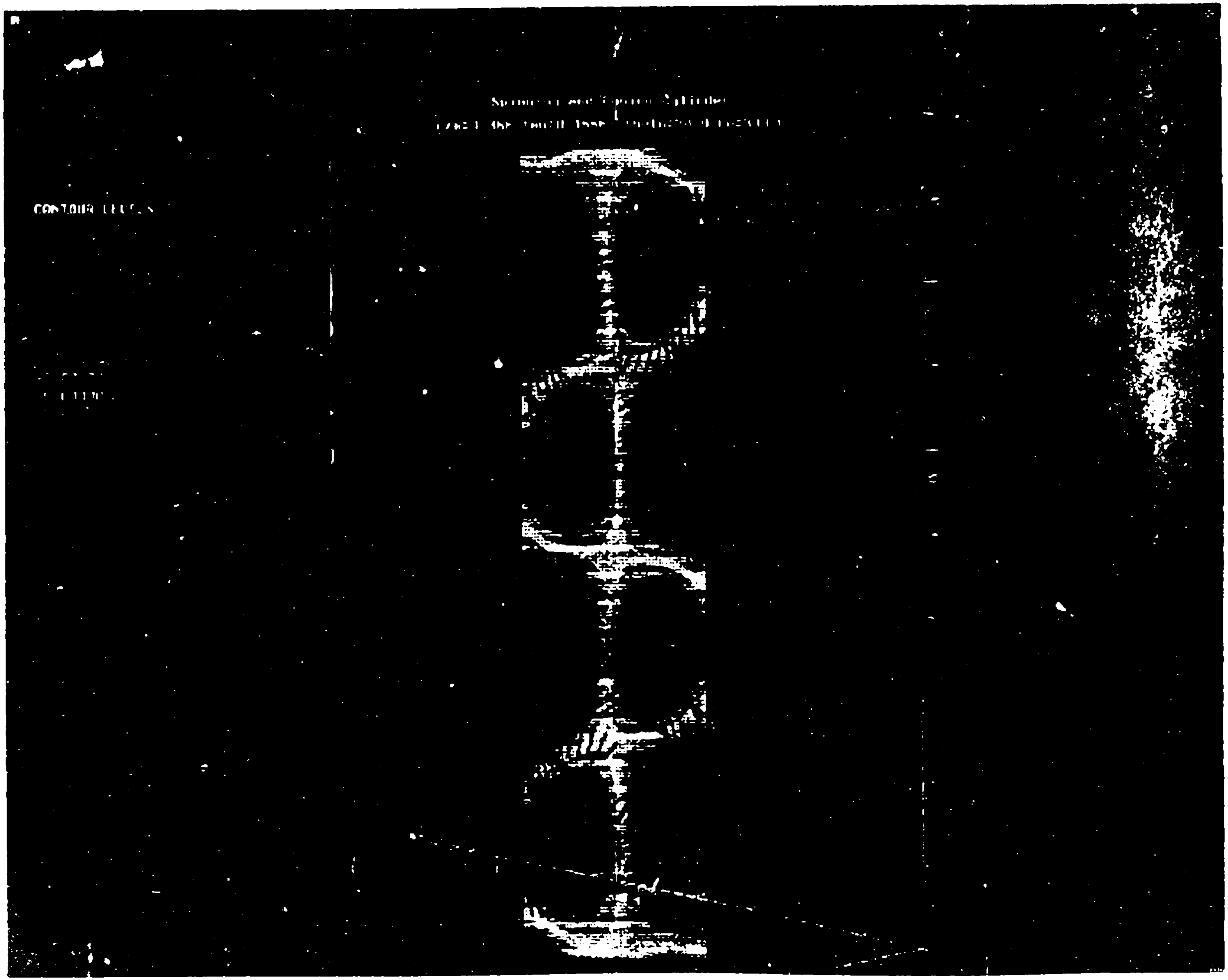
CONTOUR LEVELS

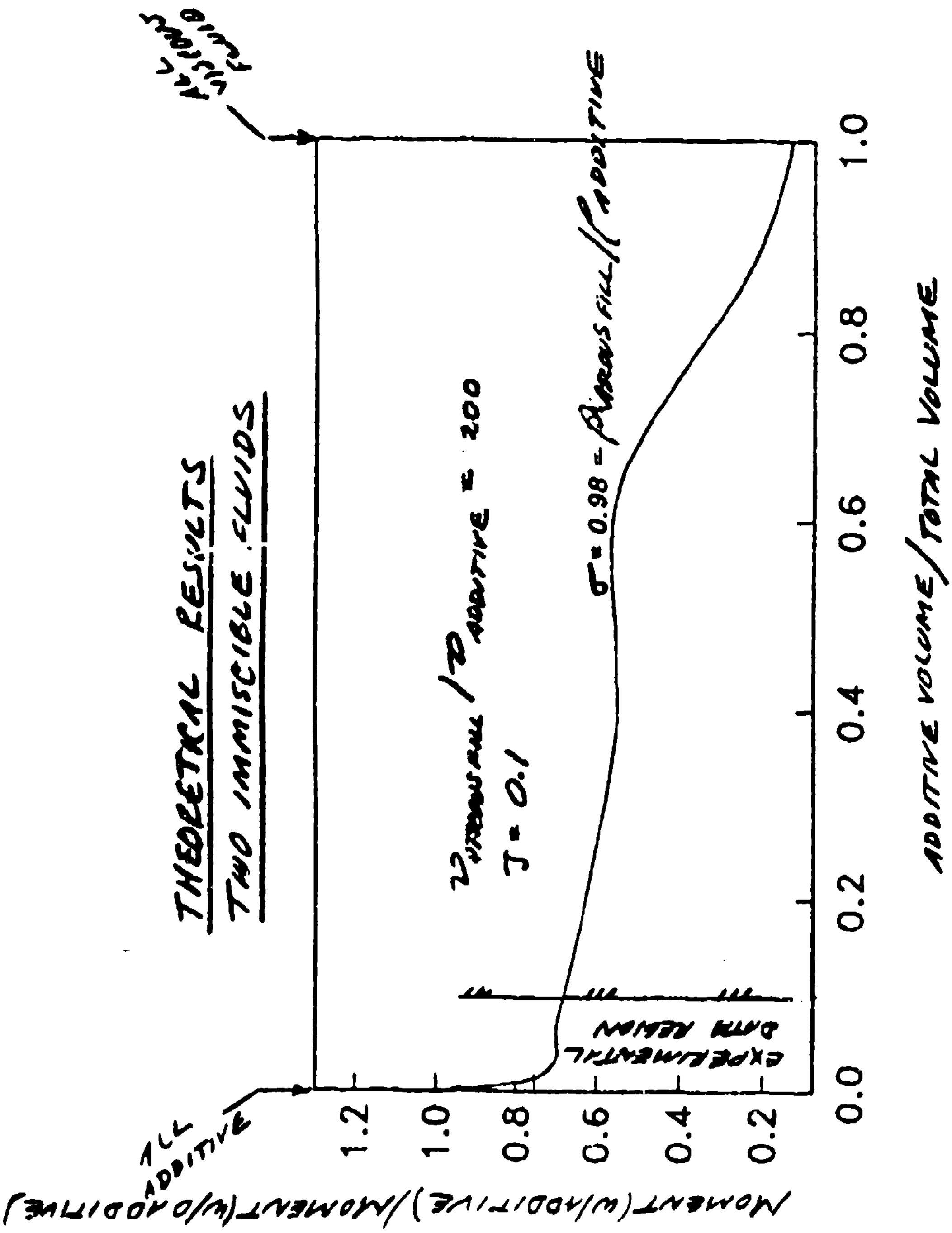
THEORETICAL RESULTS
TWO IMMISCIBLE FLUIDS
ν FIBROUS FILL / ν ADDITIVE = 200
J = 0.1
σ = 0.98 = ρ FIBROUS FILL / ρ ADDITIVE
EXPERIMENTAL DATA REGION
ALL ADDITIVE
ALL VISCOUS FLUID
MOMENT (W/ADDITIVE) / MOMENT (W/O ADDITIVE)
1.2
1.0
0.8
0.6
0.4
0.2
ADDITIVE VOLUME / TOTAL VOLUME
0.0
0.2
0.4
0.6
0.8
1.0

FLUID DYNAMICS
(FY91 ACCOMPLISHMENTS)

TITLE: FLUID-FILLED PROJECTILE FLIGHT INSTABILITIES

* Experimental: (Research studies at the CRDEC)

  * Conducted experimental investigations using CRDEC Laboratory Test Fixture For Non-Rigid Payloads:

    * Effect of two immiscible fluids with large differences in viscosity on reduction of viscous liquid-fill flight instabilities. (Concept evolved in collaboration with Dr. D. Joseph, University of Minnesota.)

    * Effect of internal surface roughness of payload compartment on creation of viscous liquid-fill flight instability.

    * Operation Desert Shield program to rapidly field artillery projectile having special liquid-fill similar to those investigated previously under the CRDEC Basic Research Program.

EFFECT OF ADDITIVE VOLUME WITH 100K CS LIQUID-FILL

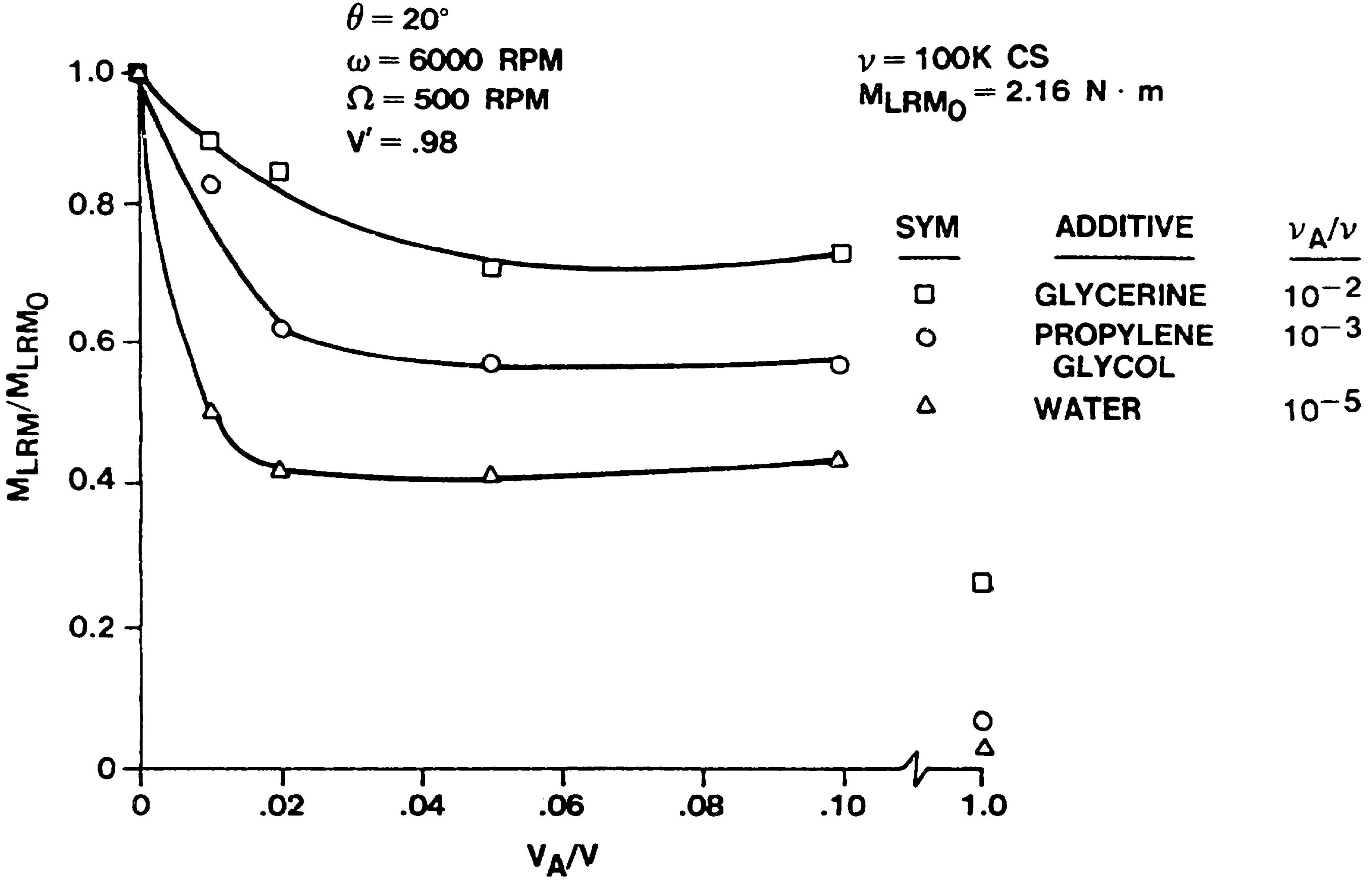

A0332-9010-A1 0187-09

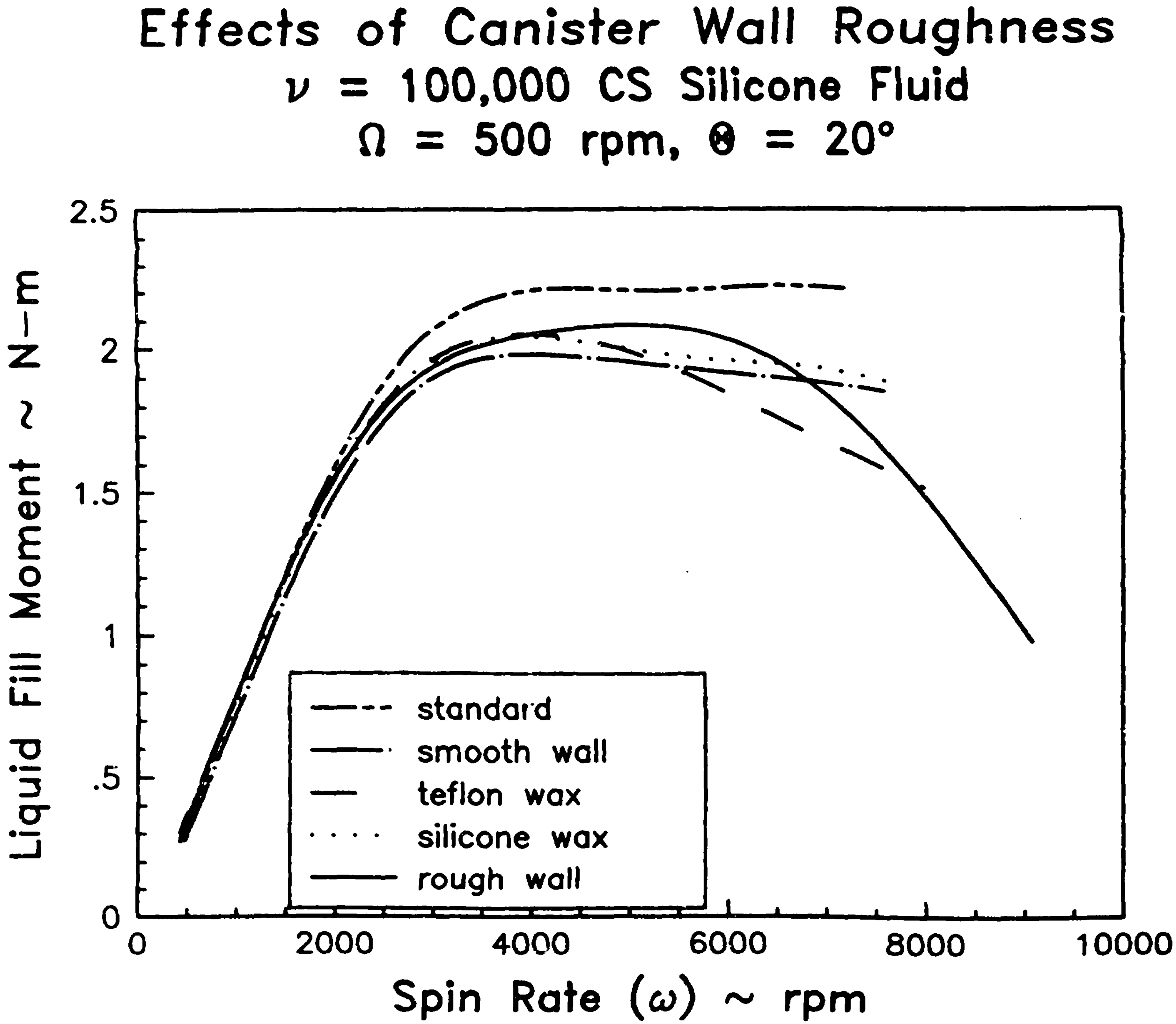
Effects of Canister Wall Roughness
ν = 100,000 CS Silicone Fluid
Ω = 500 rpm, Θ = 20°
Liquid Fill Moment ~ N-m
2.5
2
1.5
1
.5
0
2000
4000
6000
8000
10000
Spin Rate (ω) ~ rpm
standard
smooth wall
teflon wax
silicone wax
rough wall

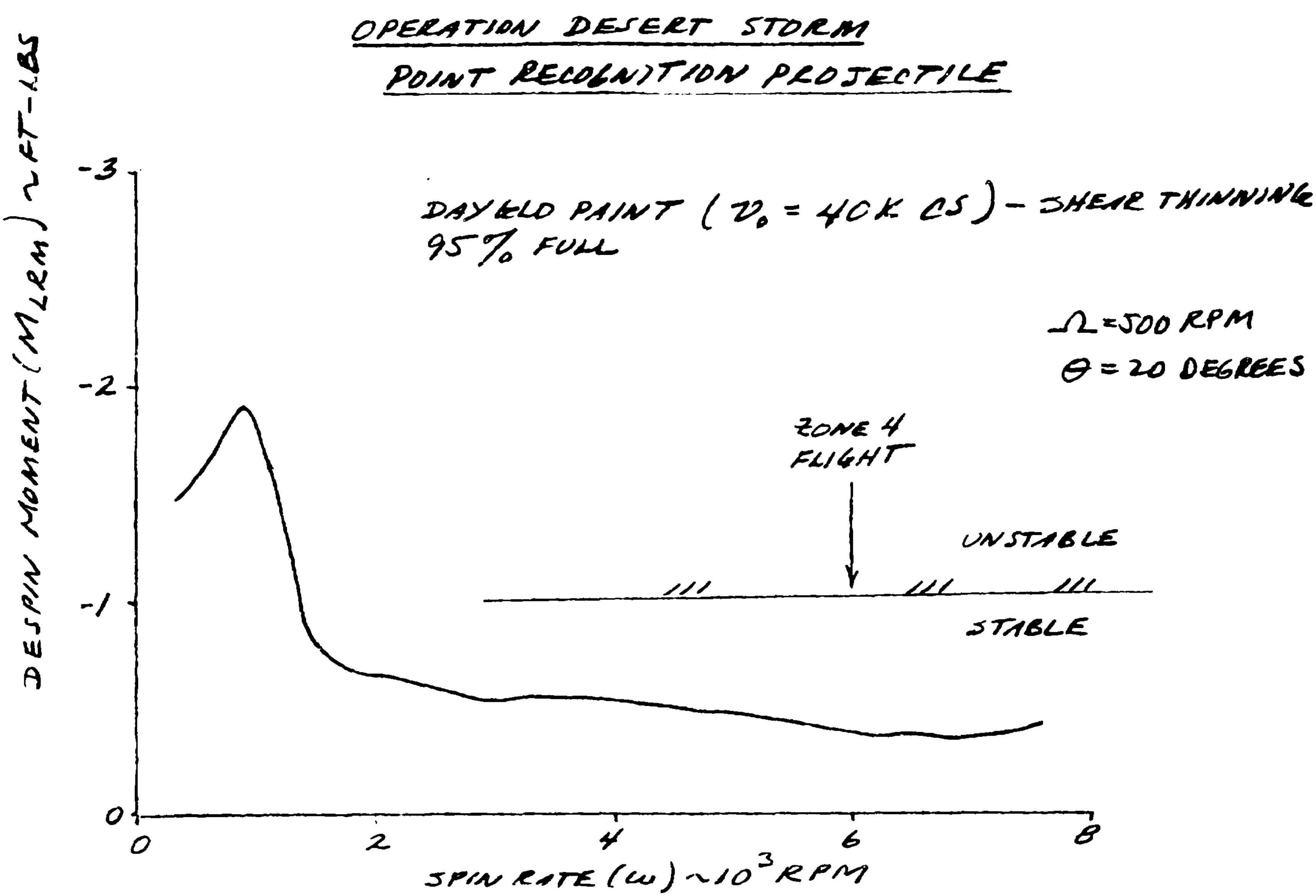

OPERATION DESERT STORM
POINT RECOGNITION PROJECTILE
DAYGLO PAINT (ν_0 = 40K CS) - SHEAR THINNING
95% FULL
Ω = 500 RPM
θ = 20 DEGREES
ZONE 4
FLIGHT
UNSTABLE
STABLE
DESPIN MOMENT (M_{LRM}) ~ FT-LBS
-3
-2
-1
0
0
2
4
6
8
SPIN RATE (ω) ~ 10^3 RPM

FLUID DYNAMICS
(FY91 ACCOMPLISHMENTS) continued

TITLE: FLUID-FILLED PROJECTILE FLIGHT INSTABILITIES

* Completed instrumented flight tests of artillery projectiles to validate experimental/theoretical results of partial fill, viscoelastic fill and immiscible, low viscosity additives.

* Modified Epicyclic Theory to include effect of viscous liquid-fill to predict flight stability using either theoretical or experimental data.

* Co-sponsored "Workplace on Problems of Rotating Liquids" at the Army High Performance Computing Research Center."

INSTRUMENTED FLIGHT TESTS

OBJECTIVE: To confirm theoretical and laboratory results through flight tests of liquid-filled artillery projectiles

TEST ITEMS: 155mm Artillery Projectiles having the following fills:

# ROUNDS	LIQUID-FILL	ADDITIVE	PREDICTED RESULTS
2	100K CS	None	Unstable
2	100K CS	5% Water	Stable
2	10K CS	None	Unstable
2	10K CS	5% Water	Stable
2	30K CS	None	Unstable
2	30K CS	5% Water	Stable
2	100K CS (Viscoelastic)	None	Stable
2	100K CS (50% Fill)	None	Unstable

FIRING CONDITIONS: Zone 4 (Transonic) with induced yaw

INSTRUMENTATION: Yaw Sondes and radar

LOCATION: Dugway Proving Ground

AO332-0103-L91 1-13324

EFFECT OF PARTIAL FILL

(NORMAL LAUNCH)

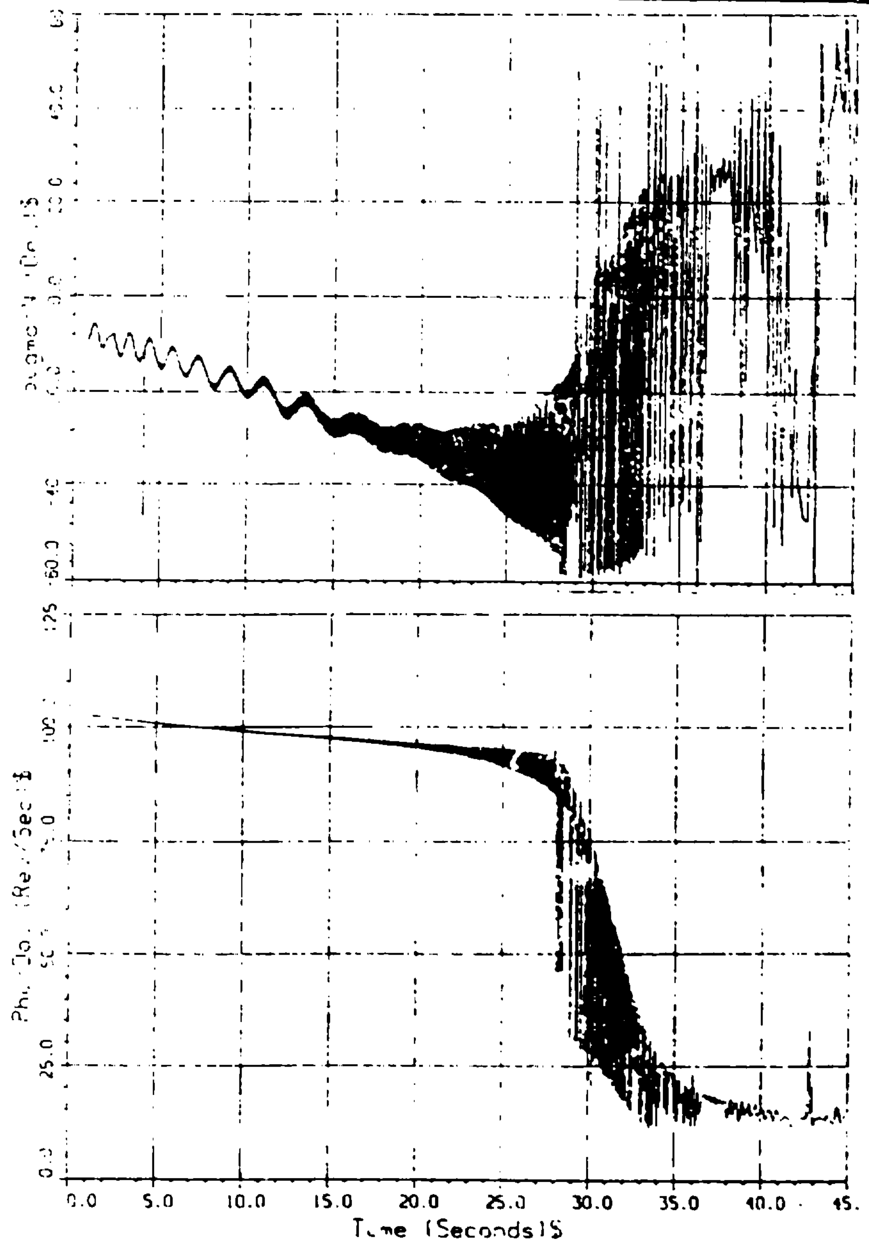

100KCS

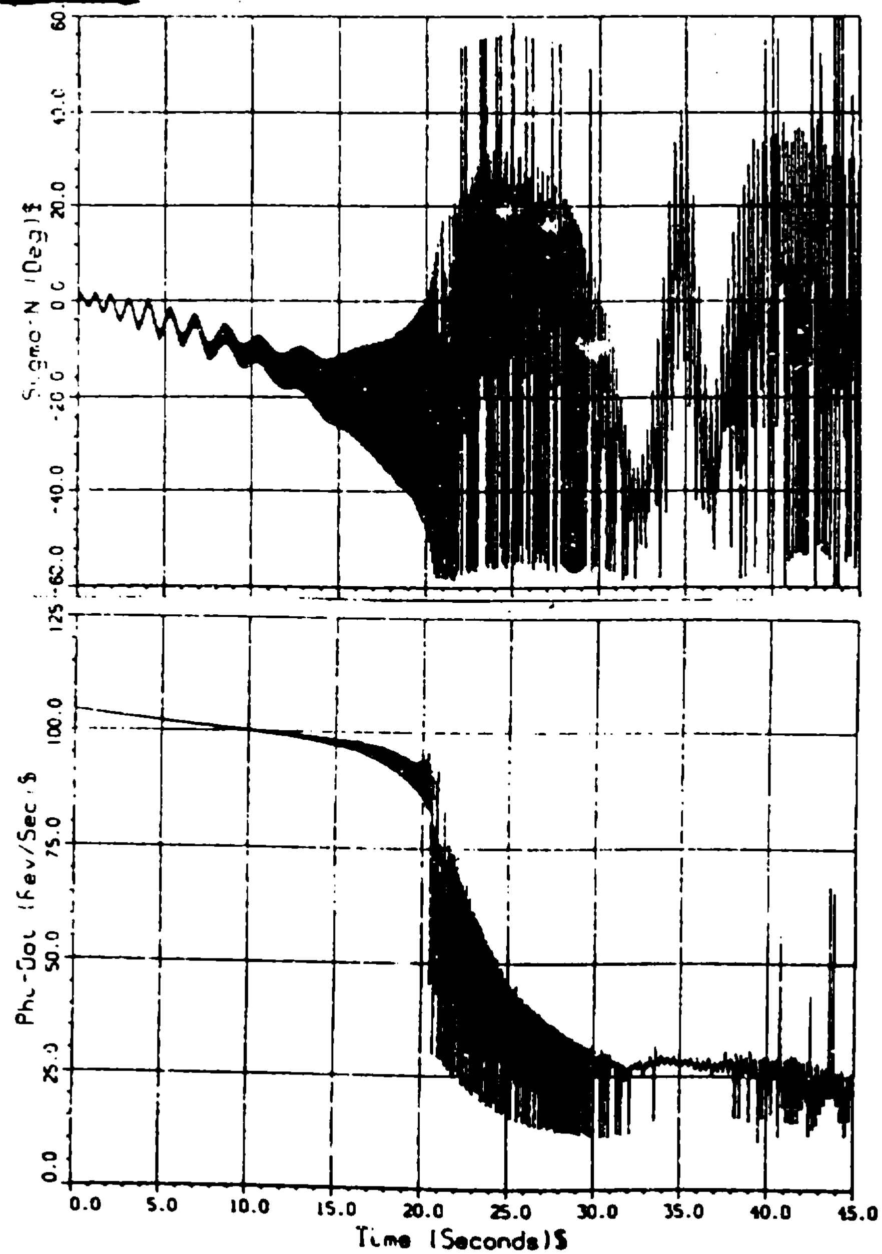

100KCS (50% FULL)

EFFECT OF VISCOELASTICITY

NORMAL LAUNCH

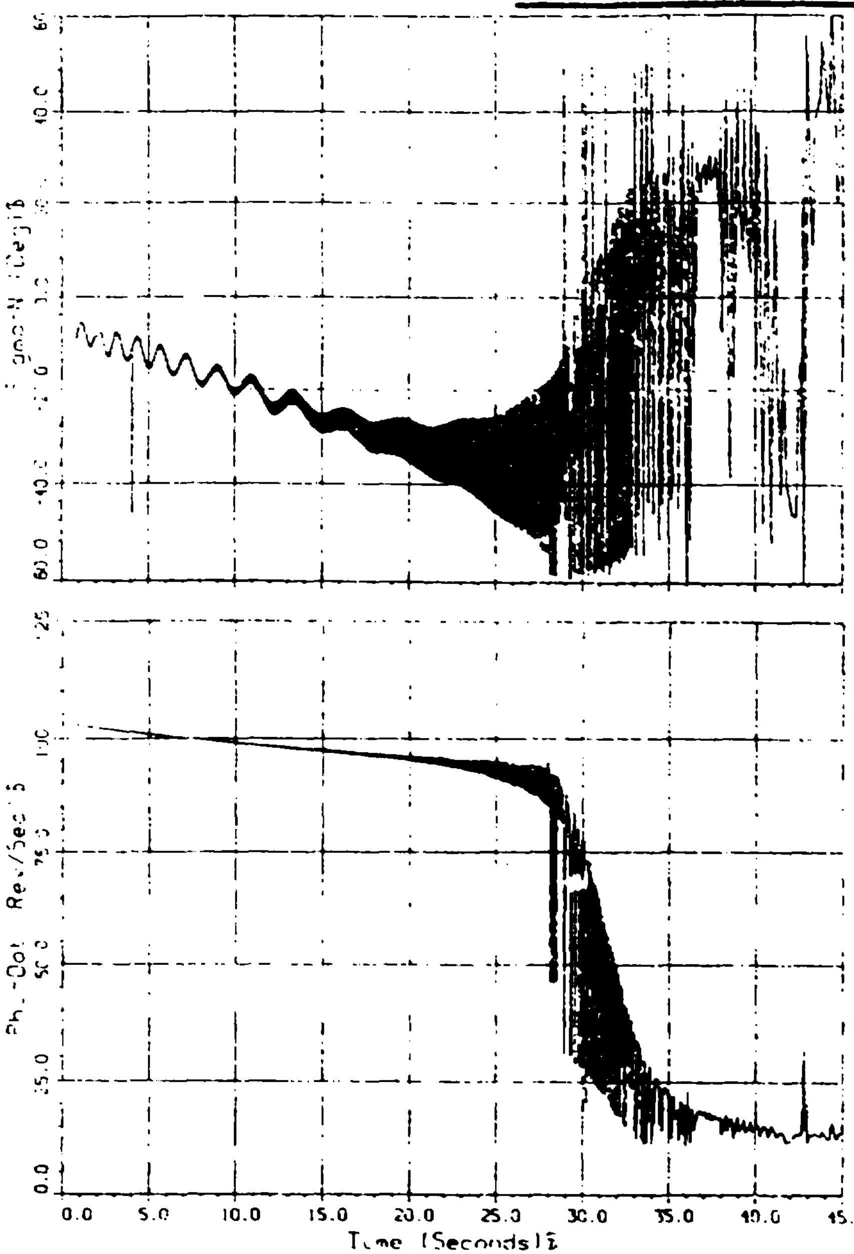

100K CS

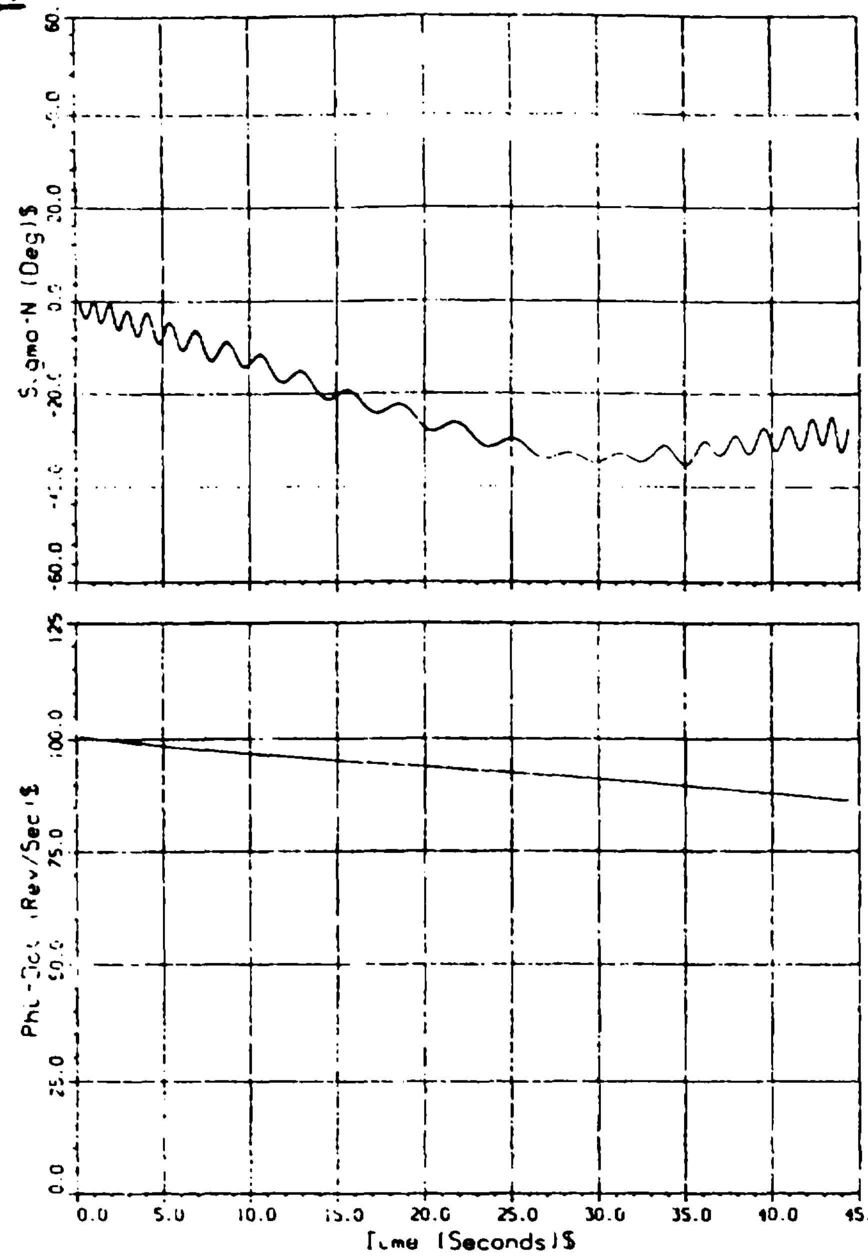

100K CS VISCOELASTIC

EFFECT OF ADDITIVE

INDUCED YAW LAUNCH

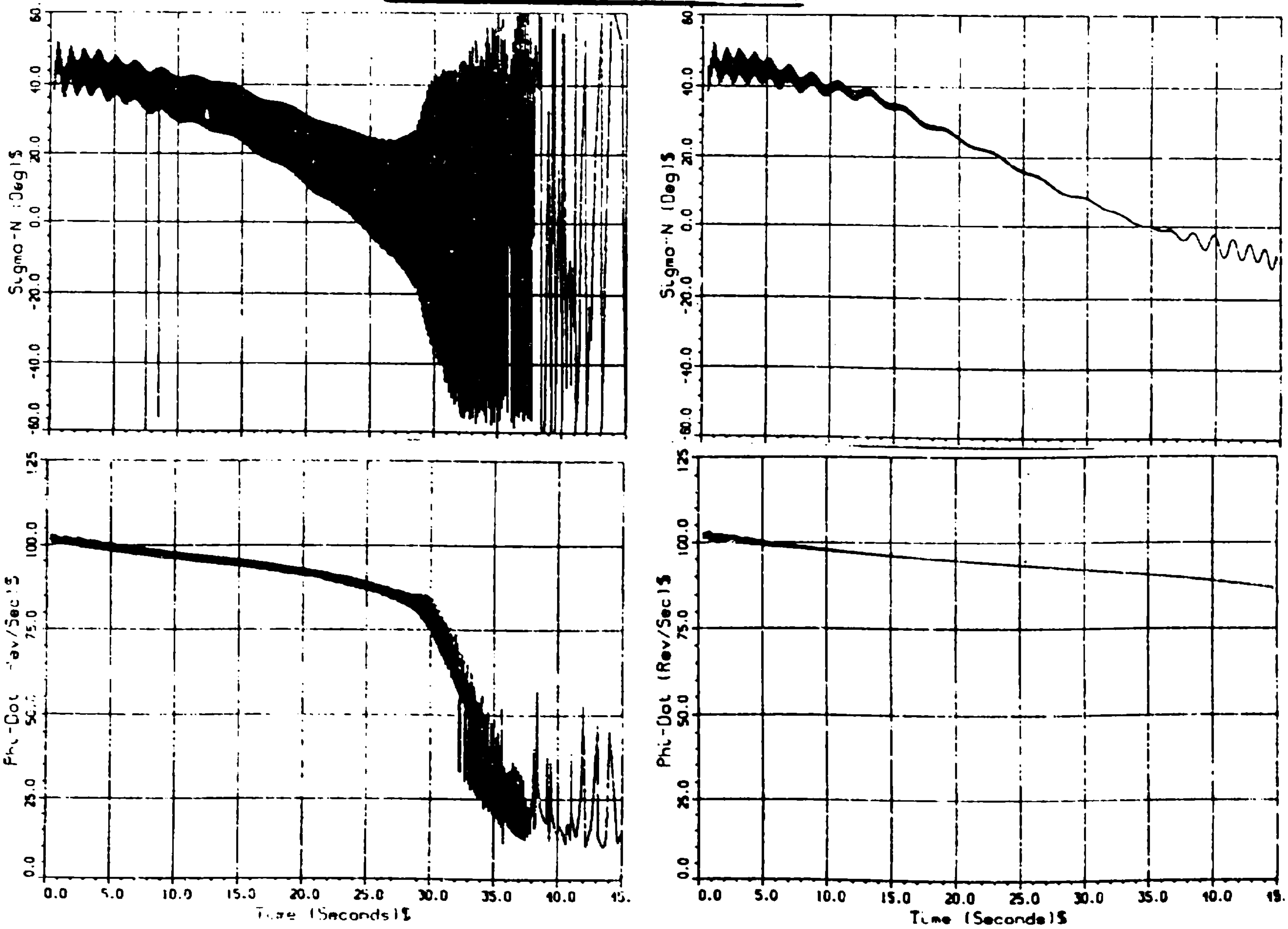

10K CS

10K CS W/ADDITIVE

EFFECT OF ADDITIVE INDUCED YAW LAUNCH

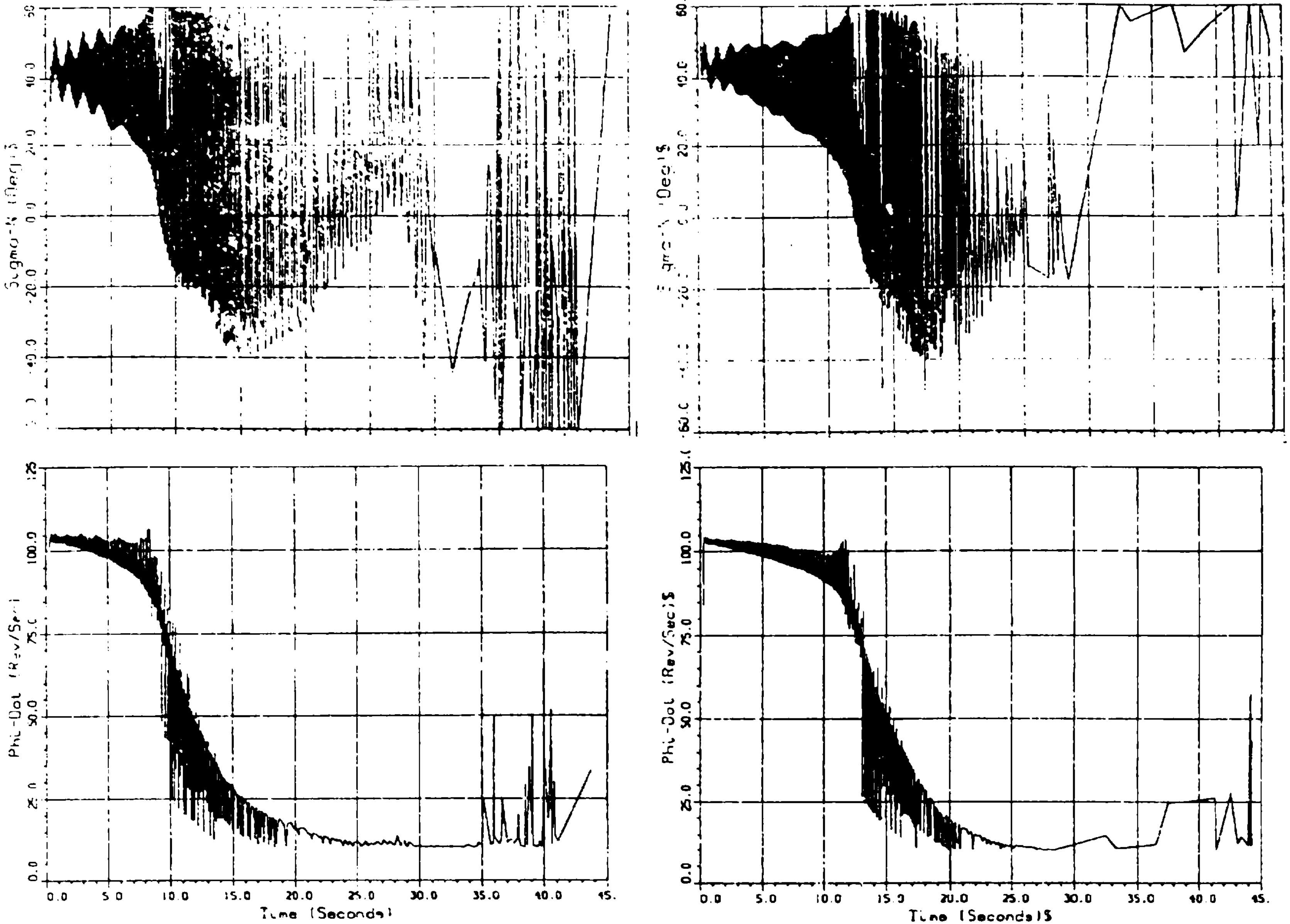

100K CS

100K CS W/ADDITIVE

FLUID DYNAMICS
FUTURE DIRECTIONS

* Continue to investigate methods to reduce or eliminate viscous liquid-fill flight instabilities.

  - Immiscible, low viscosity additives.

  - Longitudinal baffles.

* Evaluate effect of non-cylindrical and eccentrically located payload compartments on producing liquid-filled flight instabilities.

* Study neutrally buoyant, second body phenomenon related to flight stability.

* Consider flight stability effects of novel fluid-fills including slurries, powders, viscoelastic fluids, etc.

* Exploit unusual behavior of novel fluids to increase control of flight vehicles and other fluid dynamic devices.

DESPIN VERSUS KINEMATIC VISCOSITY
SPIN FIXTURE DATA

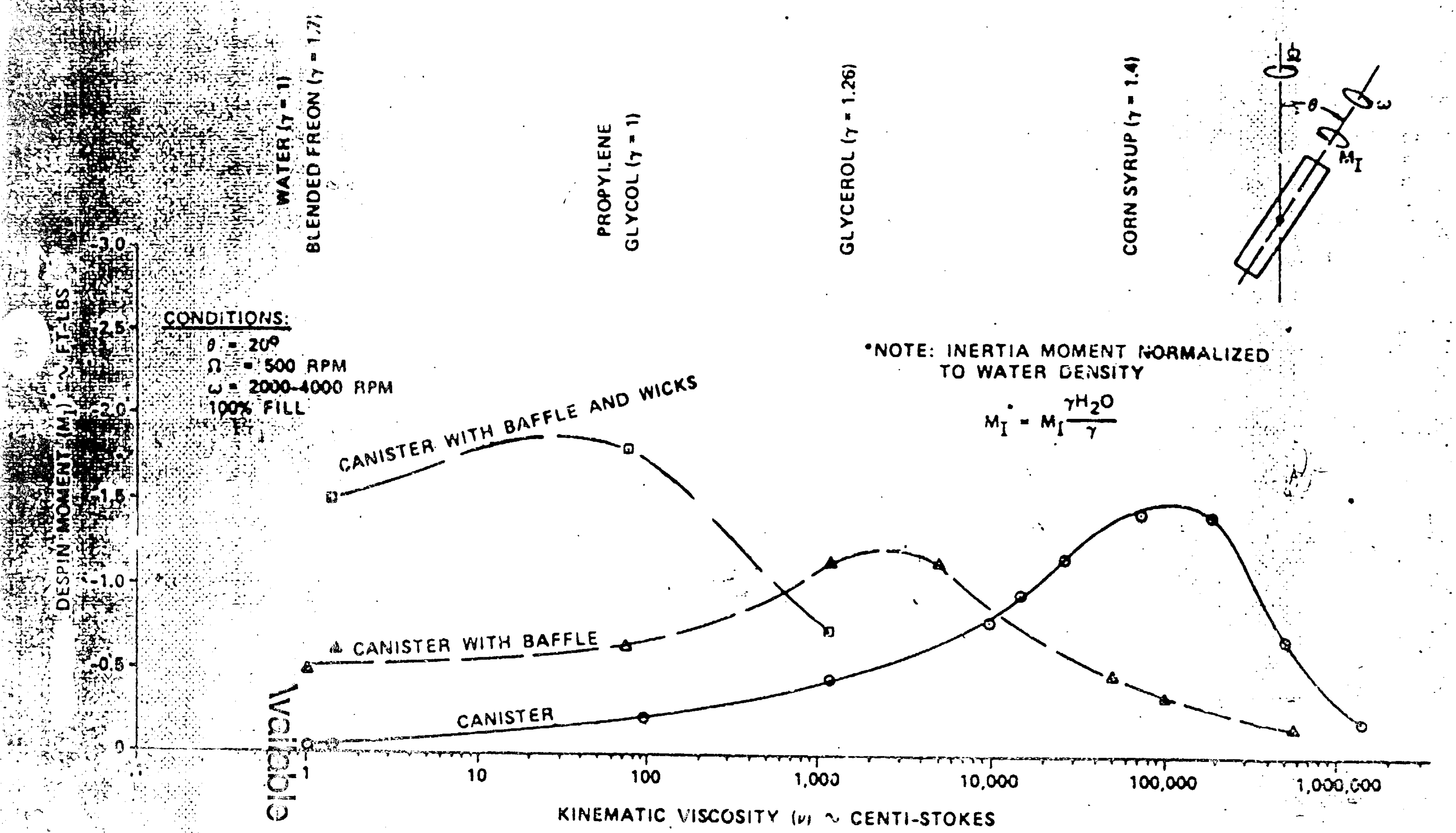

HIGHLY VISCOELASTIC FLUID WITH ADDITIVE

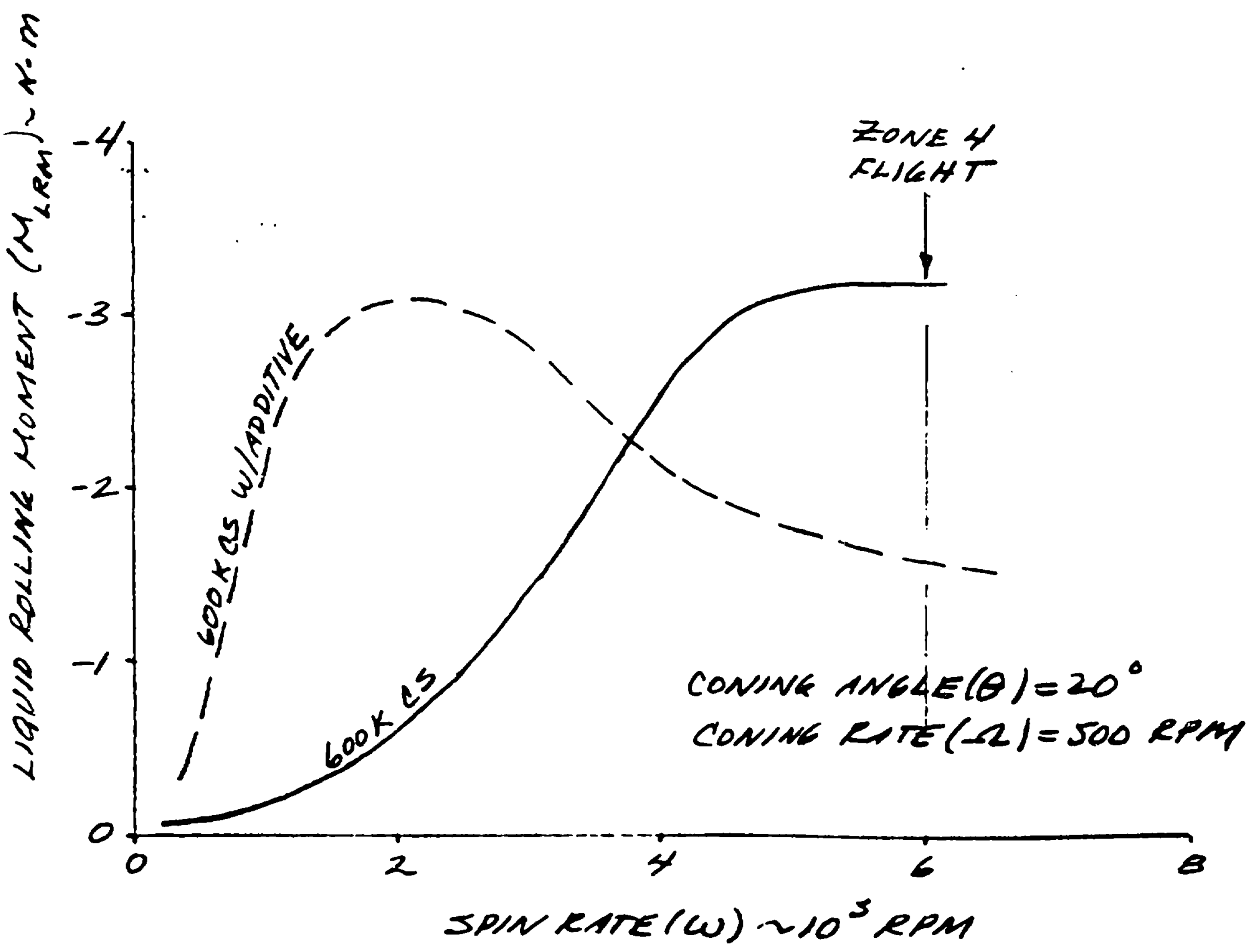

"We should have changed to winter grade!"

AREAS OF CONCERN IDENTIFIED AT ROUNDTABLE ON LIQUID-FILLED SHELL, 20-21 SEPT 1984 (not prioritized)

Effect of:

Changes in internal geometry (damp out inertial modes).

Interaction of internal flow conditions with external aerodynamics.

Unconventional internal geometry and configurations.

Partial solid/Partial liquid payloads including porous media.

Non-Newtonian fluids.

Spin-up and cone-up (Transient behavior of fluid and shell's response).

Mixing of several fluids.

Chemical Reactions in Multi-component fluid systems.

Linear vs non-linear analysis.

Thermal effects.

Understand and Predict:

Hydrodynamic and aerodynamic stability and their coupling.

Theoretical basis of bias due to frequency.

Sensitivity of shell's response to cavity aspect ratio.

Work To Do/Gaps:

Experimental (Laboratry):

Partially-filled container.

Verification of Whiting's experimental results at low angles.

Pressures at low Reynolds numbers.

Velocities.

Despin and yaw moments at all Reynolds numbers.

Experimental (Flight Test):

Yaw Sonde for different Reynolds numbers.

Identify capabilities and limitations of current facilities.

Analysis:

Establish systematic approach for all general fluids.

Exploit all methods: linear, perturbation, asymptotic, energy finite difference and finite element.

Examine bifurcation parameters.

Analyze spin-up using "matched asympototoc expansions.

Analyze conditions for Stewartson instability due to coning match.

Computations:

Eigenfrequencies for partial-fill.

CRAY II for coupling of aerodynamics and fluid dynamics.

Finite difference and finite element with adaptive grids.

Comparisons:

Analysis with computations.

Analysis with experiments.

Develop standardized units and parameters.

Determine ranges of parameters of interest to Army.

Large angle (90 degree) coning experiments.

Future Directions -
Liquid-Filled Projectiles

Experimental:

Non-cylindrical containers (all viscosities).

Longitudinal baffles to eliminate flight instabilities of viscous liquid-fills.

Immiscible, low viscosity additive to eliminate flight instabilites of viscous fills (transient effects).

Effects of non-Newtonian fluids.

Theoretical:

Purely theoretical method that can handle all viscosities (one stop approach).

viscoelastic fluids.

Computational:

Launch transient effects.

Liquid-Filled Projectile Design Handbook.

Blank

Analysis and Visualization of the Flow in a Spinning and Nutating Cylinder

Thorwald Herbert
Rihua Li
Mohamed Selmi

Department of Mechanical Engineering
The Ohio State University

Supported by
CSL - CRDC - CRDEC

Additional support by
AFOSR, NSF & OSC (Cray YMP/864)

Workshop on Problems of Rotating Fluids
AHPCRC Minneapolis, Minnesota
April 22-23, 1991

Outline

- Introduction - History
- Analytical Studies
- 3D Spectral Navier-Stokes Solver
- Eigenfunction Expansions
- Computation of the Moments
- Flight Simulations
- Extensions (Li, Selmi)
- Experimental Flow Visualization
- Computer Visualization
- Summary

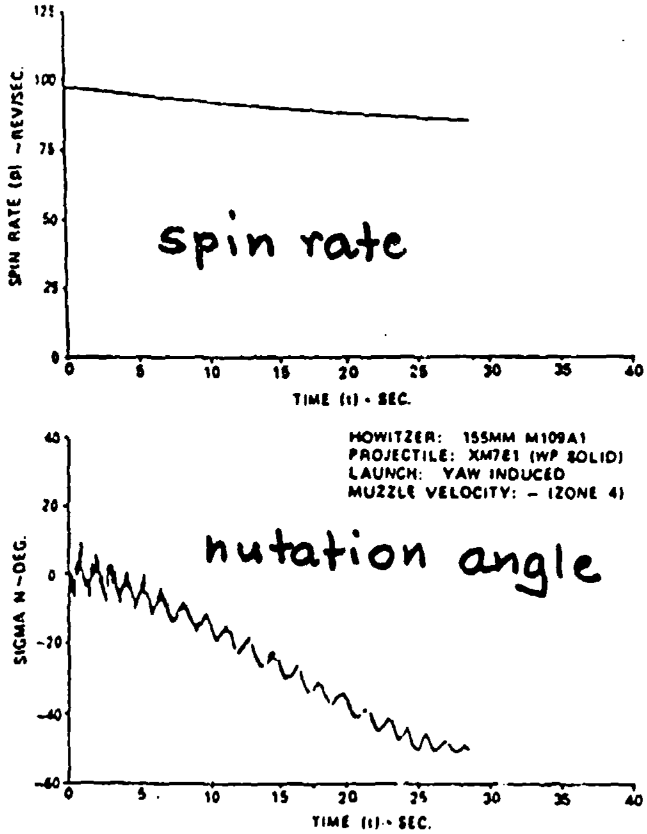

FIG.3.YAWSONDE DATA FOR XM761
STABLE FLIGHT (WP SOLID)

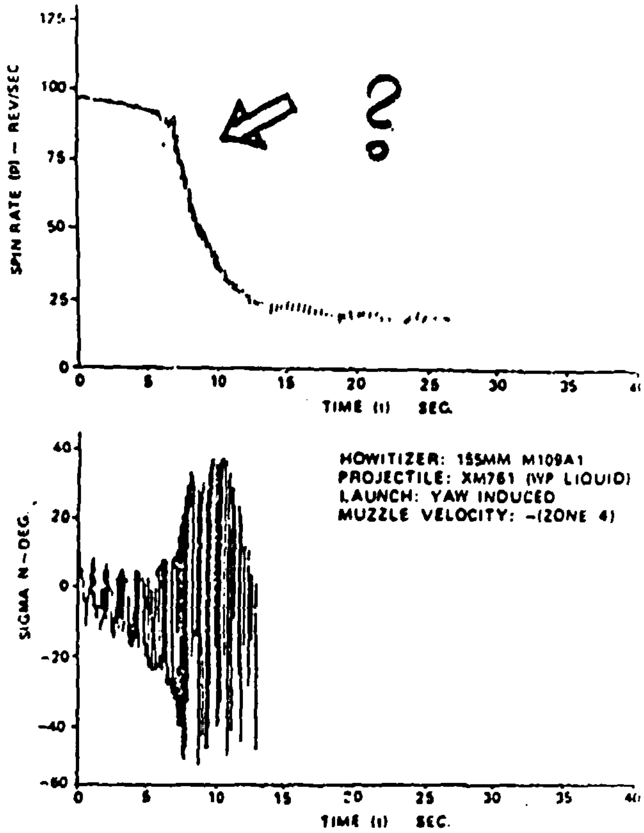

FIG.4.YAWSONDE DATA FOR XM761
UNSTABLE FLIGHT (WP LIQUID)

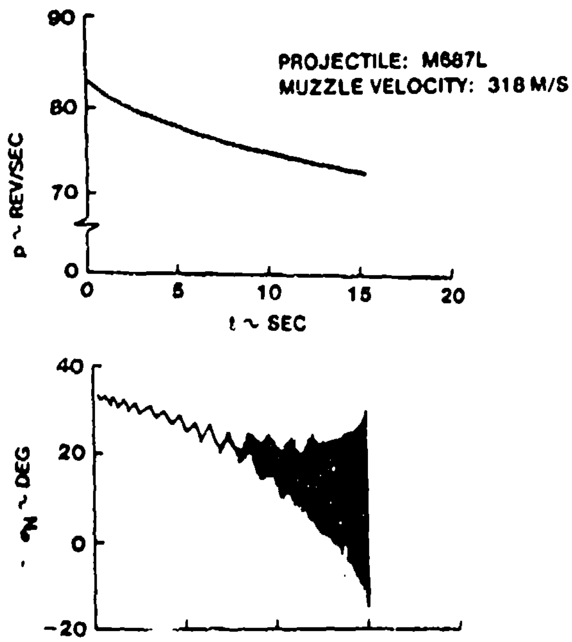

Unstable Flight Motion of Projectile With Low Viscosity Liquid Fill

Stewartson 1959
Wedemeyer 1966
inertial waves

Miller: despin moment M_z

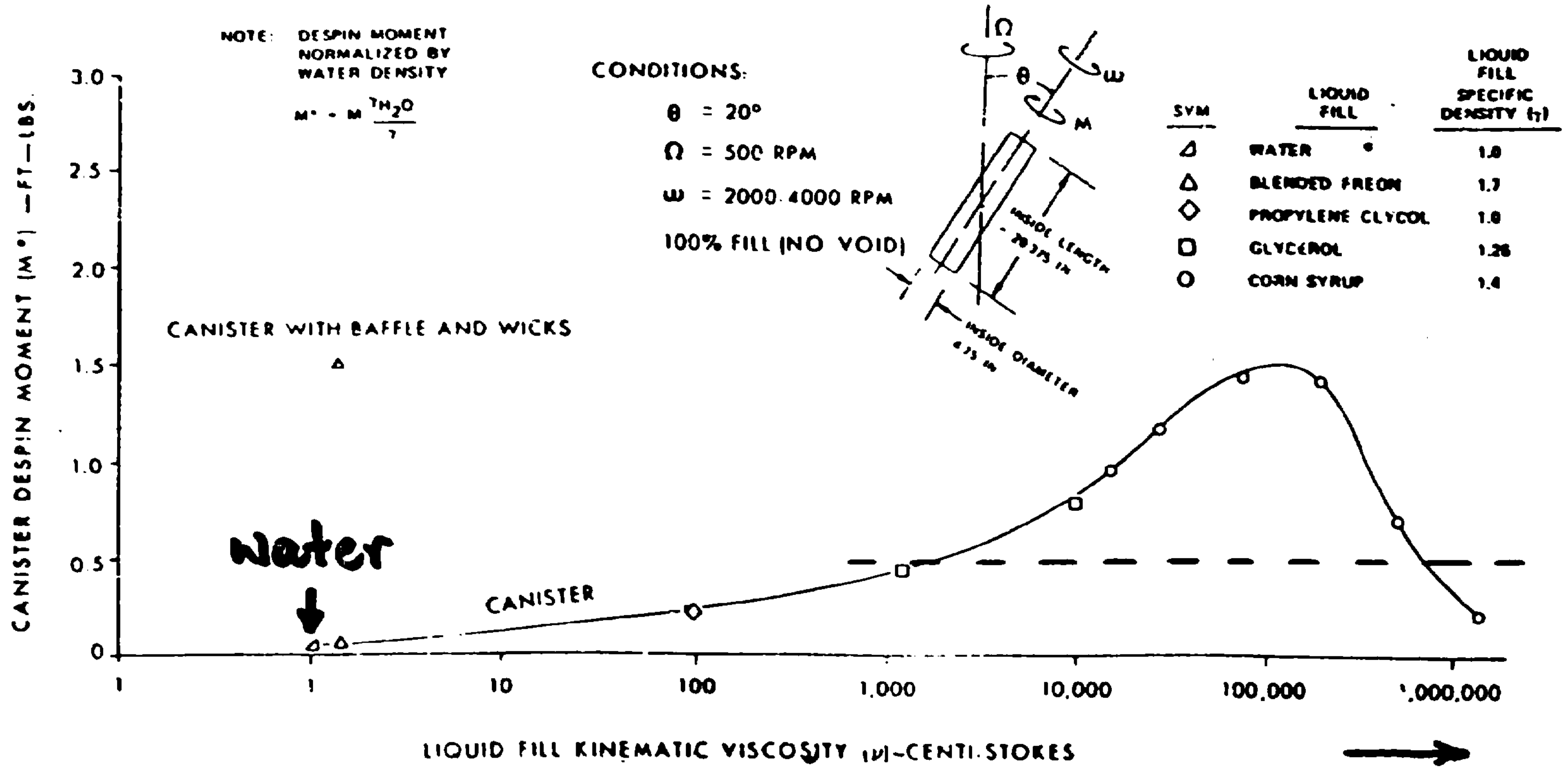

kinematic viscosity

FIG. 11. DISPIN MOMENT AS A FUNCTION OF LIQUID FILL VISCOSITY FOR A 20° CONING ANGLE

flight instability occurs at high viscosity

11

Miller: despin moment M_z

$$\Rightarrow M_z = m_e (a \Omega \sin\Theta)^2 \cdot m_z \,, \quad m_z = 0.54$$

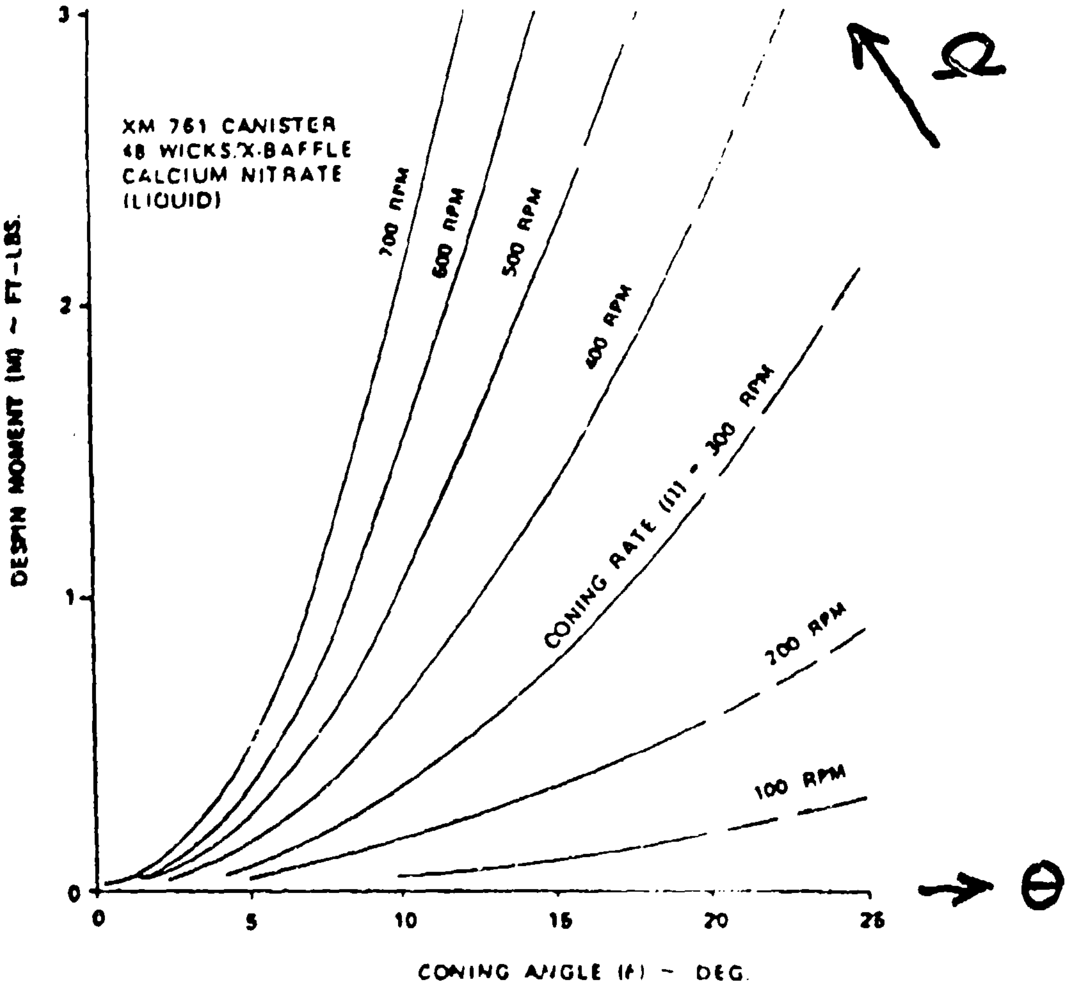

FIG.7.DESPIN MOMENT FOR THE XM761 PAYLOAD
VS CONING ANGLE AND CONING RATE

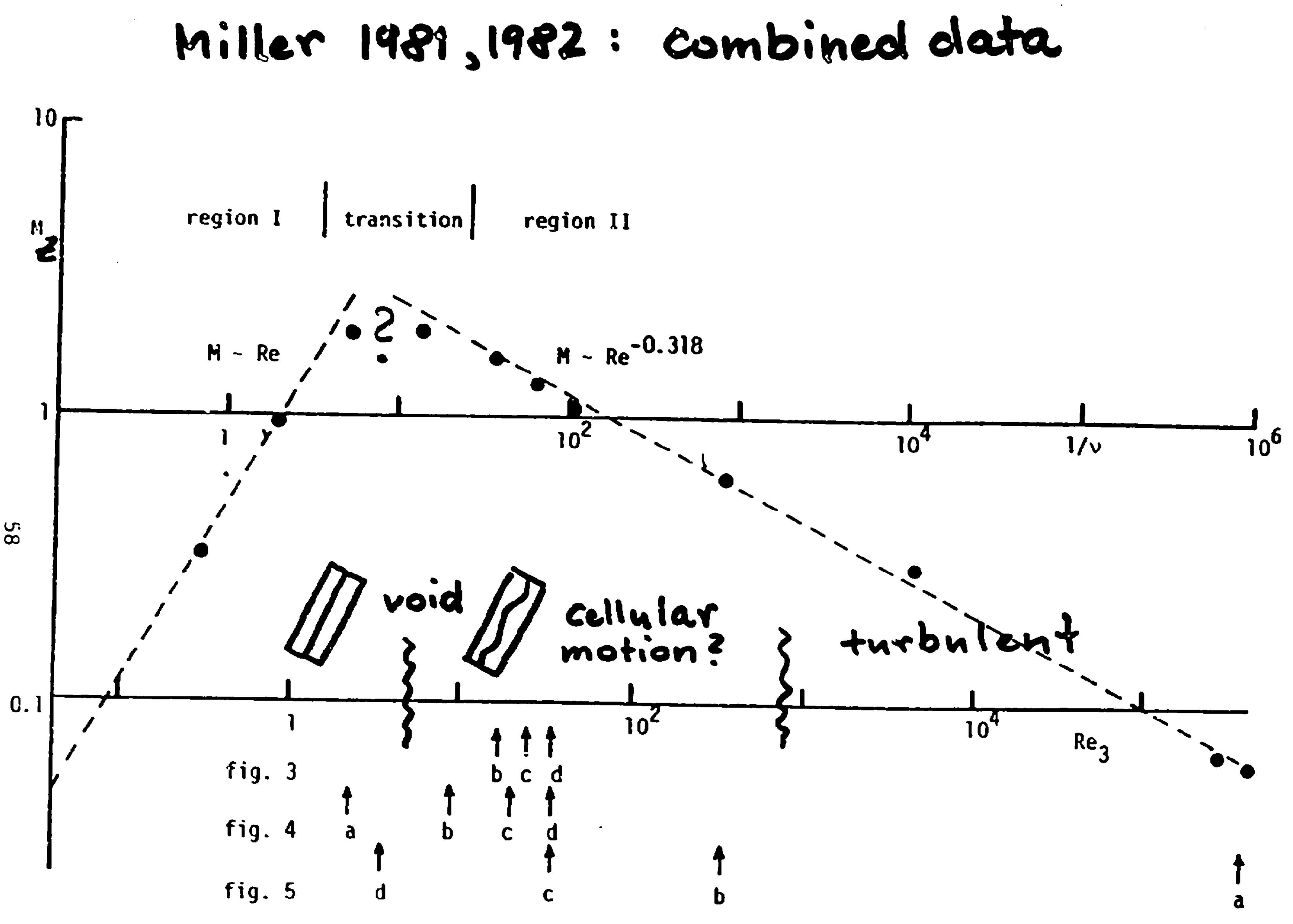
Miller 1981, 1982 : combined data
10
M
region I
transition
region II
M ~ Re
M ~ Re^-0.318
1
1
10^2
10^4
1/ν
10^6
void
cellular
motion?
turbulent
0.1
1
10^2
10^4
Re_3
fig. 3
b c d
fig. 4
a b c d
fig. 5
d c b a

Figure 3

DIMENSIONAL ANALYSIS

parameters:

∥	a	radius	<length>
	c	length/2	
∥	ω	spin rate	<time>
	Ω	nutation rate	
	Θ	nutation angle	
∥	ρ	density	<mass>
	μ	viscosity	

Π-theorem:

$7 - 3 = 4$ dimensionless groups

$\lambda = \dfrac{c}{a}$ aspect ratio $\rightarrow \eta$

$\tau = \dfrac{\Omega}{\omega}$ frequency

$\sigma = \sin\Theta$

$Re = \dfrac{\rho\,\omega\,a^2}{\mu}$ Reynolds number

$$\underline{\underline{\omega}} \rightarrow \omega' = \omega + \Omega\cos\Theta \quad ?$$

(1) Use Navier-Stokes equations in the "nutating" system (n)

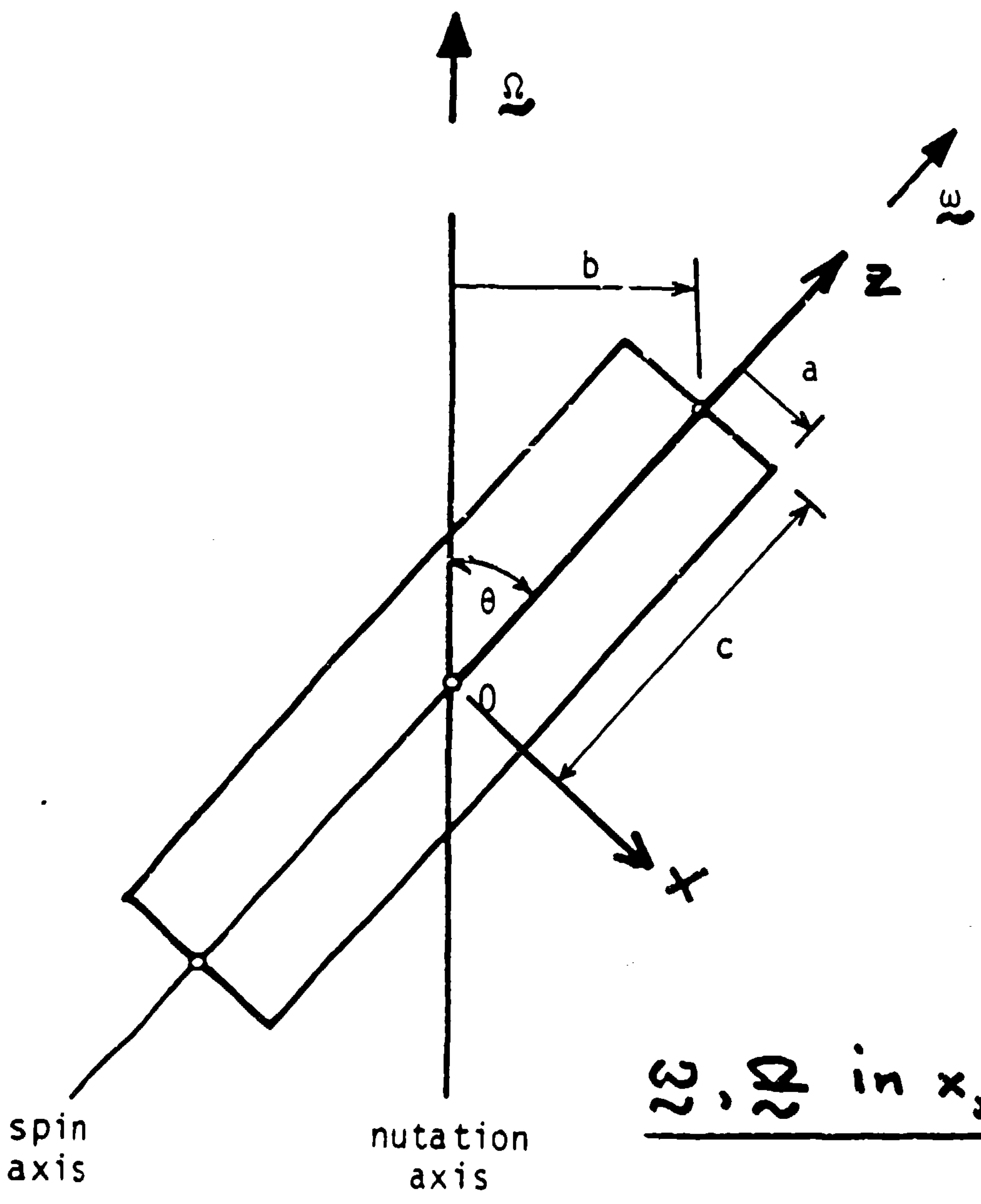

$\underset{\sim}{\omega}, \underset{\sim}{\Omega}$ in x,z-plane

Figure 1

(2) Introduce non-dimensional quantities

(3) Split $\underset{\sim}{V}_n = \underset{\sim}{V}_s + \underset{\sim}{V}_d$, $p_n = p_s + p_d$

$\underset{\sim}{V}_s$, p_s : <u>s</u>olid body rotation

$\underset{\sim}{V}_d$, p_d : <u>d</u>eviation

(4) Introduce cylindrical coordinates

$(x, y, z) \rightarrow (r, \varphi, z)$

<u>Conclusion:</u>

$$\underset{\sim}{V}_d = \mathcal{O}(\varepsilon)$$

$\varepsilon = \frac{\Omega}{\omega} \sin\Theta$ is a <u>small</u> parameter

e.g.
$$\left.\begin{array}{l} \Omega \leq 500 \text{ rpm} \\ \omega \geq 3000 \text{ rpm} \\ \Theta \leq 20^\circ \end{array}\right\} \quad \varepsilon \leq 0.057$$

(5) <u>Linearize</u> the equations in ε <u>without</u> restricting Re

(6) In the first step: <u>neglect the end effects</u>

Deviation $\underset{\sim}{v}_d$, p_d

Governing equations

continuity $$\frac{1}{r}\frac{\partial}{\partial r}(r v_r) + \frac{1}{r}\frac{\partial v_\phi}{\partial \phi} + \frac{\partial v_z}{\partial z} = 0 ,$$

$r \Longrightarrow$ $$D' v_r - \cancel{\frac{v_\phi^2}{r}} - 2(1+\tau_z) v_\phi + 2\cancel{\tau_\phi} v_z =$$

$$-\frac{\partial p_d}{\partial r} + \frac{1}{Re}[D'' v_r - \frac{v_r}{r^2} - \frac{2}{r^2}\frac{\partial v_\phi}{\partial \phi}] ,$$

$\varphi \Longrightarrow$ $$D' v_\phi + \cancel{\frac{v_r v_\phi}{r}} + 2(1+\tau_z) v_r - 2\cancel{\tau_r} v_z =$$

$$-\frac{1}{r}\frac{\partial p_d}{\partial \phi} + \frac{1}{Re}[D'' v_\phi - \frac{v_\phi}{r^2} + \frac{2}{r^2}\frac{\partial v_r}{\partial \phi}] ,$$

$z \Longrightarrow$ $$D' v_z + 2\cancel{\tau_r} v_\phi - 2\cancel{\tau_\phi} v_r = -\frac{\partial p_d}{\partial z} - \underline{\underline{2 r \tau_r}} + \frac{1}{Re} D'' v_z ,$$

$$D' = \frac{\partial}{\partial t} + \frac{\partial}{\partial \phi} + \cancel{v_r \frac{\partial}{\partial r}} + \cancel{\frac{v_\phi}{r}\frac{\partial}{\partial \phi}} + \cancel{v_z \frac{\partial}{\partial z}} ,$$

$$D'' = \frac{\partial^2}{\partial r^2} + \frac{1}{r}\frac{\partial}{\partial r} + \frac{1}{r^2}\frac{\partial^2}{\partial \phi^2} + \frac{\partial^2}{\partial z^2} ,$$

(a) linearization in ε $\Longrightarrow$ symmetries

(b) linearization in $\underset{\sim}{v}_d$

"INFINITE" CYLINDER

$$\underset{\sim}{V}_d = (0, 0, V_0) \quad , \quad p_d = 0$$

$$V_0(r,\varphi) = 2\varepsilon\,[f(r)\cos\varphi + g(r)\sin\varphi]$$

where

$$\left\| \begin{array}{l} f'' + \frac{1}{r}f' - \frac{1}{r^2}f - Re\cdot g = -Re\cdot r \\ g'' + \frac{1}{r}g' - \frac{1}{r^2}g + Re\cdot f = 0 \\ \qquad f, g = \begin{cases} 0 \text{ at } r=1 \\ \text{finite at } r=0 \end{cases} \end{array} \right.$$

Limit $Re \to 0$:

$$f = \frac{Re}{8}(r - r^3) + O(Re^3)$$

$$g = \frac{Re^2}{192}(2r - 3r^3 + r^5) + O(Re^4)$$

series for $Re \lesssim 12$

Limit $Re \to \infty$:

$$\left.\begin{array}{l} f = 0 \\ g = r \end{array}\right\} + \text{boundary layer near } r=1$$

Arbitrary Re :

- numerical solution
  (spectral method with radial Chebyshev expansion)

- analytical solution

$$V_0 = 2\varepsilon \left[f \cos\varphi + g \sin\varphi \right]$$

$$g + if = r - \frac{I_1(\sqrt{i Re}\, r)}{I_1(\sqrt{i Re})}$$

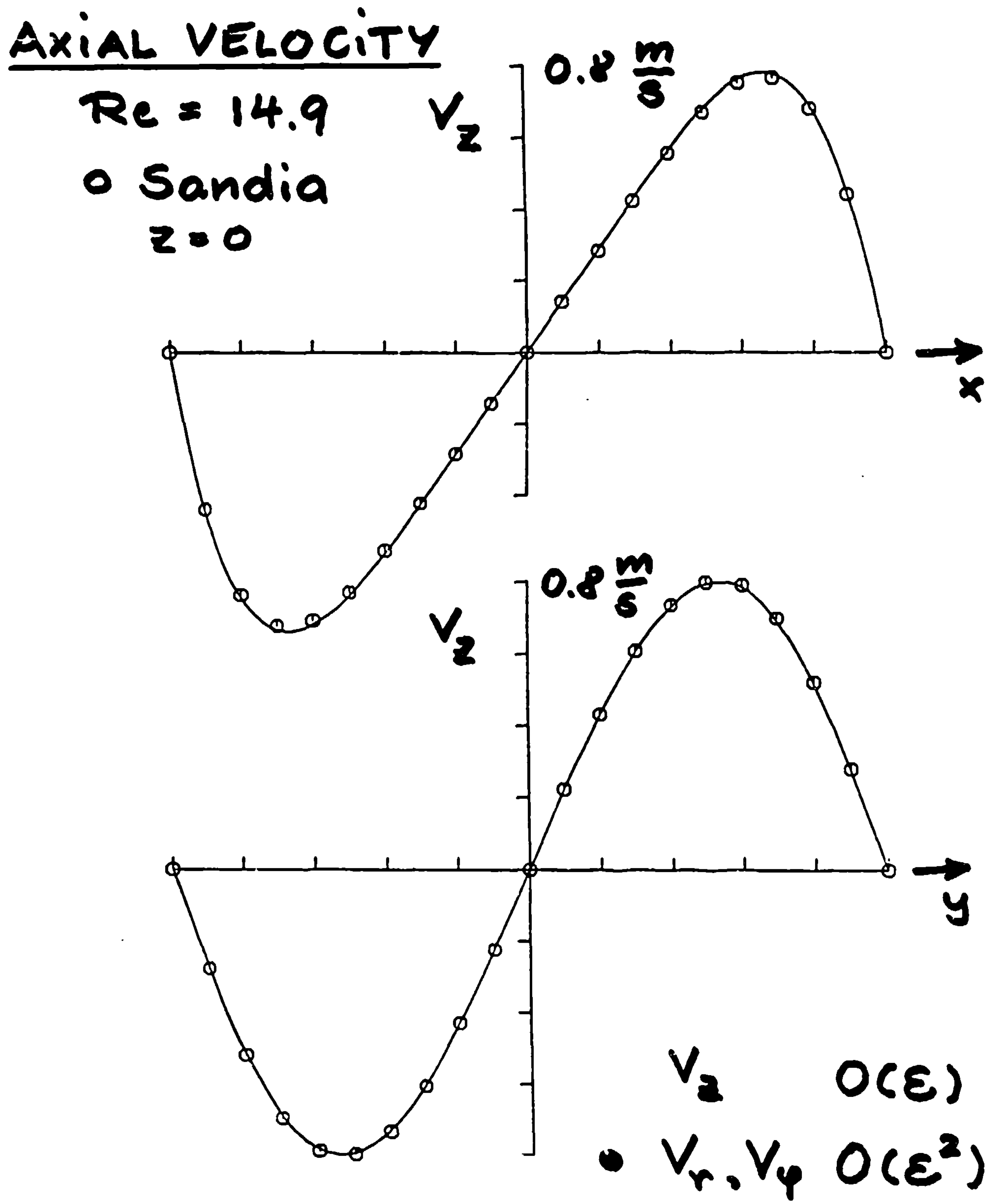

AXIAL VELOCITY
Re = 14.9
o Sandia
z = 0
V_z
0.8 m/s
x
V_z
0.8 m/s
y
V_z O(ε)
• V_r, V_φ O(ε²)

Figure 5

MOMENTS

yaw : $M_x^* = m_\ell (2\Omega a \sin\theta)(\omega a) M_x$ ∘

pitch : $M_y^* = m_\ell (2\Omega a \sin\theta)(\omega a) M_y$

due to flux of angular momentum

roll : $M_z^* = m_\ell (2\Omega a \sin\theta)^2 M_z$ ∘

due to Coriolis force

$$M_y = -\int_0^1 r^2 g\, dr = \frac{f'(1)}{Re} + \frac{1}{4} \quad \leq 0$$

$$M_z = -M_x = \int_0^1 r^2 f\, dr = -\frac{g'(1)}{Re} \quad \geq 0$$

Limit $Re \to 0$:

$$M_y = -\frac{Re^2}{1536}, \quad M_z = \frac{Re}{96} \quad (Re \lesssim 10)$$

Analytical:

$$g'(1) + i f'(1) = 2 - \sqrt{iRe}\, \frac{I_0(\sqrt{iRe})}{I_1(\sqrt{iRe})}$$

$O(\varepsilon)$: despin moment M_z

owing to Coriolis forces

NOTE : $M_z = O(\varepsilon^2)$

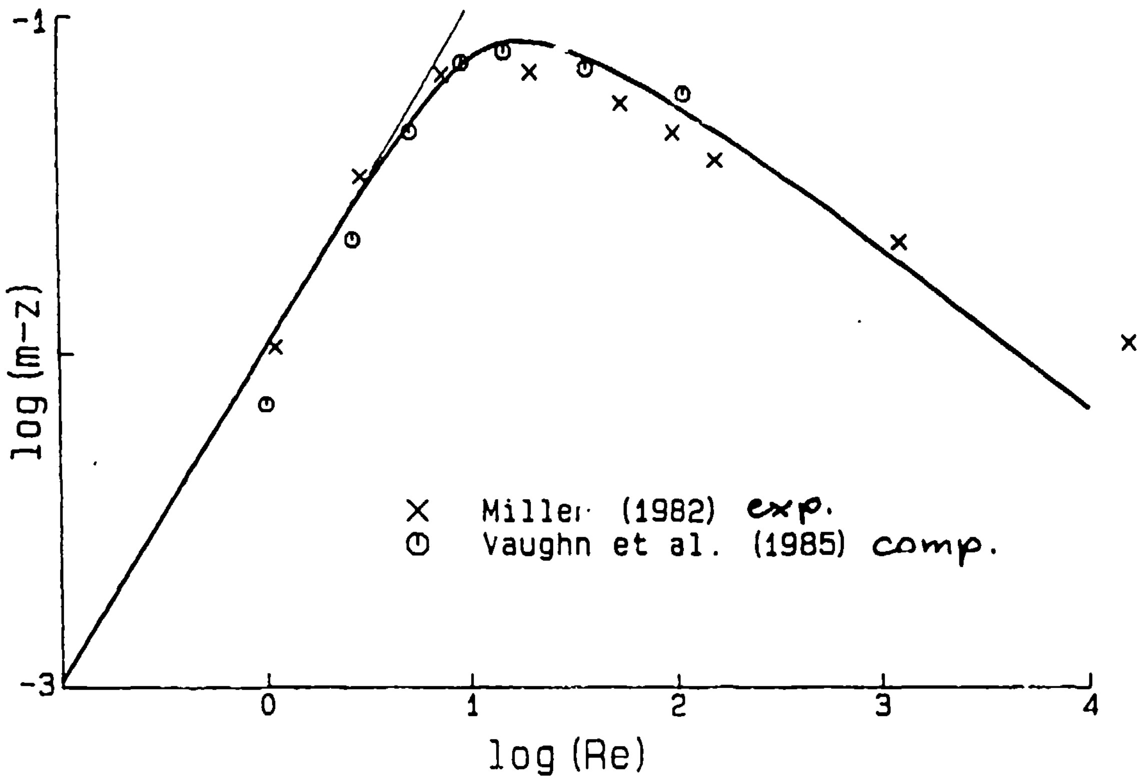

LIN7

Contours of equal axial velocity

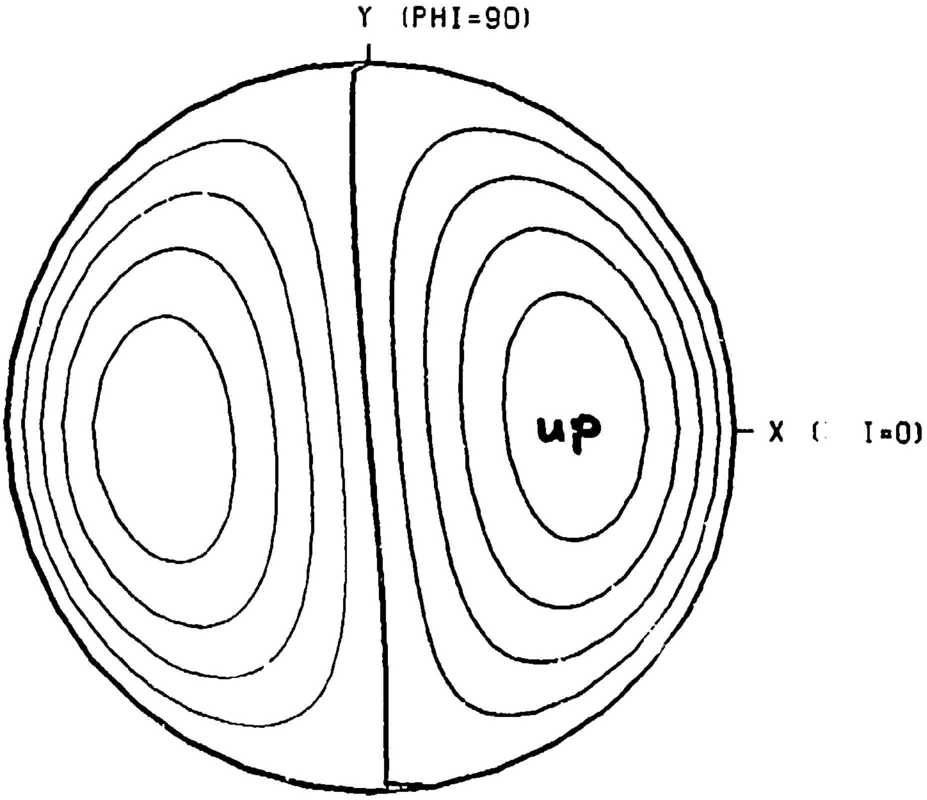

LIN5 RE= 1.00 LEVELS: 0.0100

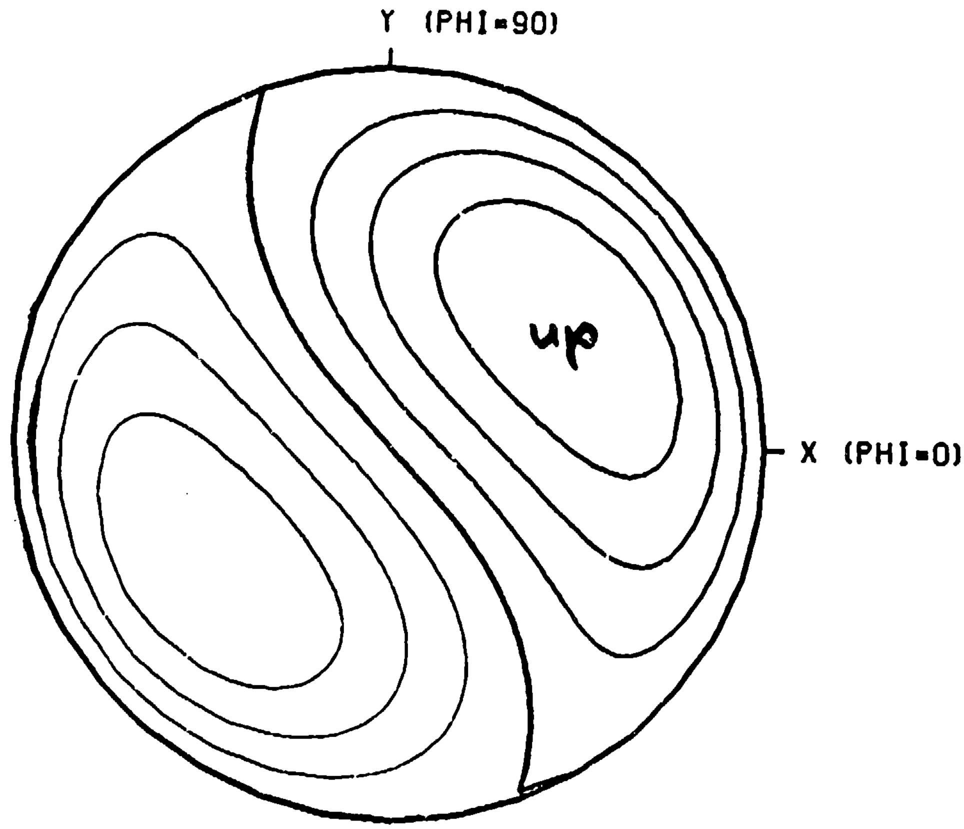

LIN5 RE= 10.00 LEVELS: 0.1000

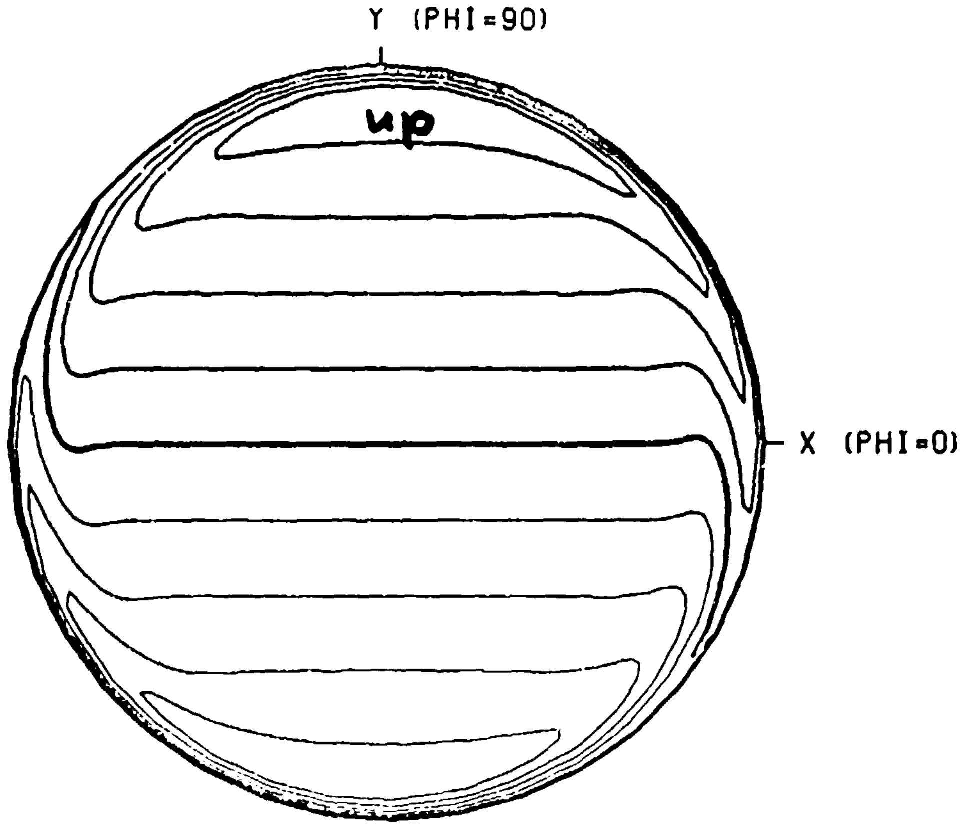

LIN5 RE= 1000.00 LEVELS: 0.2000

$O(\varepsilon^2)$ VELOCITIES V_φ, V_r

$O(\varepsilon)$:

$$V_z = 2\omega a \varepsilon [f_1 \cos\varphi + f_2 \sin\varphi]$$

$O(\varepsilon^2)$:

$$V_\varphi = \omega a \varepsilon^2 [\underline{\underline{f_3}} + f_4 \cos 2\varphi + f_5 \sin 2\varphi]$$

$$V_r = \omega a \varepsilon^2 [\qquad f_6 \cos 2\varphi + f_7 \sin 2\varphi]$$

$$f_n = f_n(r) : \quad \text{o.d.e.}$$

- f_3 : aperiodic
  effect on moment M_z

$$\Rightarrow \quad f_3 = -2 f_2$$

$$\bar{V}_\varphi = -\varepsilon V_z |_{\varphi = \frac{\pi}{2}}$$

$O(\varepsilon^2)$ DESPIN MOMENT M_z

$O(\varepsilon)$:

$$M_z = \underset{\sim}{k} \cdot \iiint_R [\underset{\sim}{r} \times (2 \overset{O(\varepsilon)}{\underset{\sim}{\Omega}} \times \overset{O(\varepsilon)}{V_z} \underset{\sim}{k}) \rho \, dR$$

no change

$O(\varepsilon^2)$:

$$M_z' = \iint_S [\underset{\sim}{r} \times \tau_{r\varphi} \underset{\sim}{e}_\varphi] \, dS$$

$\bar{V}_\varphi$, $O(\varepsilon^2)$

$$\Longrightarrow \quad M_z' = M_z$$

since $\bar{V}_\varphi = -\varepsilon V_z \,\Big|_{\varphi = \frac{\pi}{2}}$

EXISTING CODES

Natural variables v_r, v_φ, v_z, p

Vaughn, Oberkampf & Wolfe (1983, 1985)

finite differences $11 \times 24 \times 21$

$10^4 - 10^5$ time steps

22,176 data

6-48 min Cray 1S

$Re \lesssim 100$

Strikwerda & Nagel (1986)

finite differences in r, z

pseudospectral in φ

line SOR

Rosenblat, Gooding & Engleman (1986)

finite elements

$Re \lesssim 1000$

All codes have nearly the same performance:

6-12 hrs / solution on VAX 8600

NAVIER-STOKES SOLVER

- deviation from solid-body rotation is governed by a small parameter

→ good approximation from linear equations

→ few Fourier modes in φ

- low Reynolds number range

→ few Chebyshev modes in r, z

- Spectral collocation method:

$$v_r = \sum_{\ell=1}^{L} \sum_{m=1}^{M} \sum_{n=1}^{N} a_{\ell mn} R_\ell(r)\, \Phi_m(\varphi)\, Z_n\left(\frac{z}{\lambda}\right)$$

similar for v_φ, v_z, p

— symmetries are exploited

— boundary conditions implicitly satisfied by expansion functions

— interior (sine) collocation points to avoid corner problem and spurious pressure terms

SPECTRAL CODE

4 natural variables

$\Longrightarrow$ $\left.\begin{array}{l}\text{linear}\\ \text{nonlinear}\end{array}\right\}$ algebraic system

of dimension $4 \times L \times M \times N$

Gauss elimination +

modified Newton iteration

Typically: $L = M = N = 5$ $\quad 4LMN = 500$

- Rapid convergence (Newton)
- Rapid convergence in φ, r, z
- Semi-analytical solution
- Small data volume
- Extensions
  - stability analysis
  - unsteady problems

- Apollo DN 300 (Cray 1S / 2000)
  - 5-5-5 (500) 90 min
  - 4-3-4 (192) ≈ 3 min

ANALYSIS OF LIQUID MOMENTS

for engineering design!

- quasi-steady motion

A) Navier-Stokes, 3D, nonlinear
   $Re \lesssim 1000$, 5 - 60 sec/solution
   Herbert & Li (spectral code)

B) Boundary layer approximation
   $Re \gtrsim 1000$, ?
   Murphy

C) Perturbation expansion in
   $\varepsilon = \frac{\Omega}{\omega} \sin\theta$ (large $c/a = \eta$)
   all Re, 0.05 sec/solution
   Herbert & Li

D) Spatial eigenfunction expansion
   (linearized, M_x (M_z) only)
   $Re \lesssim 1000$, 10 - 1800 sec/solution
   Hall, Sedney, Gerber

CONCLUSIONS

- results agree at $Re = 1000$ to within a few percent
- linearization in $\varepsilon = \frac{\Omega}{\omega} \sin\theta$ causes small error
- time per solution is acceptable
- time per flight simulation is considerable (1000 solutions)

can we do better ?

Eigenfunction expansion

Governing Equations

- Navier-Stokes equations
- Nutating (aeroballistic) coordinates
- Linearized in $\varepsilon = \dfrac{\Omega}{\omega}\sin\theta$

$$\nabla \cdot \mathbf{v} = 0$$

$$\frac{\partial}{\partial\phi}\mathbf{v} + 2\boldsymbol{\tau} \times \mathbf{v} + \nabla p_d - \frac{1}{Re}\nabla^2\mathbf{v} = -2r\,\tau_r\,\mathbf{e}_k$$

where

$$\nabla^2 = \frac{\partial}{\partial r^2} + \frac{1}{r}\frac{\partial}{\partial r} + \frac{1}{r^2}\frac{\partial^2}{\partial\phi^2} + \frac{\partial^2}{\partial z^2}$$

$$\boldsymbol{\tau} = (\tau_r, \tau_\phi, 1 + \tau_z)\,, \quad \begin{cases} \tau_r = -\dfrac{\Omega}{\omega}\sin\theta\cos\phi \\ \tau_\phi = \dfrac{\Omega}{\omega}\sin\theta\sin\phi \\ \tau_z = \dfrac{\Omega}{\omega}\cos\theta \end{cases}$$

- Take the curl $\nabla \times$ of the momentum equations
- Take the curl $\nabla \times$ of the resulting equations
- Apply $\left(\frac{\partial}{\partial \phi} - \frac{1}{Re}\nabla^2\right)$ to the resulting equations

$$\frac{\partial^2}{\partial \phi^2}\nabla^2 \mathbf{v} - \frac{2}{Re}\frac{\partial}{\partial \phi}\nabla^4 \mathbf{v} + \frac{1}{Re^2}\nabla^6 \mathbf{v} + 4(1+\tau_z)^2\frac{\partial^2 \mathbf{v}}{\partial z^2} = 0$$

- Introduce Fourier series for $\mathbf{v}$

$$\mathbf{v} = \sum_{n=-\infty}^{\infty} \hat{\mathbf{v}}_n(r, z)e^{in\phi}$$

- For the moments, we need only $\hat{v}_{z1}$, $\hat{v}_{\phi 0}$

$$\nabla^2 \hat{v}_z + \frac{2i}{Re}\nabla^4 \hat{v}_z - \frac{1}{Re^2}\nabla^6 \hat{v}_z - 4(1+\tau_z)^2\frac{\partial^2 \hat{v}_z}{\partial z^2} = 0$$

where

$$\nabla^2 = \frac{\partial}{\partial r^2} + \frac{1}{r}\frac{\partial}{\partial r} - \frac{1}{r^2} + \frac{\partial^2}{\partial z^2}$$

Scaled Equations and Boundary Conditions

- Introduce $v_z = \hat{v}_{z\,1}$

$$\tilde{r} = qr \ , \ \tilde{z} = qz$$

$$q^2 = iRe \ , \ q = (1+i)\sqrt{Re/2} \ ,$$

complex, large ?

$$\tilde{\nabla}^2 = \frac{\partial^2}{\partial \tilde{r}^2} + \frac{1}{\tilde{r}}\frac{\partial}{\partial \tilde{r}} - \frac{1}{\tilde{r}^2} + \frac{\partial^2}{\partial \tilde{z}^2}$$

- Governing equation for v_z

$$\tilde{\nabla}^2 v_z - 2\tilde{\nabla}^4 v_z + \tilde{\nabla}^6 v_z - 4(1+\tau_z)^2 \frac{\partial^2 v_z}{\partial \tilde{z}^2} = 0$$

single sixth-order PDE

- Boundary conditions at the ends:

$$v_z = 0$$

$$\frac{\partial v_z}{\partial z} = 0$$

$$-\frac{\partial^3 v_z}{\partial \tilde{z}^3} + 2\tilde{\nabla}_1^2 \frac{\partial^3 v_z}{\partial \tilde{z}^3} + \frac{\partial^5 v_z}{\partial \tilde{z}^5} = 0$$

where

$$\tilde{\nabla}_1^2 = \frac{\partial^2}{\partial \tilde{r}^2} + \frac{1}{\tilde{r}}\frac{\partial}{\partial \tilde{r}} - \frac{1}{\tilde{r}^2}$$

- Boundary conditions at the wall:

$$v_z = 0$$

$$\frac{\partial}{\partial\tilde{r}}(\tilde{\nabla}_1^4 v_z) + 2\frac{\partial}{\partial\tilde{r}}\tilde{\nabla}_1^2\frac{\partial^2 v_z}{\tilde{z}^2} + \frac{\partial^5 v_z}{\partial\tilde{r}\,\partial\tilde{z}^4}$$
$$-\frac{\partial}{\partial\tilde{r}}\tilde{\nabla}_1^2 v_z - \frac{\partial^3 v_z}{\partial\tilde{r}\,\partial\tilde{z}^2} - 2(1+\tau_z)\frac{1}{\tilde{r}}\tilde{\nabla}_1^2 v_z = \frac{2(1+\tau_z)\varepsilon}{iq}$$

$$2(1+\tau_z)[\frac{\partial v_z}{\partial\tilde{r}} - \frac{\partial}{\partial\tilde{r}}\tilde{\nabla}_1^2 v_z - 2\frac{\partial^3 v_z}{\partial\tilde{r}\,\partial\tilde{z}^2} + \frac{1}{\tilde{r}}\frac{\partial v_z}{\partial\tilde{r}}]$$
$$-\frac{1}{\tilde{r}}\tilde{\nabla}_1^2 v_z + \frac{1}{\tilde{r}}\tilde{\nabla}_1^4 v_z + \frac{2}{\tilde{r}}\tilde{\nabla}_1^2\frac{\partial^2 v_z}{\partial\tilde{z}^2} = \frac{2(1+\tau_z)\varepsilon}{iq}$$

where

$$\tilde{\nabla}_1^2 = \frac{\partial^2}{\partial\tilde{r}^2} + \frac{1}{\tilde{r}}\frac{\partial}{\partial\tilde{r}} - \frac{1}{\tilde{r}^2}$$

SPATIAL EIGENFUNCTIONS

Assume $$V_z = W(\tilde{r})\, F(\tilde{z})$$
$$\tilde{\nabla}_1^2 W - BW = 0$$

then $$W(\tilde{r}) = I_1(\sqrt{B}\,\tilde{r})$$
$$F(\tilde{z}) = \sum_{i=1}^{3} c_i \cos a_i \tilde{z}$$

is a solution of the PDE if a_i are roots of

$$a^6 - a^4(3B-2) + a^2[3B^2 - 4B + 1 - 4(1+\tau_z)^2] - (B^3 - 2B^2 + B) = 0$$

The end-wall conditions are satisfied if

$$\begin{aligned}&(a_1^2 - a_2^2)(2B-1-a_1^2-a_2^2)\, a_1 \tan(a_1 q\eta)\, a_2 \tan(a_2 q\eta)\\ &+ (a_2^2 - a_3^2)(2B-1-a_2^2-a_3^2)\, a_2 \tan(a_2 q\eta)\, a_3 \tan(a_3 q\eta)\\ &+ (a_3^2 - a_1^2)(2B-1-a_3^2-a_1^2)\, a_3 \tan(a_3 q\eta)\, a_1 \tan(a_1 q\eta)\\ &= 0\end{aligned}$$

and two of the c_i are properly chosen

Roots $B(a)$, $a_{1n} \approx \dfrac{(2n+1)\pi}{2q\eta}$

$Re = 2$

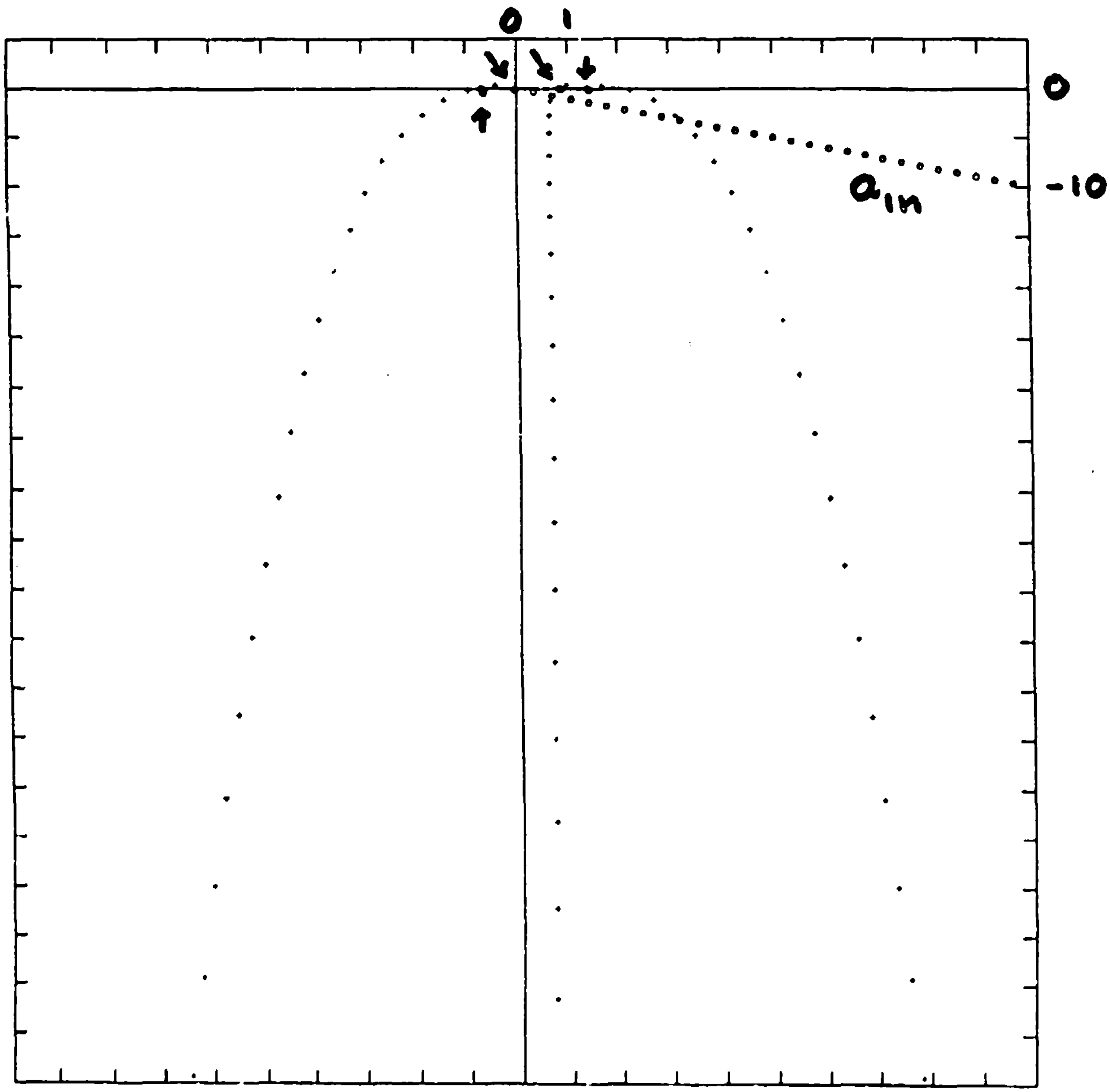

isolated roots $a=0$: $B = 0, 1, 1$

$a_2^2 = a_3^2$ real

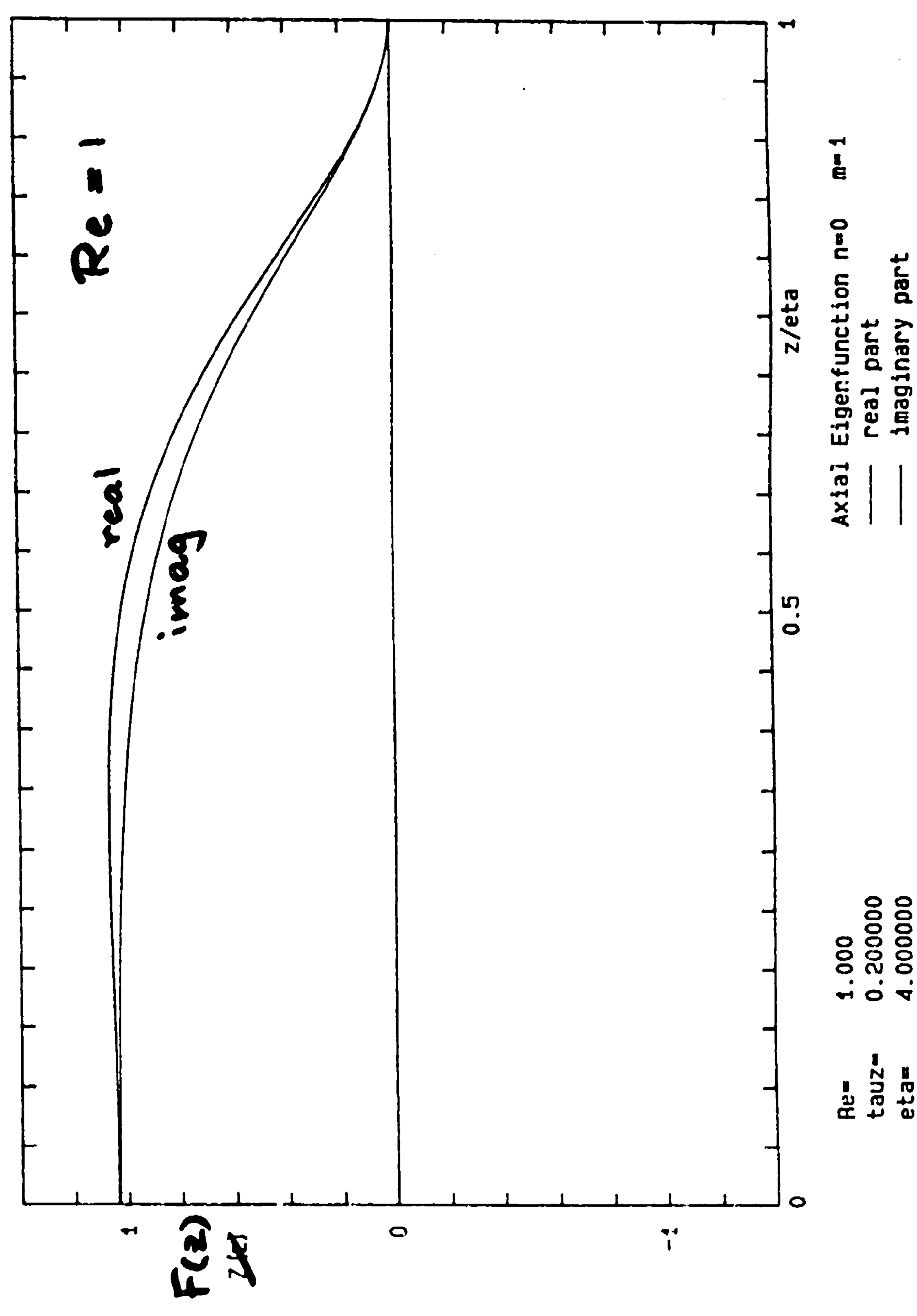
Re = 1
real
imag
F(z)
1
0
-1
0
0.5
1
z/eta
Axial Eigenfunction n=0 m=1
real part
imaginary part
Re= 1.000
tauz= 0.200000
eta= 4.000000

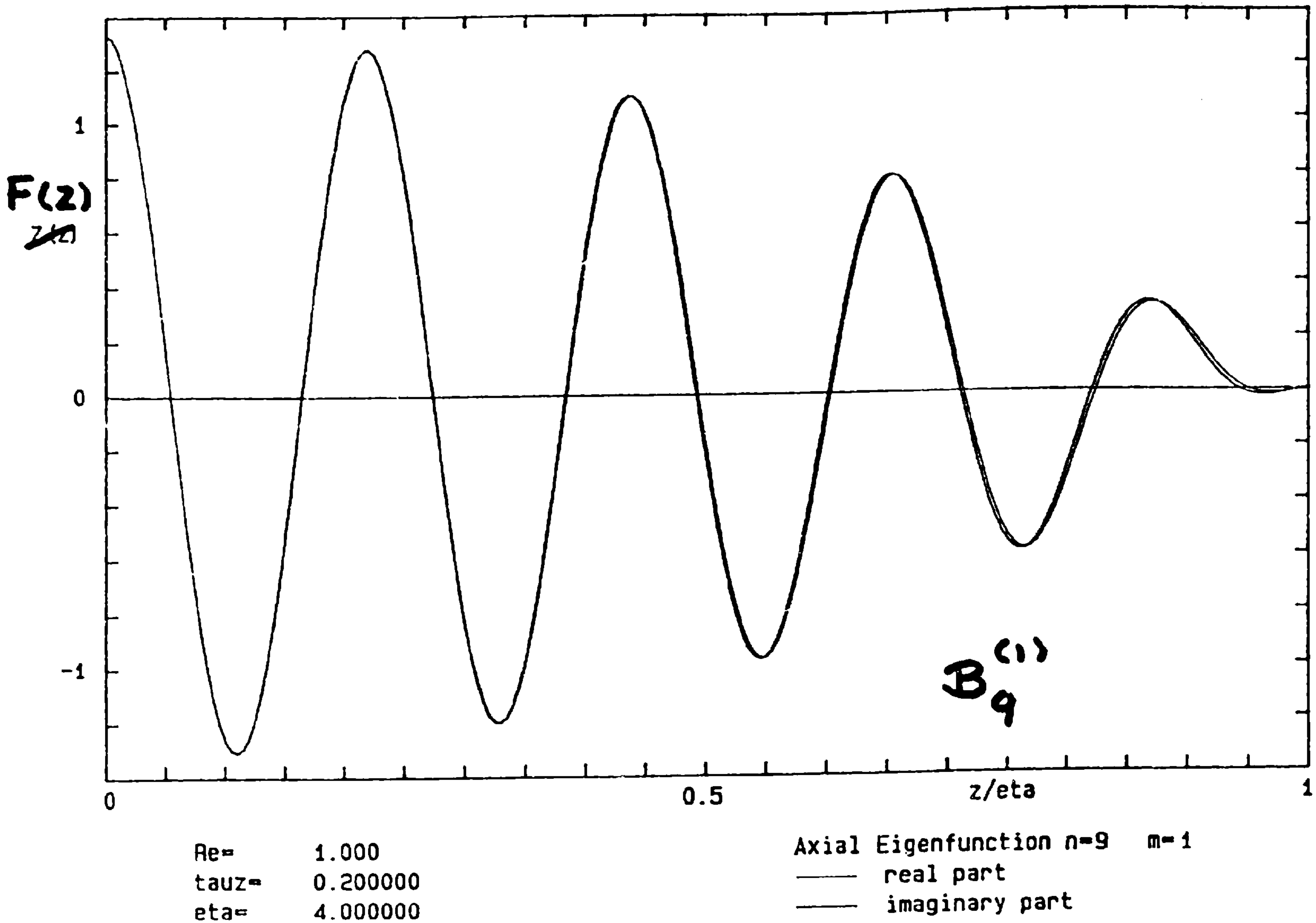
F(z)
~~Z(z)~~
1
0
-1
0
0.5
z/eta
1
$B_9^{(1)}$
Re= 1.000
tauz= 0.200000
eta= 4.000000
Axial Eigenfunction n=9 m=1
real part
imaginary part

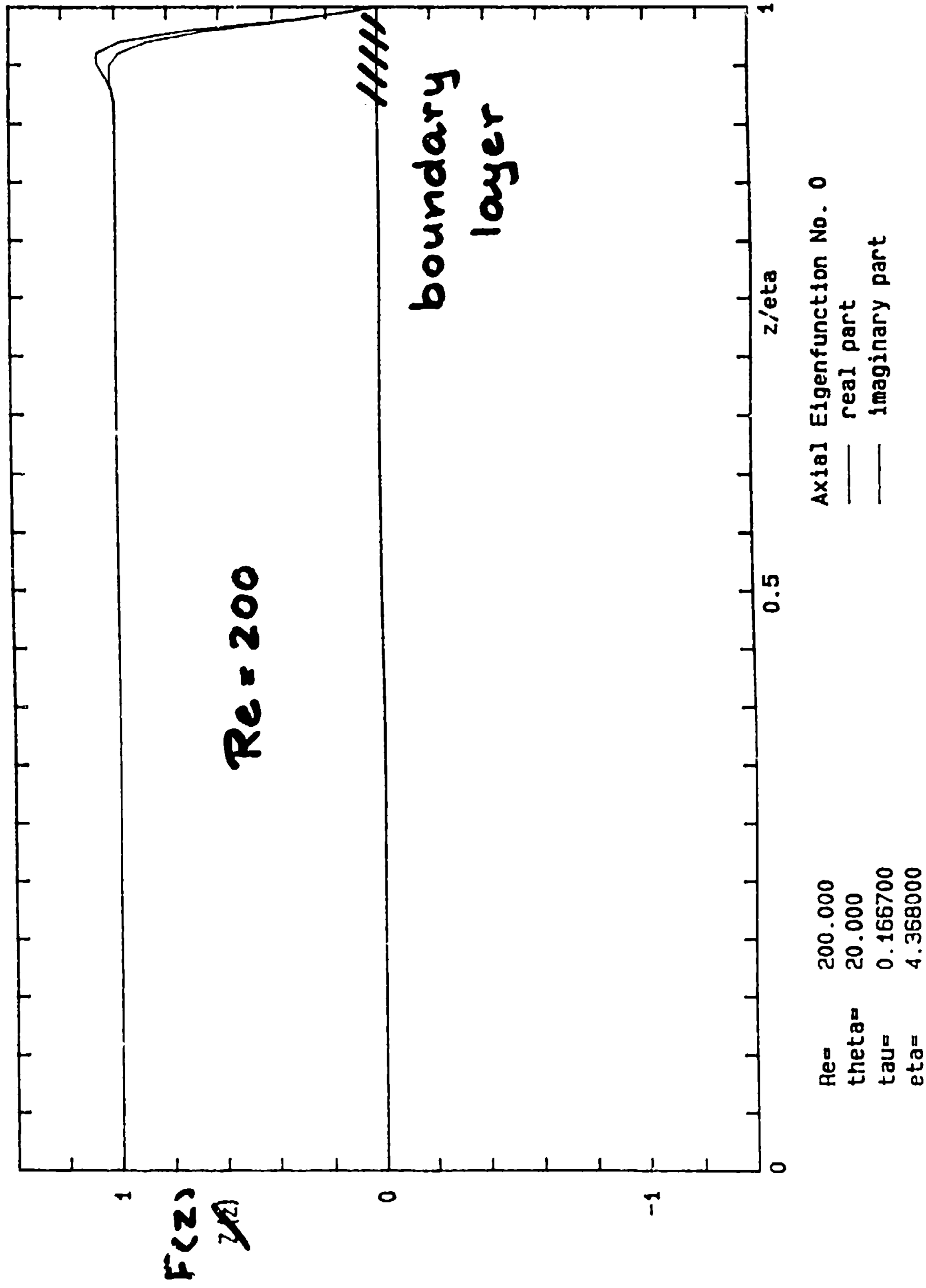

Re = 200
boundary layer
F(z)
z/eta
0
0.5
1
-1
Axial Eigenfunction No. 0
real part
imaginary part
Re= 200.000
theta= 20.000
tau= 0.166700
eta= 4.368000

SERIES SOLUTION FOR v_{z1}

$$v_{z1} = \sum_{n=1}^{N} \sum_{m=1}^{3} \underbrace{A_{nm}} W_{nm}(\tilde{r}) F_{nm}(\tilde{z})$$

$$W_{nm} = I_1(\sqrt{B_n^{(m)}}\,\tilde{r})$$

Determine A_{nm} from boundary conditions on the side wall, $\tilde{r} = q$

1) by collocation method

2) by least squares

CONVERGENCE

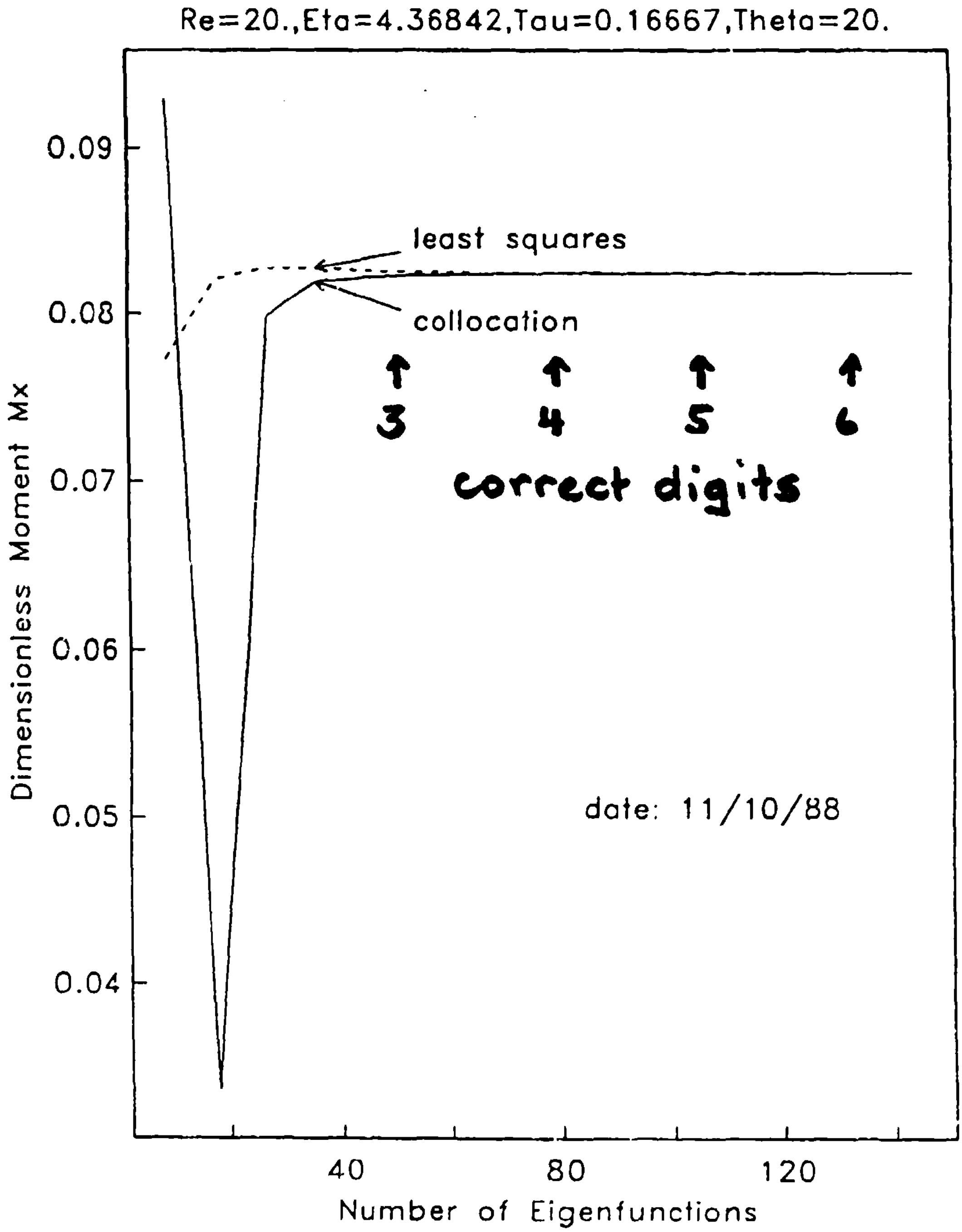

Complete Fill: Roll moment vs. Aspect ratio

$\theta = 2, \tau = 0.083333$

up to 25000

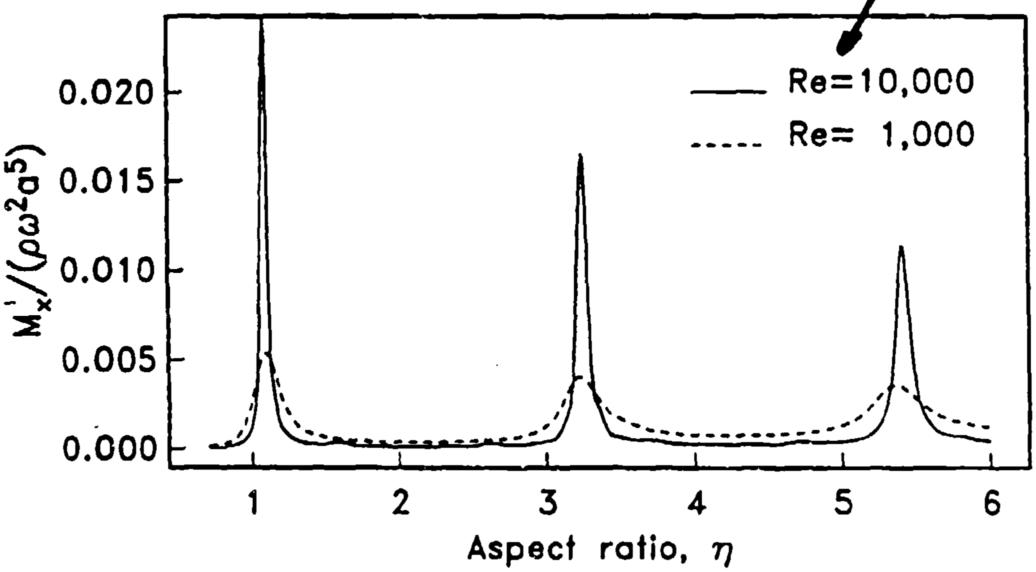

CONCLUSIONS

- The PDE for v_{z1} is a good basis for more efficient moment calculation
- Knowledge of the analytical structure of v_{z1} replaces trial-and-error approach
- Spatial eigenfunctions in z are an alternative to HSG (in r)
- Results of eigenfunction expansion agree with spectral NS results at small ε (linearization)
- Both methods work easily at Re = 100(
- Roots calculated up to Re = 10^6
- Solutions calculated up to Re = 25 000

MOMENTS

- Surface approach (standard):

  $\iint_S$ stresses on inside wall

  pressure

  velocity gradients

  difference of large numbers

- Volume approach:

  $\iiint_V$ Coriolis terms in the fluid

  Rosenblat's relations

  axial & azimuthal velocities

For given fields, the <u>volume</u> approach provides <u>more accurate</u> moments

With the volume approach, estimates for the moments can be obtained from the analytical results

CALCULATION OF MOMENTS

$$M_x = 2\frac{\Omega}{\omega}\cos\theta \int_{-\eta}^{\eta}\int_0^{2\pi}\int_0^1 v_z \underbrace{r^2\cos\varphi}\, dr\, d\varphi\, dz$$

$$M_y = \underbrace{\frac{\Omega}{\omega}}_{\varepsilon}\sin\theta \int_{-\eta}^{\eta}\int_0^{2\pi}\int_0^1 \underline{v_\varphi}\, r^2\, dr\, d\varphi\, dz$$

$$+2\frac{\Omega}{\omega}\cos\theta \int_{-\eta}^{\eta}\int_0^{2\pi}\int_0^1 v_z \underbrace{r^2\sin\varphi}\, dr\, d\varphi\, dz$$

$$M_z = M_x \tan\theta$$

Let $\underset{\sim}{v}(r,\varphi,z) = \sum_{n=-\infty}^{\infty} \hat{\underset{\sim}{v}}_n(r,z)\, e^{in\varphi}$

then we need only

$$v_{z1}(r,z),\quad \underbrace{v_{\varphi 0}(r,z)}_{\text{small effect}}$$

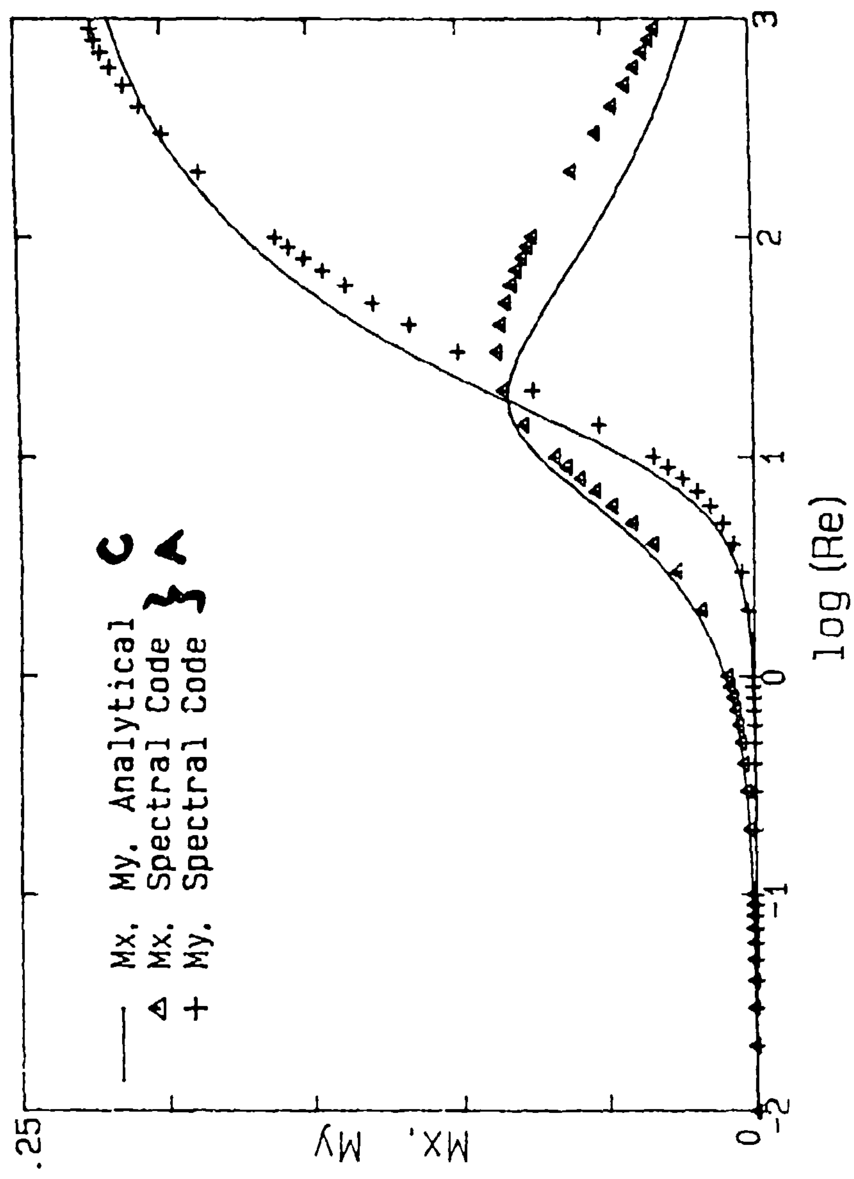

Mx. My. Analytical C
Mx. Spectral Code A
My. Spectral Code
.25
0
Mx, My
-2
-1
0
1
2
3
log (Re)

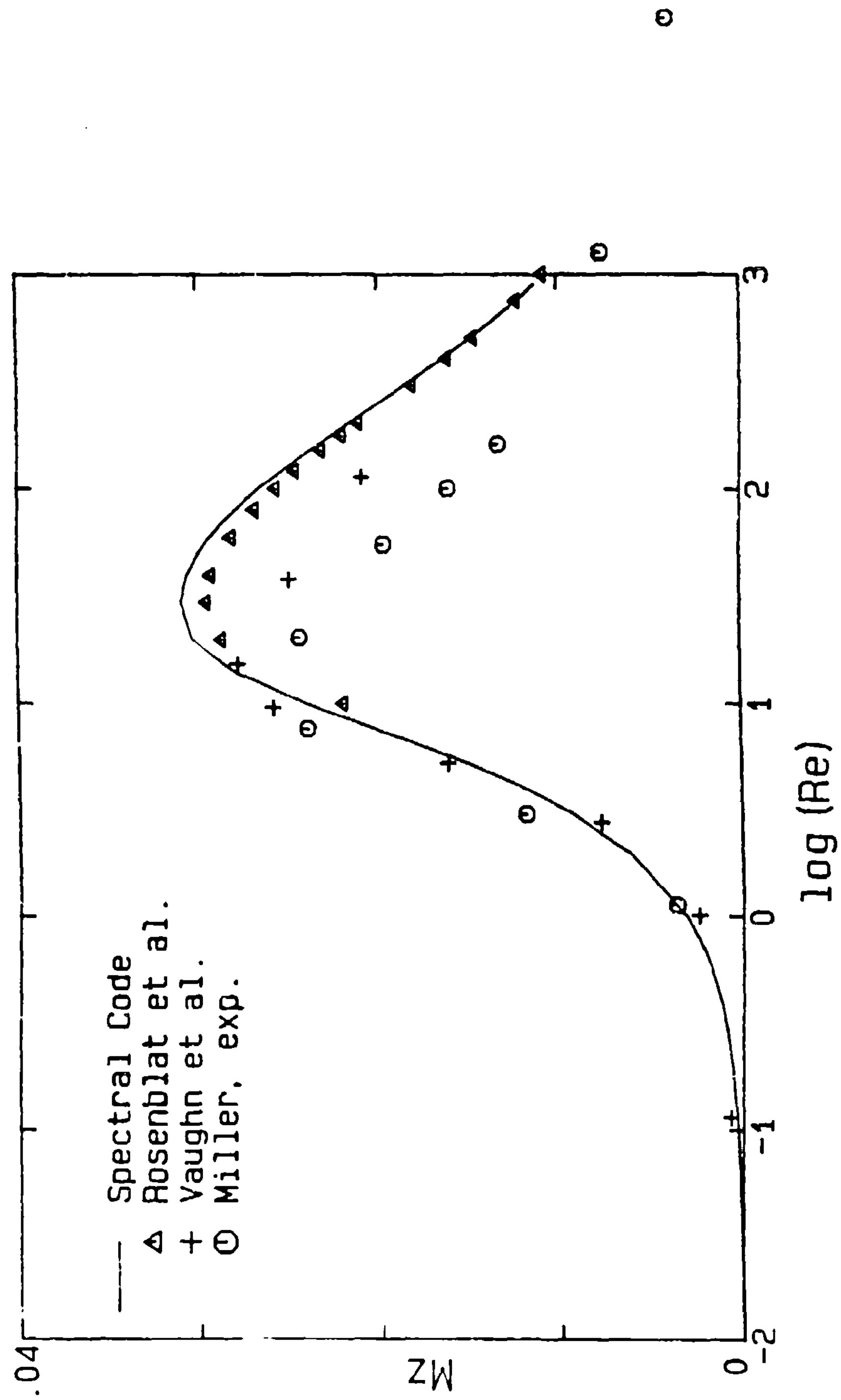
Spectral Code
Rosenblat et al.
Vaughn et al.
Miller, exp.
Mz
.04
0
log (Re)
-2
-1
0
1
2
3

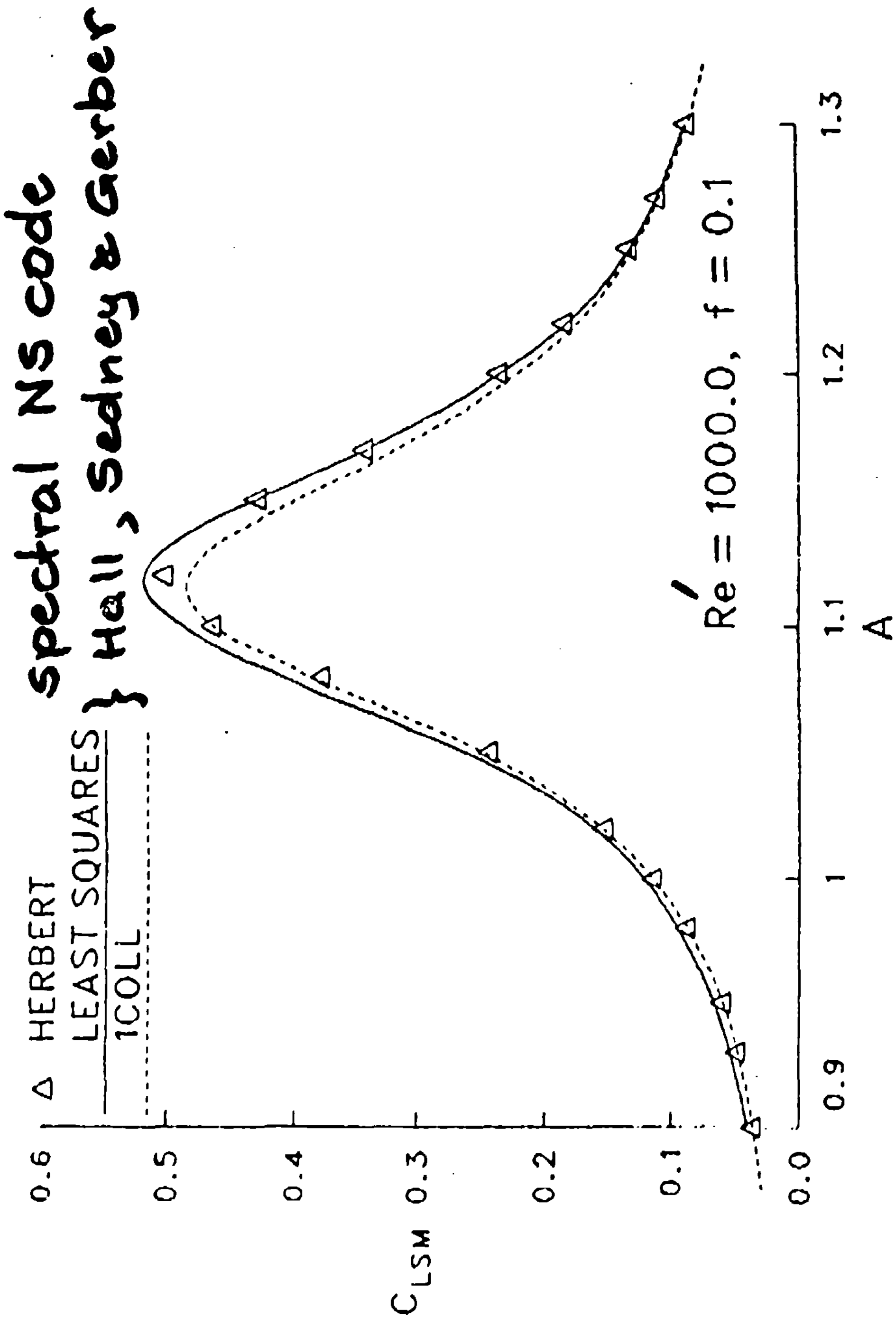

Δ HERBERT
LEAST SQUARES
1COLL
spectral NS code
} Hall, Sedney & Gerber
C_{LSM}
0.6
0.5
0.4
0.3
0.2
0.1
0.0
0.9
1
1.1
1.2
1.3
A
Re = 1000.0, f = 0.1

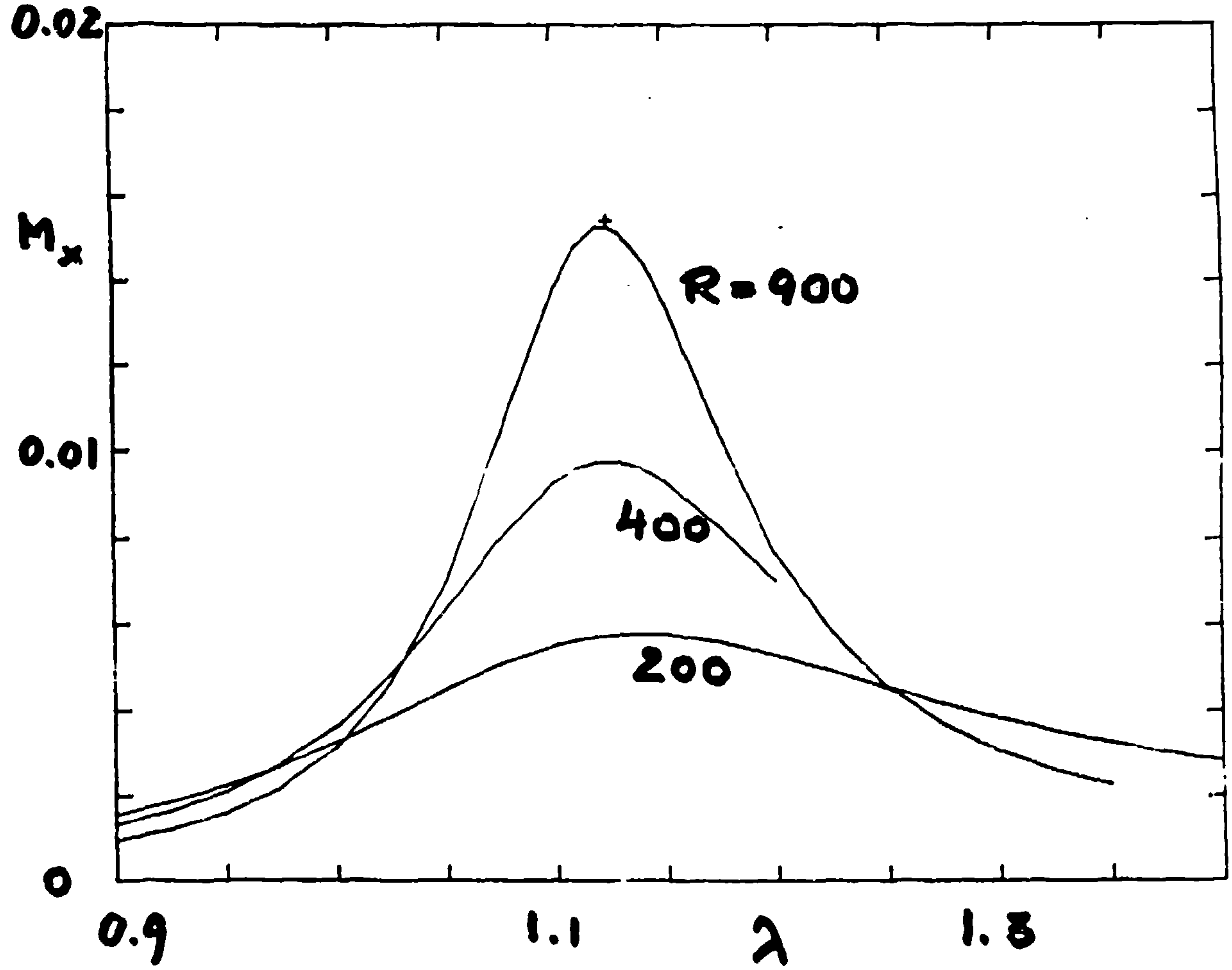

Resonance with inertial waves

FLIGHT INSTABILITIES:

- Resonance with inertial waves (high Reynolds number)
- Viscous secondary flow (medium Reynolds number)

FLIGHT SIMULATION:

Vaughn, Wolfe, Oberkampf 1985

shell data
aerodynamic data (table)
payload data
liquid moments (table)
launch data

integration 30-100s, $\Delta t = 2 \cdot 10^{-5}$ s

Trajectory

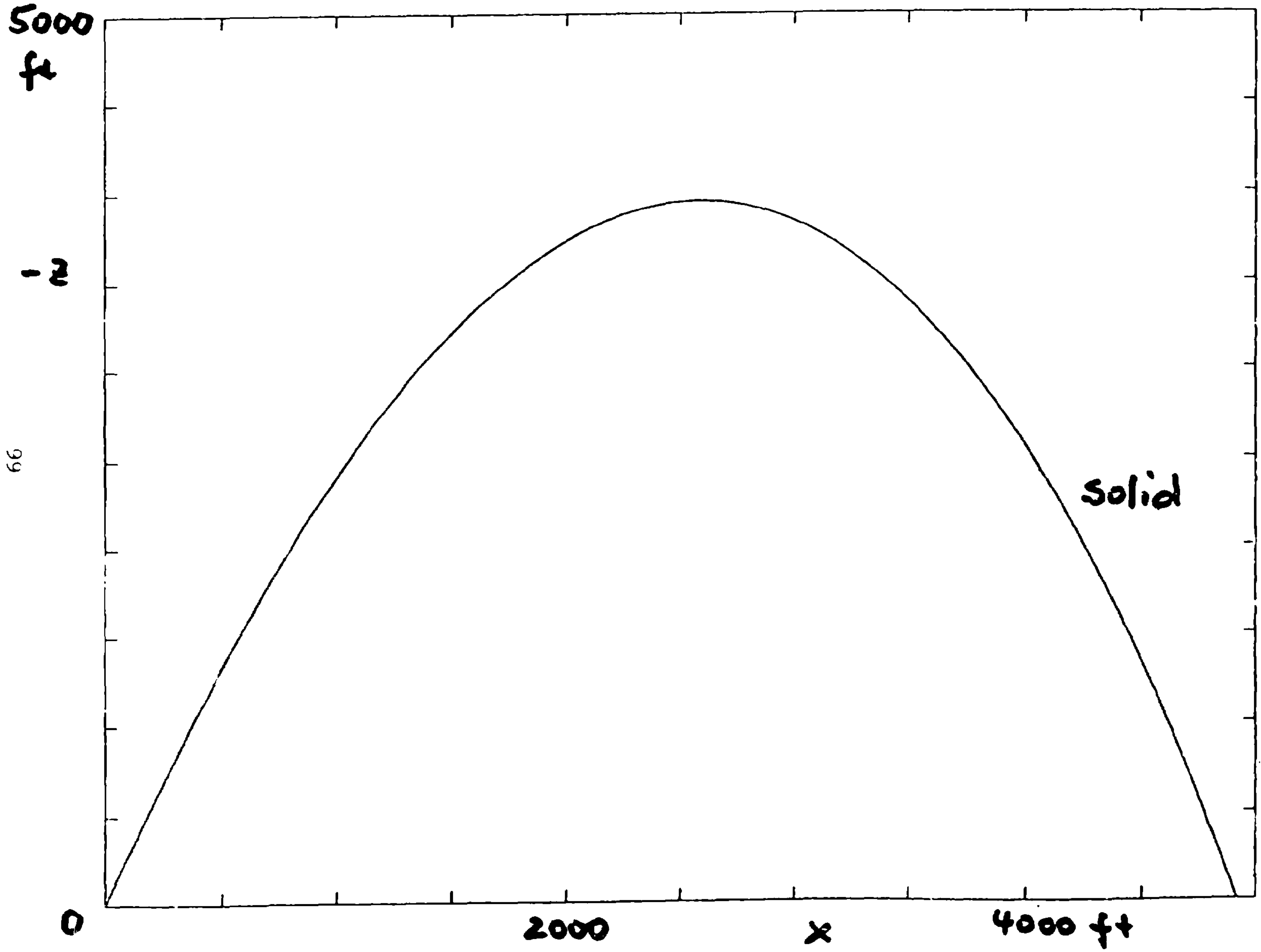

Trajectory, $r = -3$

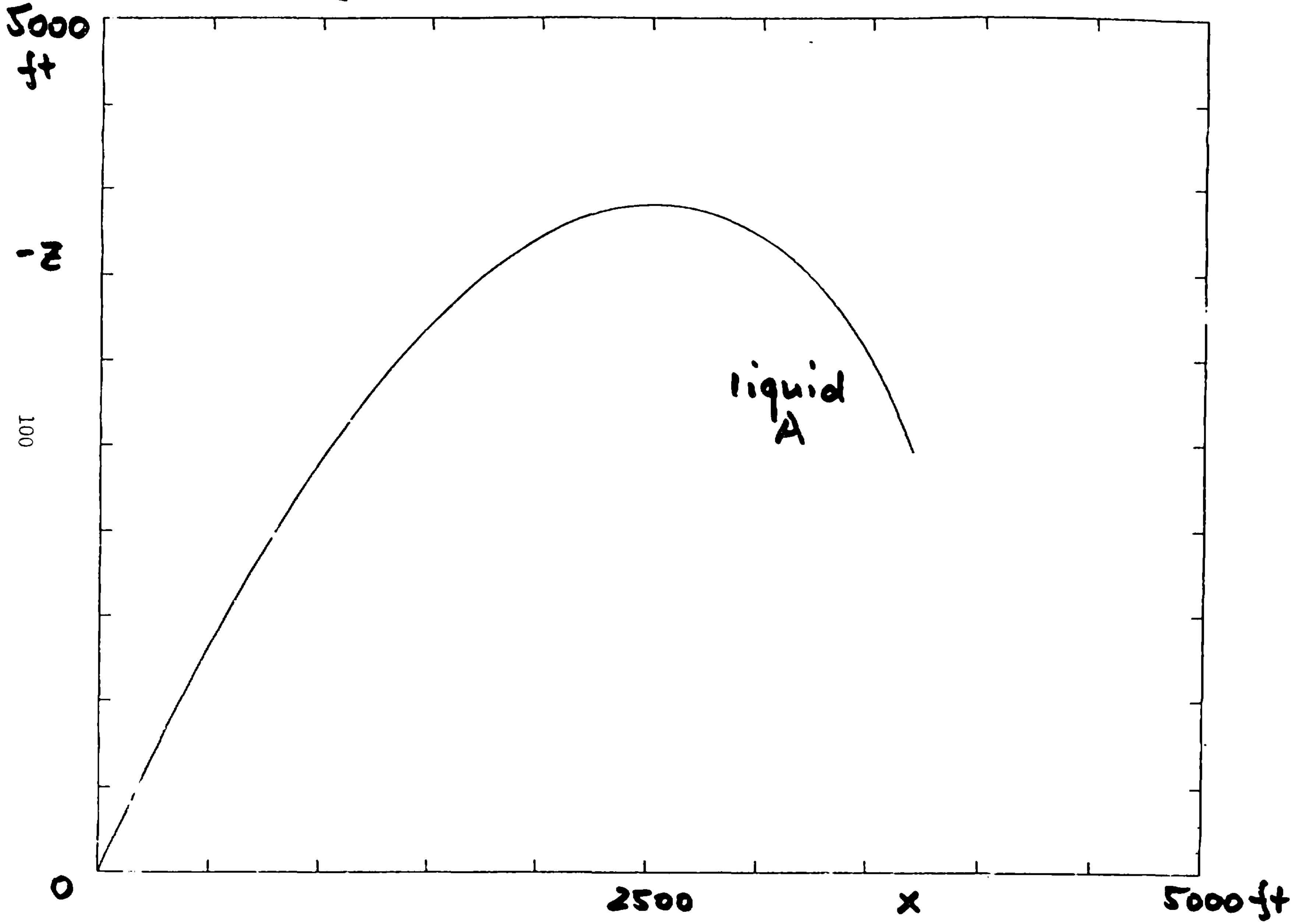

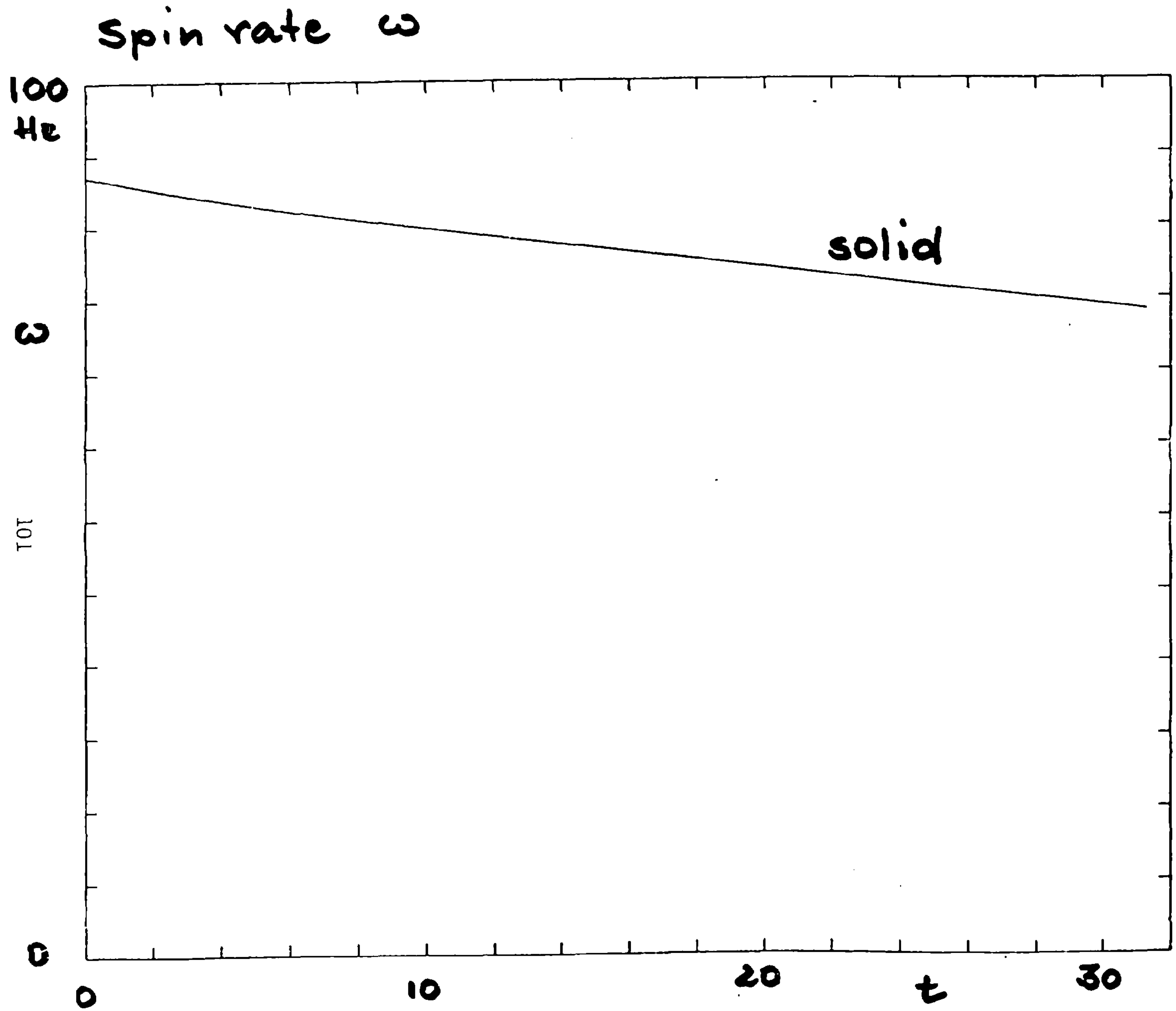
Spin rate ω
100
He
ω
0
solid
0
10
20
t
30

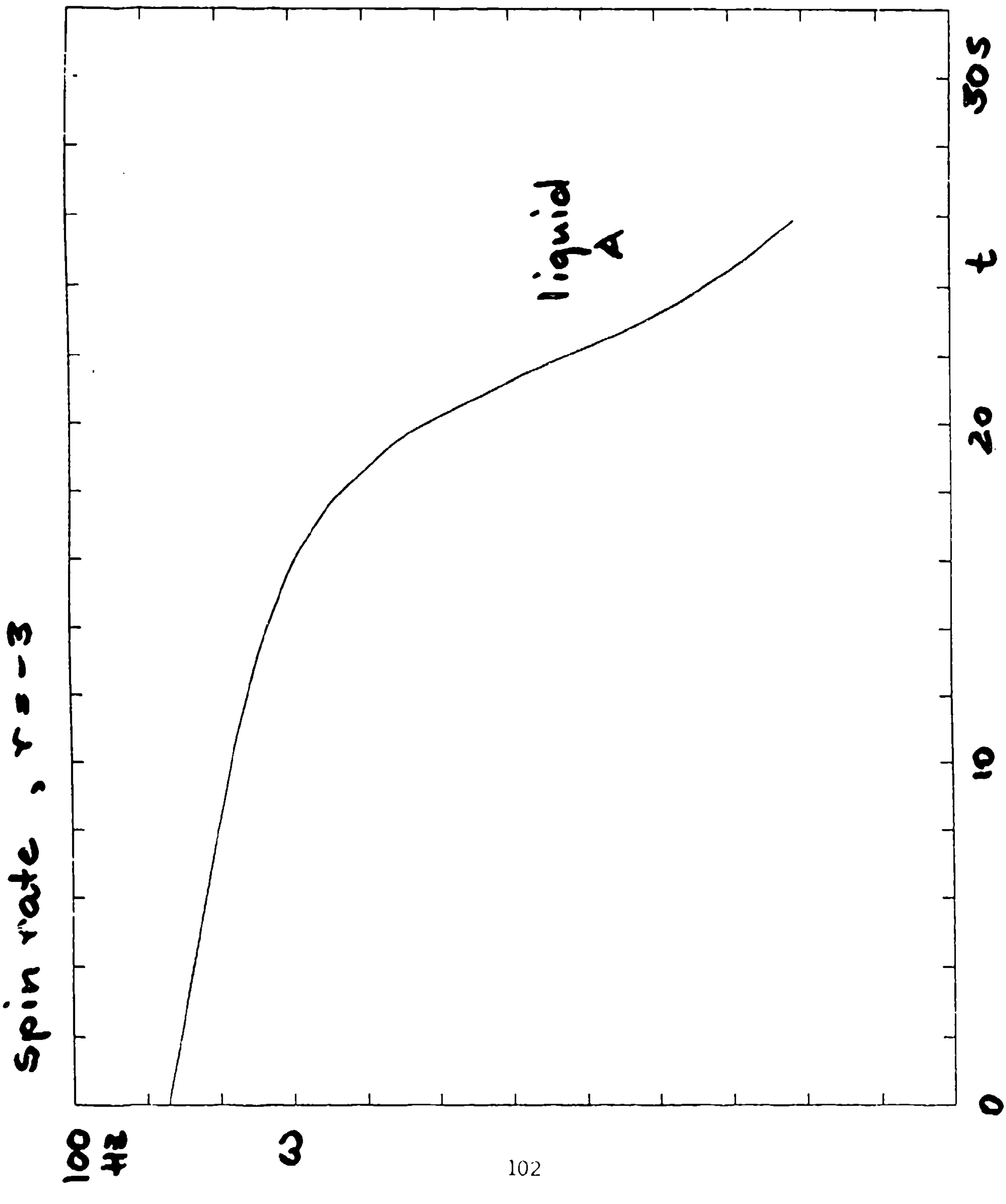

spin rate , r = -3
liquid A
100 Hz
3
0
10
20
30 s
t

FLIGHT SIMULATION: Angle of attack

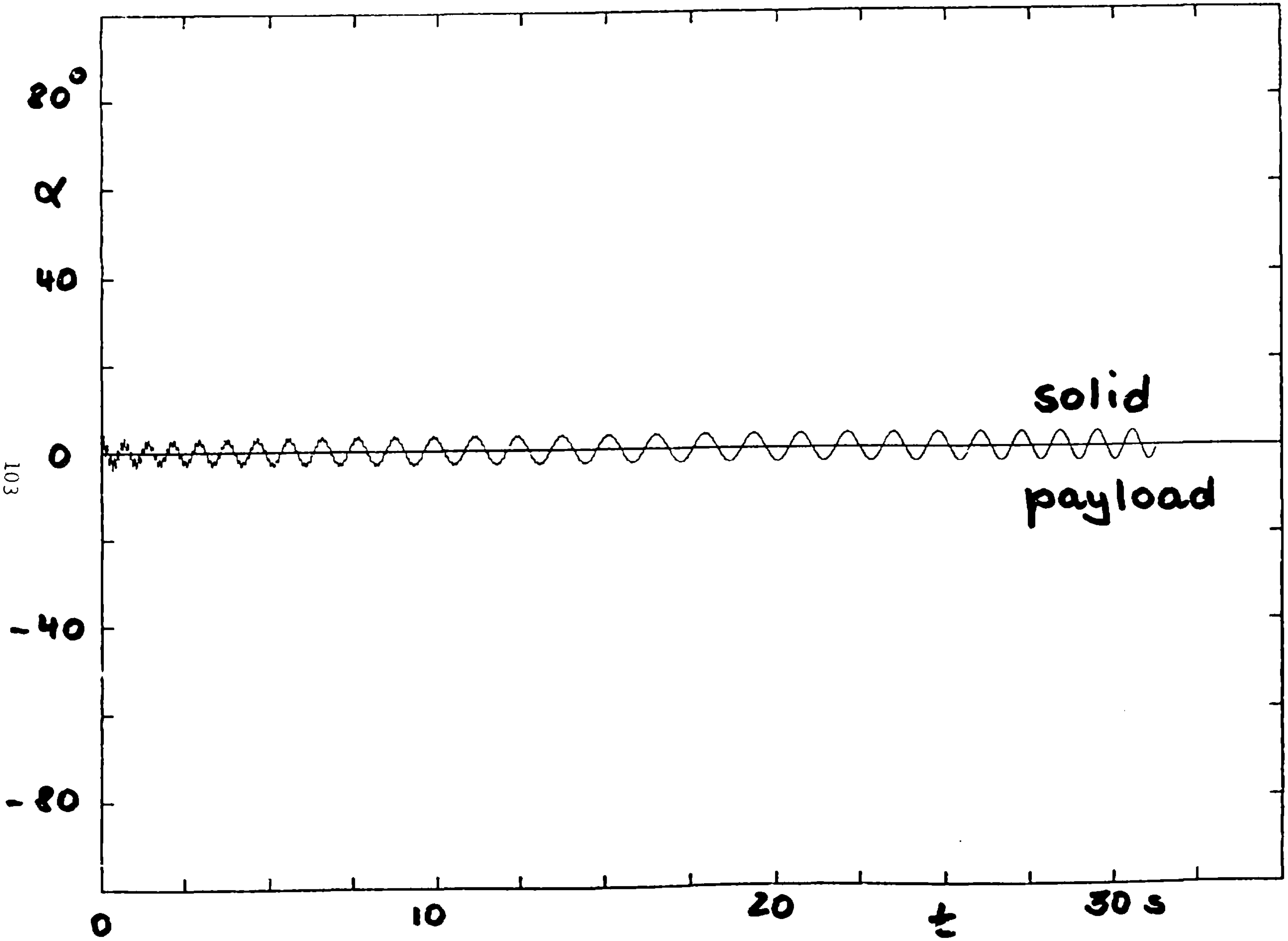

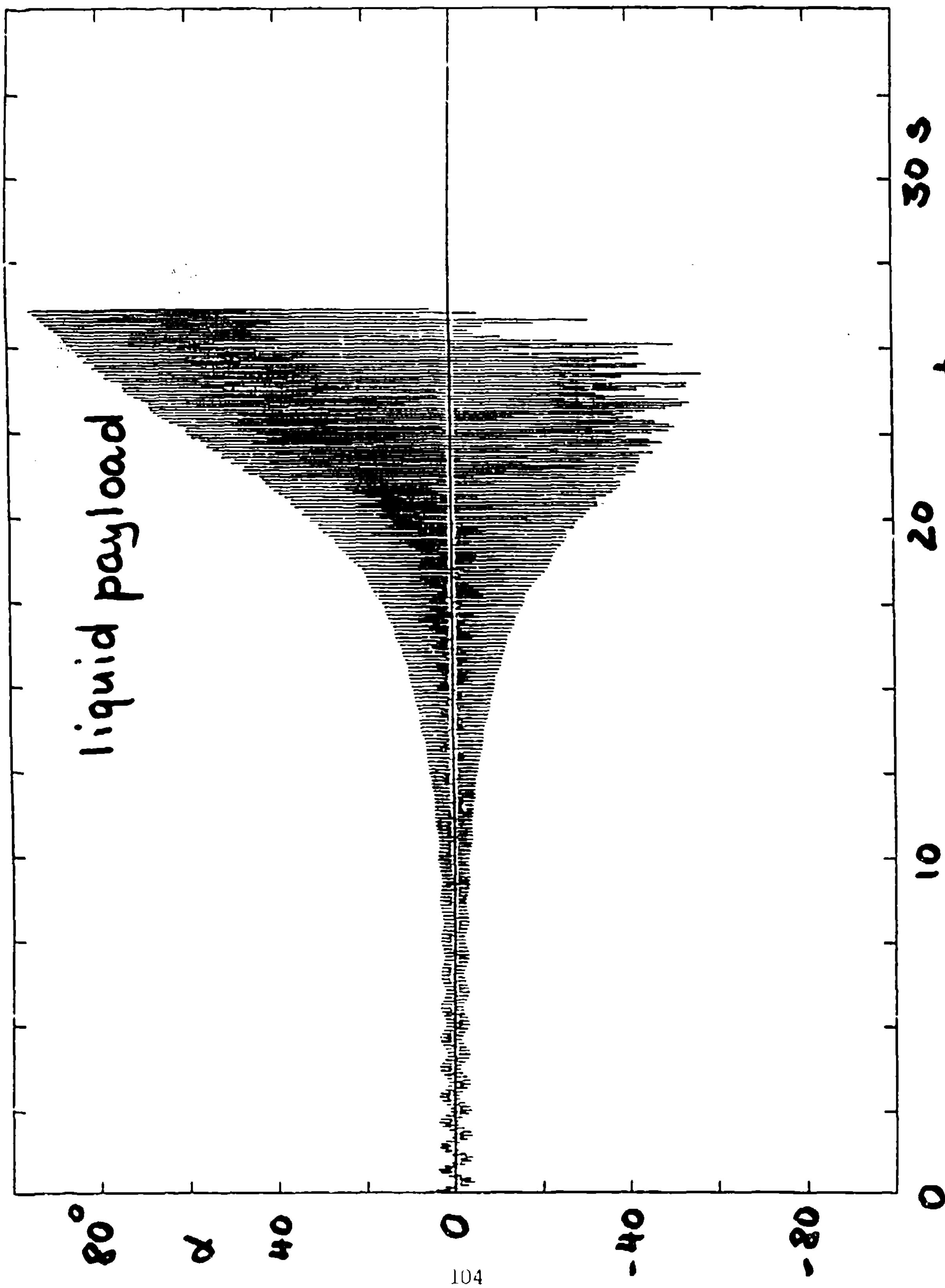
liquid payload
80°
α
40
0
-40
-80
0
10
20
t
30 s

EXPERIMENTAL STUDIES

Goal: Show feasibility of flow visualizations in a properly scaled model

Restrictions: low cost ($\leq$ \$500)
use available equipment
utilize "cheap" labor

⇒ Senior Student Project:
David Pierpont

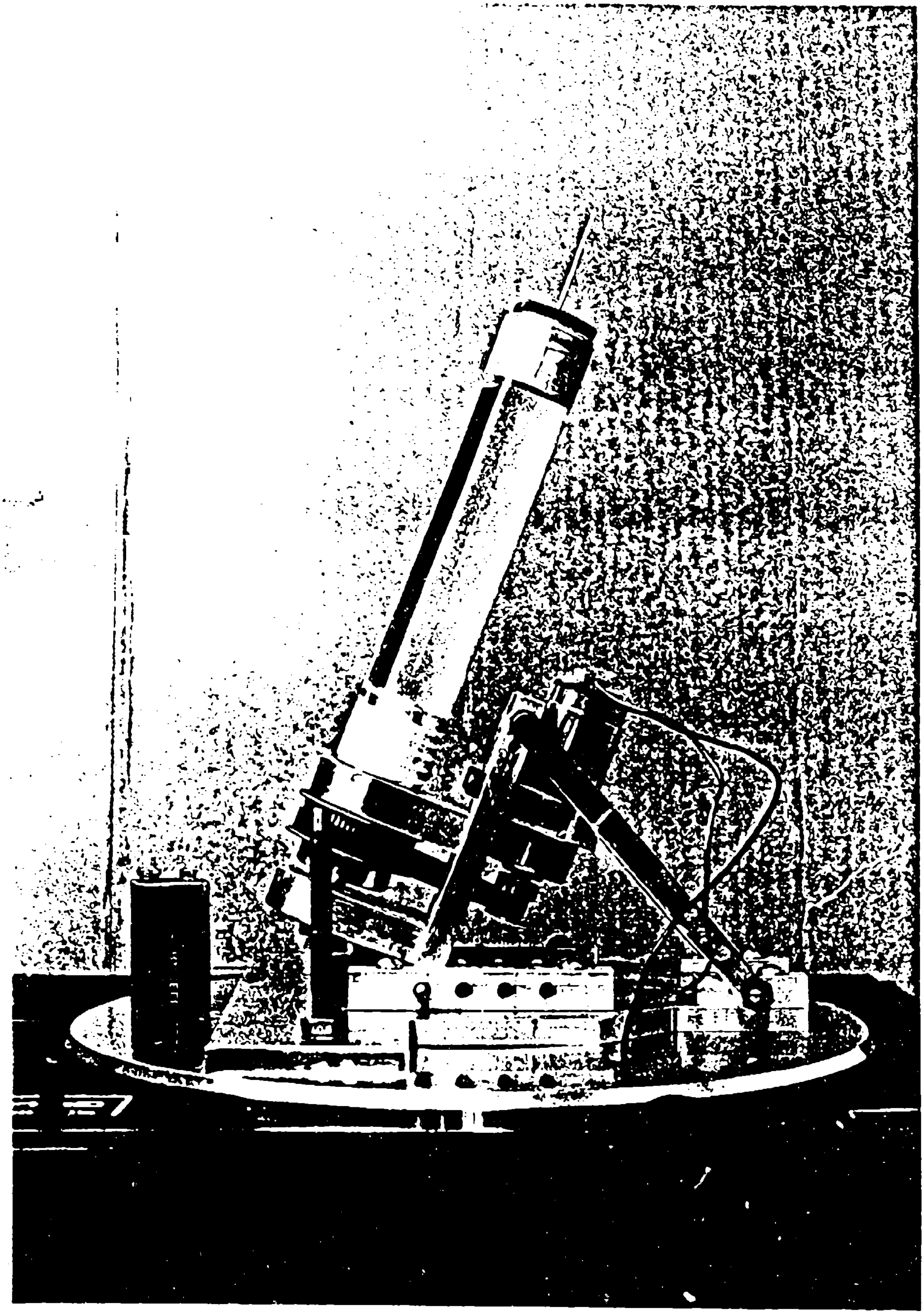

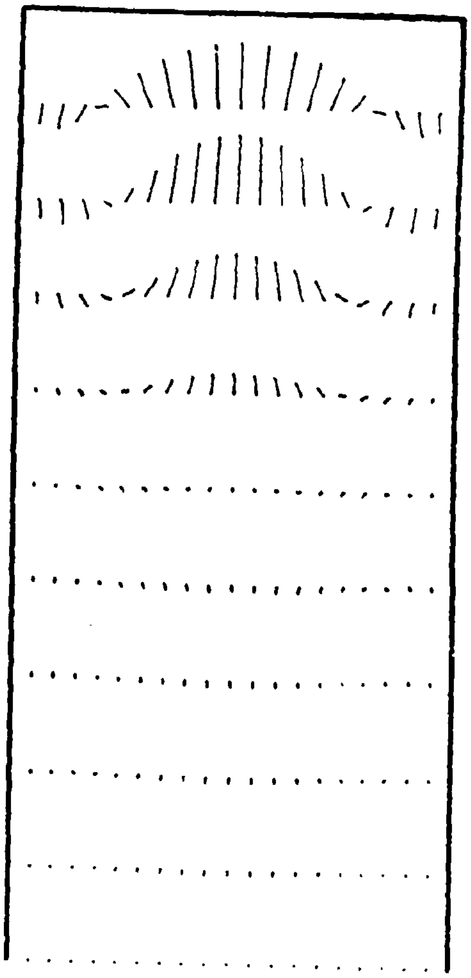

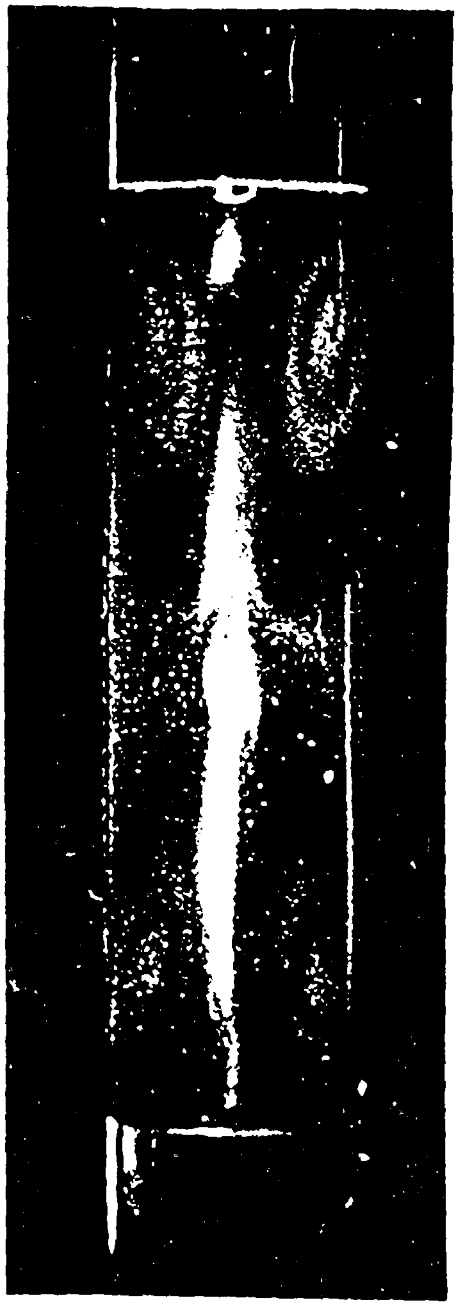

Mean

Re ≈ 30

NSY_5 / NSY_1 Velocity Field - Type 0

Re=	20.000	Cut at Phi= 0	
Theta=	20.000	Scale: ——	0.00200
Tau=	0.1667	Points:	6 radial
Lambda=	4.3680		5 azimuthal
			8 axial

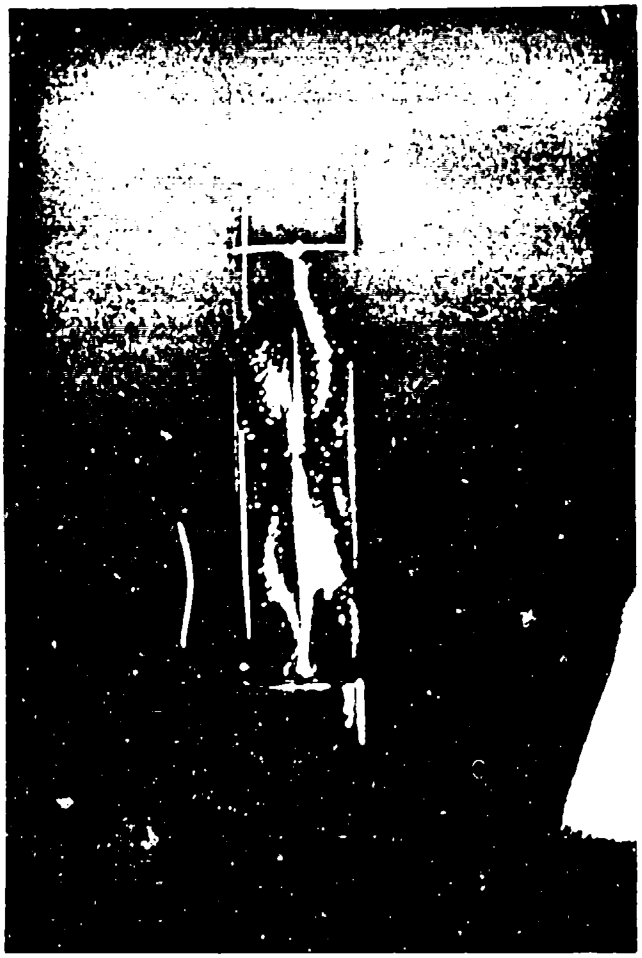
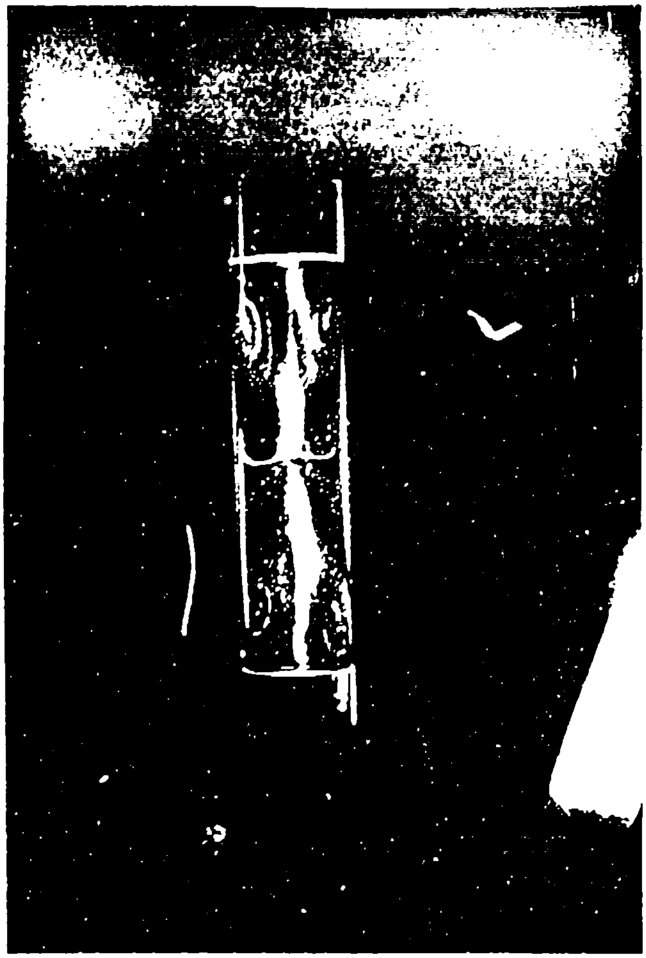

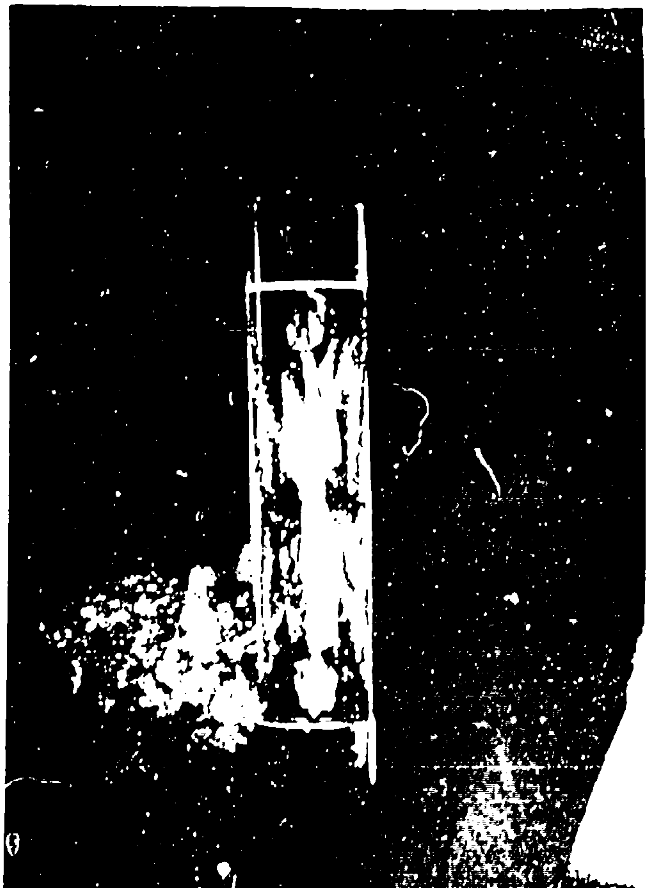

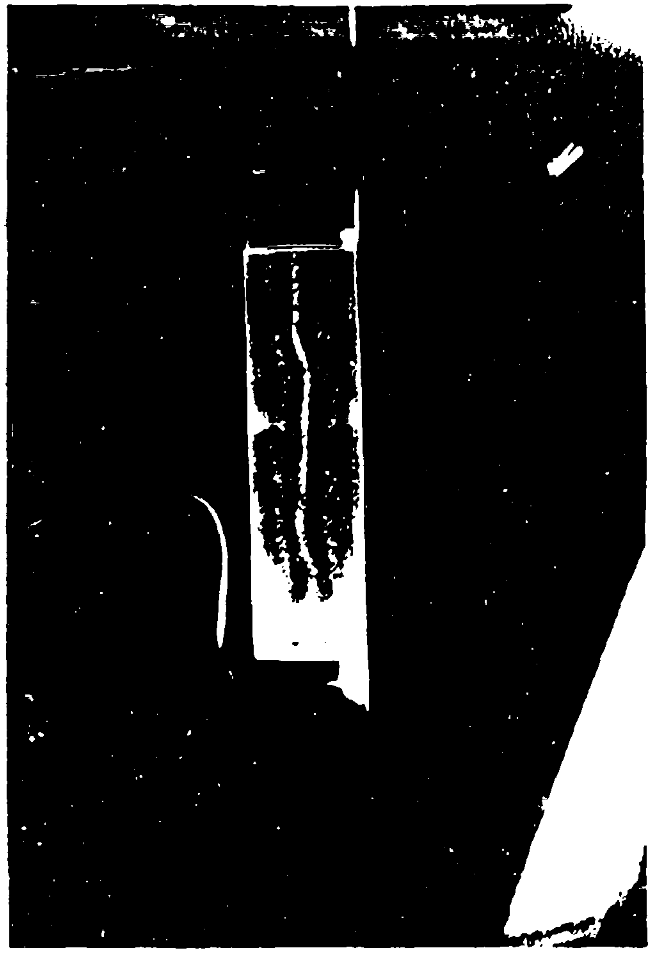

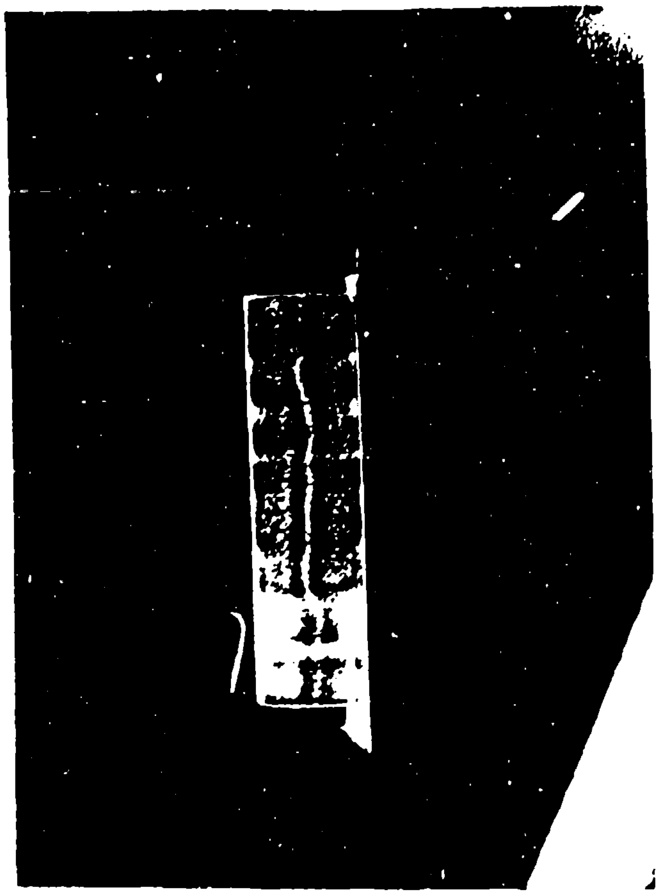

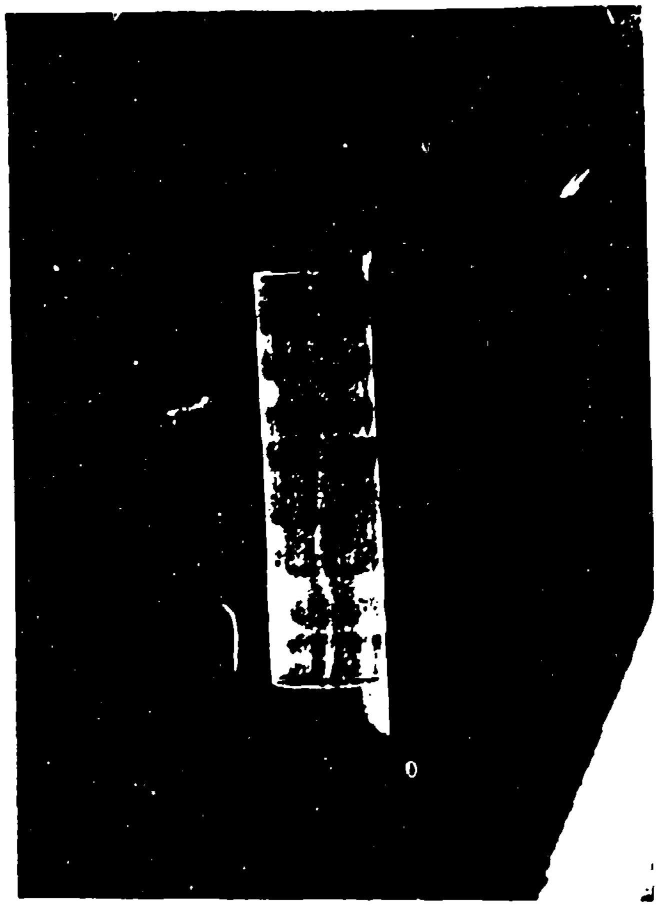

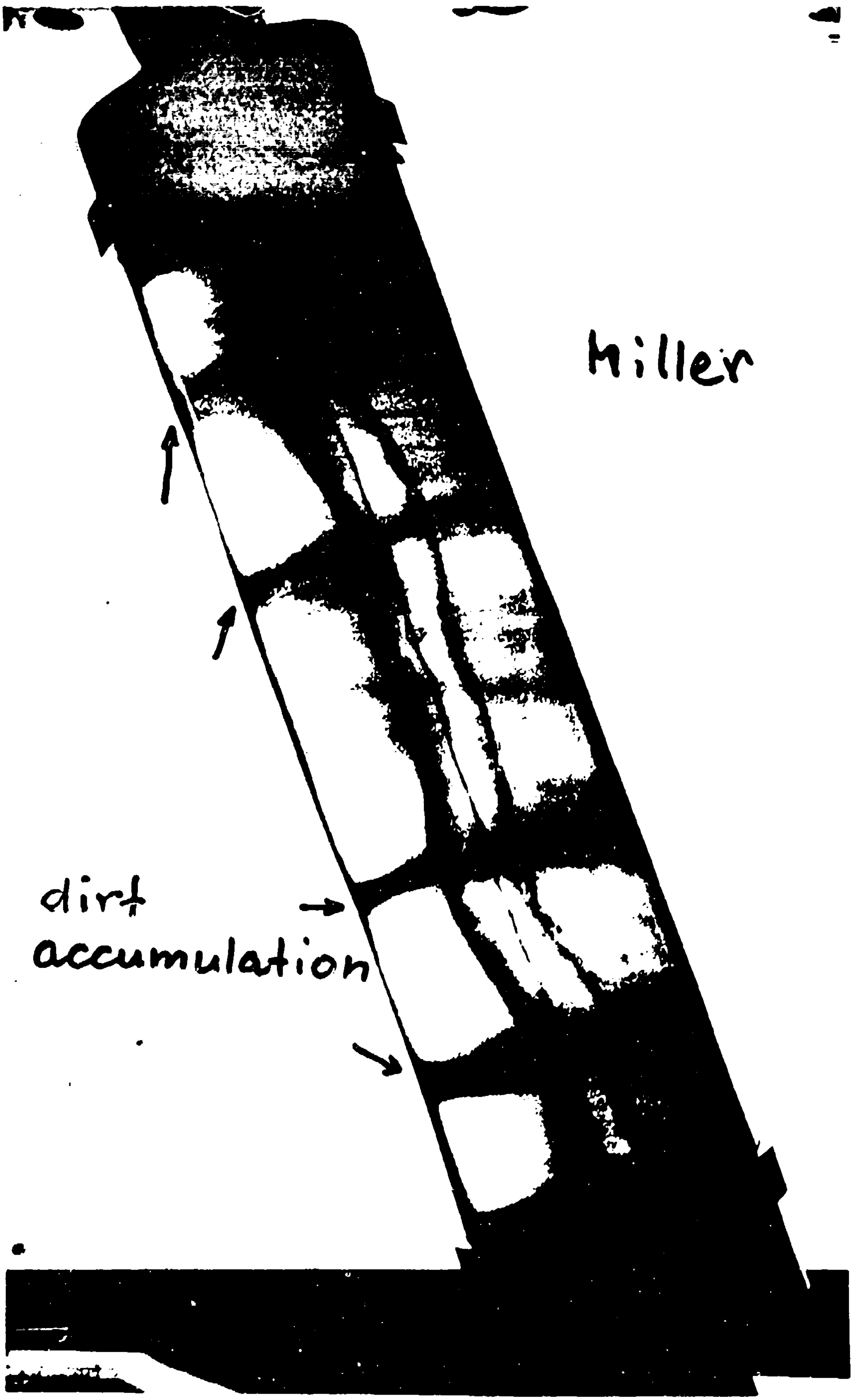
Miller
dirt
accumulation

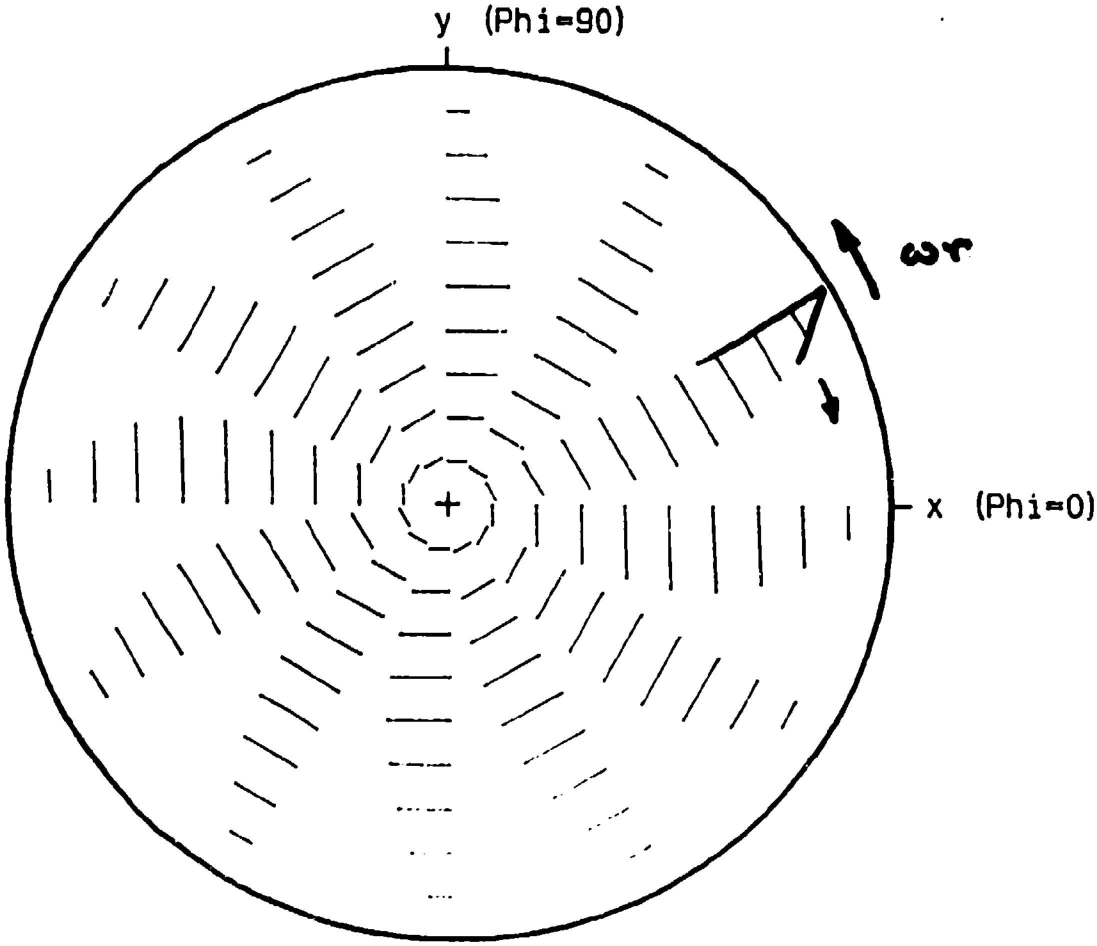

NSY_5 / NSY_1 Velocity Field - Type 0

Re=	20.000	Cut at z= 0.000	
Theta=	20.000	Scale: —— 0.00300	
Tau=	0.1667	Points:	6 radial
Lambda=	4.3680		5 azimuthal
			8 axial

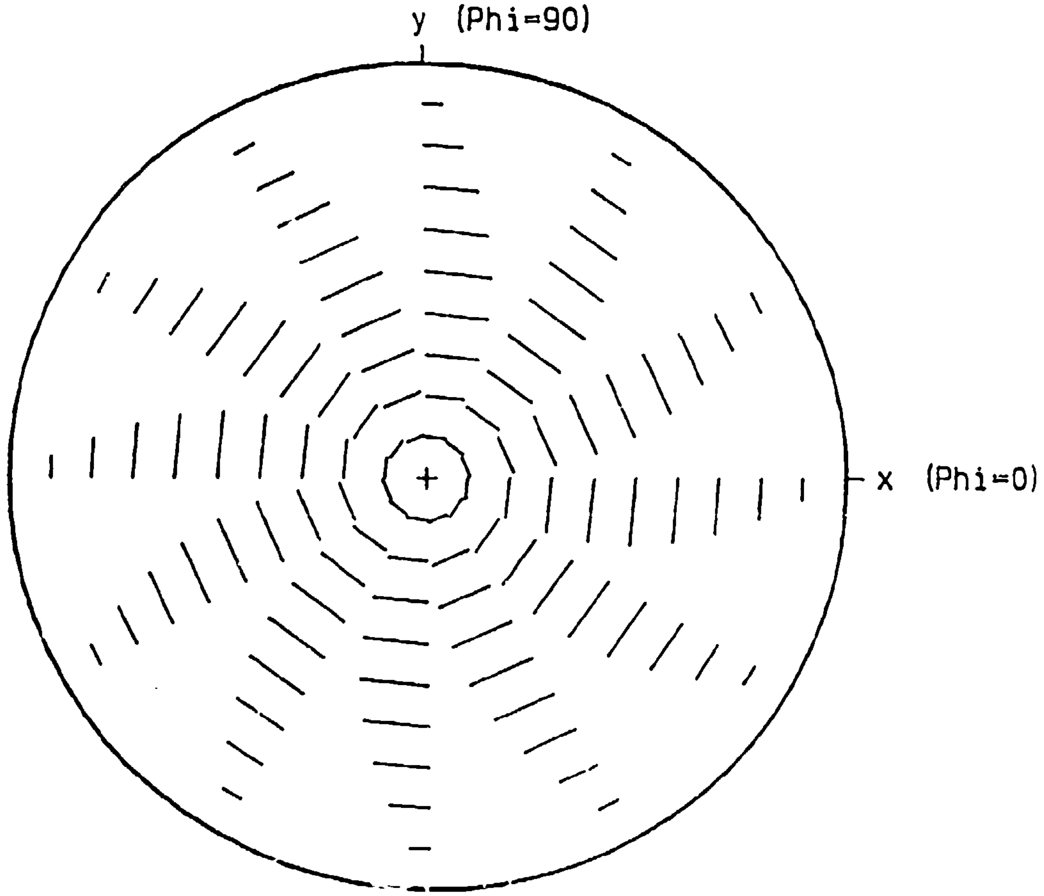

NSS (Sym.) Mean Velocity Field

Re=	14.950	Cut at z=	0.800
Theta=	20.000	Scale:	——— 0.00250
Tau=	0.1667	Points:	5 radial
Lambda=	4.3684		5 azimuthal
			5 axial

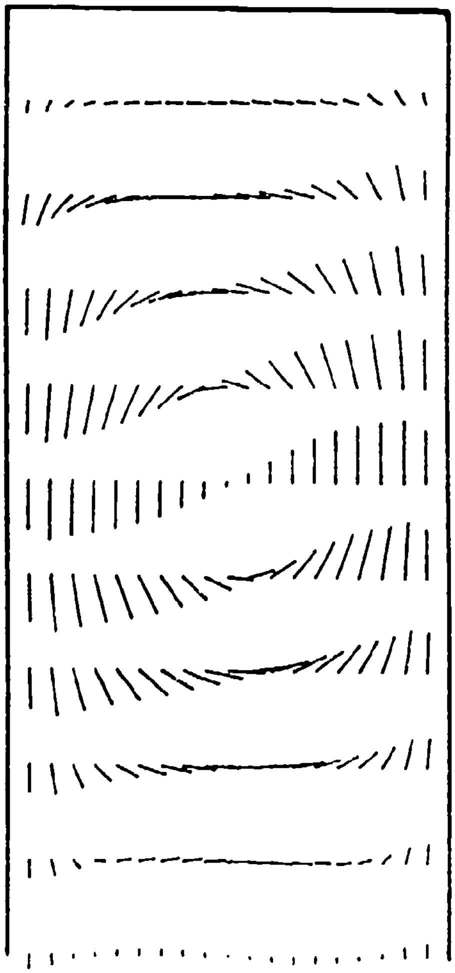

NSY_5 / NSY_1 Velocity Field - Type 0

Re=	300.000	Cut at Phi= 90	
Theta=	20.000	Scale: ———	0.20000
Tau=	0.1667	Points:	6 radial
Lambda=	4.3680		5 azimuthal
			8 axial

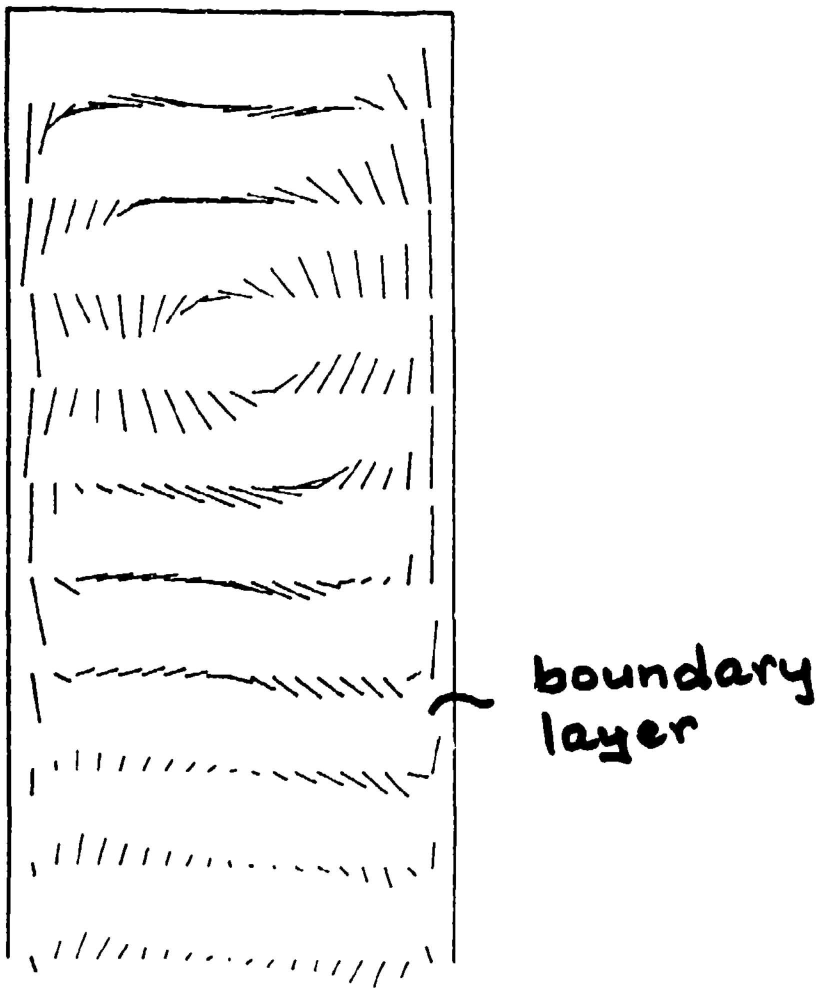

NSY_5 / NSY_1 Velocity Field - Type 0

Re=	300.000	Cut at Phi= 0	
Theta=	20.000	Scale: ——	0.05000
Tau=	0.1667	Points:	6 radial
Lambda=	4.3680		5 azimuthal
			8 axial

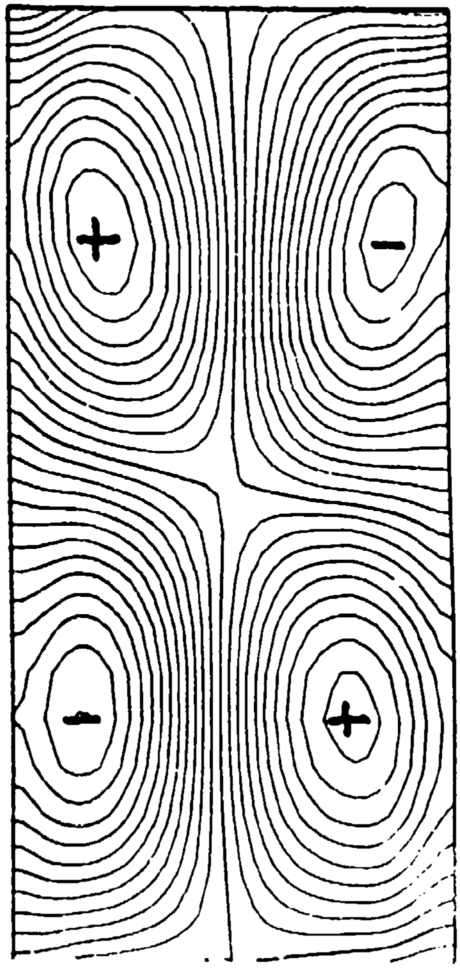

NSY_5 / NSY_1 Pressure Field - Type 0

Re=	300.000	Cut at Phi= 0	
Theta=	20.000	Levels:	0.00500
Tau=	0.1667	Points:	6 radial
Lambda=	4.3680		5 azimuthal
			8 axial

Miller 1982

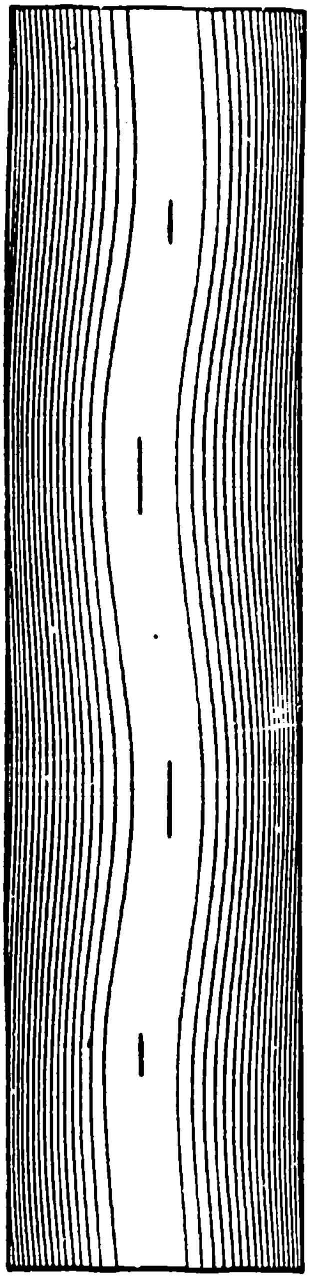

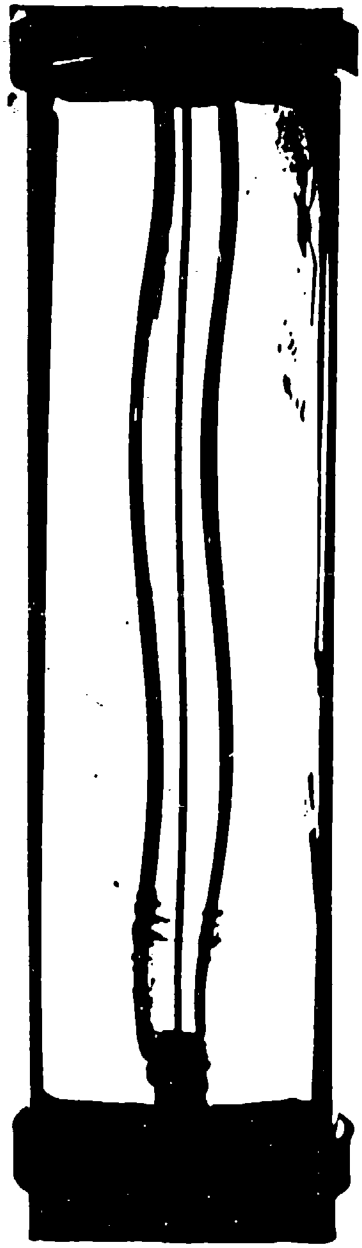

Total

NSY_5 / NSY_1 Pressure Field - Type 0

Re=	300.000	Cut at Phi= 0	
Theta=	20.000	Levels:	0.04000
Tau=	0.1667	Points:	6 radial
Lambda=	4.3680		5 azimuthal
			8 axial

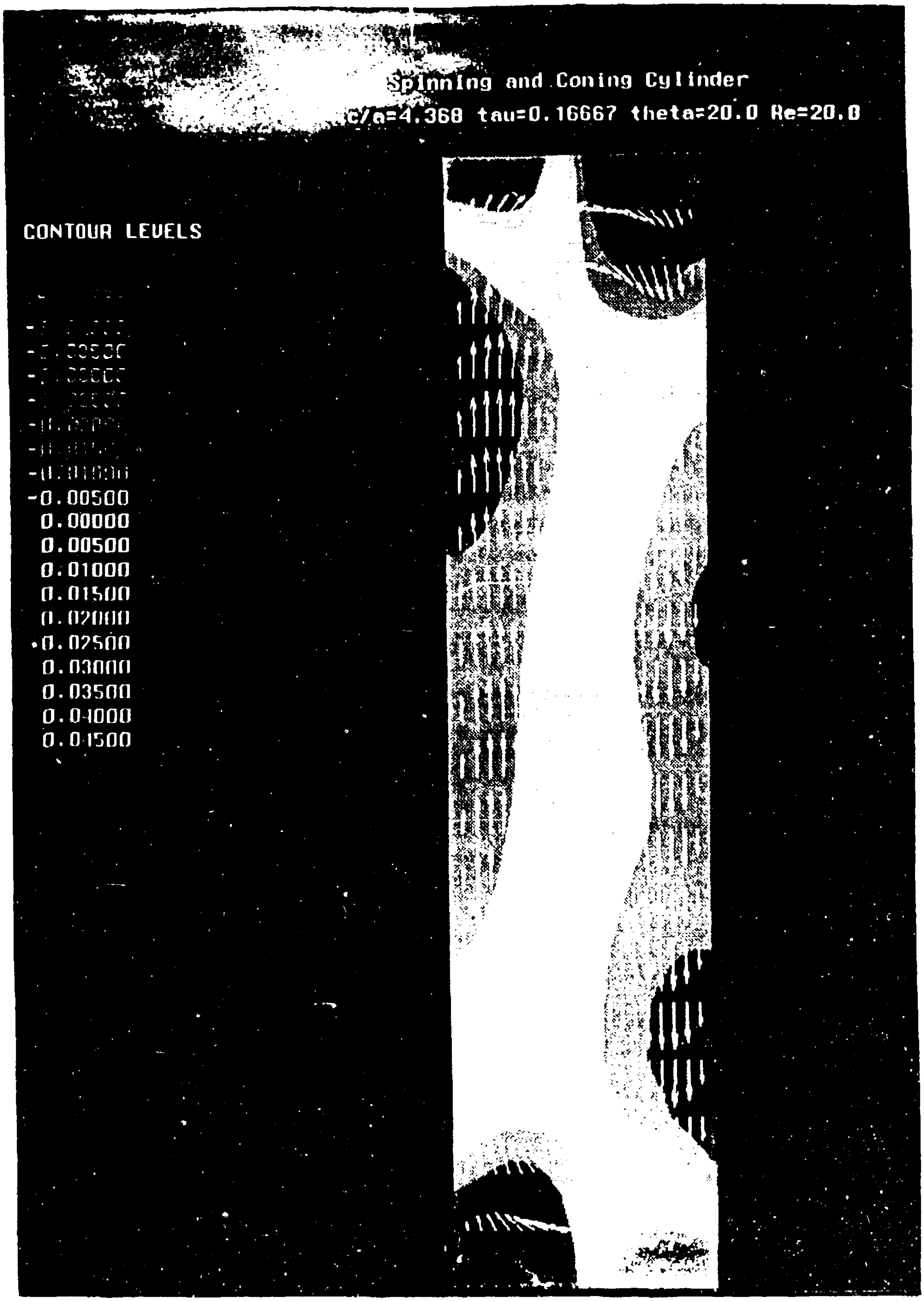
Spinning and Coning Cylinder
c/a=4.368 tau=0.16667 theta=20.0 Re=20.0
CONTOUR LEVELS
-0.00500
0.00000
0.00500
0.01000
0.01500
0.02000
0.02500
0.03000
0.03500
0.04000
0.04500

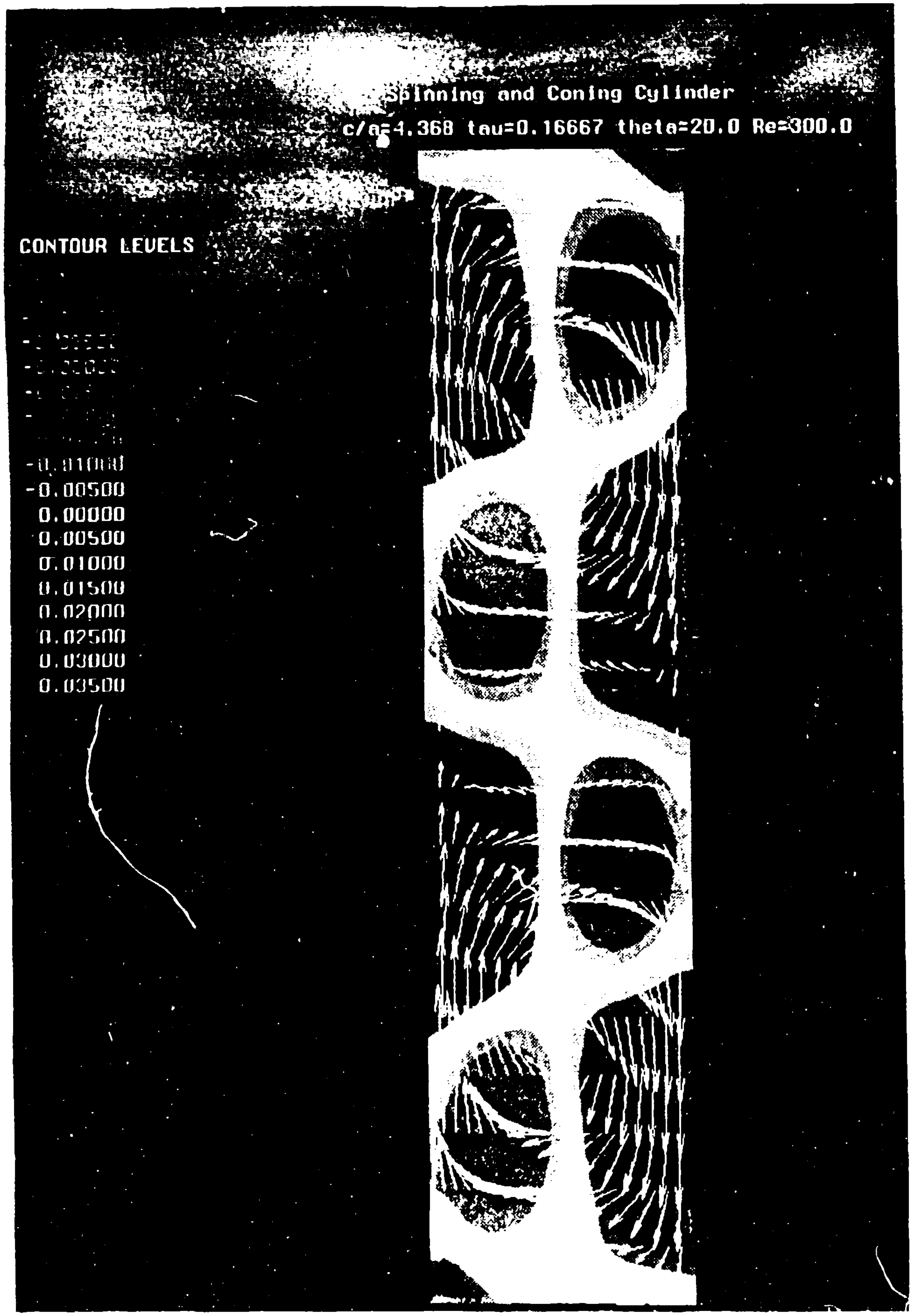
Spinning and Coning Cylinder
c/a=4.368 tau=0.16667 theta=20.0 Re=300.0
CONTOUR LEVELS
-0.01000
-0.00500
0.00000
0.00500
0.01000
0.01500
0.02000
0.02500
0.03000
0.03500

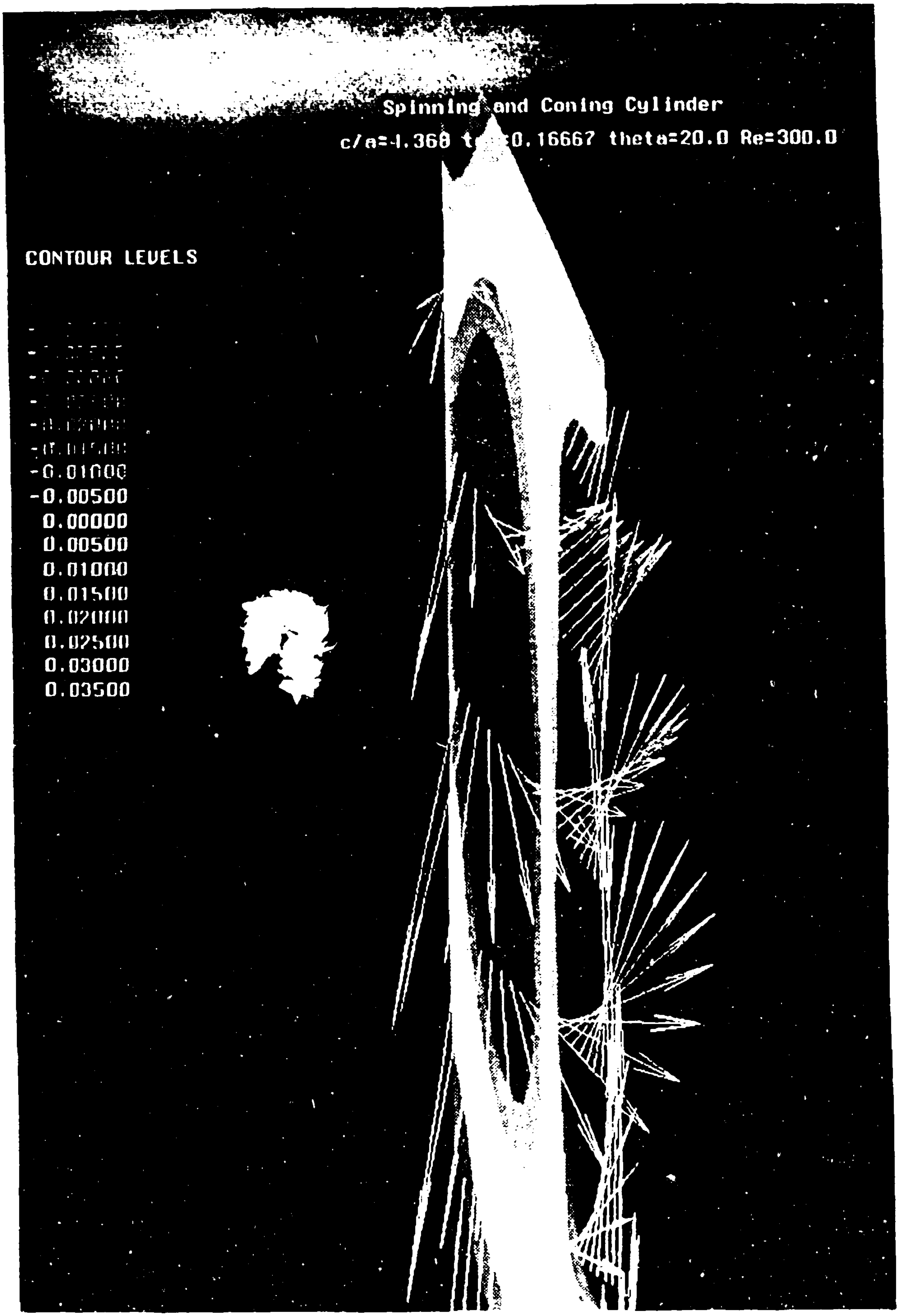
Spinning and Coning Cylinder
c/a=-1.368
0.16667 theta=20.0 Re=300.0
CONTOUR LEVELS
-0.01000
-0.00500
0.00000
0.00500
0.01000
0.01500
0.02000
0.02500
0.03000
0.03500

Blank

ROTATING FLUIDS WORKSHOP

A CENTRIFUGAL SPECTROMETER

Harvey Greenspan

Massachusetts Institute of Technology

22-23 April 1991

Army High Performance Computing Research Center
University of Minnesota

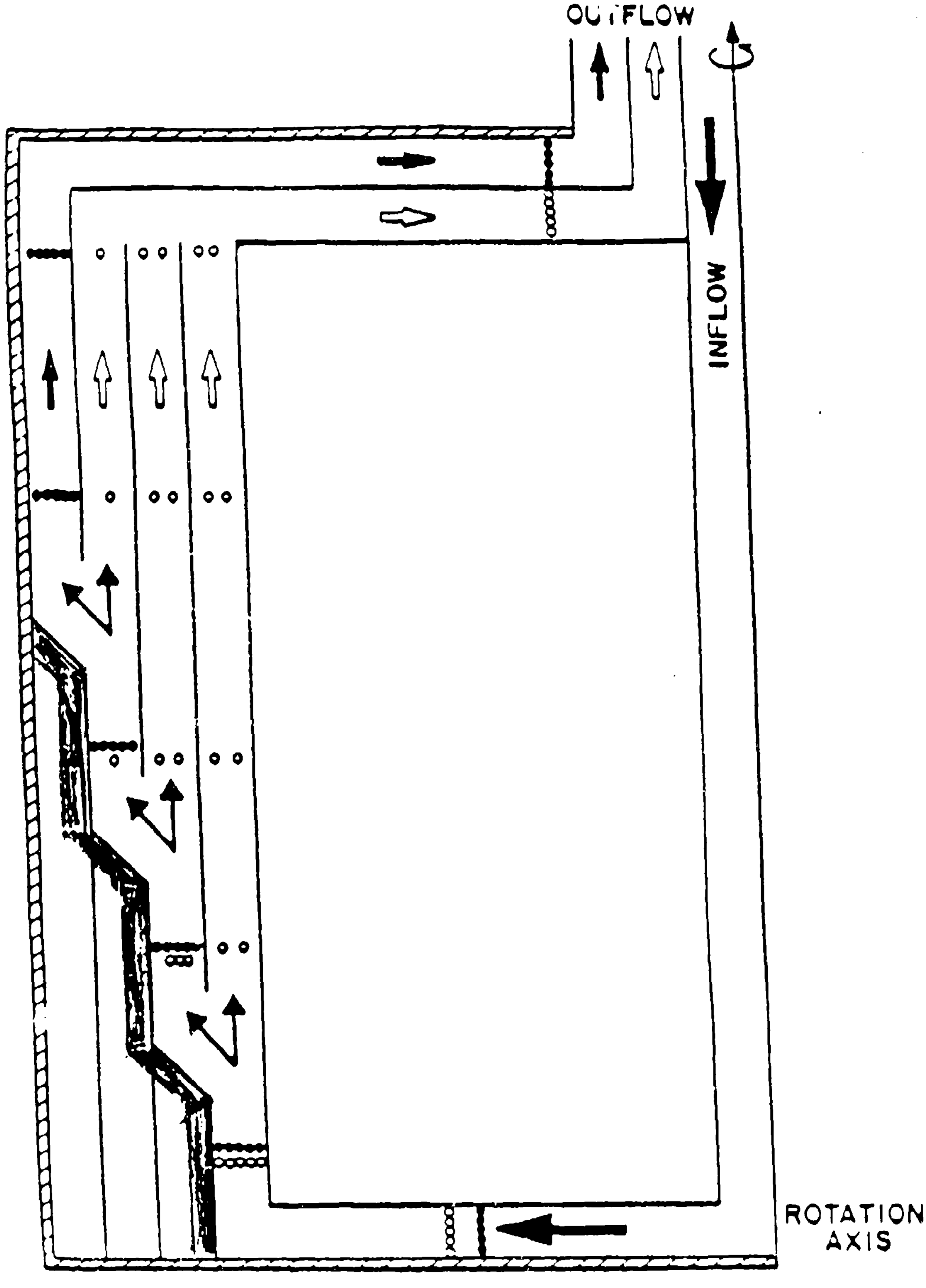
OUTFLOW
INFLOW
ROTATION AXIS

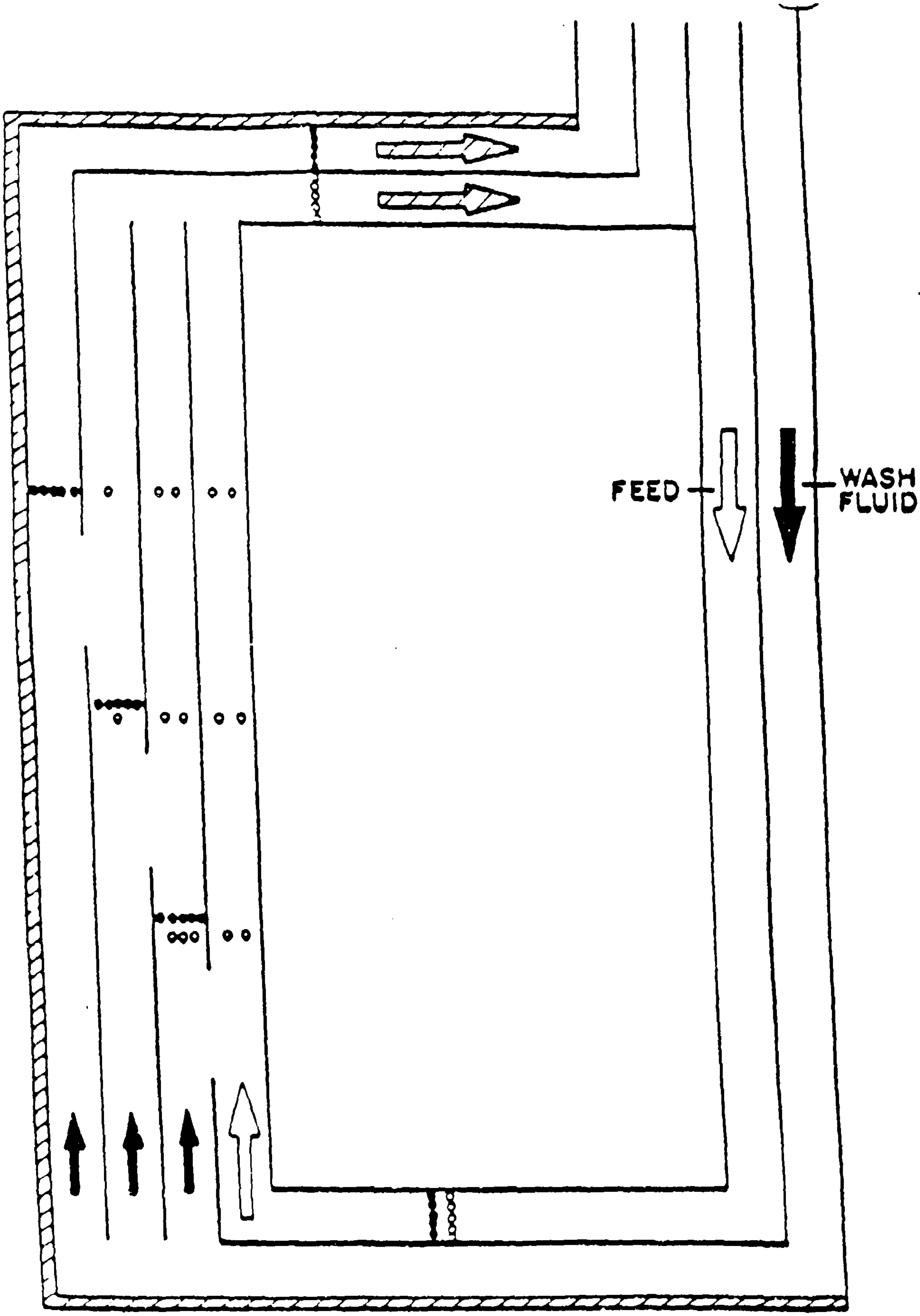
FEED
WASH
FLUID

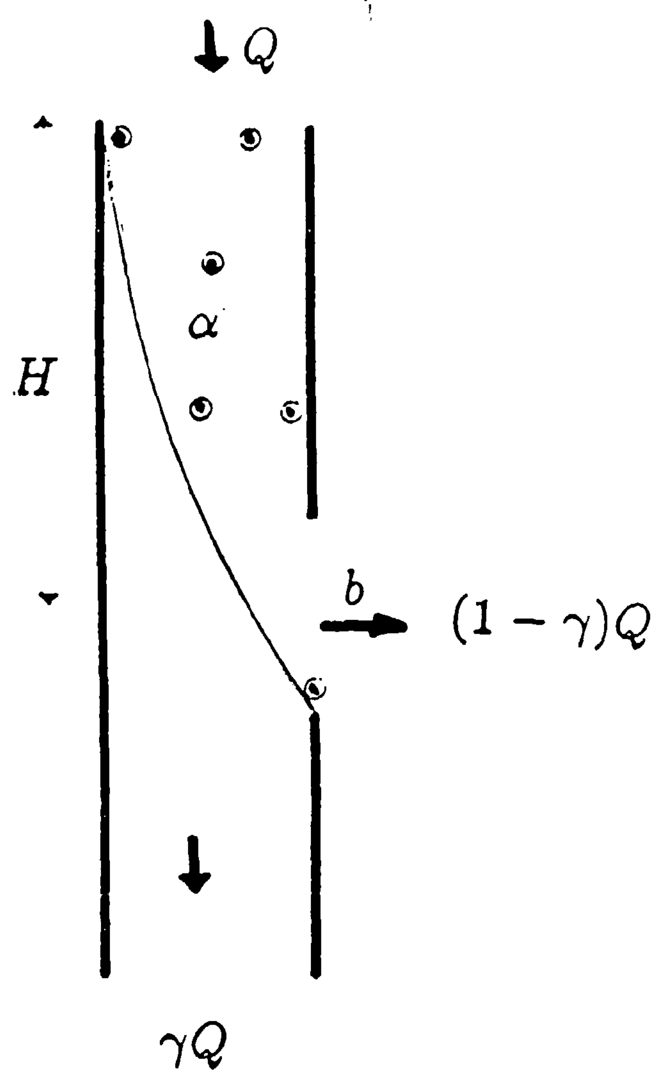

$$Q_p = \alpha(1-\gamma)Q$$
$$+\alpha U_s(H+b)2\pi R$$

If $Q_p = \alpha Q$,

$$U_s = \gamma Q/(H+b)2\pi R$$

SMALL PARTICLES

$$\frac{a_1}{a_2} = \sigma$$

% OUT OF SLOT $= 1 - \gamma(1-\sigma^2)$

% REMAINING $= \gamma(1-\sigma^2)$

$$\nabla \cdot \mathrm{q} = 0$$

$$\frac{\partial}{\partial t}\mathrm{q} \; + R_0 \mathrm{q} \cdot \nabla \mathrm{q}$$
$$+ 2\hat{k} \times \mathrm{q} = -\nabla P + E \nabla^2 \mathrm{q}$$

$$\mathrm{q}_p = \mathrm{q} + \frac{\epsilon \beta}{R_0} r \hat{r}$$

$$\epsilon = \frac{\rho_P - \rho_F}{\rho_F}; \quad \beta = \frac{2}{9} \frac{a^2 \Omega}{\nu}$$

$$E = \frac{\nu}{\Omega H^2}, R_0 = \frac{V}{\Omega H}$$

$$\text{B.C.} \quad \mathrm{q} = \mathrm{U}_W = U_W \hat{n}$$

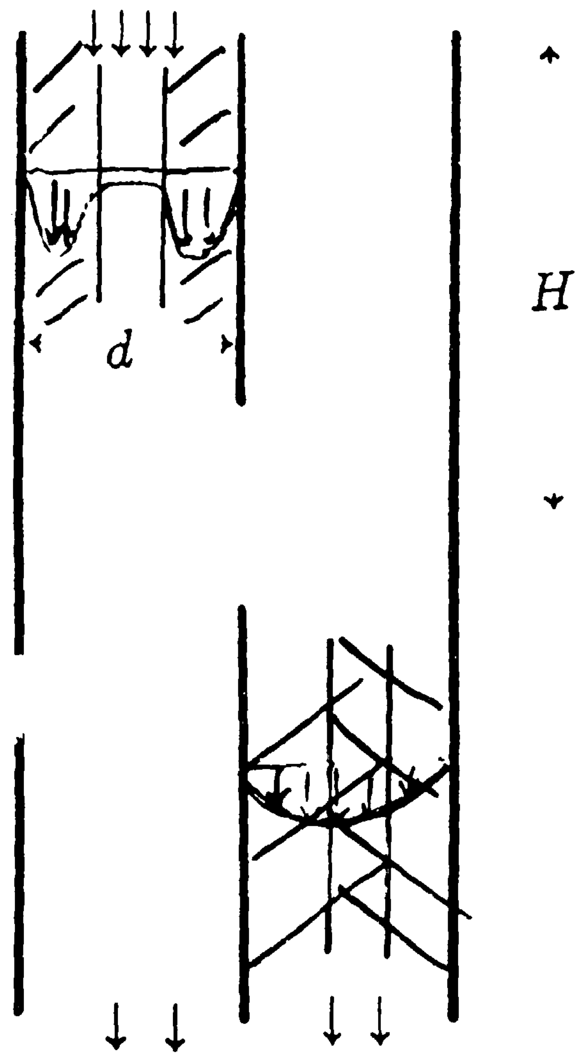

VERTICAL B. L. SCALE $\sim (\nu/\Omega H^2)^{1/3} H$

$\sim E^{1/3} H$

ENTRY LENGTH $\sim d^3\Omega/4\nu$

$R_0 \sim E^{1/3}$ N. L. EFFECTS

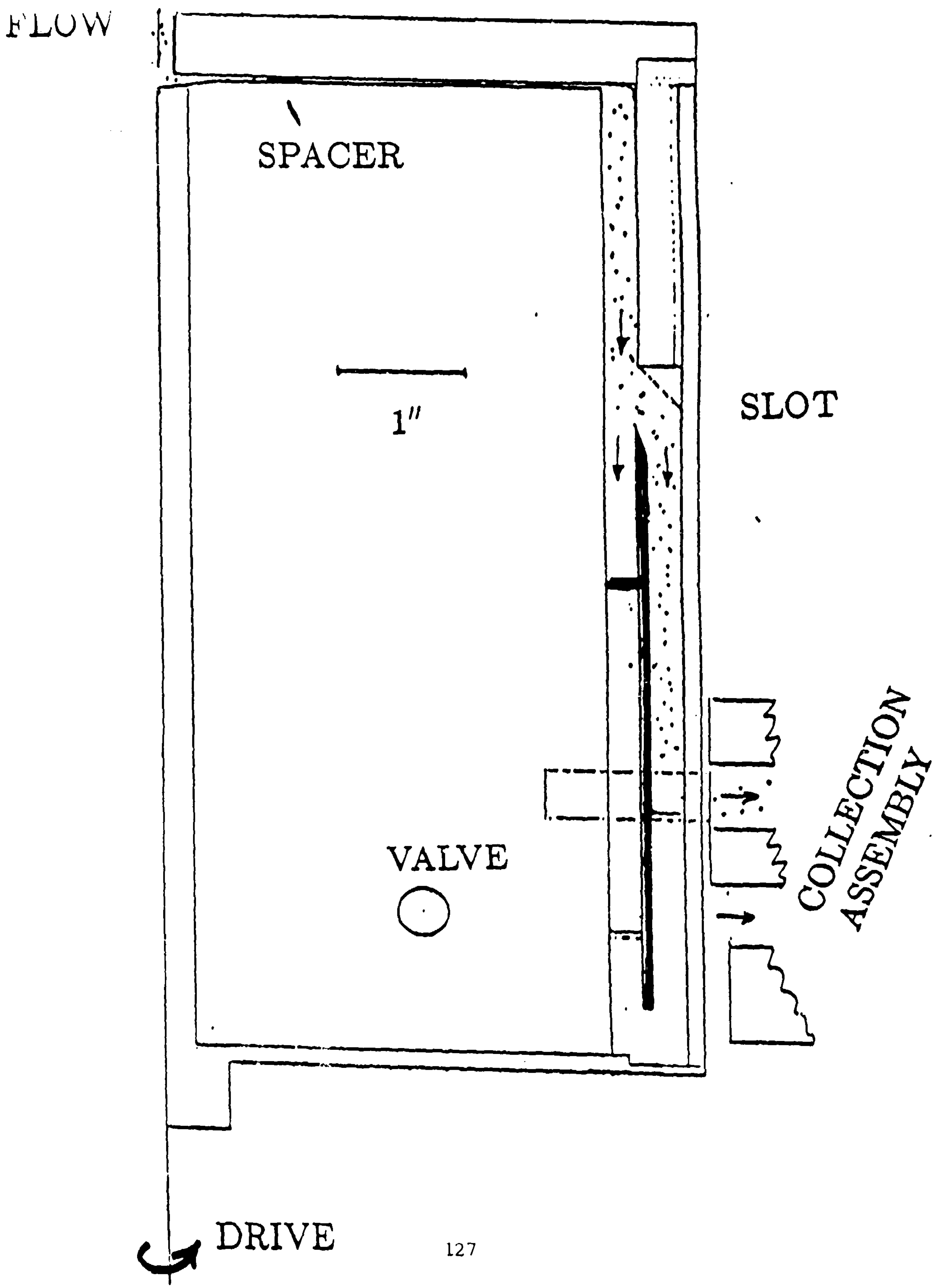
FLOW
SPACER
1″
SLOT
VALVE
COLLECTION ASSEMBLY
DRIVE

PARTICLE PATHS

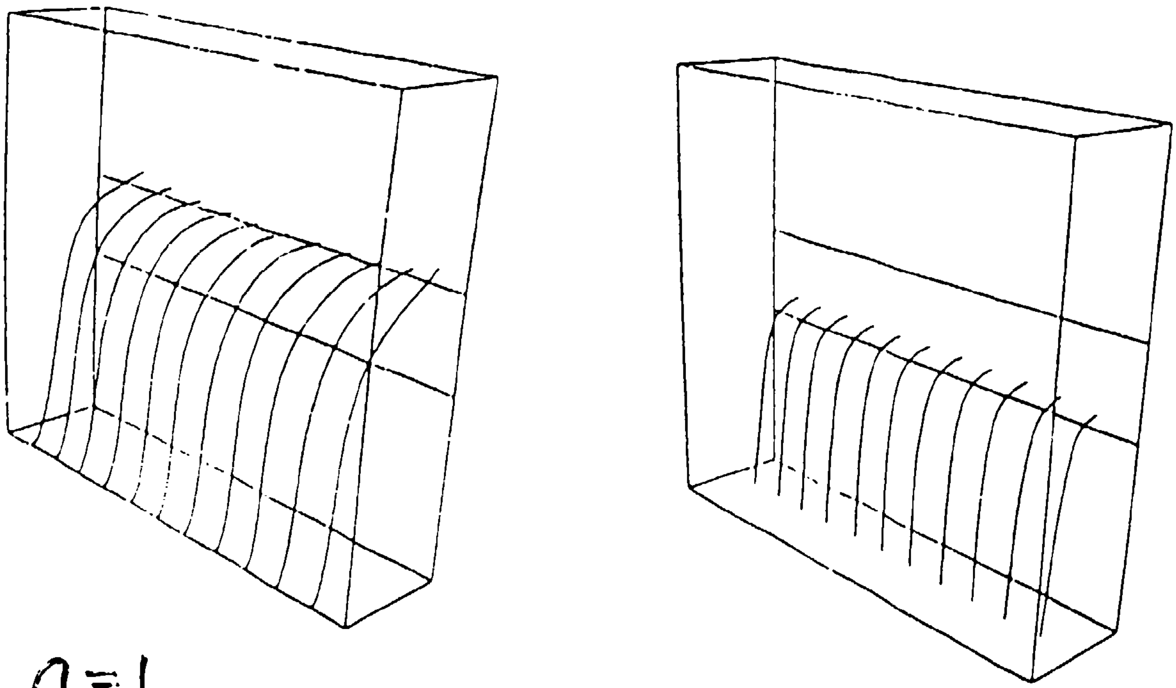

$a=1$

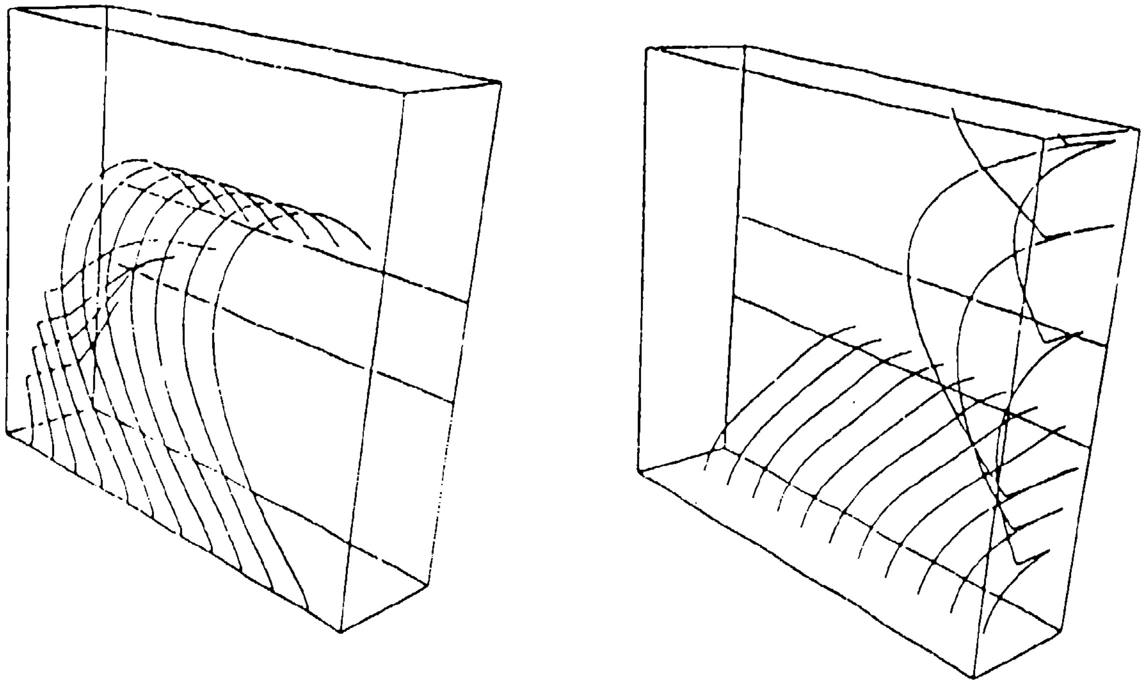

$a=3$

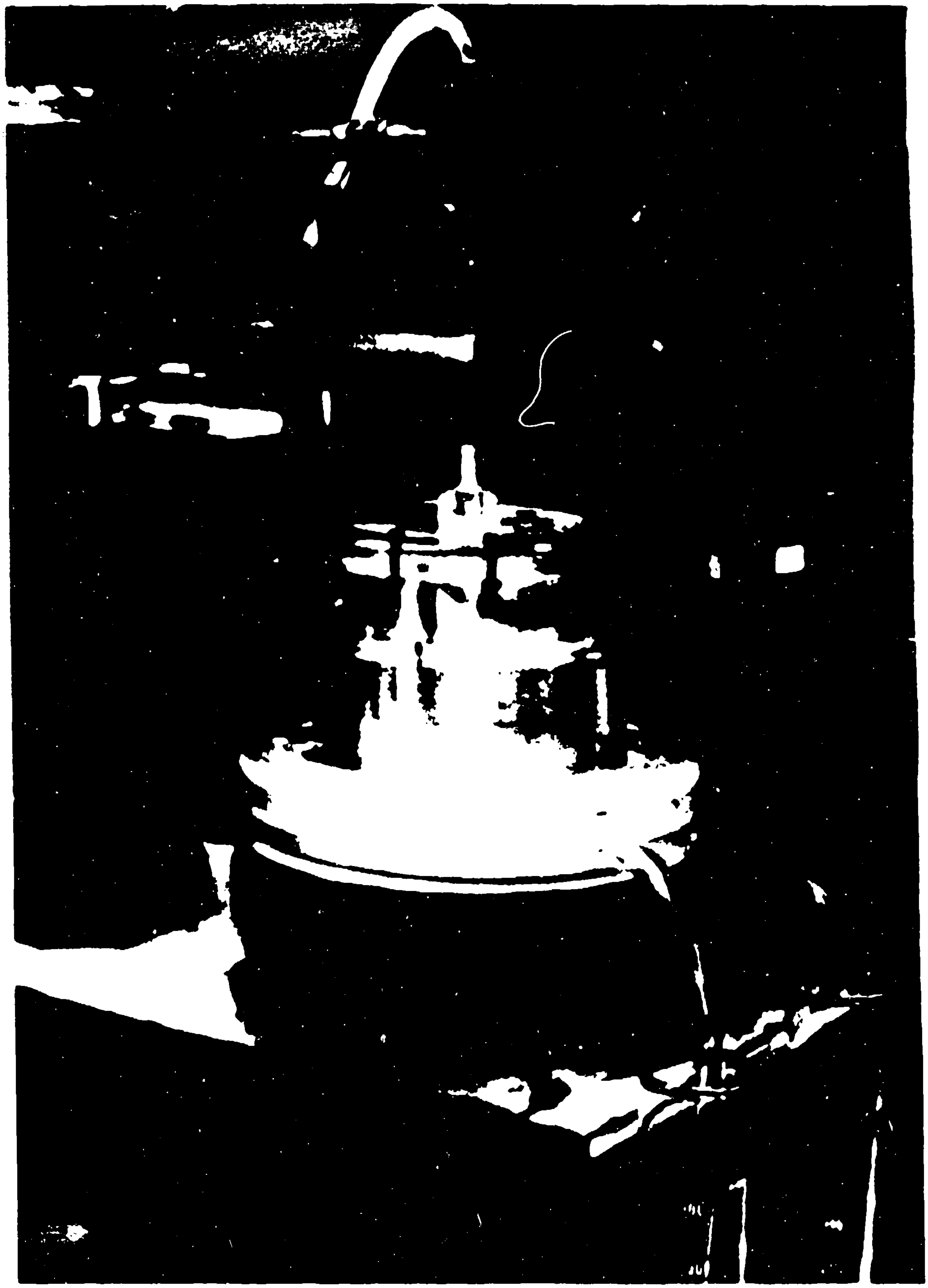

Blank

US ARMY
LABORATORY COMMAND

Moment Exerted by a Viscous Liquid in a Spinning, Coning Container

Charles Murphy
Ballistic Research Laboratory

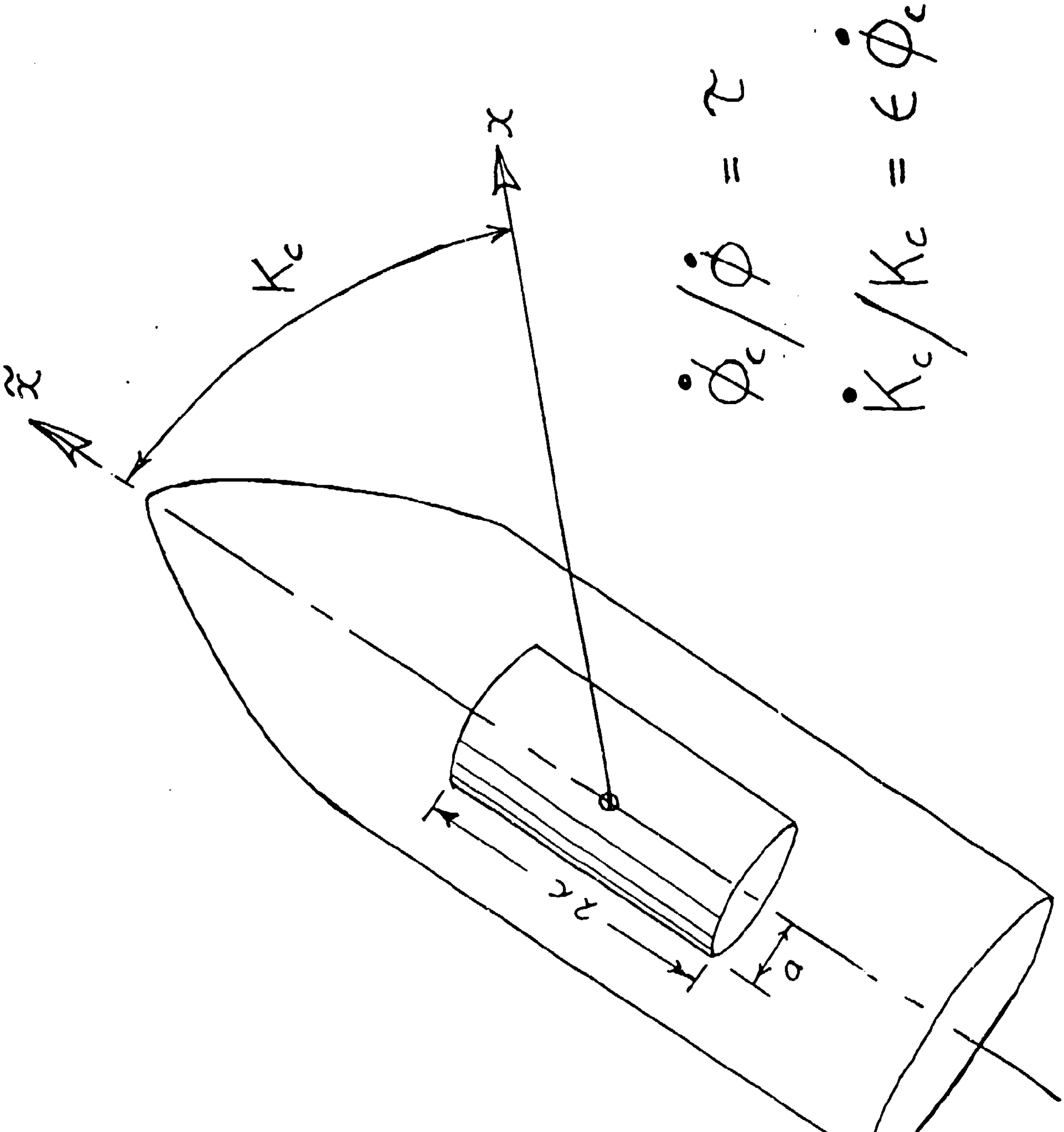
$\tilde{x}$
x
K_c
a
$\dot{\phi}_c / \dot{\phi} = \tau$
$\dot{K}_c / K_c = \epsilon \dot{\phi}_c$

LINEAR LIQUID MOMENT

$$m_L a^2 \phi^2 \tau [C_{LSM} + \iota C_{LIM}](\beta + \iota\alpha)$$

where C_{LSM} and C_{LIM} are

functions of τ, ε, Re and shape

26 July '82

Classical Method

1. Linear perturbation functions expressed as sums of products of functions of one variable

$$p = \sum c_k \, R_k(r,\lambda_k) \sin \lambda_k z \, , \ldots$$

2. Boundary conditions satisfied by proper selection of c_k, λ_k, and the b.c. of the R_k functions

LIQUID-FILLED CYLINDER THEORY

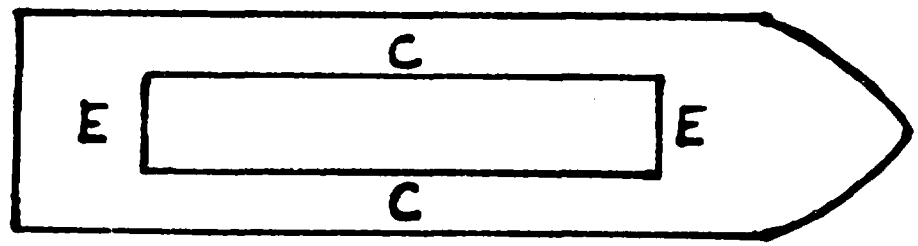

	λ_k	
1958 STEWARTSON (INVISCID)	$k\pi/2$	(E)
1965 STEWARTSON-WEDEMEYER (BL)	$k\pi/2(1+\delta_c)$	(E)
1970 KITCHENS-GERBER-SEDNEY (LNS-BL)	$k\pi/2(1+\delta_c)$	(E)
1986 HALL-SEDNEY-GERBER (LNS)	COMPUTED	(C)

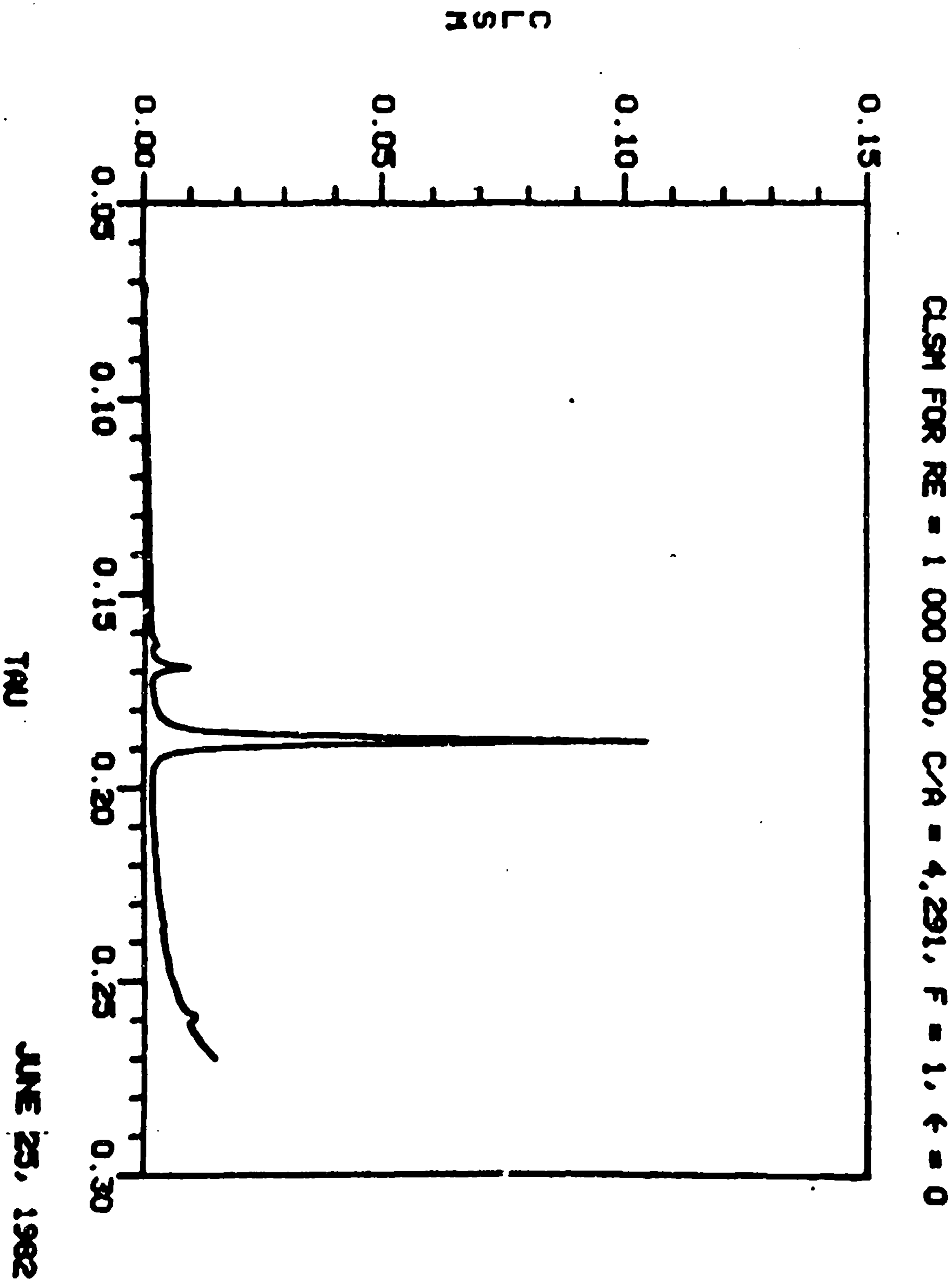
CLSM FOR RE = 1 000 000, C/A = 4.291, F = 1, ε = 0
CLSM
0.00
0.05
0.10
0.15
TAU
0.05
0.10
0.15
0.20
0.25
0.30
JUNE 25, 1982

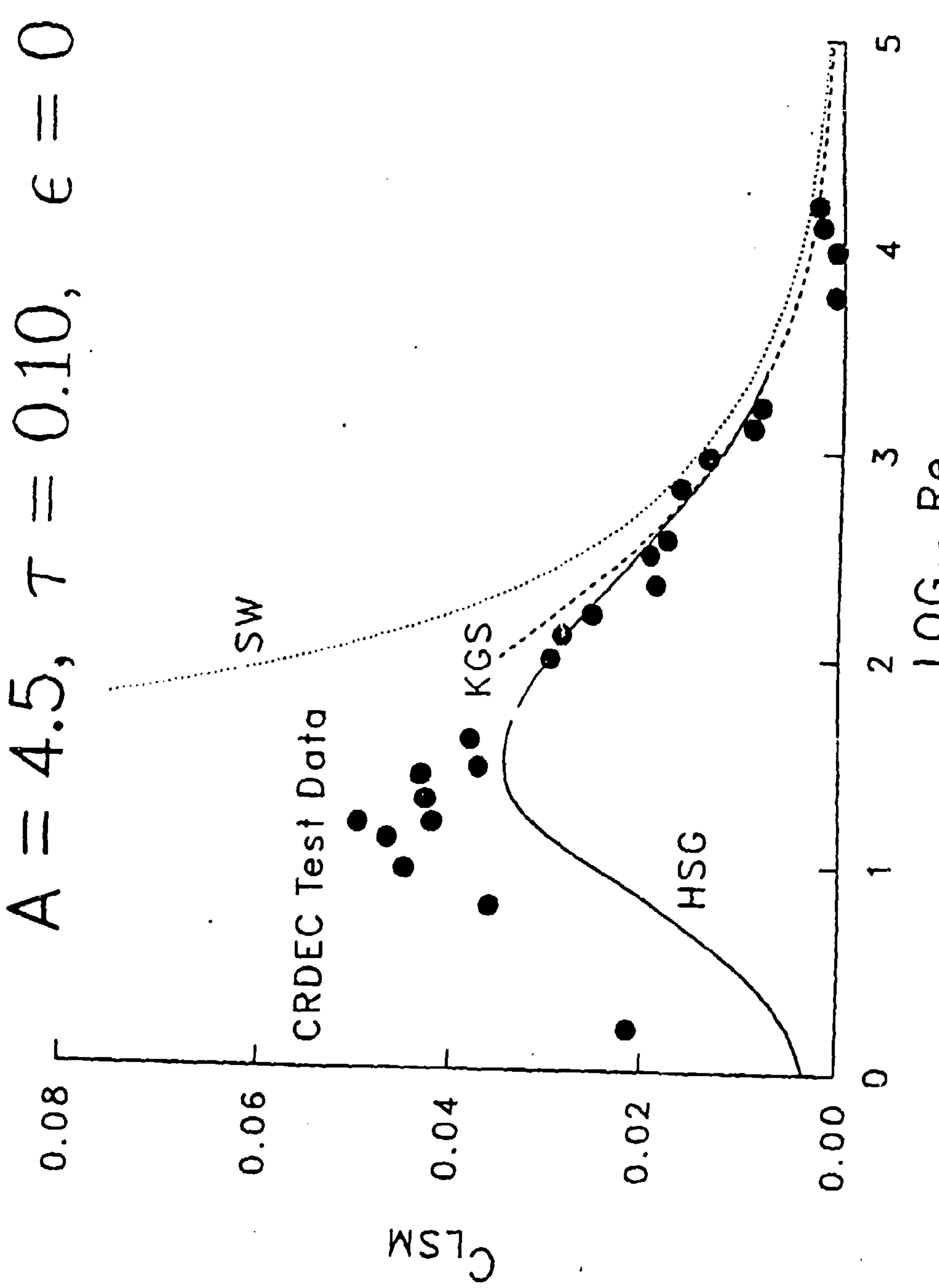

A = 4.5, τ = 0.10, ε = 0
SW
KGS
CRDEC Test Data
HSG
C_LSM
0.08
0.06
0.04
0.02
0.00
0
1
2
3
4
5
LOG10 Re

ANGULAR MOMENTUM

US ARMY
LABORATORY COMMAND

BALLISTIC RESEARCH LABORATORY

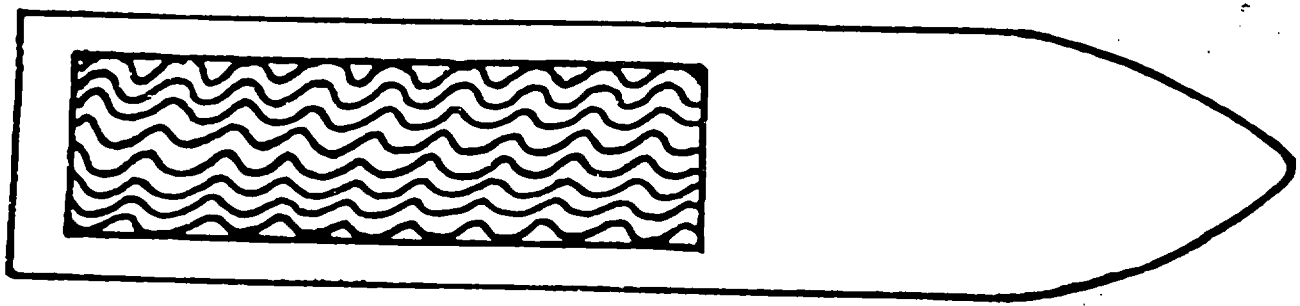

$$\vec{L} = \iiint \vec{R} \times \vec{V} \rho r \, d\theta \, dr \, dx$$

MOMENTUM DERIVATIVE

US ARMY
LABORATORY COMMAND

BALLISTIC RESEARCH LABORATORY

$$\vec{L} = (L_1, L_2, L_3)$$

$$\vec{M}_p = -\frac{d\vec{L}}{dt}$$

$$= -(\dot{L}_1, \dot{L}_2, \dot{L}_3) - \vec{\Omega}_c \times \vec{L}$$

$$M_p = \dot{\phi}_c \Big[-L_3 \sin\alpha_c \, \hat{e}_{xc} + L_3 \cos\alpha_c \, \hat{e}_{xc}$$
$$+ \left(L_1 \sin\alpha_c - L_2 \cos\alpha_c \right) \hat{e}_{zc} \Big]$$

$$\therefore \quad \boxed{M_{pRM} = -\tan\alpha_c \, M_{pSM}}$$

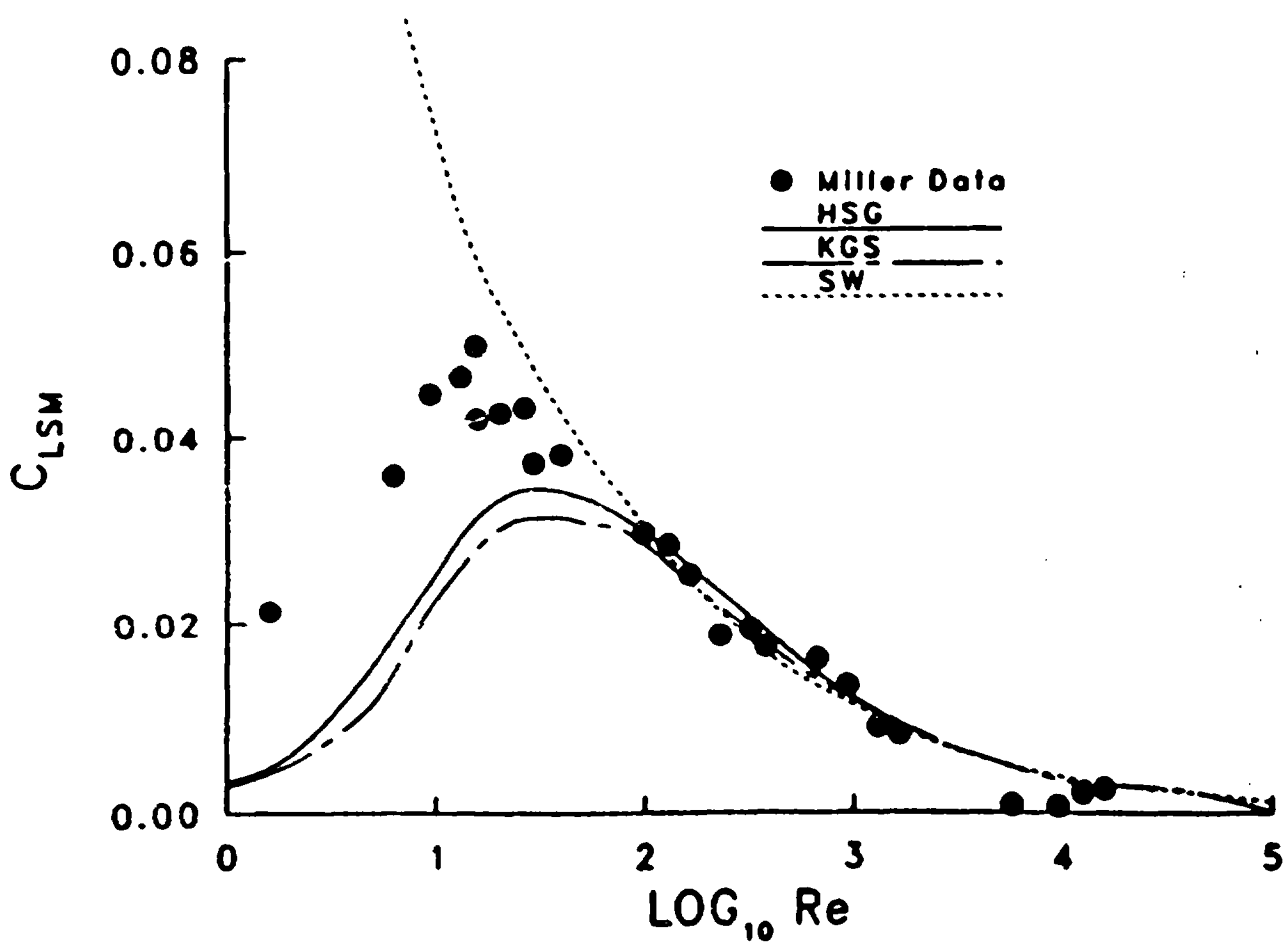

C_{LSM} vs. $\log_{10}$ Re
for $A = 4.5$, $\tau = 0.1$. Comparison with Miller data.

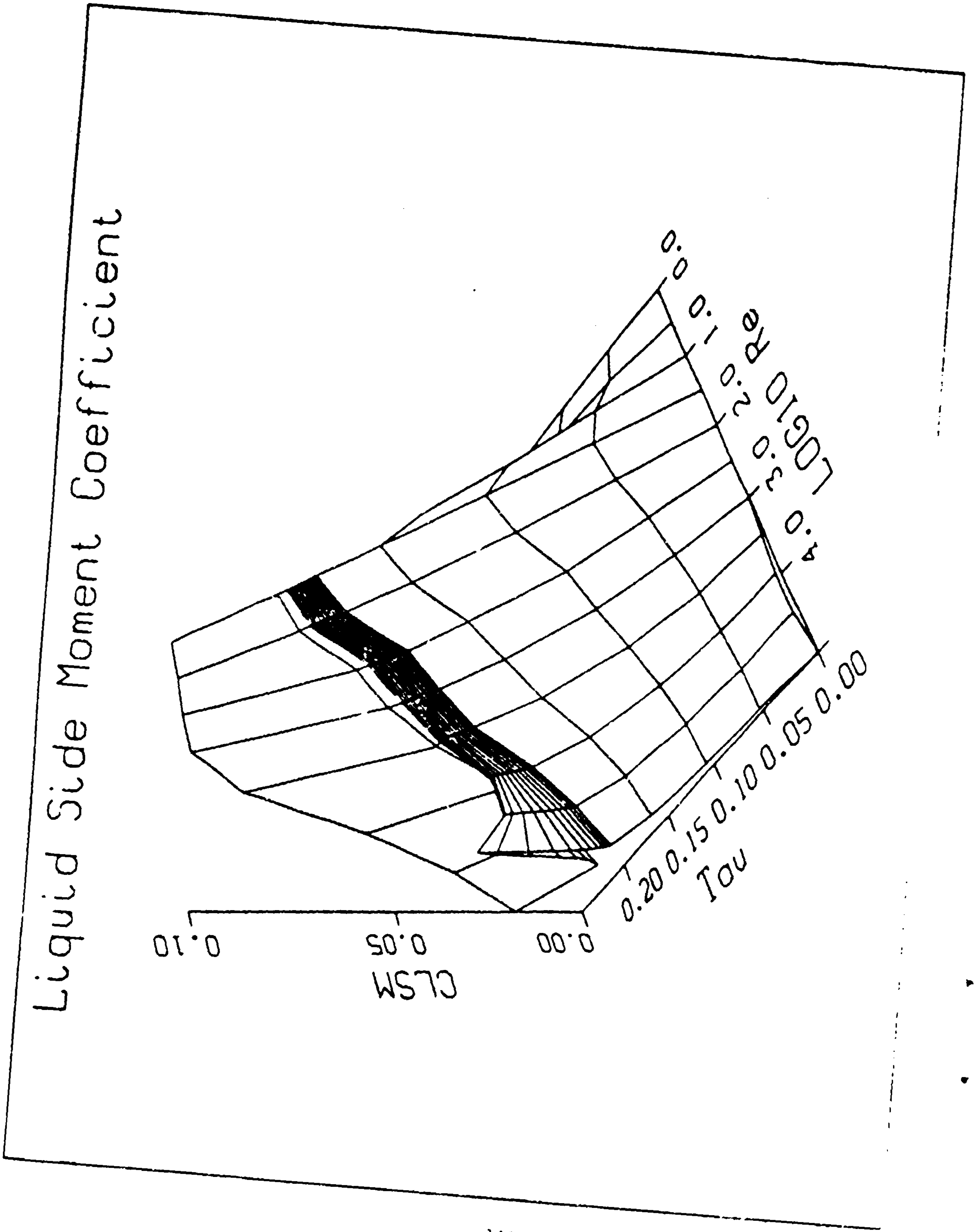
Liquid Side Moment Coefficient
CLSM
0.00
0.05
0.10
Tau
0.20 0.15 0.10 0.05 0.00
LOG10 Re
0.0 1.0 2.0 3.0 4.0

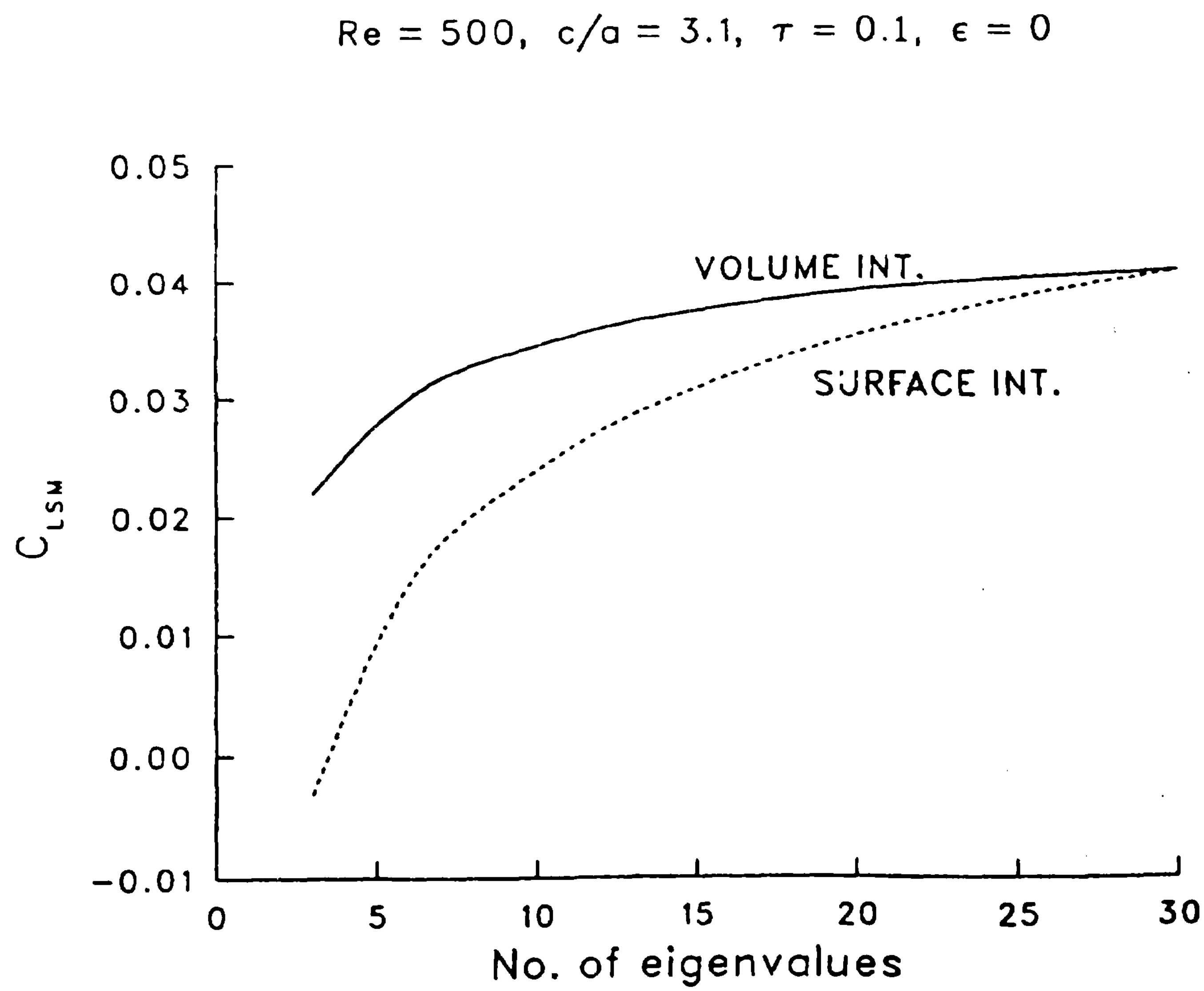
Re = 500, c/a = 3.1, τ = 0.1, ε = 0
VOLUME INT.
SURFACE INT.
C_LSM
0.05
0.04
0.03
0.02
0.01
0.00
-0.01
0
5
10
15
20
25
30
No. of eigenvalues

Partial Fill/Central Rod

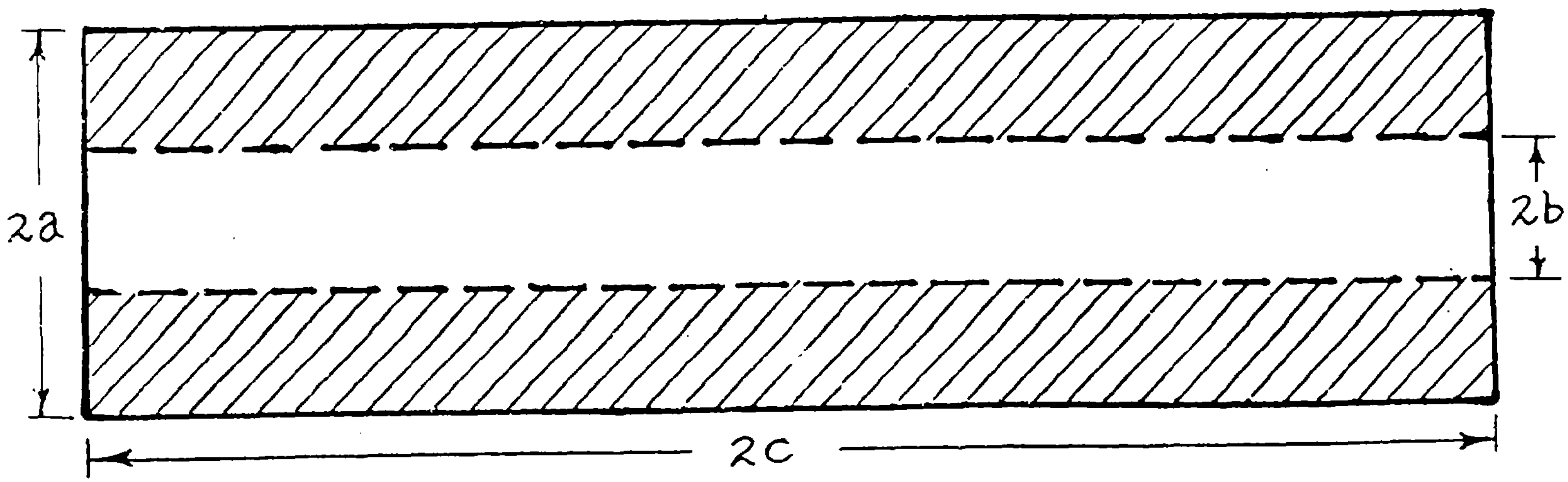

- Use b.c. at inner cylinder in differential equation for $R_k(r)$
- Extend Mermagen Tables to b/a = .1, .3 so that initial values of λ_k's can be determined

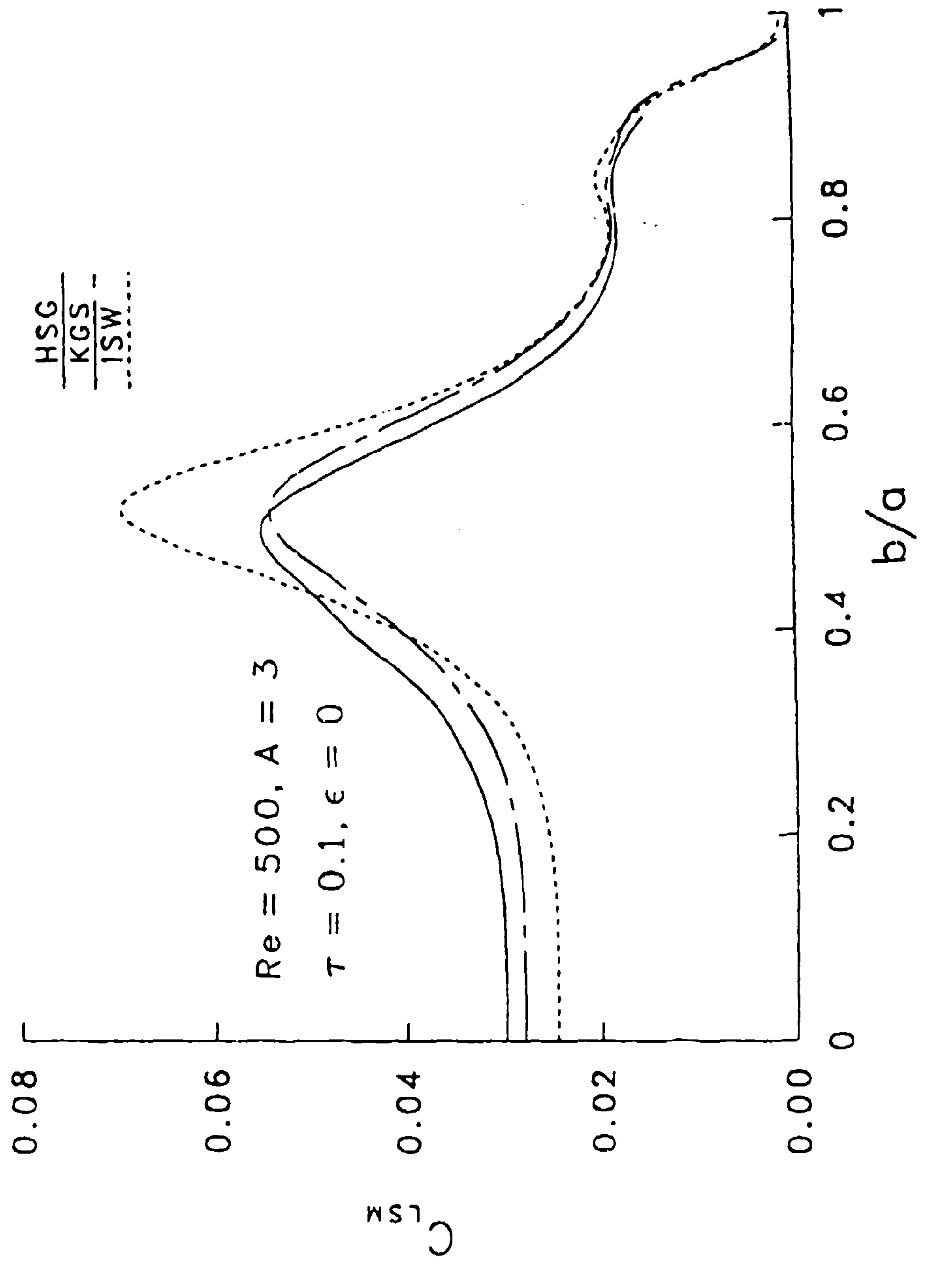

Partial Fill: C_{LSM} vs. b/a

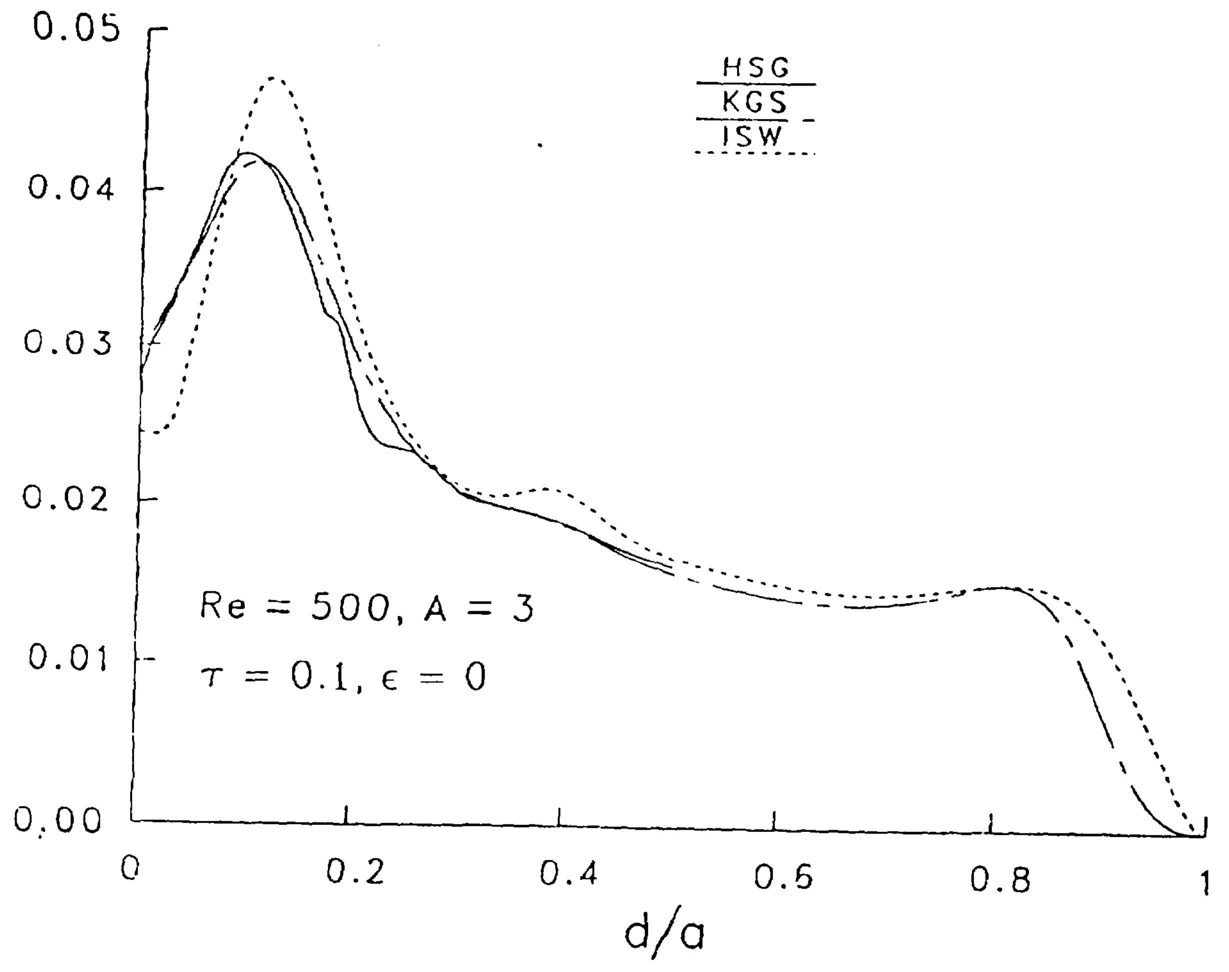

Central Rod: C_{LSM} vs. d/a

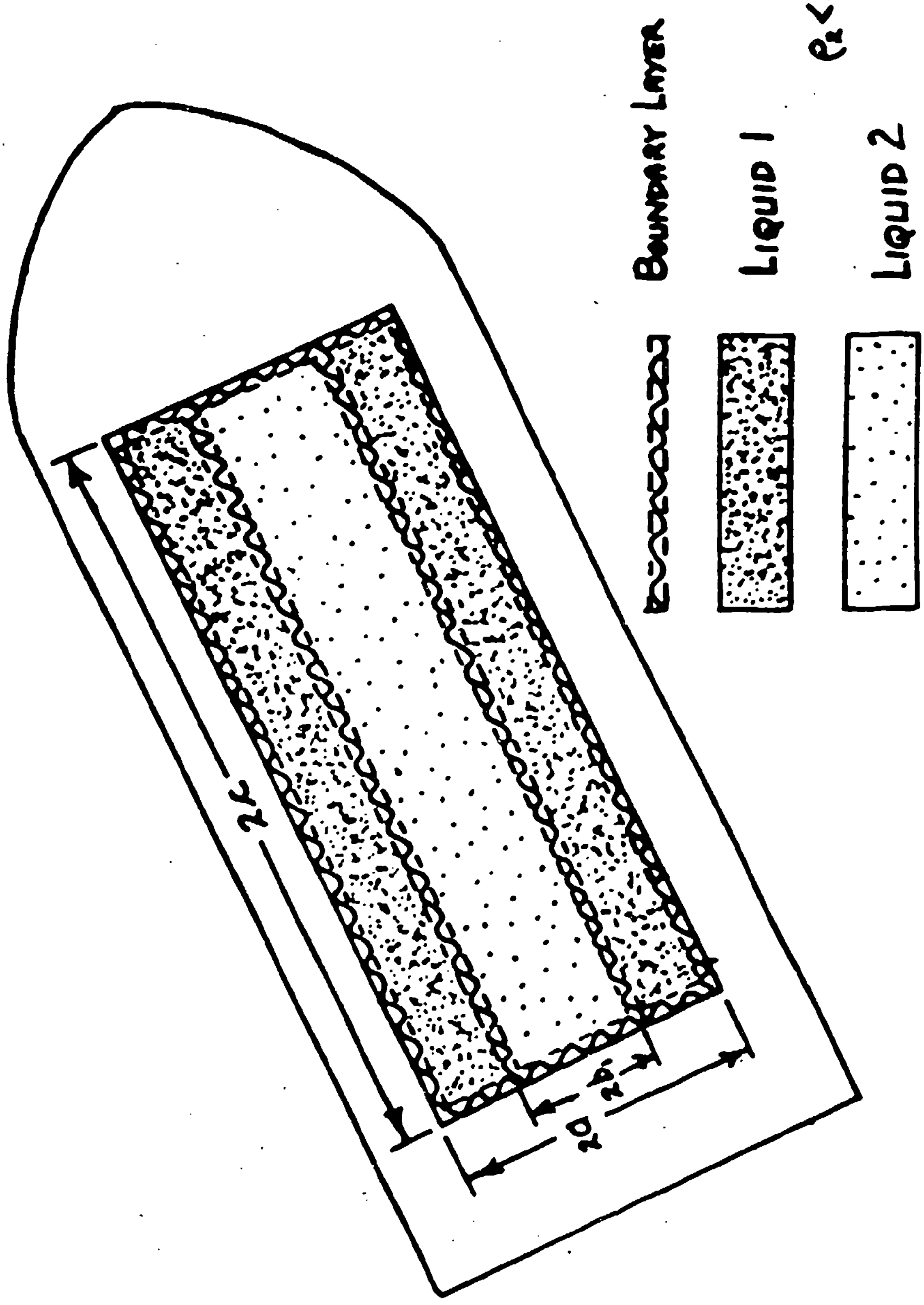
BOUNDARY LAYER
LIQUID 1
LIQUID 2
$\rho_2 < \rho_1$
2c
2a
2b

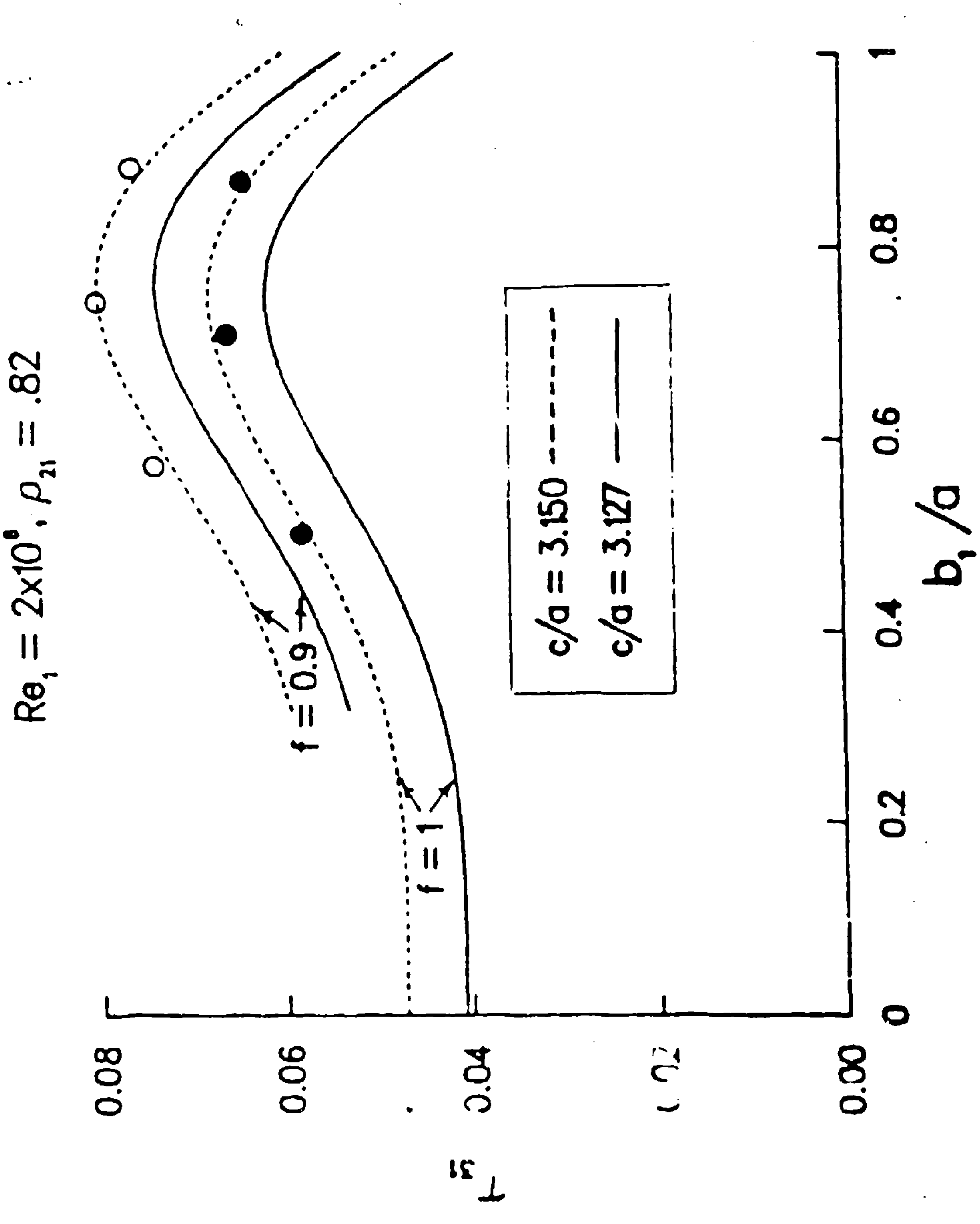

Re₁ = 2x10⁶, ρ₂₁ = .82
f = 0.9
f = 1
c/a = 3.150
c/a = 3.127
0.08
0.06
0.04
0.00
0
0.2
0.4
0.6
0.8
1
b₁/a
T₃₁

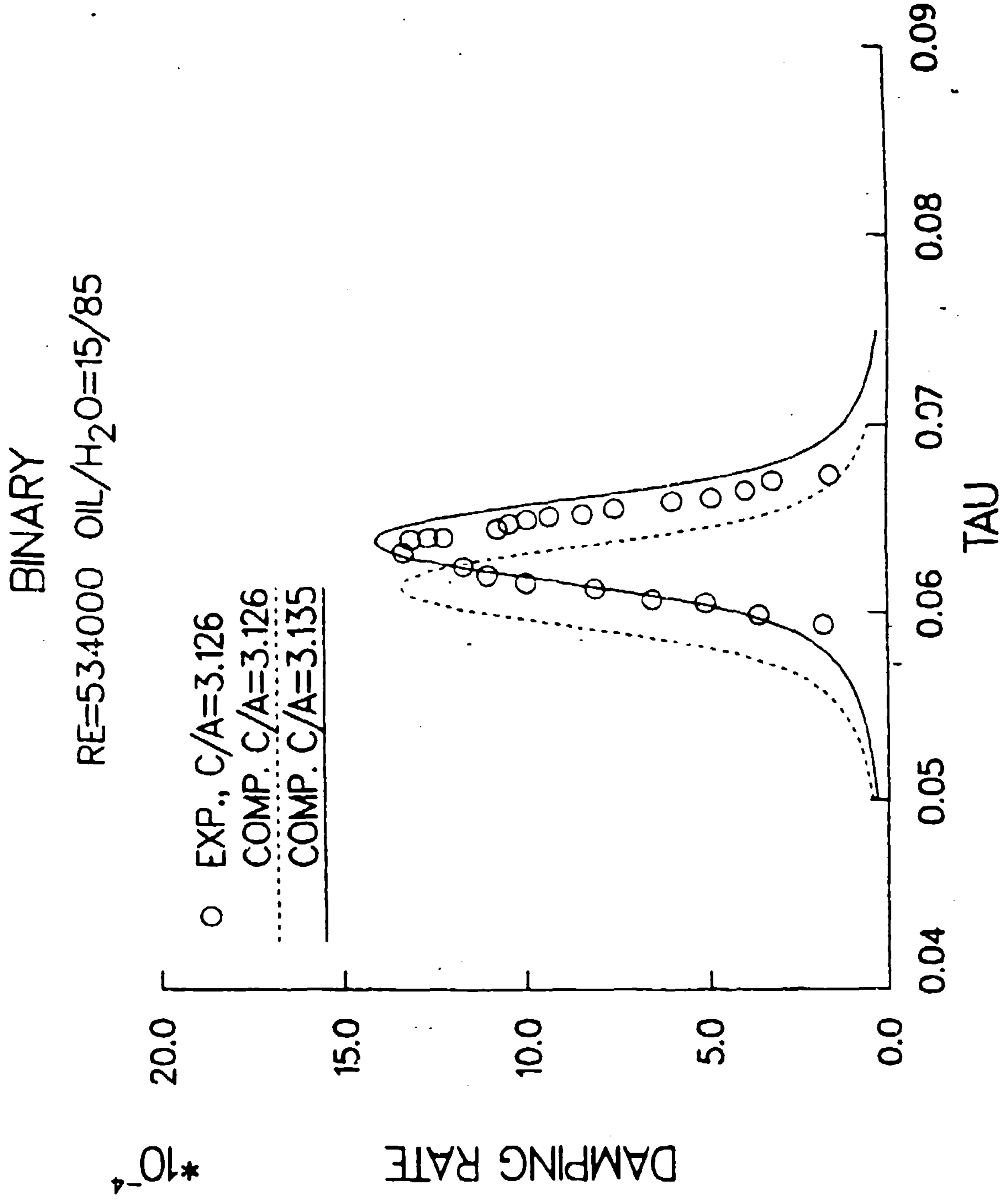

BINARY
RE=534000 OIL/H2O=15/85
EXP., C/A=3.126
COMP. C/A=3.126
COMP. C/A=3.135
DAMPING RATE
*10^-4
20.0
15.0
10.0
5.0
0.0
0.04
0.05
0.06
0.07
0.08
0.09
TAU

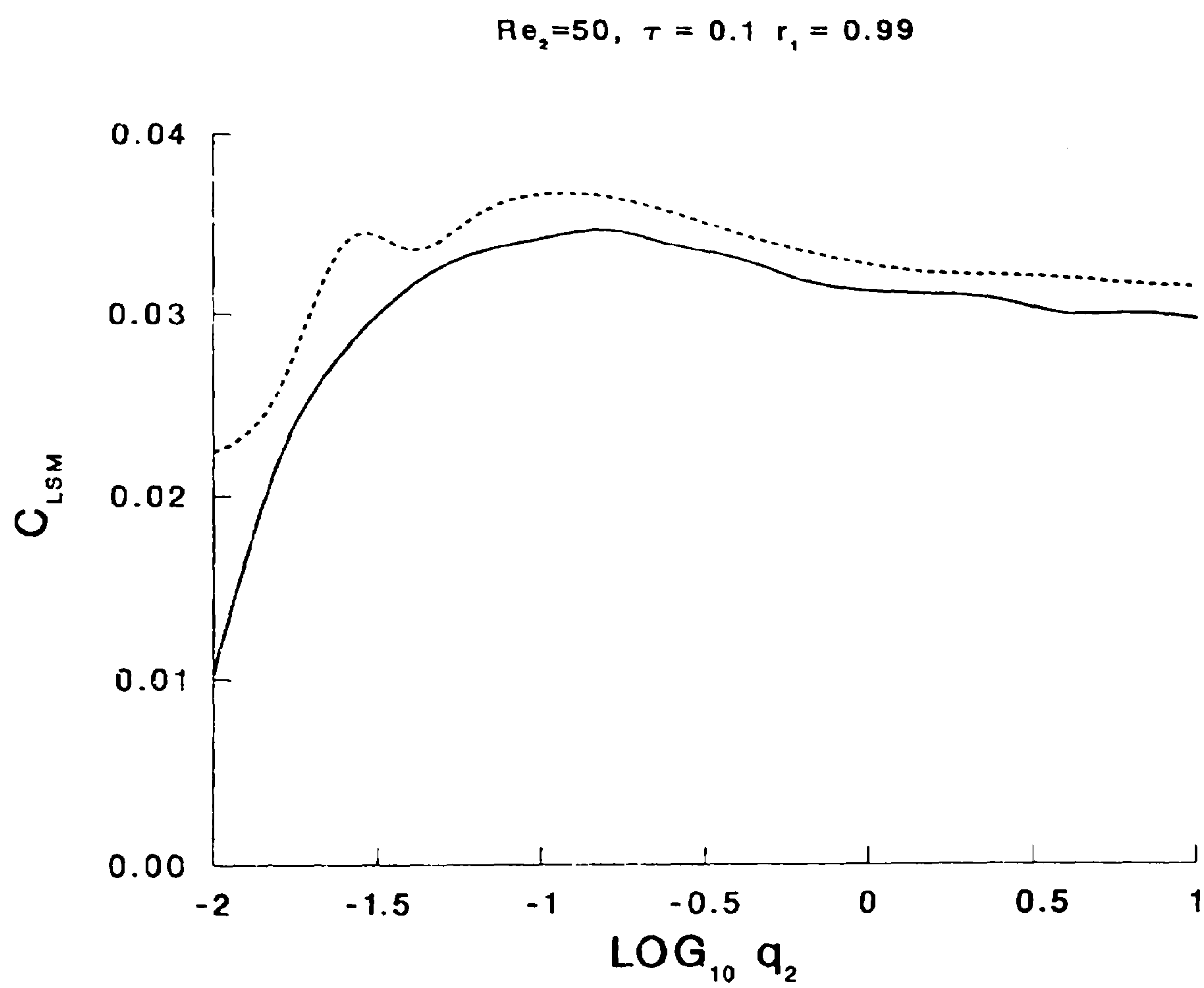

Re2=50, τ = 0.1 r1 = 0.99
0.04
0.03
0.02
0.01
0.00
C LSM
-2
-1.5
-1
-0.5
0
0.5
1
LOG10 q2

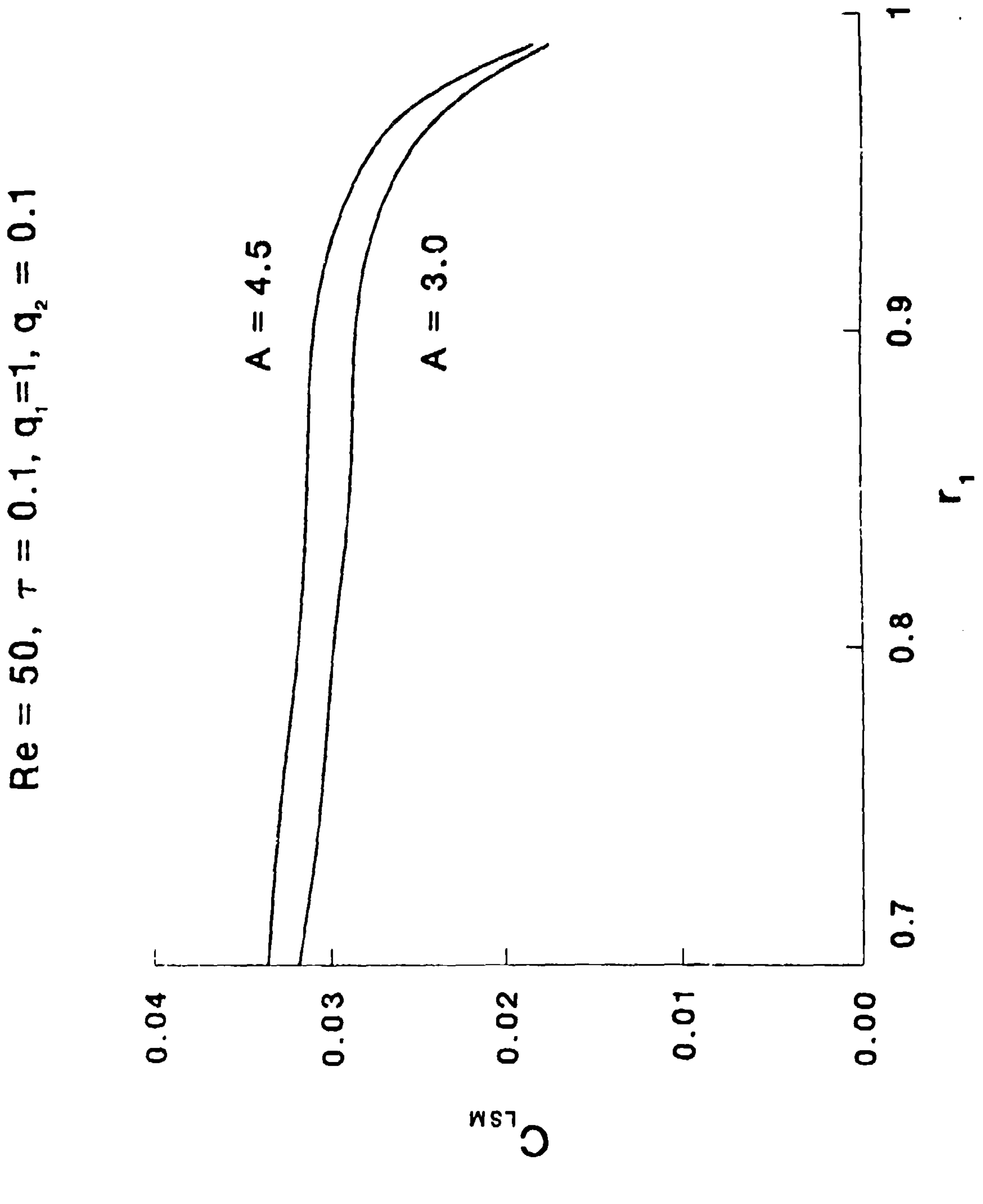

Re = 50, τ = 0.1, q₁=1, q₂ = 0.1
A = 4.5
A = 3.0
0.04
0.03
0.02
0.01
0.00
C_LSM
0.7
0.8
0.9
1
r₁

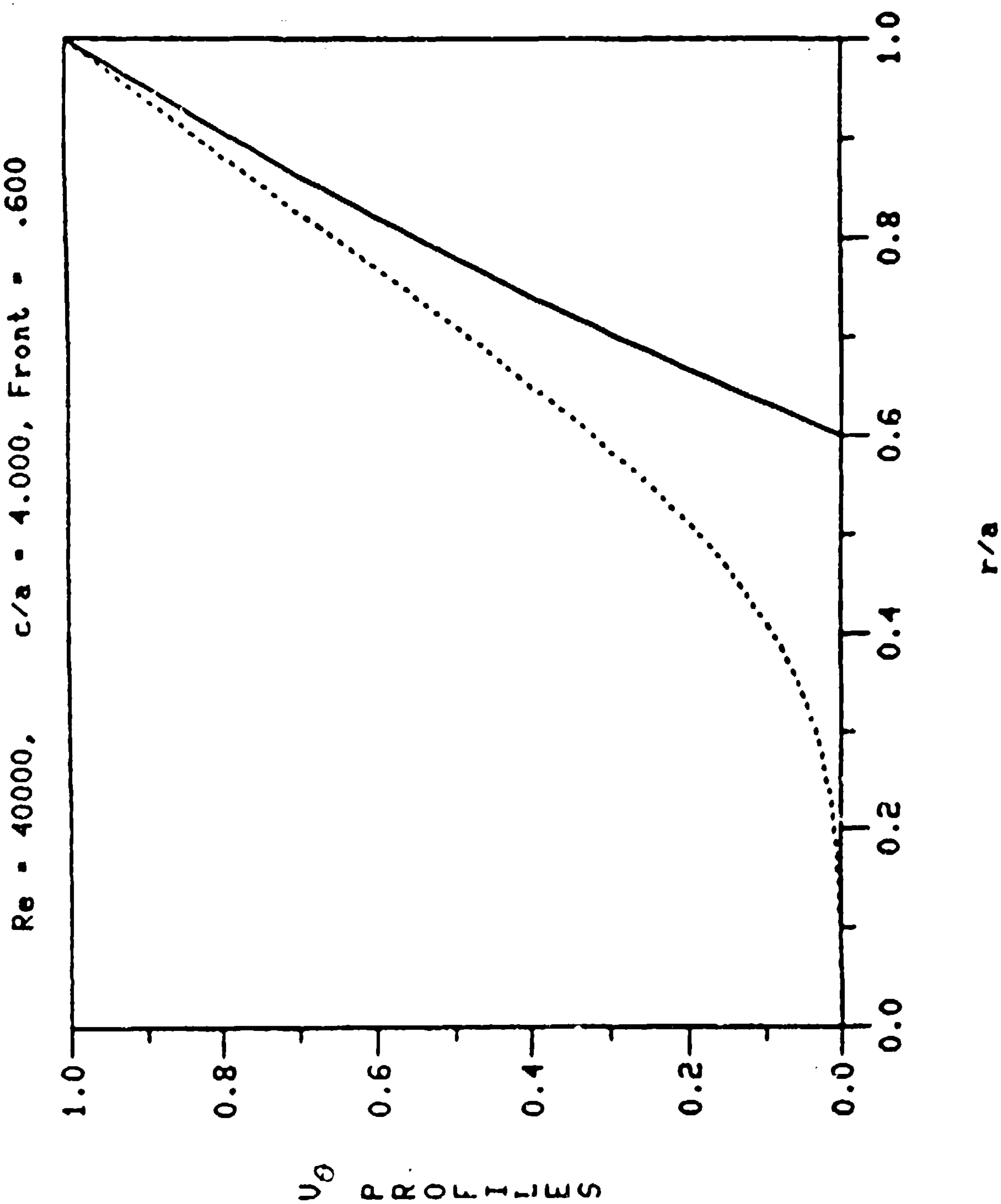

Re = 40000, c/a = 4.000, Front = .600
r/a
V_θ PROFILES
0.0
0.2
0.4
0.6
0.8
1.0

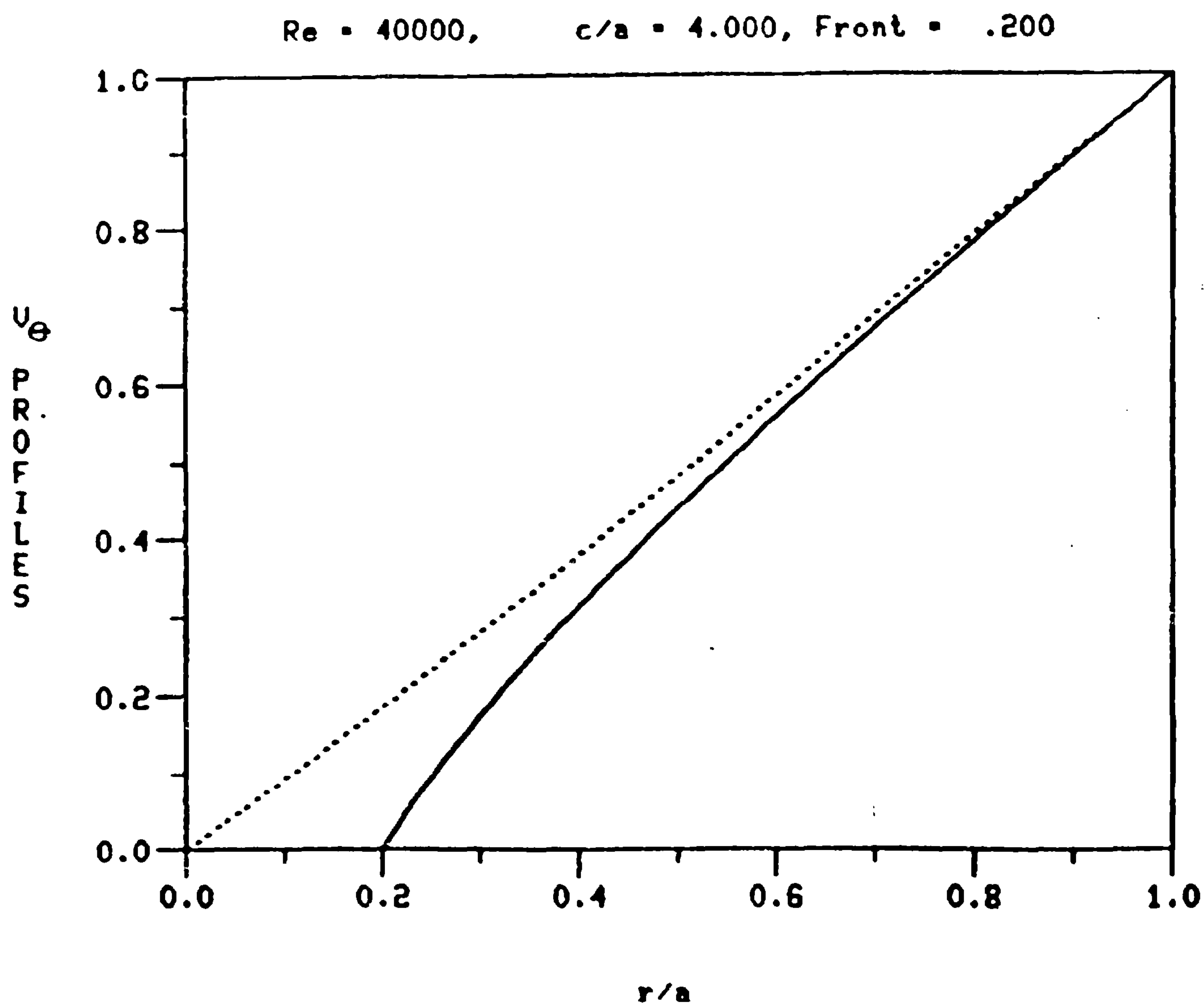
Re = 40000, c/a = 4.000, Front = .200
V_θ PROFILES
1.0
0.8
0.6
0.4
0.2
0.0
0.0
0.2
0.4
0.6
0.8
1.0
r/a

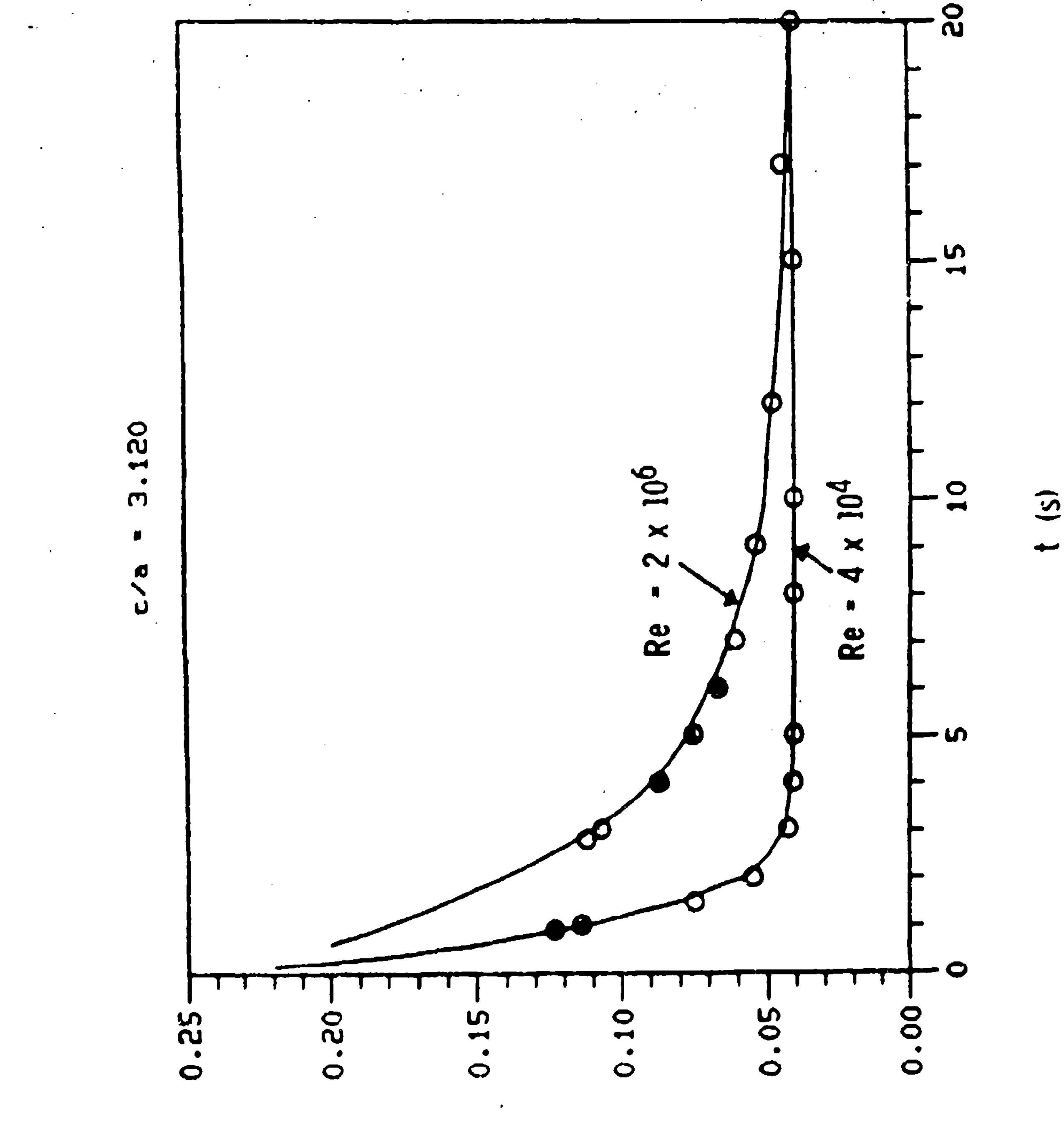
c/a = 3.120
Re = 2 x 10^6
Re = 4 x 10^4
t (s)
Tau
0.25
0.20
0.15
0.10
0.05
0.00
0
5
10
15
20

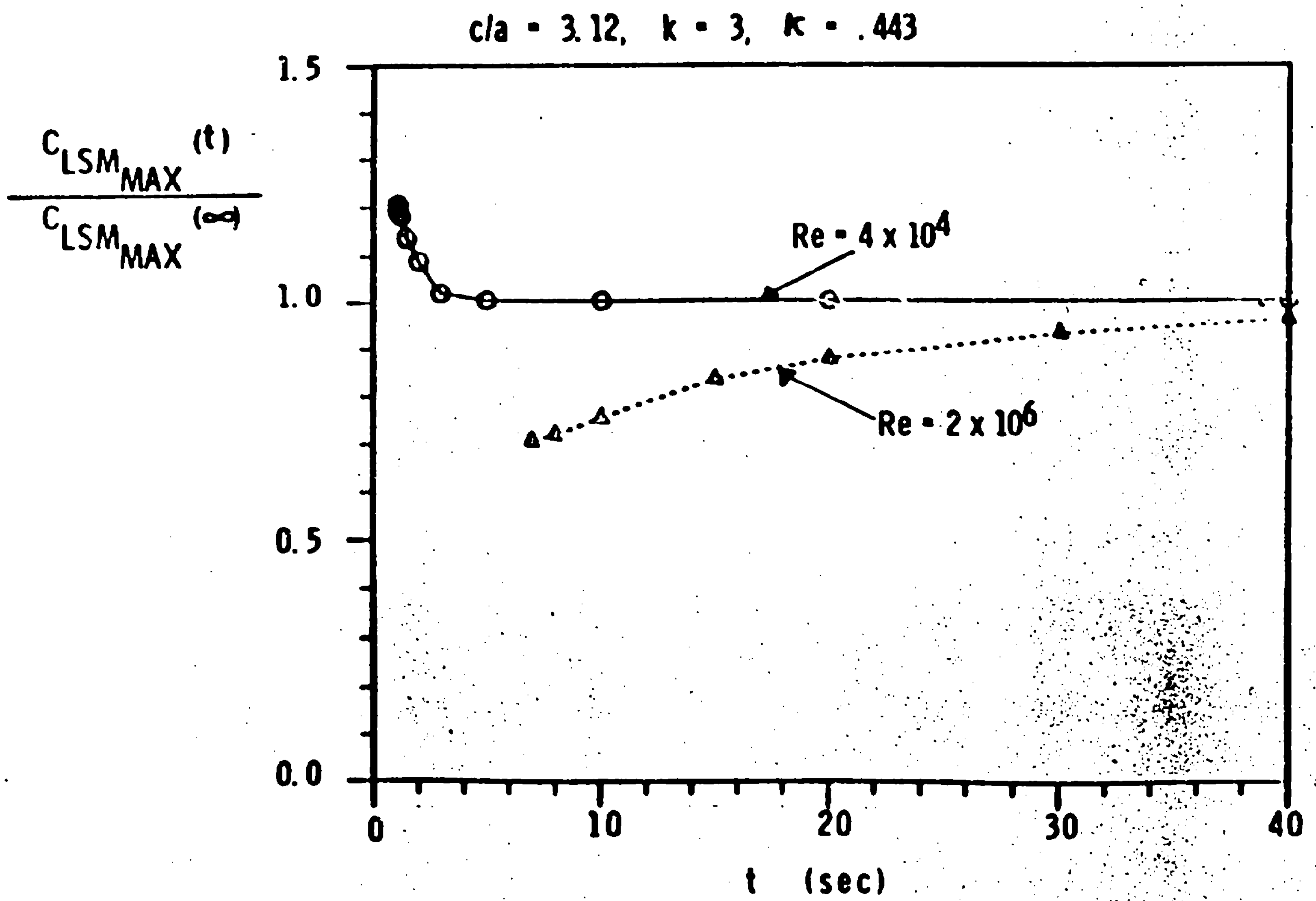
c/a = 3.12, k = 3, κ = .443
$\frac{C_{LSM_{MAX}}(t)}{C_{LSM_{MAX}}(\infty)}$
1.5
1.0
0.5
0.0
Re = 4 x 10^4
Re = 2 x 10^6
0
10
20
30
40
t (sec)

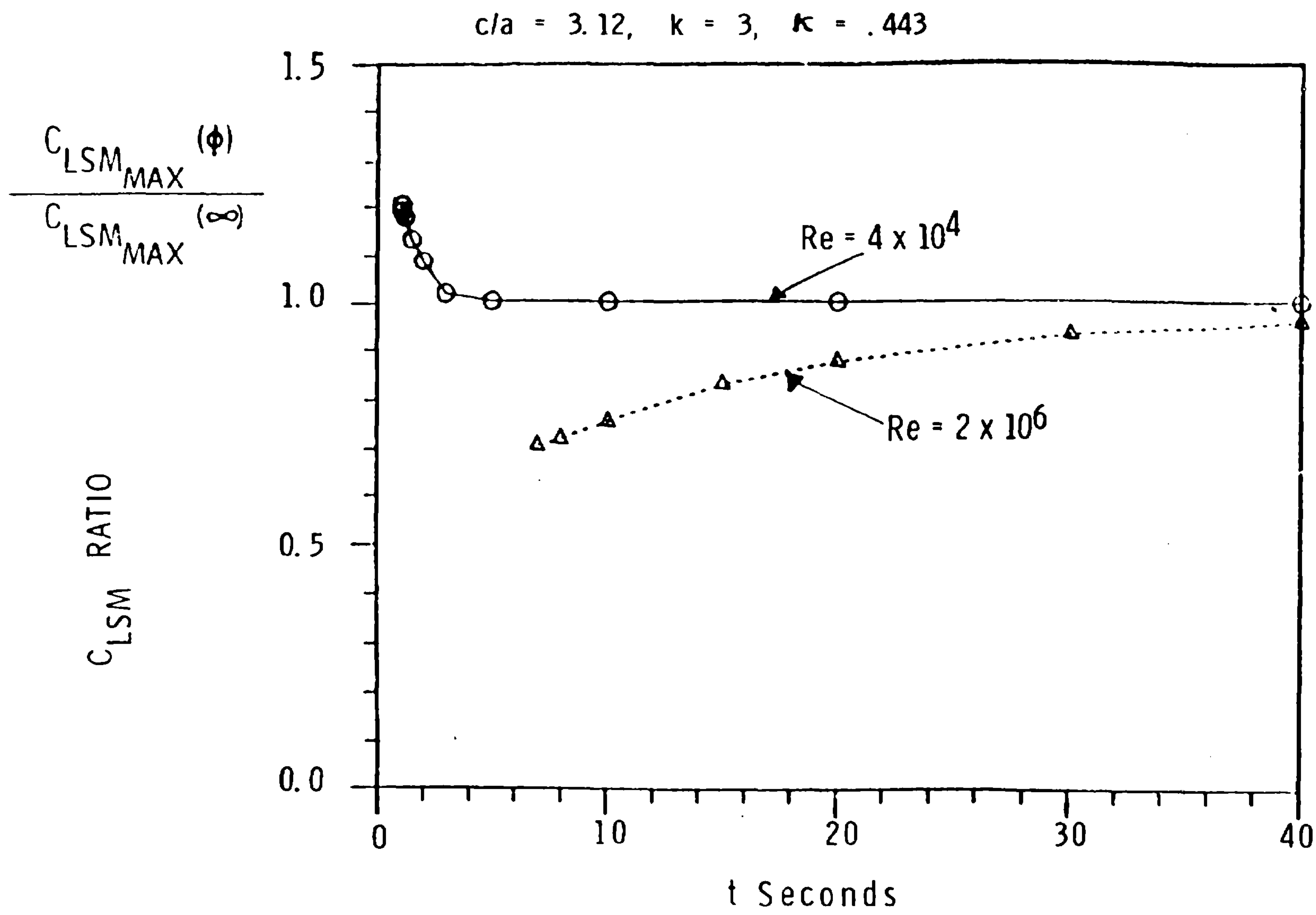

Figure 8. Ratio of Maximum Side Moment Coefficients vs Roll Angle, ϕ for $Re = 4 \times 10^4$, 2×10^6, $c/a = 3.12$, $k = 3$, $n = 1$.

SUMMARY

1. Cylindrical Payloads can be computed by classical methods for all Reynolds numbers.

2. CFD is required for other payload shapes and time accurate computations.

3. 6 DOF calculations include liquid moments.

Blank

NUMERICAL STUDY OF UNSTEADY 3D FLOWS IN A SPINNING AND NUTATING CYLINDER

R. LI & TH. HERBERT

RESEARCH FUNDED BY CRDEC

DEPARTMENT OF MECHANICAL ENGINEERING

THE OHIO STATE UNIVERSITY

COLUMBUS, OHIO

APRIL 1991

PREVIOUS WORK: STEADY STATE ONLY

* FDM (USE ARTIFICIAL COMPRESSIBILITY)
  VAUGH, OBERKAMPF & WOLFE (1985, JFM)

* FDM IN R & Z, FOURIER METHOD IN ϕ.
  STRIKWERDA & NAGEL (1988, J. COMPUT. PHYS)

* SCM (SPECTRAL COLLOCATION METHOD)
  HERBERT & LI (1990, J. AIAA)

PRESENT WORK: UNSTEADY (SPIN-DOWN)

Ω AND θ ARE FIXED, WHILE $\omega(t)$ IS GIVEN.

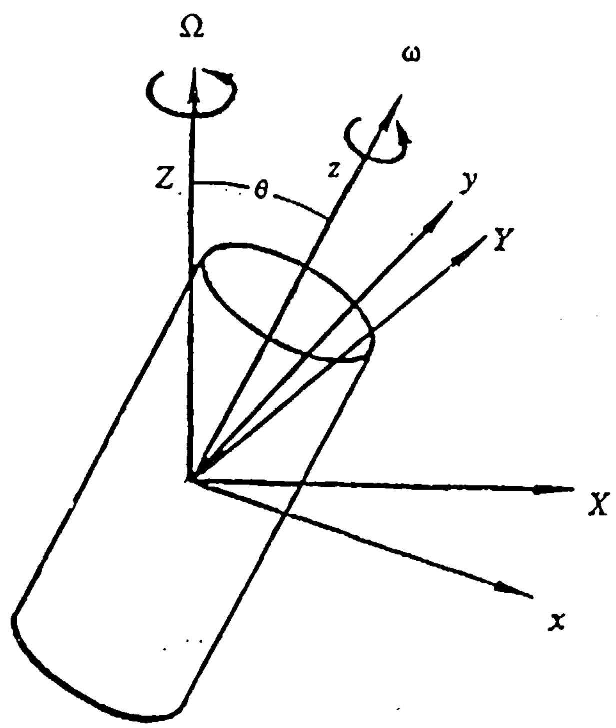

Fig. 1 A sketch of a nutating and spinning cylinder. The frame $(x-y-z)$ is rotating with respect to the fixed frame $(X-Y-Z)$ with the angular velocity Ω.

VELOCITY-VORTICITY FORMULATION

$$\frac{\partial}{\partial t}\mathbf{O} + (\mathbf{V}\cdot\nabla)\,\mathbf{O} = (\mathbf{O}\cdot\nabla)\mathbf{V} + \nu\nabla^2\mathbf{O} + 2\Omega\cdot\nabla\mathbf{V} - 2\dot{\Omega} \quad (1)$$

$$\nabla^2\mathbf{V} = \nabla\times\mathbf{O} \quad (2)$$

ν : KINETIC VISCOSITY

Ω : ANGULAR VELOCITY OF NUTATION

V : VELOCITY

O : VORTICITY $\quad (\mathbf{O} = -\nabla\times\mathbf{V})$

REFERENCE QUANTITIES FOR NONDIMENSIONALIZATION:

RADIUS a, DENSITY ρ, AND ω_{ref}

NUMERICAL METHOD

* FDM IN R & Z (UNIFORM GRID: 20 PTS IN R; 40 PTS IN Z);
* FOURIER METHOD IN ϕ (6 FOURIER MODES);
* VISCOUS TERMS - MULTISTEP IMPLICIT;
* CONVECTIVE TERMS - MULTISTEP EXPLICIT;
* 2ND ORDER ACCURACY IN SPACE & TIME;
* ITERATION: LINE GAUSS-SEIDEL RELAXATION WITH ZEBRA PATTERN (VECTORIZATION).

CALCULATION OF MOMENTS :

VOLUME INTEGRAL

SURFACE INTEGRAL

VOLUME INTEGRAL APPROACH

$$\mathbf{M} = \int \mathbf{r} \times \frac{D\mathbf{V}}{Dt} dV = \frac{\partial}{\partial \mathrm{t}} \mathbf{J} + \mathbf{\Omega} \times \mathbf{J} \tag{3}$$

IF WE DECOMPOSE THE VELOCITY FIELD INTO

$$\mathrm{V} = \mathbf{V}^r + \mathbf{V}^d \tag{4}$$

$\mathbf{V}^r$: RIGID BODY MOTION; $\mathbf{V}^d$: DEVIATION.

THEN

$$\mathbf{J} = \mathbf{J}^r + \mathbf{J}^d \tag{5}$$

WHERE

$$\mathbf{J}^d = (A^d_{23}, \quad -A^d_{13}, \quad A^d_{12}) \tag{6}$$

INTEGRALS (DIMENSIONLESS)

$$A^d_{13} = \int V^d_z r \cos\phi r dr d\phi dz \tag{7}$$

$$A^d_{23} = \int V^d_z r \sin\phi r dr d\phi dz \tag{8}$$

$$A^d_{12} = \frac{1}{2} \int V^d_\phi r^2 dr d\phi dz \tag{9}$$

(INDEED, ONLY NEED FUNDAMENTAL OF V^d_z AND DISTORTION OF THE MEAN OF V^d_ϕ).

DIMENSIONLESS COMPONENTS OF MOMENT

$$M_x = 2\dot{A}^d_{23} \qquad + 2\varepsilon A^d_{13} / \tan\theta \tag{10}$$

$$\overline{M}_y = -2\dot{A}^d_{13} \qquad + 2\varepsilon(A^d_{12} + A^d_{23}/\tan\theta) \tag{11}$$

$$M_z = 2\dot{A}^d_{12} + \eta\pi\dot{\omega}(t) \qquad + 2\varepsilon A^d_{13} \tag{12}$$

$$M_y = \overline{M}_y + \varepsilon\omega(t)\eta\pi + \varepsilon^2\eta\pi(-\frac{2}{3}\eta^2 + \frac{1}{2})/\tan\theta \tag{13}$$

PARAMETERS: $\varepsilon = \Omega\sin\theta/\omega_{ref}$, $\eta = c/a$ (ASPECT RATIO)

WHERE

(1) COMPONENTS DUE TO THE UNSTEADINESS OF RELATIVE MOTION (THE TERM $\frac{\partial}{\partial t}\mathbf{J}$)

RIGID BODY: (0, 0, $\eta\pi\dot{\omega}(t)$)

DEVIATION: ($2\dot{A}^d_{23}$, $-2\dot{A}^d_{13}$, $2\dot{A}^d_{12}$)

(2) COMPONENTS DUE TO THE CORIOLIS ACCELERATION

RIGID BODY: (0, $\varepsilon\omega(t)\eta\pi$, 0)

DEVIATION: ($2\varepsilon A^d_{13}/\tan\theta$, $2\varepsilon(A^d_{12} + A^d_{23}/\tan\theta)$, $2\varepsilon A^d_{13}$)

(3) COMPONENTS DUE TO THE CENTRIPETAL ACCELERATION

RIGID BODY: (0, $\varepsilon^2\eta\pi(-\frac{2}{3}\eta^2 + \frac{1}{2})/\tan\theta$, 0)

RESULTS AND DISCUSSIONS

(1) CALCULATION OF STEADY STATES

* START FROM RIGID BODY MOTION
* COMPARE WITH SCM (5 FOURIER MODES in ϕ,
  5 CHEBYSHEV POLYNOMIALS IN RADIUS,
  5 CHEBYSHEV POLYNOMIALS IN HALF LENGTH.)
* Ω = 500 RPM, ω = 3000 RPM, θ = 20 DEG, $\omega_{ref} = \omega$,
  $\eta = c/a = 4.368$, Re = $a^2\omega/\nu$.
* 0.3 TO 2 MINUTES IN CRAY Y-MP FOR Re < 200.

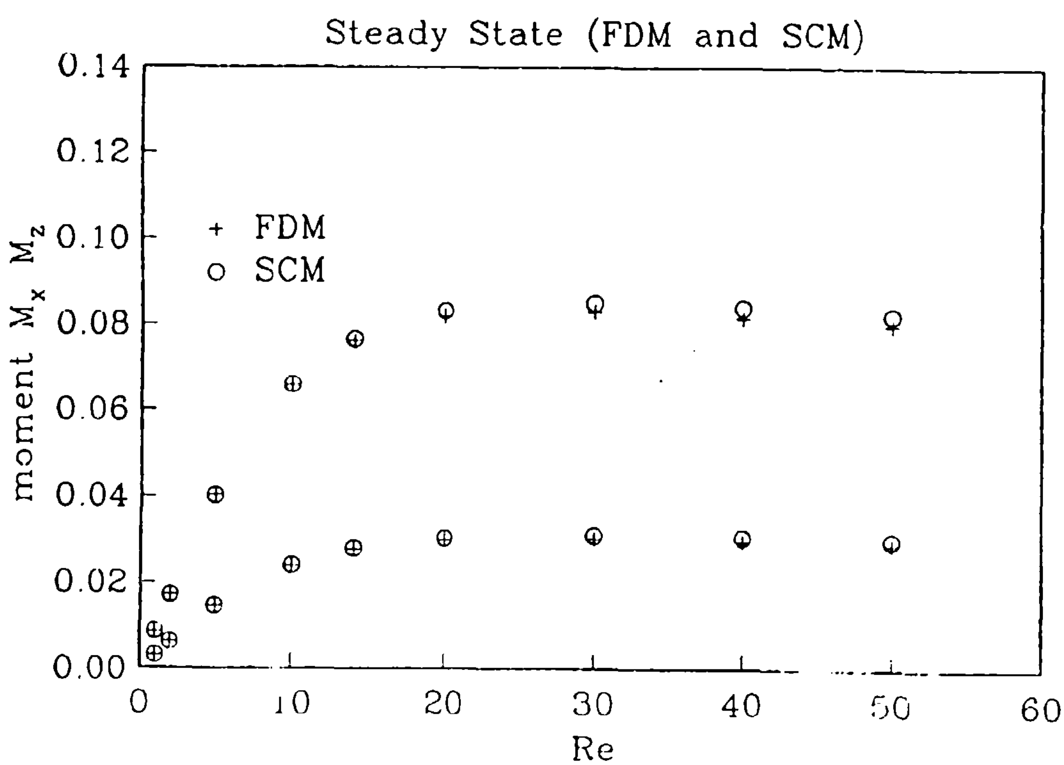

(2) SPIN-DOWN OF 60 KCS FLUID

* $\Omega = 500$ RPM, $\theta = 20$ DEG, $\eta = 4.4955$.

  $\omega_{ref} = 2\Omega = 1000$ RPM.

  "INSTANTANEOUS REYNOLDS NO." : $Re = a^2\omega(t)/\nu$.

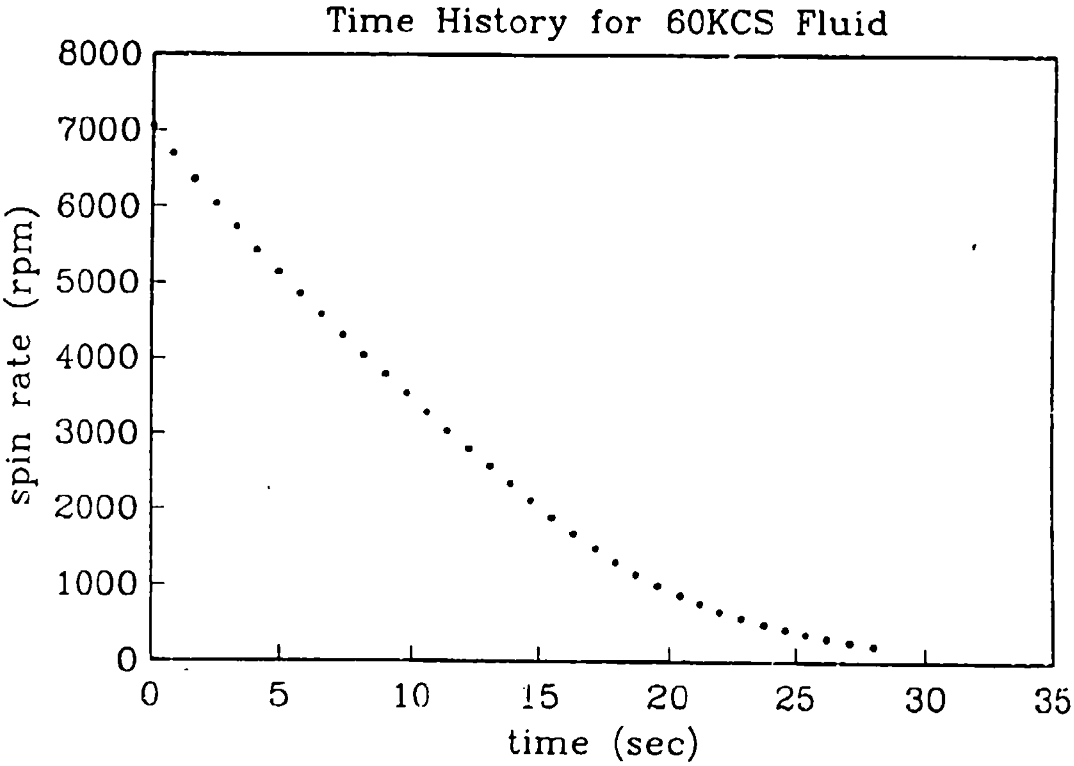

(A) CALCULATE STEADY STATES AT DIFFERENT SPIN RATE.

(B) START FROM STEADY STATE AT $t = 0$, USE THE GIVEN $\omega(t)$ AS TIME-DEPENDENT BOUNDARY, RUN THE "QUASI-STEADY" SPIN-DOWN.

* TIME $t = 0$ TO $t = 3000$

  $\Delta t = 0.02$, 150,000 TIMESTEP, 5 HRS. IN CRAY.

EXAMPLE FOR STEP (A): STEADY STATE AT $\omega = 6800$ RPM

A_1 : FUNDAMENTAL OF $V_z^d(r = 0.5, z = 0, \phi = 0)$

A_0 : DISTORTION OF MEAN FLOW OF $V_\phi^d(r = 0.5, z = 0, \phi = 0)$

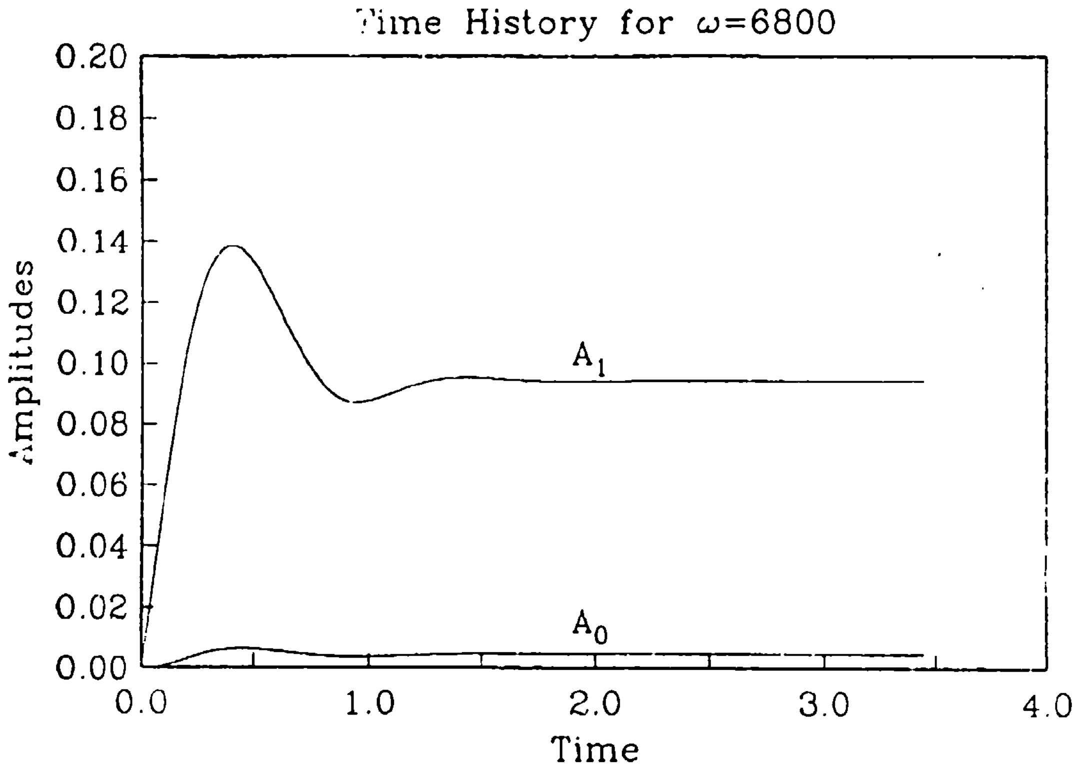

FLUID DEVELOPS FROM RIGID BODY MOTION TO STEADY STATE RAPIDLY.

THE INTEGRALS OF UNSTEADY ("QUASI-STEADY") ARE THE SAME AS THOSE OF STEADY STATE.

CONCLUSION : THE UNSTEADY FLOW FIELD ADAPTS VERY QUICKLY TO THE SLOWLY CHANGING BOUNDARY CONDITIONS.

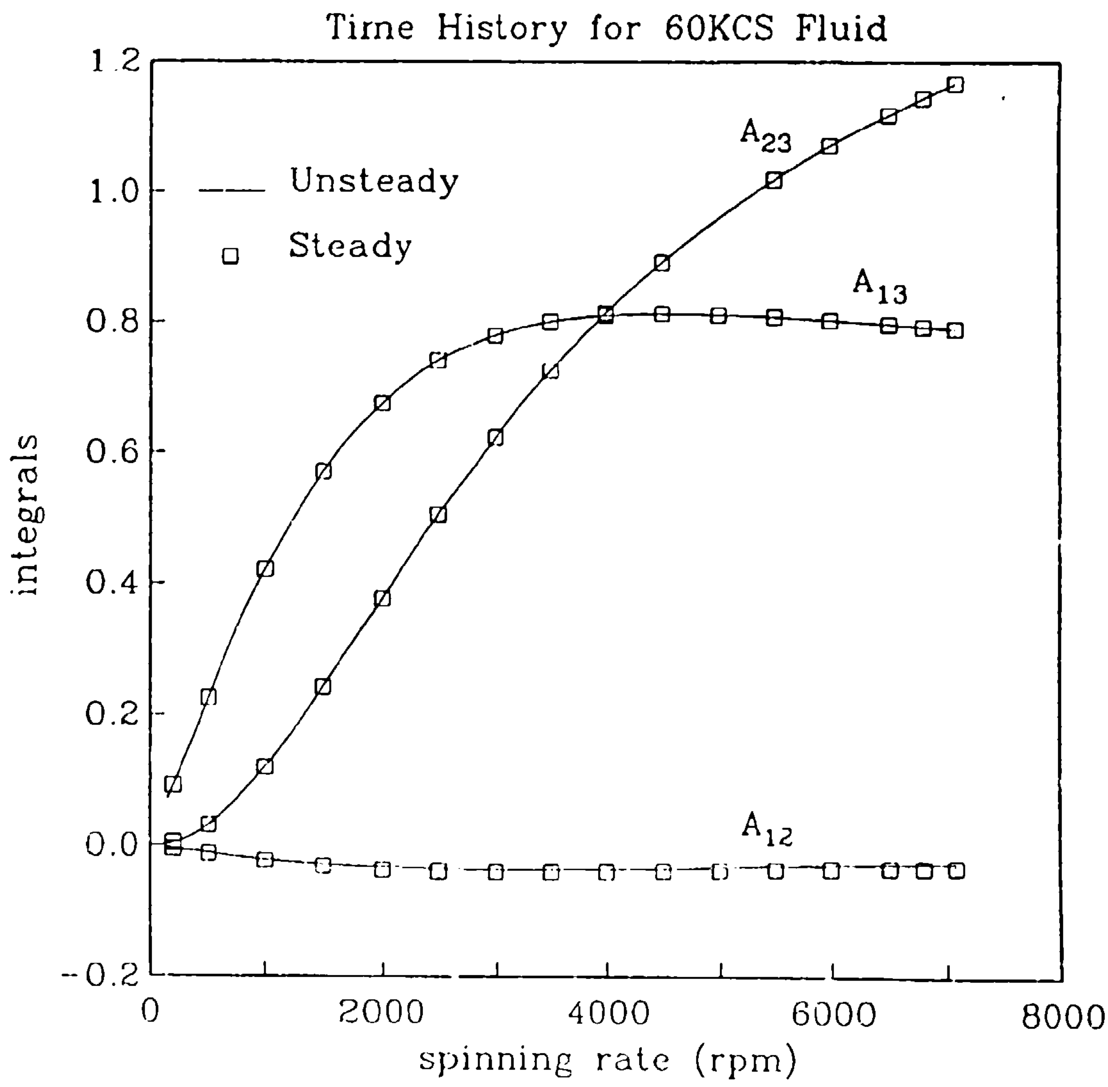

M_x and $\overline{M}_y$ OF UNSTEADY ("QUASI-STEADY") ARE THE SAME AS THOSE OF STEADY STATE.

M_z OF UNSTEADY ("QUASI-STEADY") IS BELOW THAT OF STEADY STATE.

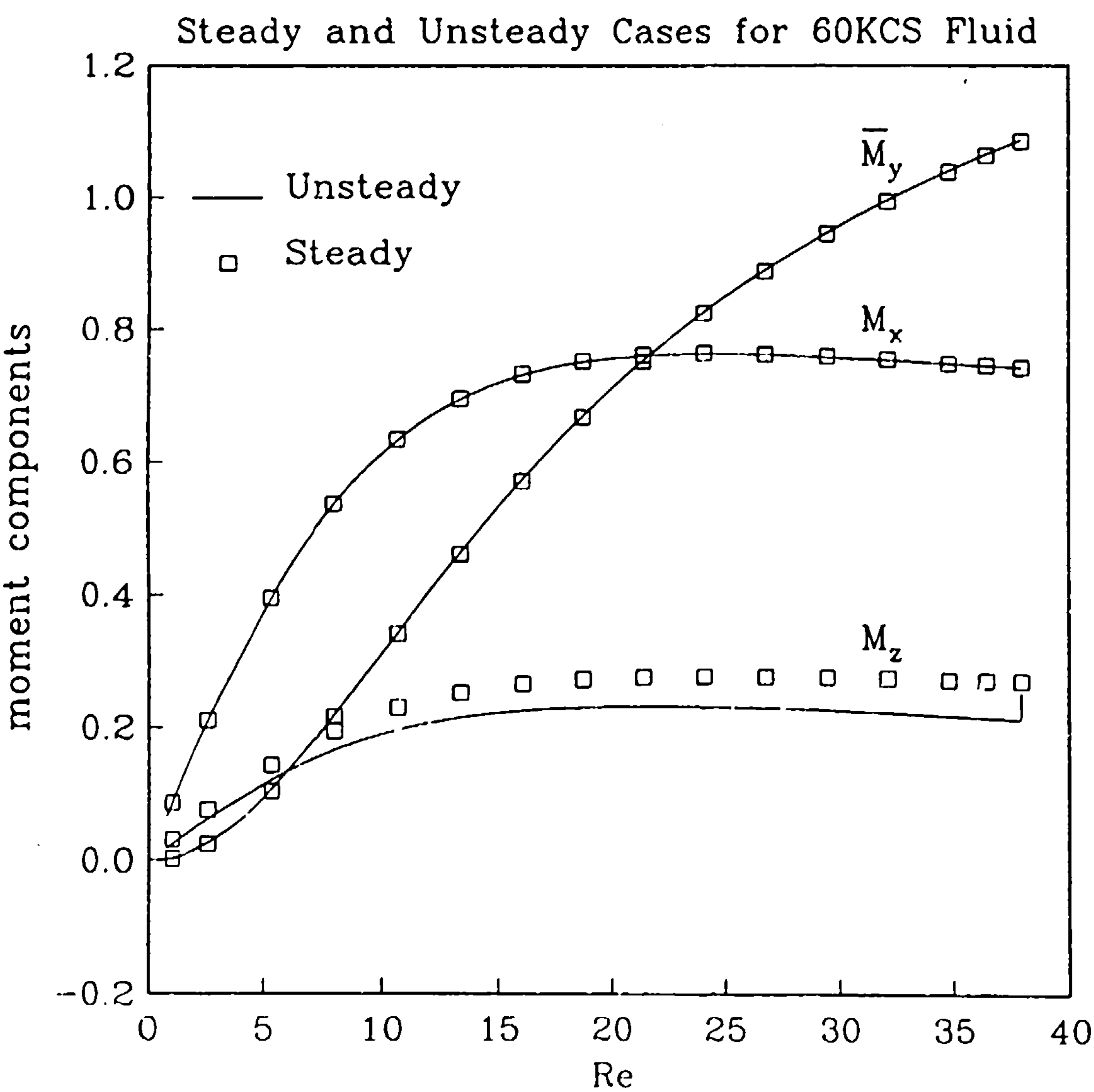

THE CONTRIBUTION OF TIME DERIVATIVES OF INTEGRALS OF UNSTEADY ("QUASI-STEADY") TO THE MOMENT COMPONENTS ARE NEGLIGIBLE.

THE CHANGE OF SPIN RATE, $\dot{\omega}(t)$, HAS CERTAIN EFFECT ON THE RESULTS OF M_z (NOTE: $\eta\pi\dot{\omega}(t)$ REPRESENTS THE UNSTEADY RIGID BODY MOTION).

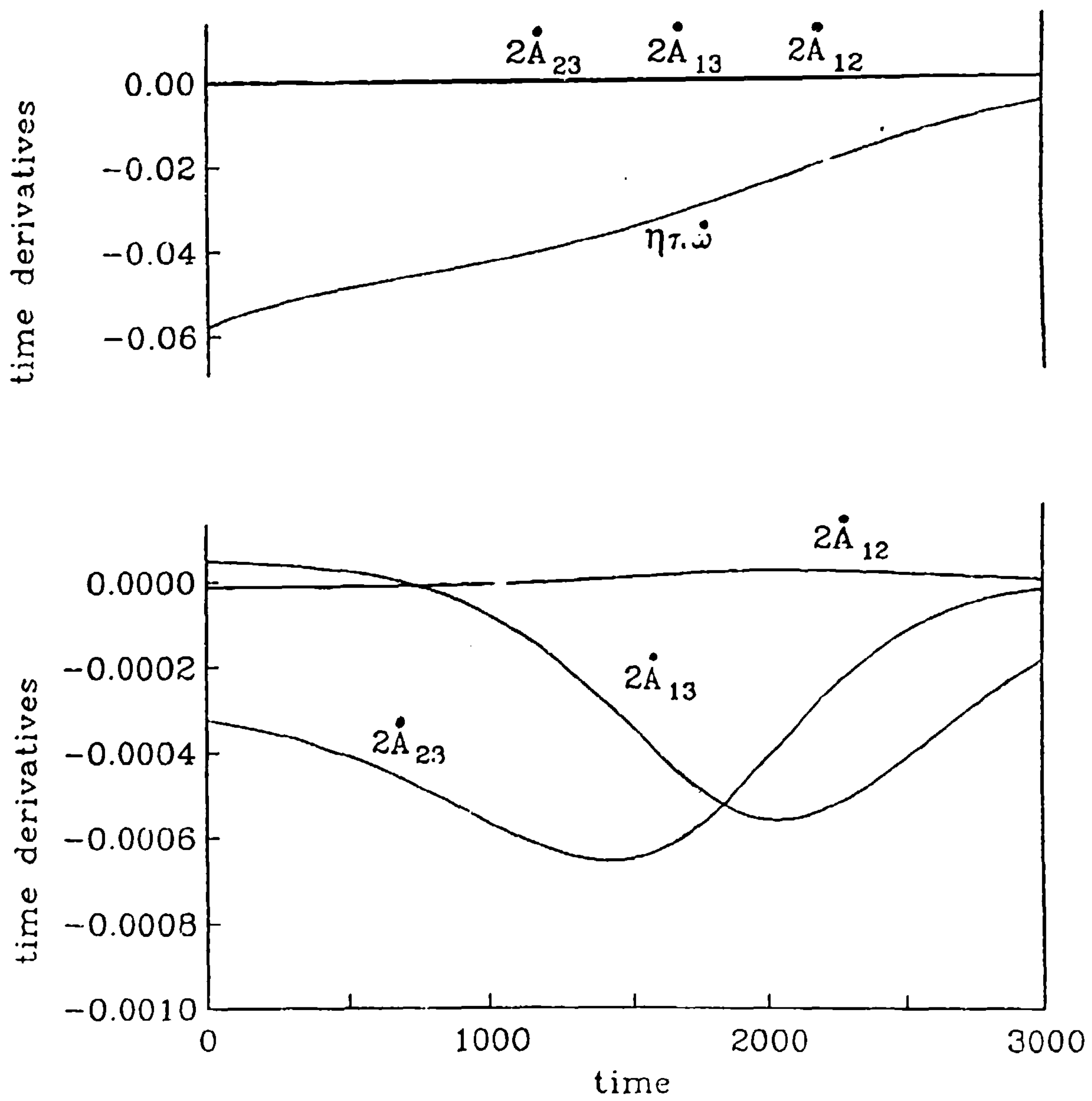

(3) SPIN-DOWN OF 10 KCS FLUID

SIMILAR RESULTS TO 60 KCS FLUID.

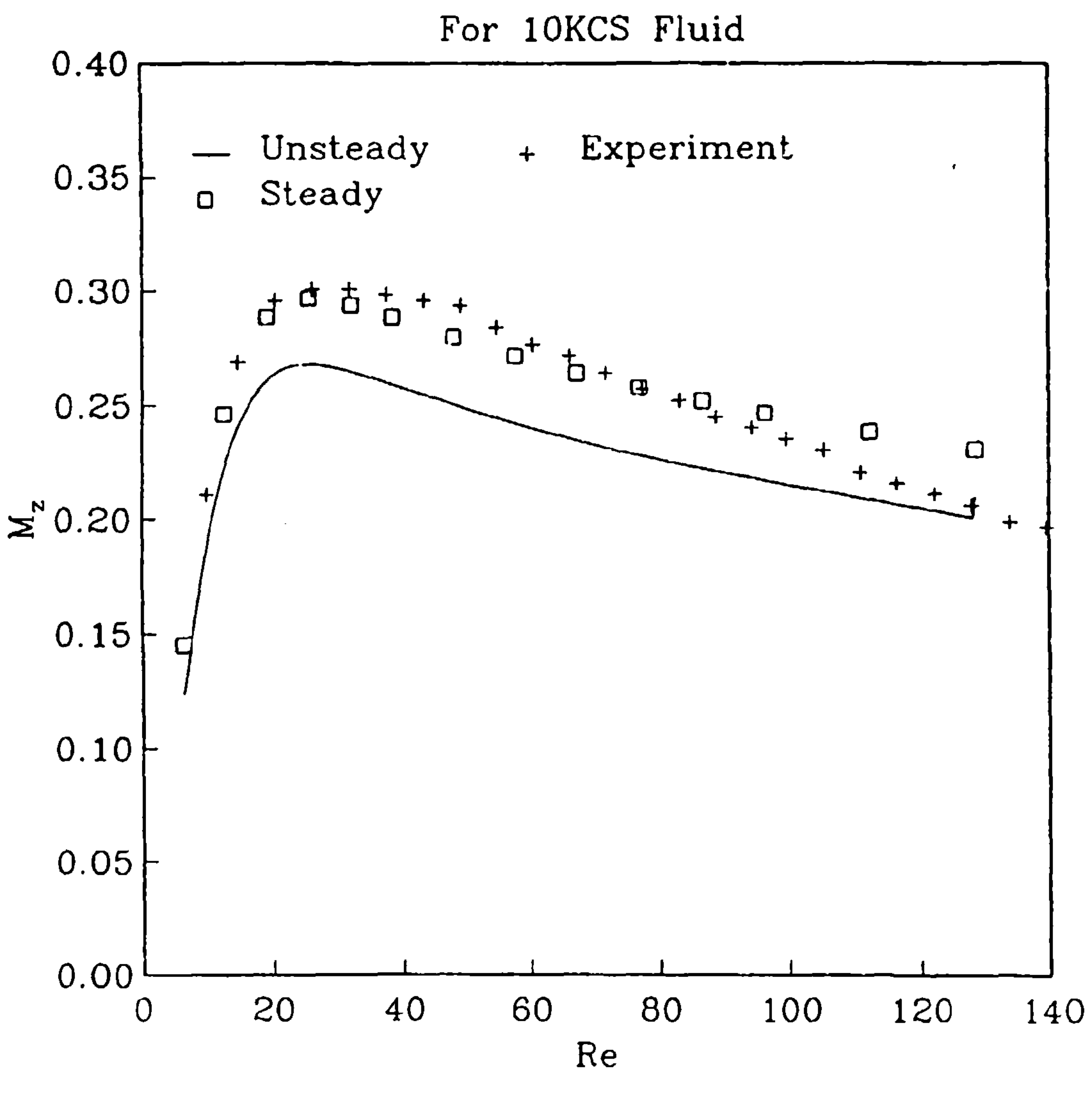

SUMMARY

(1) FOR MOMENT $\mathbf{M} = \frac{\partial}{\partial t}\mathbf{J} + \mathbf{\Omega} \times \mathbf{J}$, THE VISCOUS FLOW HAS LITTLE EFFECTS TO THE TERM $\frac{\partial}{\partial t}\mathbf{J}$, BUT IMPORTANT CONTRIBUTION TO THE TERM RELATED TO CORIOLIS ACCELERATION WHICH IS INCLUDED IN THE TERM $\mathbf{\Omega} \times \mathbf{J}$.

(2) THE MOMENTS OBTAINED FROM THE "QUASI-STEADY" SPIN-DOWN EXPERIMENTS CAN BE REGARDED AS THOSE FOR STEADY STATES IF THEY ARE CORRECTED BY TAKING THE UNSTEADY RIGID BODY MOTION (THE TERM $\eta\pi\dot{\omega}(t)$) INTO ACCOUNT.

(3) FOR STEADY FLOW, $M_Z = -M_x \sin\theta + M_z \cos\theta = 0$

BUT FOR UNSTEADY FLOW,

$$M_Z = -M_x^d \sin\theta + M_z^d \cos\theta = -2(\dot{A}_{23}^d \sin\theta - \dot{A}_{12}^d \cos\theta) + \lambda\pi\dot{\omega}(t)\cos\theta$$

(4) THE FORMULA OF MOMENT CAN BE EASILY EXTENDED TO THE UNSTEADY CASE THAT BOTH Ω AND ω ARE CHANGING WHILE θ IS FIXED (FOR EXAMPLE, "SPIN-UP").

Modelling Non-Newtonian Behavior

R. Li

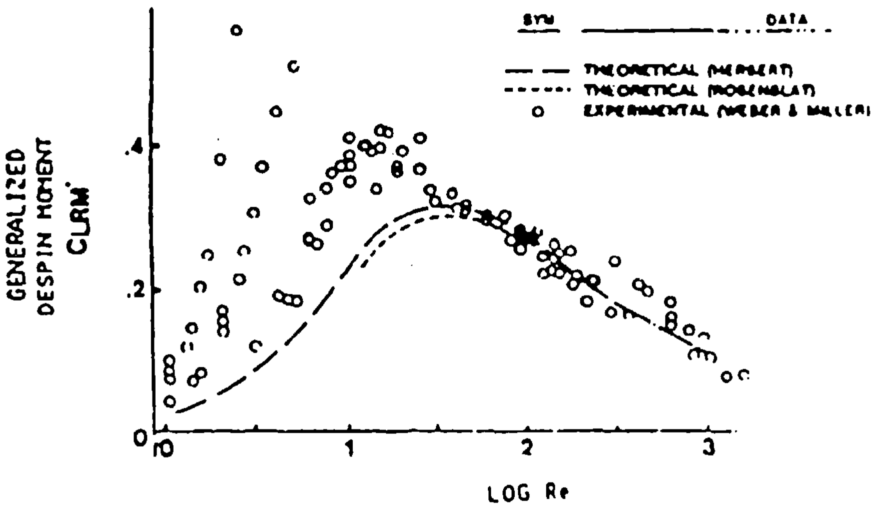

Obvious non-Newtonian behavior for high viscosity Silicone 200 fluids (for example, $\nu \geqslant 60$ kcs)

S. Rosenblat et. al. (1986)

Analytical work (perturbation method)

Numerical Studies (FEM)

No measured data from experiments available.

R. P. Tytus (1989, CRDEC)

measured Silicone 200 fluids

used the formula of differential model derived by Rosenblat to calculate the despin moment — good agreement was not achieved.

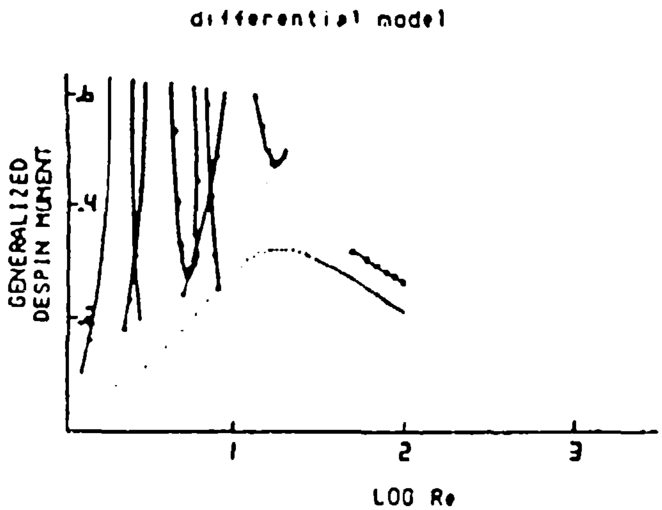

Problem: two terms are missing in Rosenblat's formula.

The corrected formula seems better for 100 kcs.

Future work: 1. Check other high viscosities;

2. 3-D numerical studies.

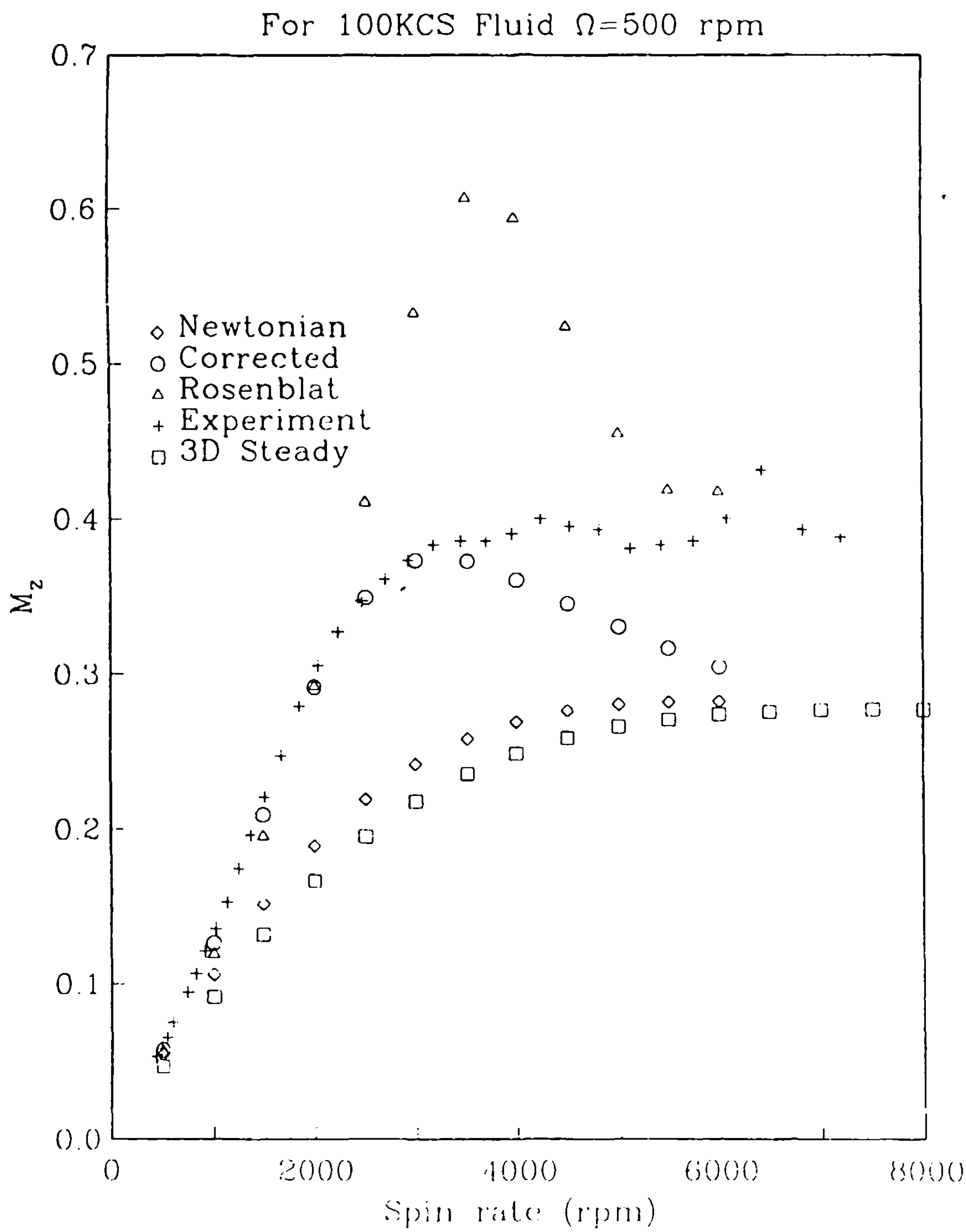
For 100KCS Fluid Ω=500 rpm
0.7
0.6
0.5
0.4
0.3
0.2
0.1
0.0
M_z
Newtonian
Corrected
Rosenblat
Experiment
3D Steady
0
2000
4000
6000
8000
Spin rate (rpm)

BALLISTIC RESEARCH LABORATORY

US ARMY
LABORATORY COMMAND

Numerical Simulation for Non-Cylindrical Liquid-Filled Containers

Michael J. Nusca

Free Flight Aerodynamics Branch
Launch and Flight Division, U.S. Army BRL
Aberdeen Proving Ground, MD 21005

Presented at the AHPCRC Workshop on Problems of Rotating Fluids, University of Minnesota, April 22-23, 1991

Non-Cylindrical Containers
Previous Analytical and Experimental Work

- Theory: Wedemeyer, BRL Report No. 1326, 1966
  - Linear Euler equations (Re $= \infty$)
  - Small variation of sidewall radius with axial length, $|da/dz| \ll 1$
  - Approximate eigenfrequencies computed

- Experiments: Karpov, BRL Report No. 1332, 1966
  - Investigated rounded endwall corners. For corner radii $\leq 60\%$ of the cylinder radius, eigenfrequencies remain constant for constant liquid volume.
  - Investigated conical reduction of cylinder ends. The fill ratio at which the eigenfrequency = gyroscope nutational frequency increases with cone angle.
  - Data shows that Wedemeyer's theory is valid for $|da/dz| \leq .2$

Overview

- Steady, Low Reynolds Number Flow (1988-1989)
  - Strikwerda's code for cylindrical geometry (1985)
  - Central & spectral finite-differencing, LSOR method
  - Psuedo-compressibility, pressure update from $\nabla \cdot \vec{V}$
  - Aeroballistic coordinate system
  - Reformulated for generalized geometry, **UWISC/BRL**
  - Volume integral method for $C_{\mathrm{LRM}}, C_{\mathrm{LSM}}$

- Unsteady, Arbitrary Reynolds Number Flow (1990-1991)
  - Rockwell **USA-IN3** code (Chakravarthy & Pan)
  - Time accurate, upwind TVD method
  - Psuedo-compressibility with $\nabla \cdot \vec{V} = 0$ at each Δt
  - Continuity equation incl. moving grid, inertial coord. system
  - Generalized geometry, Zonal mesh
  - Volume integral method for $C_{\mathrm{LRM}}, C_{\mathrm{LSM}}$ added
  - Turbulence and separated flow models

Configuration and Nomenclature

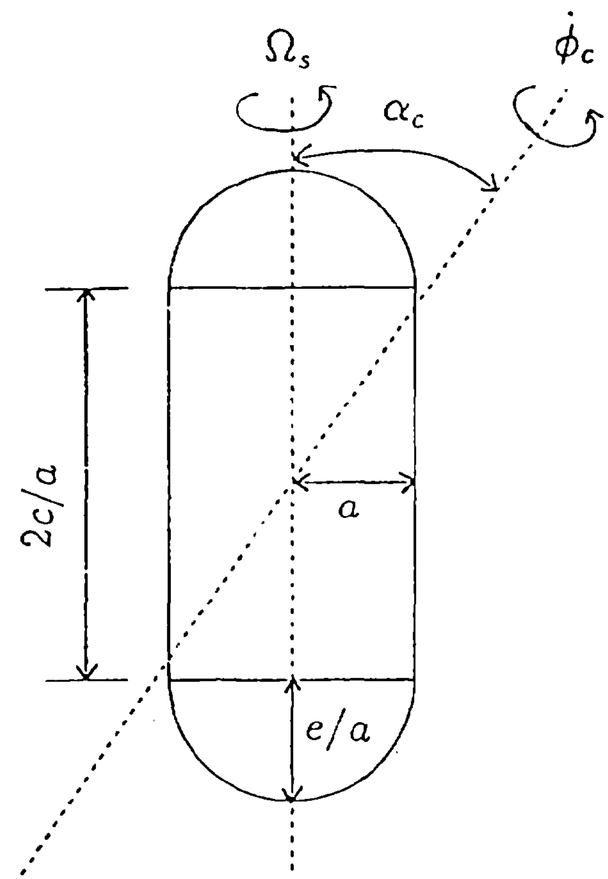

Computational Grid

Cylinder/Hemispherical Endcaps

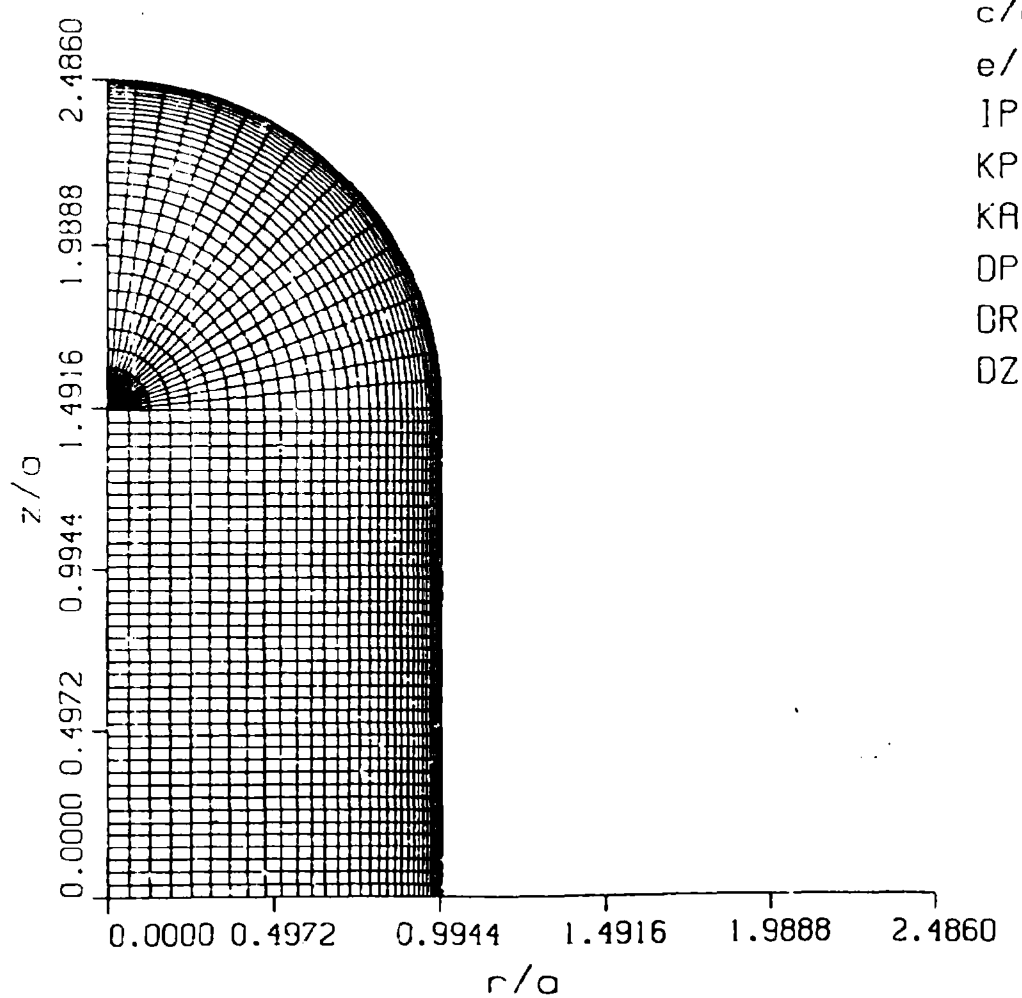

c/a	=	1.48600
e/a	=	1.00000
IPTS	=	31
KPTS	=	117
KAPPTS	=	19
DPHI (D)	=	0.00000
DRWALL	=	0.00700
DZWALL	=	0.00000

Computational Grid

Truncated Ellipsoid

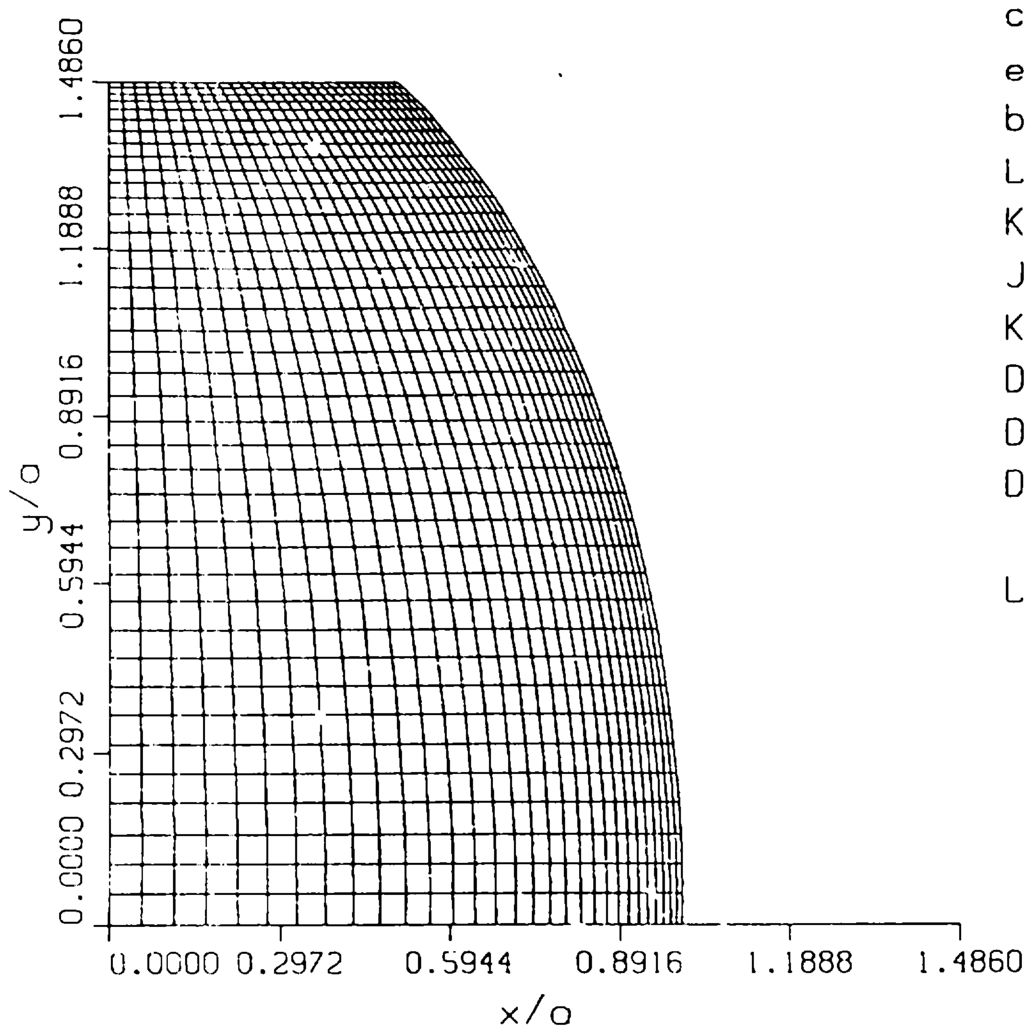

c/a	=	1.48600
e/a	=	0.00000
b/a	=	0.50000
LPTS	=	21
KPTS	=	81
JPTS	=	31
KAPPTS	=	1
DPHI (D)	=	100.000
DXWALL	=	0.01000
DYWALL	=	0.01000
LPOINT	=	1

UWISC/BRL – Governing Equations

- 3D Navier-Stokes equations (inertial, cartesian coordinate system)

$$\rho\frac{\mathrm{D}\vec{V}}{\mathrm{D}t} = -\nabla p + \mu\nabla^2\vec{V} \qquad \nabla\cdot\vec{V} = \delta \qquad p^{m+1} = p^m - \beta\left(\nabla\cdot\vec{V}^{m+1}\right)$$

- Equations transformed to non-inertial reference frame; $\partial/\partial t = 0$
  Reference frame rotates with angular velocity $\dot{\phi}_c$ about coning axis

- Cylindrical coordinate system r, ϕ, z with velocities u, v, w
  Same coordinate system for endcaps; grid lines not aligned in r, z

- Equations, variables non-dimensionalized by a and $a\dot{\phi}$
  Reynolds No., precessional frequency; $\mathrm{Re} = a^2\dot{\phi}/\nu$, $\tau = \dot{\phi}_c/\dot{\phi}$

- Solid-body rotation subtracted from $\vec{V}$ and p redefined;

$$\vec{V} = \vec{V}_{\text{computed}} + \vec{V}_{\text{solid-body}} + \vec{\tau}\times\vec{r}$$

$$p = p_{\text{computed}} + \frac{r^2}{2} + r^2\tau\cos\alpha_c + \frac{\tau^2}{2}\left[(r\cos\phi\cos\alpha_c + z\sin\alpha_c)^2 + r^2\sin^2\alpha_c\right]$$

UWISC/BRL – Boundary Conditions

- Container walls: no-slip for velocity, extrapolation for pressure
  - Axisymmetric geometry requires

$$u_{I,j,k} = v_{I,j,k} = w_{I,j,k} = 0 \qquad p_{I,j,k} = 3p_{I-1,j,k} - 3p_{I-2,j,k} + p_{I-3,j,k}$$

  - Cylindrical geometry also requires

$$u_{i,j,1} = u_{i,j,K} = v_{i,j,1} = v_{i,j,K} = w_{i,j,1} = w_{i,j,K} = 0$$
$$p_{i,j,1} = 3p_{i,j,2} - 3p_{i,j,3} + p_{i,j,4} \qquad p_{i,j,K} = 3p_{i,j,K-1} - 3p_{i,j,K-2} + p_{i,j,K-3}$$

- Container z-axis $(r/a = 0)$: interpolation from interior points

$$u_{1,j,k} = \frac{1}{3}\left(\frac{4}{J}\sum_{j=1}^{J} u_{2,j,k} - \frac{1}{J}\sum_{j=1}^{J} u_{3,j,k}\right) \qquad \text{(similarly for } v, w\text{)}$$
$$p_{1,j,k} = \frac{1}{3}\left(\frac{4}{J}\sum_{j=1}^{J} p_{2,j,k} - \frac{1}{J}\sum_{j=1}^{J} p_{3,j,k}\right)$$

- Container axis at interface of cylinder and endcaps $(r = 0, z = |c/a|)$ assigned equal values (obtained from interpolation)

UWISC/BRL – Numerical Method

- Follows that of Strikwerda
- Central finite differences for r and z derivatives
- Psuedo-spectral differences for the ϕ derivatives
- Line-successive-over-relaxation (LSOR) solution scheme
- Psuedo-compressibility method
  - $\nabla \cdot \vec{V} = \delta$ where δ is 2nd order truncation error

$$p^{m+1} = p^m - \beta\left(\nabla \cdot \vec{V}^{m+1}\right)$$

where m is the iteration index and β is a parameter

Liquid-Induced Moments

- Conservation of Angular Momentum
  (Control volume **V**, surface **S**, constant angular rate Ω)

$$\begin{aligned}\vec{M} &= \int_{\mathrm{S}} \left(\vec{r} \times \vec{F}\right) \mathrm{dS} \\ &= \int_{\mathrm{V}} \vec{r} \times \left(2\vec{\Omega} \times \vec{V}\right) \rho \mathrm{dV} + \int_{\mathrm{V}} \vec{r} \times \left[\vec{\Omega} \times \left(\vec{\Omega} \times \vec{r}\right)\right] \rho \mathrm{dV} + \int_{\mathrm{S}} \left(\vec{r} \times \vec{V}\right) \rho \vec{V} \cdot \mathrm{dS} \\ &= (M_x, M_y, M_z)\end{aligned}$$

Note, $\vec{V} \cdot \mathrm{dS} \equiv 0$ on **S**

- Herbert and Rosenblat have shown,

$$M_x = \frac{2\cos\alpha_c}{\tau} \int_{-\eta}^{\eta} \int_0^{2\pi} \int_0^{r_{\max}} \left[w r^2 \cos\phi\right] \mathrm{d}r \mathrm{d}\phi \mathrm{d}z \qquad \mathrm{M_z} = -\mathrm{M_x} \tan\alpha_c$$

- Thus,

$$C_{\mathrm{LSM}} = \frac{1}{\pi (c/a) \tan\alpha_c} \int_{-\eta}^{\eta} \int_0^{2\pi} \int_0^{r_{\max}} \left[w r^2 \cos\phi\right] \mathrm{d}r \mathrm{d}\phi \mathrm{d}z \qquad C_{\mathrm{LRM}} = -C_{\mathrm{LSM}} \tan\alpha_c$$

where, $\eta = c/a, r_{\max} = 1$ for cylindrical **V** and $\eta = c/a + e/a, r_{\max} = r_{\max}(z)$ for axisymmetric **V**

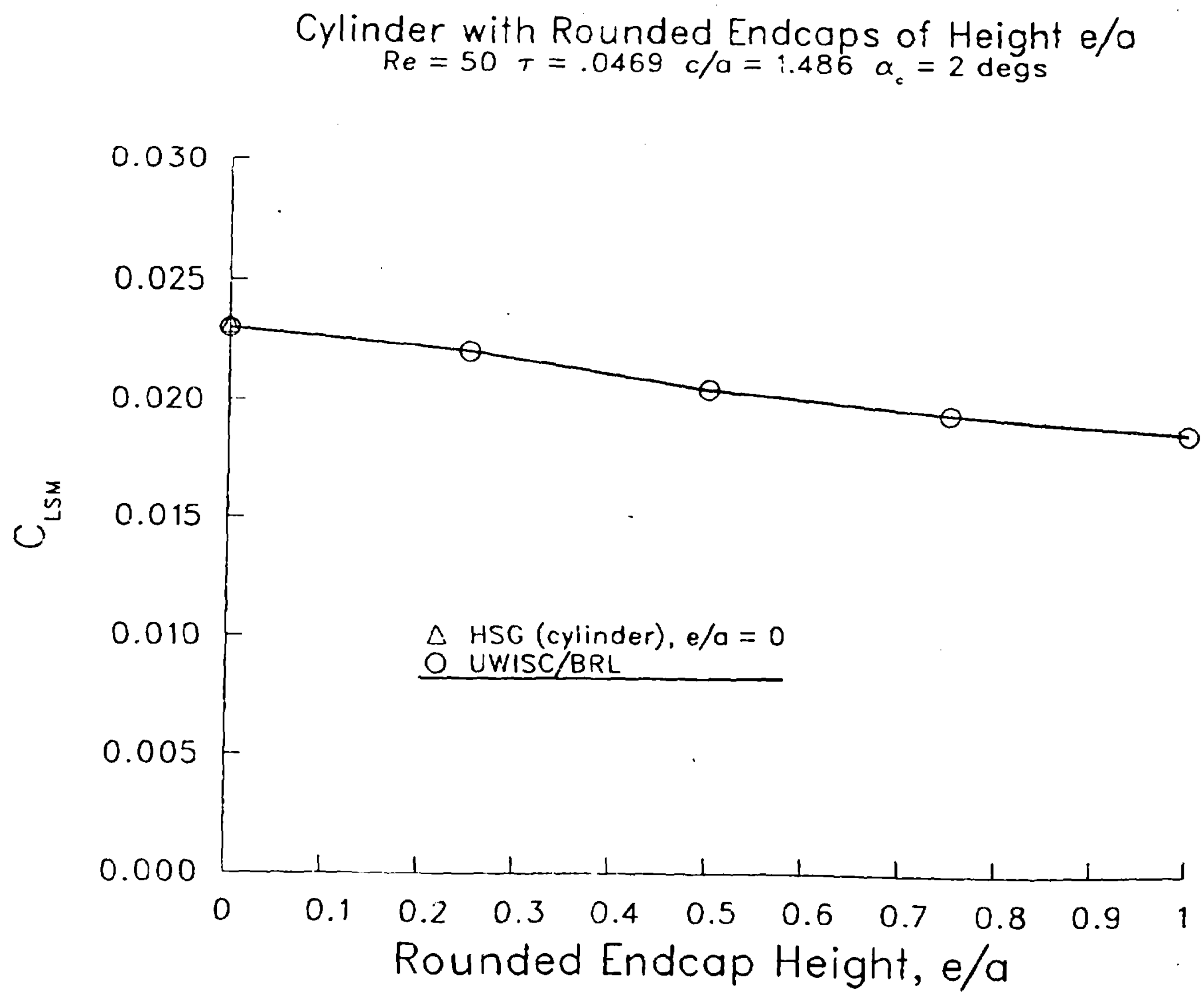
Cylinder with Rounded Endcaps of Height e/a
Re = 50 τ = .0469 c/a = 1.486 αc = 2 degs
C LSM
0.030
0.025
0.020
0.015
0.010
0.005
0.000
0
0.1
0.2
0.3
0.4
0.5
0.6
0.7
0.8
0.9
1
Rounded Endcap Height, e/a
△ HSG (cylinder), e/a = 0
○ UWISC/BRL

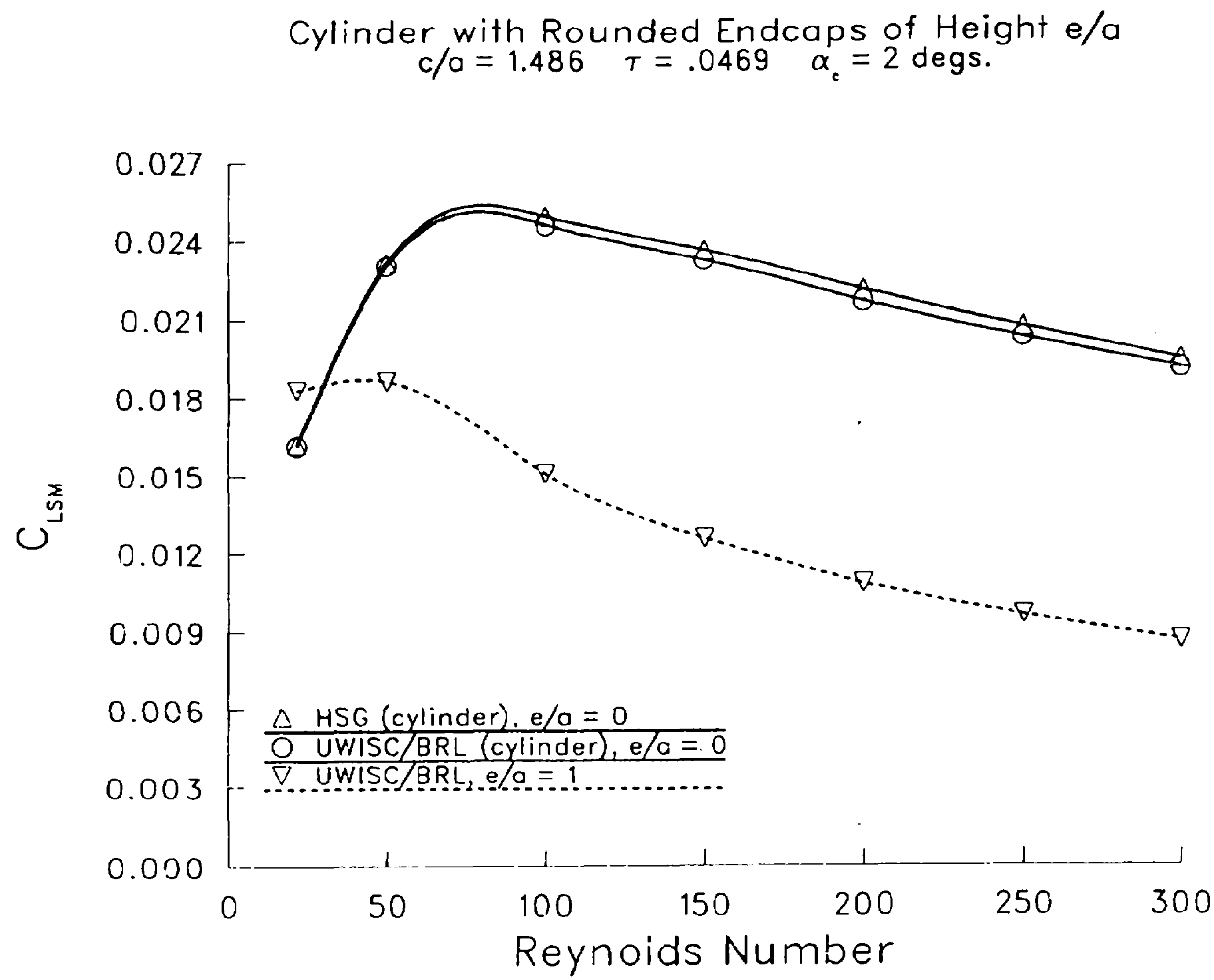
Cylinder with Rounded Endcaps of Height e/a
c/a = 1.486   τ = .0469   αc = 2 degs.
C_LSM
0.027
0.024
0.021
0.018
0.015
0.012
0.009
0.006
0.003
0.000
0
50
100
150
200
250
300
Reynolds Number
△ HSG (cylinder), e/a = 0
○ UWISC/BRL (cylinder), e/a = 0
▽ UWISC/BRL, e/a = 1

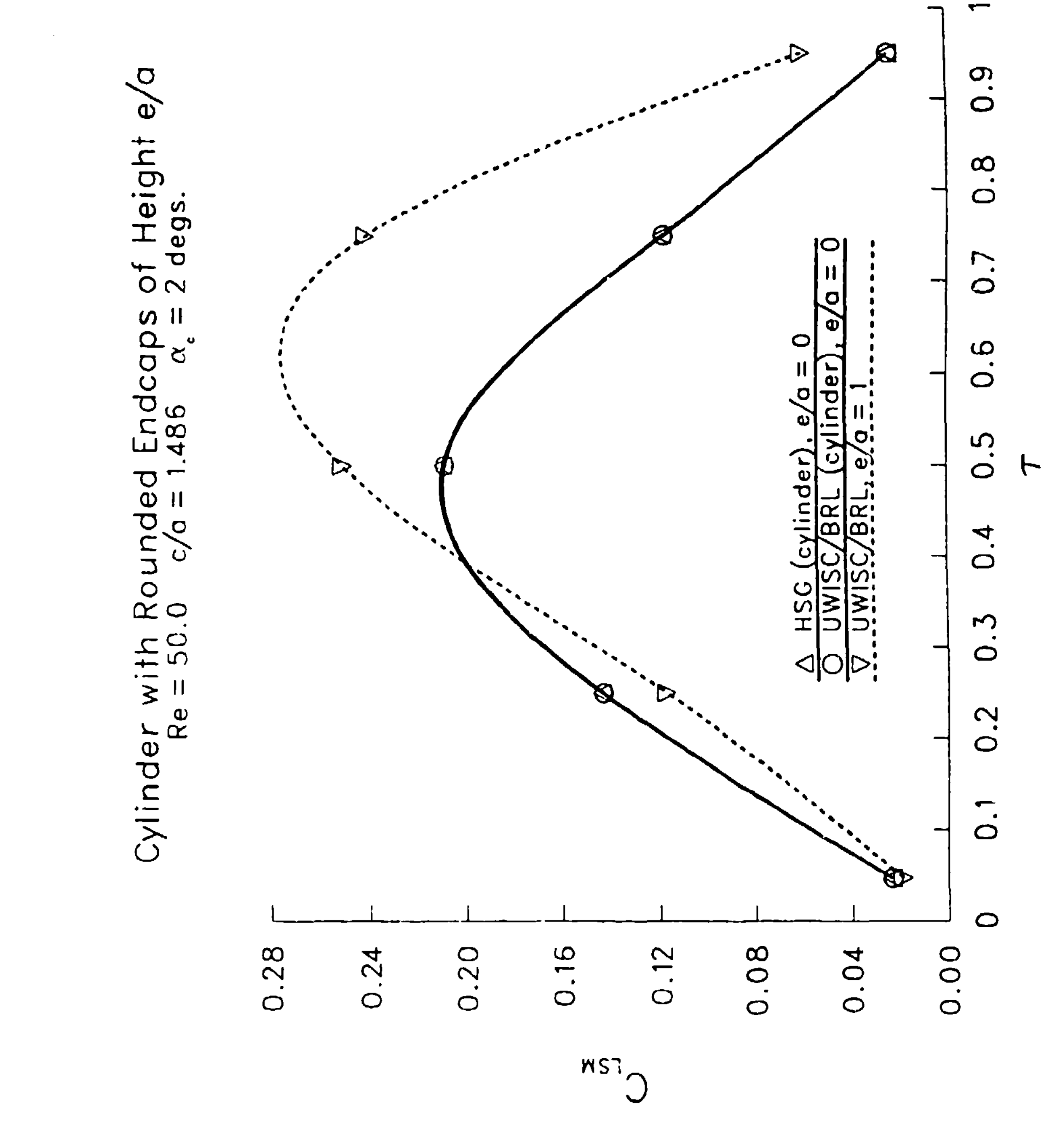
Cylinder with Rounded Endcaps of Height e/a
Re = 50.0 c/a = 1.486 α_c = 2 degs.
△ HSG (cylinder), e/a = 0
○ UWISC/BRL (cylinder), e/a = 0
▽ UWISC/BRL, e/a = 1
C_{LSM}
0.00
0.04
0.08
0.12
0.16
0.20
0.24
0.28
0
0.1
0.2
0.3
0.4
0.5
0.6
0.7
0.8
0.9
1
τ

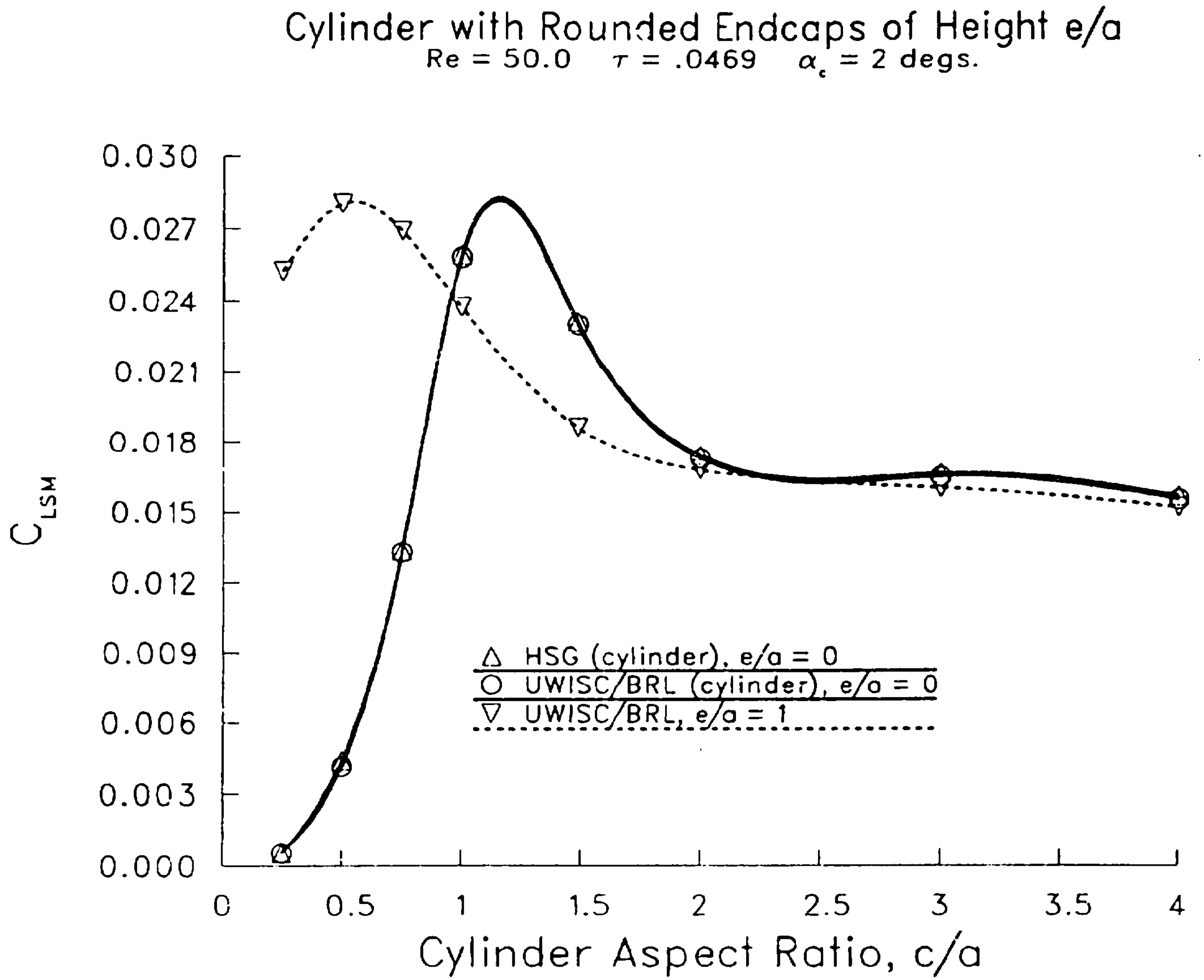
Cylinder with Rounded Endcaps of Height e/a
Re = 50.0   τ = .0469 α_c = 2 degs.
C_{LSM}
0.030
0.027
0.024
0.021
0.018
0.015
0.012
0.009
0.006
0.003
0.000
0
0.5
1
1.5
2
2.5
3
3.5
4
Cylinder Aspect Ratio, c/a
△ HSG (cylinder), e/a = 0
○ UWISC/BRL (cylinder), e/a = 0
▽ UWISC/BRL, e/a = 1

UWISC/BRL – Conclusions

- Finite-Difference Navier-Stokes code
  - Three-dimensional equations
  - Steady-state flow
  - Psuedo-spectral ϕ differencing
  - Implicit LSOR solution scheme

- Rewritten to generalized axisymmetric geometry
  - Efficient for Re $\leq$ 300

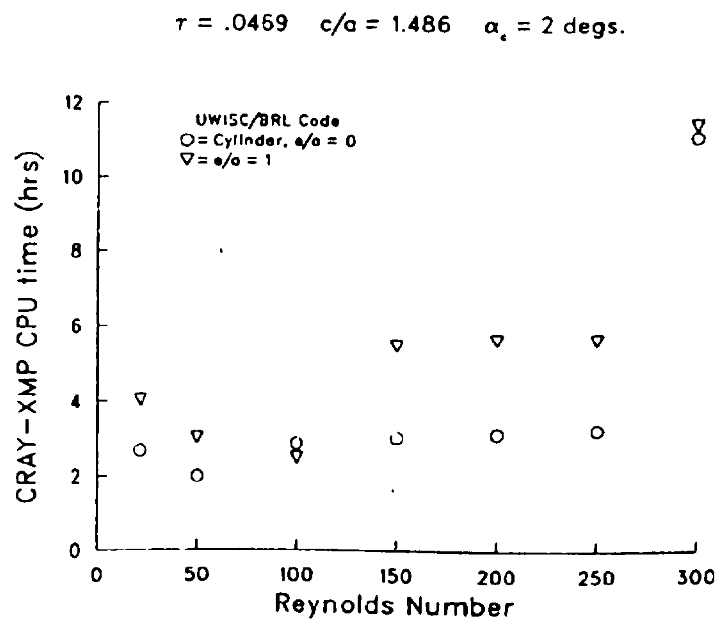

USA-IN3 – Governing Equations

- 3D Navier-Stokes equations (inertial, cartesian coordinate system)

$$\frac{\partial \bar{Q}}{\partial t} + \frac{\partial \bar{E}}{\partial x} + \frac{\partial \bar{F}}{\partial y} + \frac{\partial \bar{G}}{\partial z} = 0$$

$$\bar{Q} = \begin{pmatrix} p \\ u \\ v \\ w \end{pmatrix}, \bar{E} = \begin{pmatrix} \beta u \\ u^2 + p \\ vu \\ wu \end{pmatrix}, \bar{F} = \begin{pmatrix} \beta v \\ uv \\ v^2 + p \\ wv \end{pmatrix}, \bar{G} = \begin{pmatrix} \beta w \\ uw \\ vw \\ w^2 + p \end{pmatrix}$$

$$\nabla \cdot \vec{V} = 0 \quad \text{when} \quad \frac{\partial p}{\partial t} = 0 \quad (\beta = \text{artificial compressibility factor})$$

- Equations transformed to generalized inertial coordinates

$$\frac{\partial Q}{\partial \tau} + \frac{\partial E}{\partial \xi} + \frac{\partial F}{\partial \eta} + \frac{\partial G}{\partial \zeta} = 0$$

$$Q = \frac{\bar{Q}}{J} \qquad E = \frac{\xi_t}{J} I_d \bar{Q} + \frac{\xi_x}{J}\bar{E} + \frac{\xi_y}{J}\bar{F} + \frac{\xi_z}{J}\bar{G}$$

$$F = \frac{\eta_t}{J} I_d \bar{Q} + \frac{\eta_x}{J}\bar{E} + \frac{\eta_y}{J}\bar{F} + \frac{\eta_z}{J}\bar{G} \qquad G = \frac{\zeta_t}{J} I_d \bar{Q} + \frac{\zeta_x}{J}\bar{E} + \frac{\zeta_y}{J}\bar{F} + \frac{\zeta_z}{J}\bar{G}$$

- I_d matrix accounts for moving grid zones

USA-IN3 – Numerical Method

- Finite-Volume implementation of upwind finite-difference scheme

$$\frac{\partial Q}{\partial \tau} + \left(E_{j+\frac{1}{2},k} - E_{j-\frac{1}{2},k}\right) + \left(F_{j,k+\frac{1}{2}} - F_{j,k-\frac{1}{2}}\right)$$

  where j, k denote the volume vertices in ξ and η

- Upwind scheme based on Roe's flux limiters

$$\hat{f}_{m+\frac{1}{2}} \equiv \frac{1}{2}\left[f(q^{+}_{m+\frac{1}{2}}) + f(q^{-}_{m+\frac{1}{2}}) - |\bar{A}|\,(q^{+}_{m+\frac{1}{2}} - q^{-}_{m+\frac{1}{2}})\right]$$

  $\hat{f}_{m+\frac{1}{2}}$ = numerical flux at cell surface $m + \frac{1}{2}$, m-direction

  $q^{+}_{m+\frac{1}{2}}, q^{-}_{m+\frac{1}{2}}$ = right, left states of cell surface $m + \frac{1}{2}$

  $|\bar{A}|$ = flux Jacobian of intermediate $\bar{q}$ state

- Implicit time discretization up to third-order accurate
  - Sub-iteration guarantees divergence-free solution at each Δt
  - ADI and various Gauss-Seidel methods in either full-block or diagonalized formulation

USA-IN3 – Boundary Conditions

- Inertial coordinate system utilized
  - Wall conditions on velocity
  - Neumann-type BC for wall p using characteristics or extrapolation

- Grid node velocities specified for steady coning motion

USA-IN3 Result

Vortex Shedding Behind a Circular Cylinder

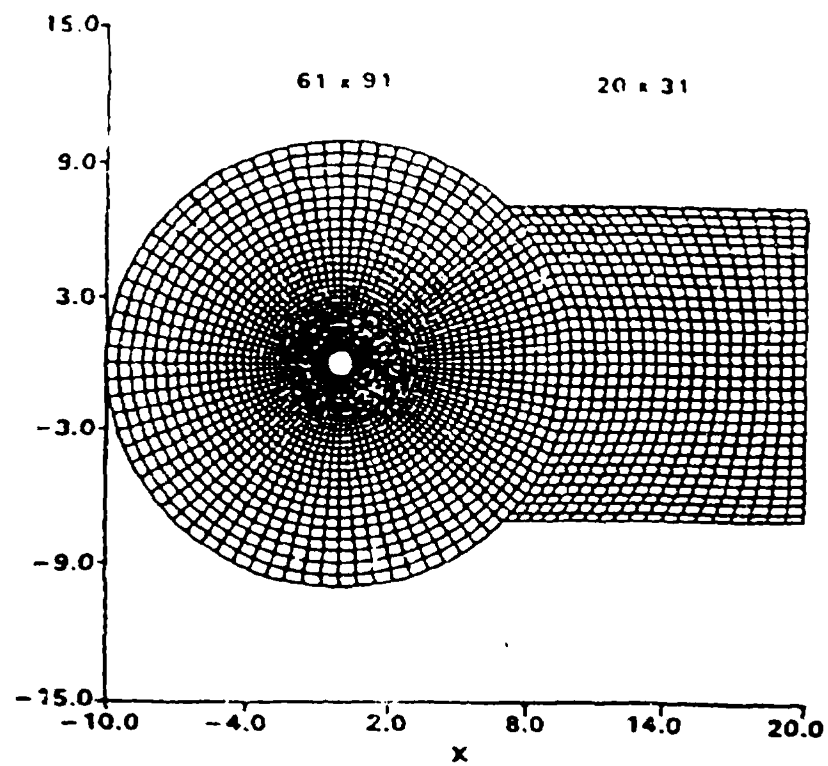

USA-IN3 Result

Vortex Shedding Behind a Circular Cylinder ($Re_D = 2000$)

Strouhal Number = .21 (experimental), .23 (computed)

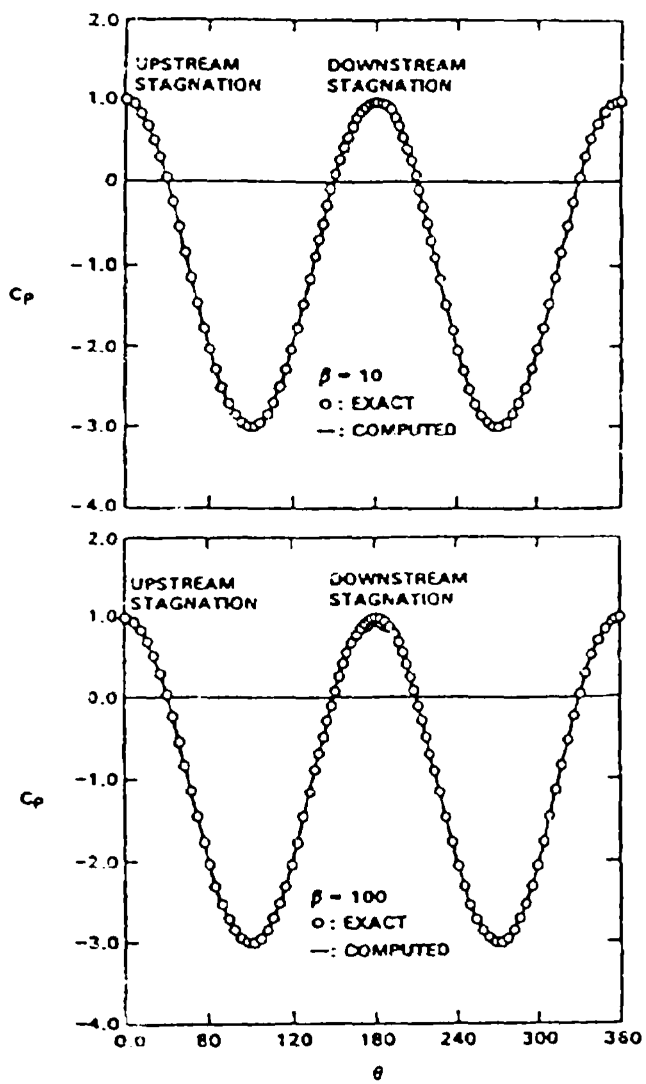

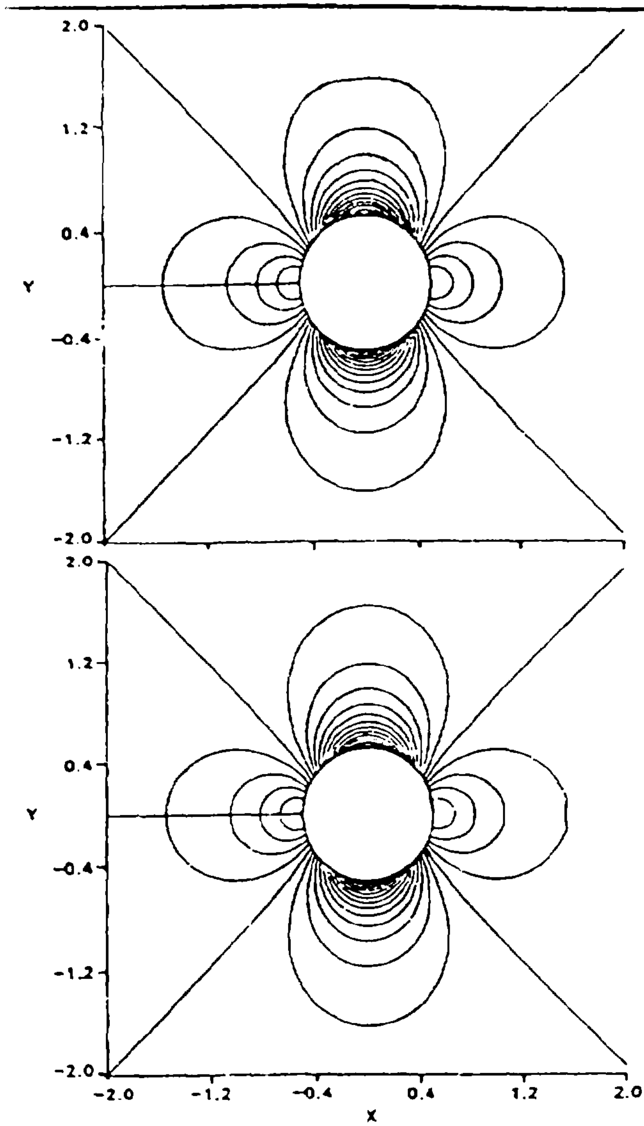

USA-IN3 Result

Vortex Shedding Behind a Sphere ($Re_D = 2000$)

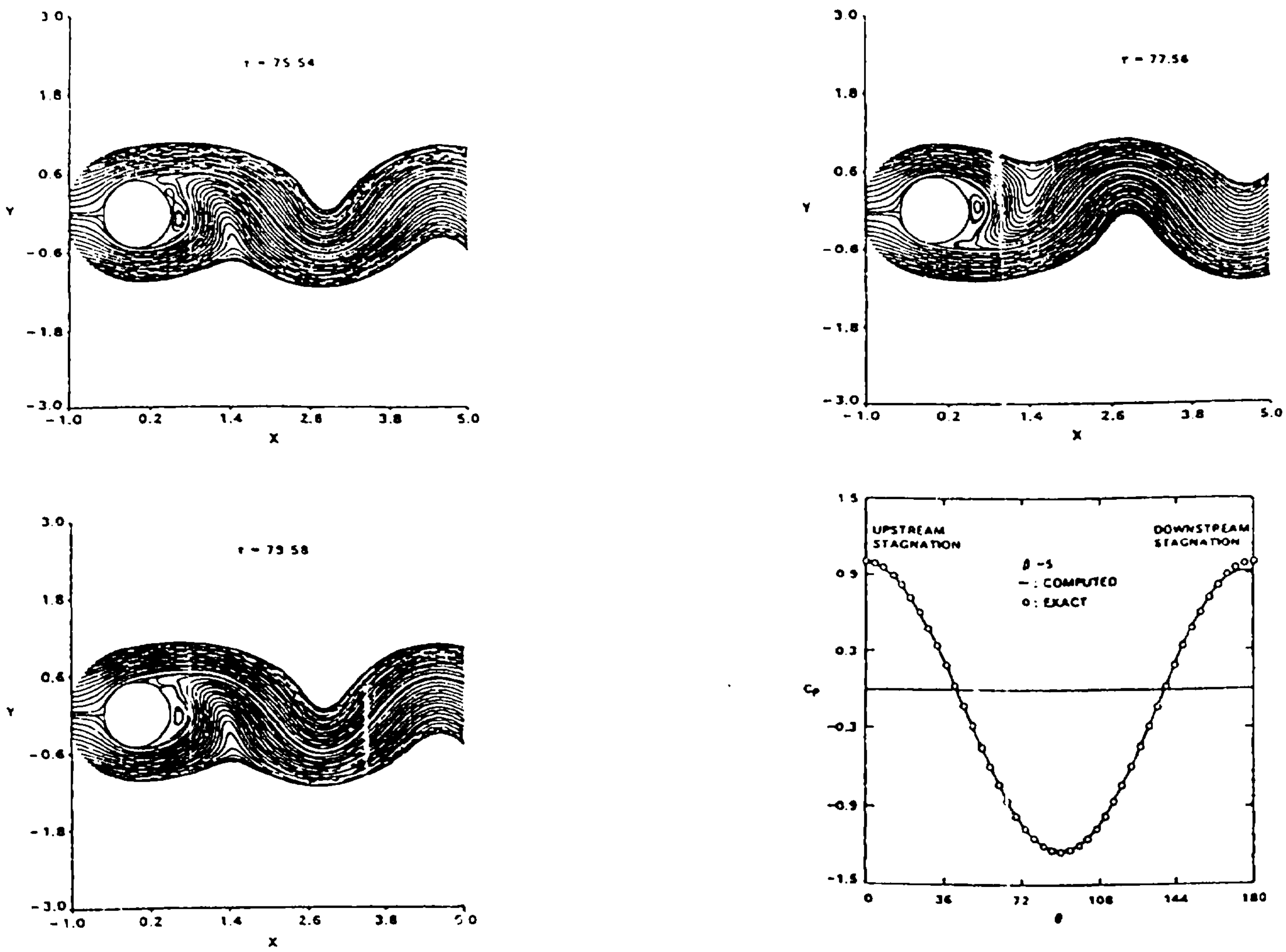

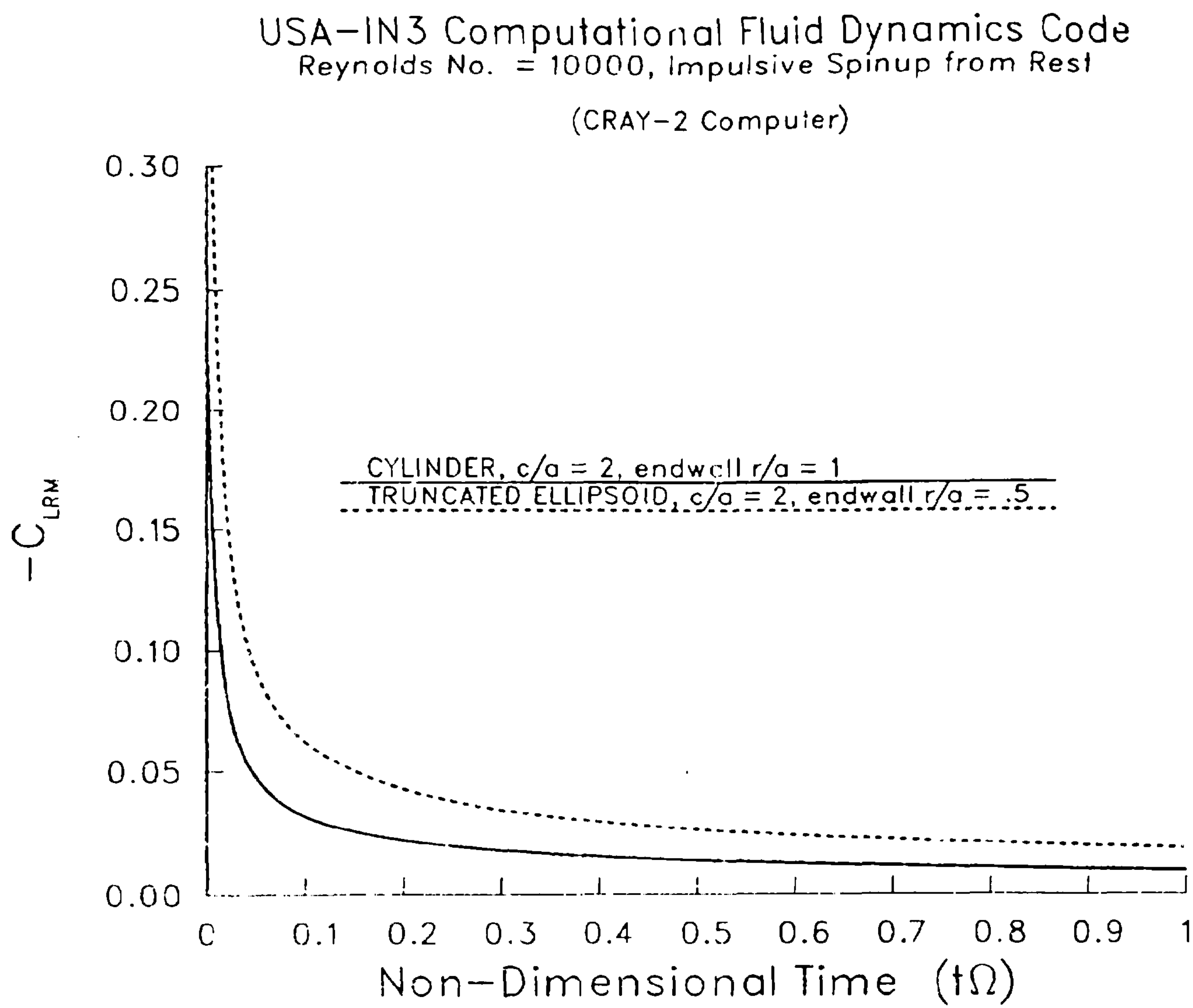
USA-IN3 Computational Fluid Dynamics Code
Reynolds No. = 10000, Impulsive Spinup from Rest
(CRAY-2 Computer)
0.30
0.25
0.20
0.15
0.10
0.05
0.00
$-C_{LRM}$
CYLINDER, c/a = 2, endwall r/a = 1
TRUNCATED ELLIPSOID, c/a = 2, endwall r/a = .5
0
0.1
0.2
0.3
0.4
0.5
0.6
0.7
0.8
0.9
1
Non-Dimensional Time (tΩ)

Future Work

- For steady coning motion:
  - Compare UWISC/BRL and USA-IN3, $10 \leq \mathrm{Re} \leq 300$
  - Numerical experiments using USA-IN3 for $10 \leq \mathrm{Re} \leq 1\mathrm{x}10^6$
    - Cylinder with rounded endcaps
    - Truncated ellipsoid
    - Investigate small α_c nonlinearities in C_{LSM} at large Re

- Unsteady coneup and spinup

Blank

Motion of two Immiscible Fluids in a Spinning and Coning Cylinder

Mohamed Selmi

Department of Mechanical Engineering
The Ohio State University

Supported by
CRDEC & OSC (CRAY YMP/864)

Workshop on Problems of Rotating Fluids
AHPCRC Minneapolis, Minnesota
April 22-23, 1991

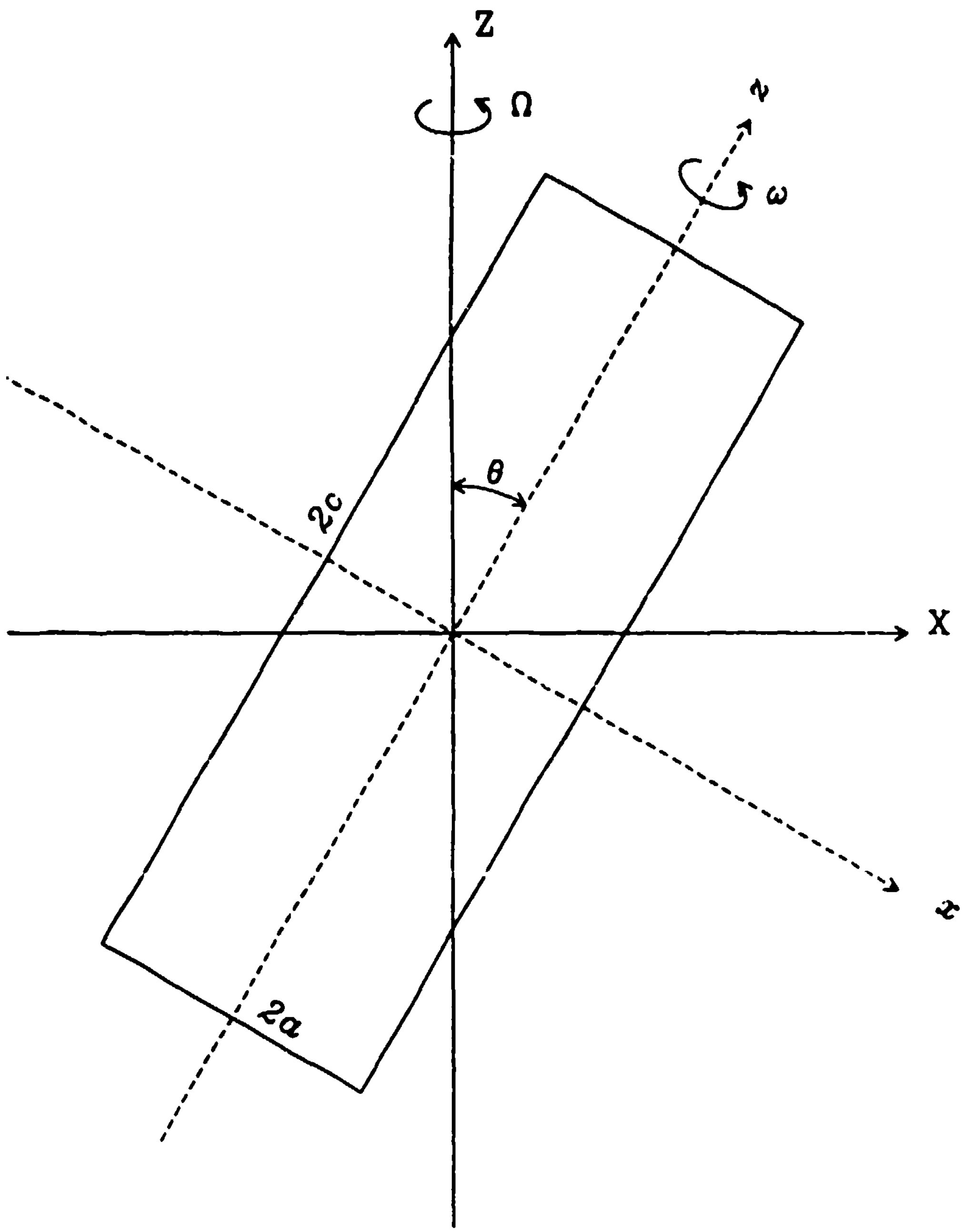

Description of Geometry

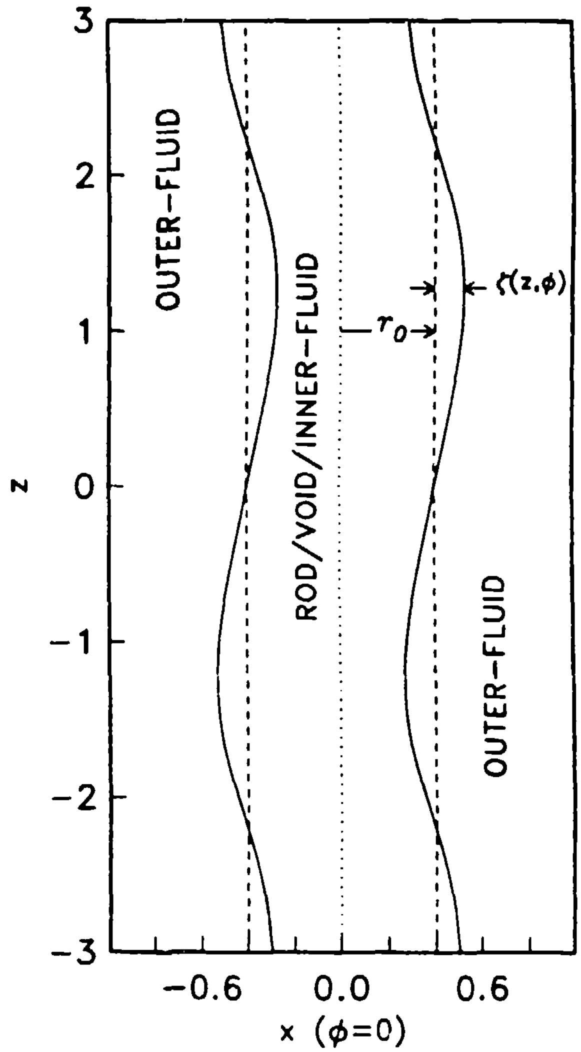

Nomenclature sketch

GOVERNING EQUATIONS

$$(x, y, z) \qquad \text{or} \qquad (r, \phi, z)$$

$$\frac{D\,\mathbf{V}}{D\,t} + 2\,\Omega \times \mathbf{V} + \Omega \times (\Omega \times \mathbf{r}) = -\frac{1}{\rho}\nabla P + \nu \nabla^2 \mathbf{V}$$

$$\nabla \cdot \mathbf{V} = 0$$

REFERENCE QUANTITIES

Length:	a
Velocity:	ωa
Pressure:	$\rho \omega^2 a^2$
Time :	ω^{-1}

NON-DIMENSIONAL PARAMETERS

Aspect ratio : $\eta = \dfrac{c}{a}$

Coning frequency : $\tau = \dfrac{\Omega}{\omega}$

Nutation angle : θ

Inner-fluid Reynolds No: $Re_0 = \dfrac{\omega a^2}{\nu_0}$

Outer-fluid Reynolds No: $Re_1 = \dfrac{\omega a^2}{\nu_1}$

Density ratio : $\dfrac{\rho_0}{\rho_1}$

Fill ratio : $\dfrac{V_1}{V} = 1 - r_0^2$

Fill radius : r_0

FLOW DECOMPOSITION

$$\mathbf{V} = \mathbf{V}^r + \mathbf{V}^d, \qquad P = -\frac{1}{2}(1+\tau_z)^2 r_0^2 + p^r + p^d$$

$$\mathbf{V}^r = r\,\hat{e}_\phi$$

$$p^r = \frac{1}{2}[r^2(1+\tau_z)^2 + r^2\tau_\phi^2 + z^2\varepsilon^2 - 2\,r\,z\,\tau_z\,\tau_r]$$

$$\tau_z = \tau\cos\theta, \qquad \varepsilon = \tau\sin\theta$$

$$\tau_\phi = \varepsilon\sin\phi, \qquad \tau_r = -\varepsilon\cos\phi$$

$$\mathbf{V}^d = v_r\,\hat{e}_r + v_\phi\,\hat{e}_\phi + v_z\,\hat{e}_z$$

Complete Fill: Roll moment vs. Reynolds Number

$\eta = 4.368,\ \theta = 20,\ \tau = 0.16667$

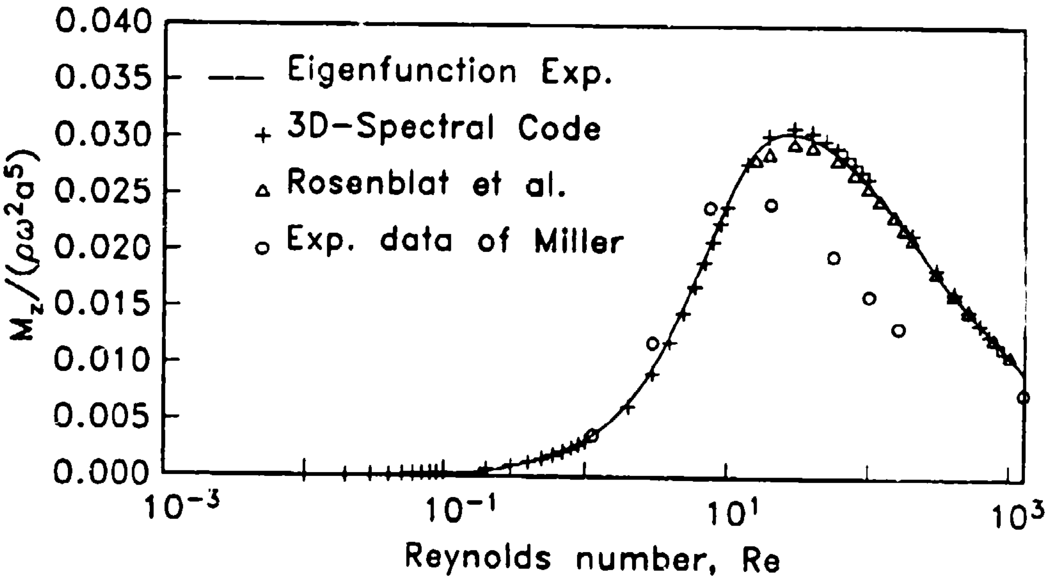

Complete Fill: Pitch moment vs. Reynolds Number

$\eta = 4.368, \ \theta = 20, \ \tau = 0.16667$

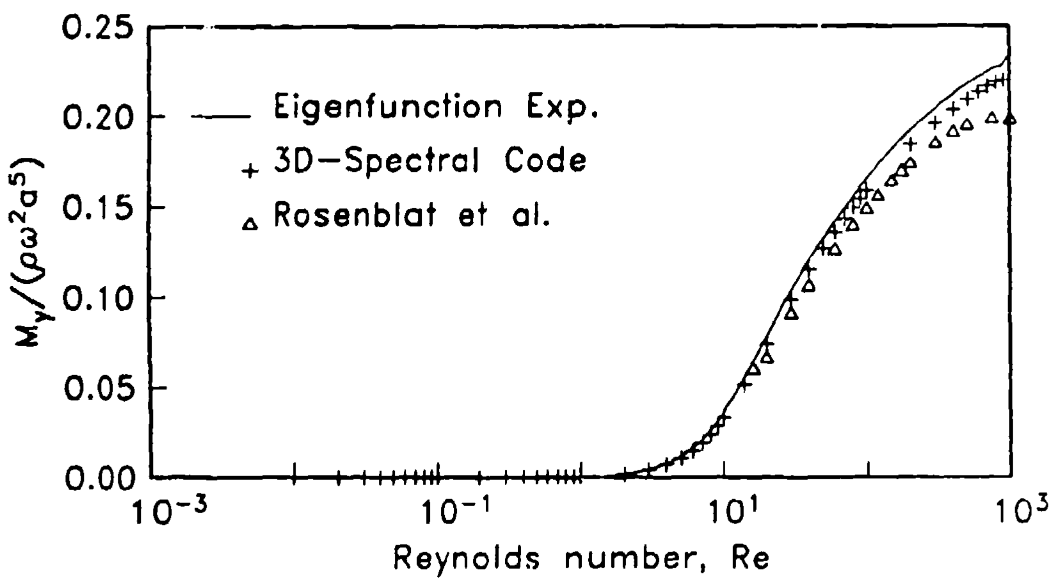

Complete Fill: Roll moment vs. Aspect ratio

$\theta = 2, \tau = 0.083333$

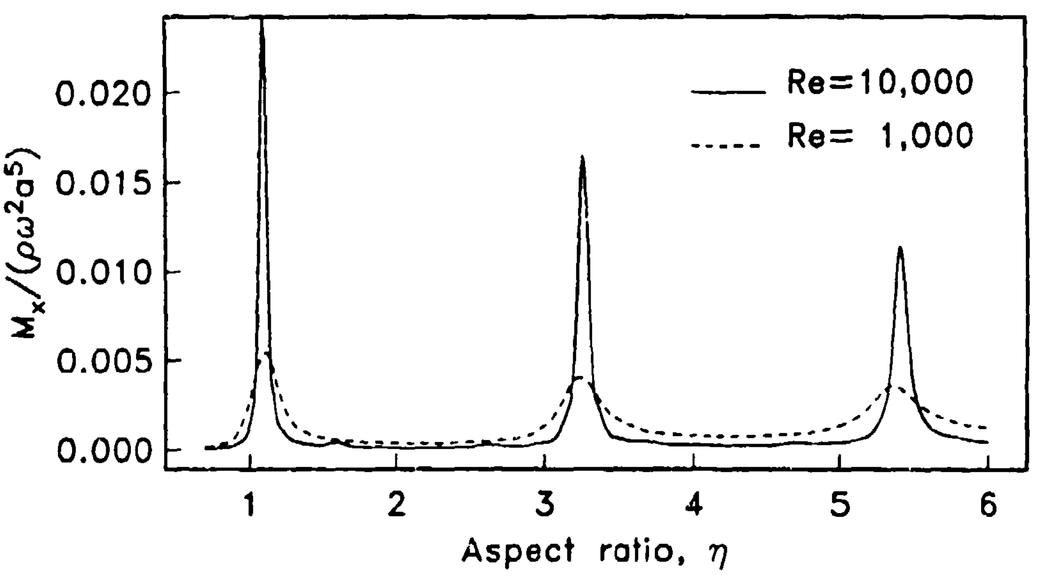

Two Fluids: Roll moment ratio vs. Fill ratio

$\eta = 4.5,\ \theta = 1,\ \tau = 0.008$

$Re_0 = 25,\ Re_1 = 10^4$

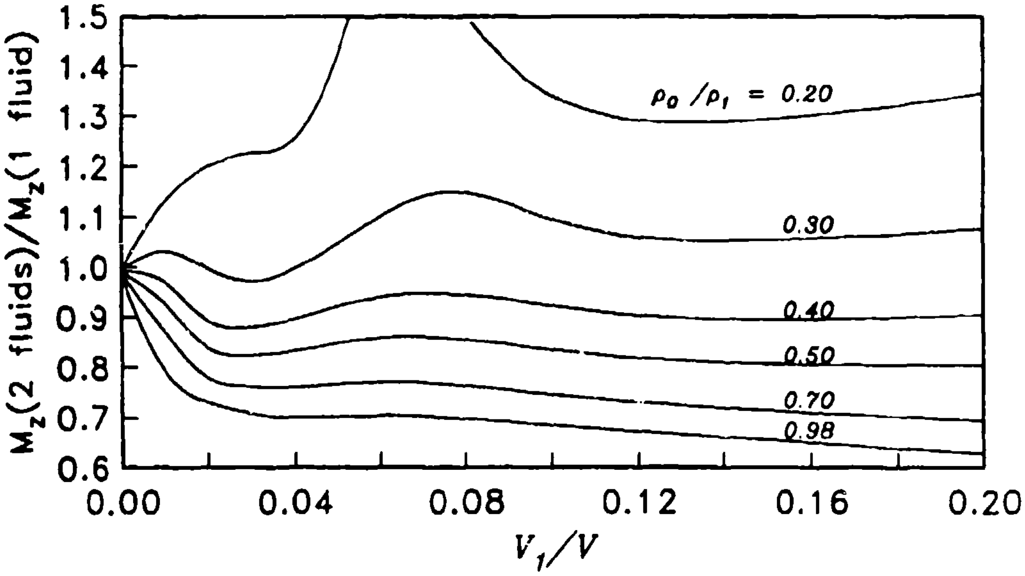

Two Fluids: Roll moment ratio vs. Fill ratio

$\eta = 4.5, \ \theta = 1, \ \tau = 0.008$

$Re_0 = 25, \ Re_1 = 10^4$

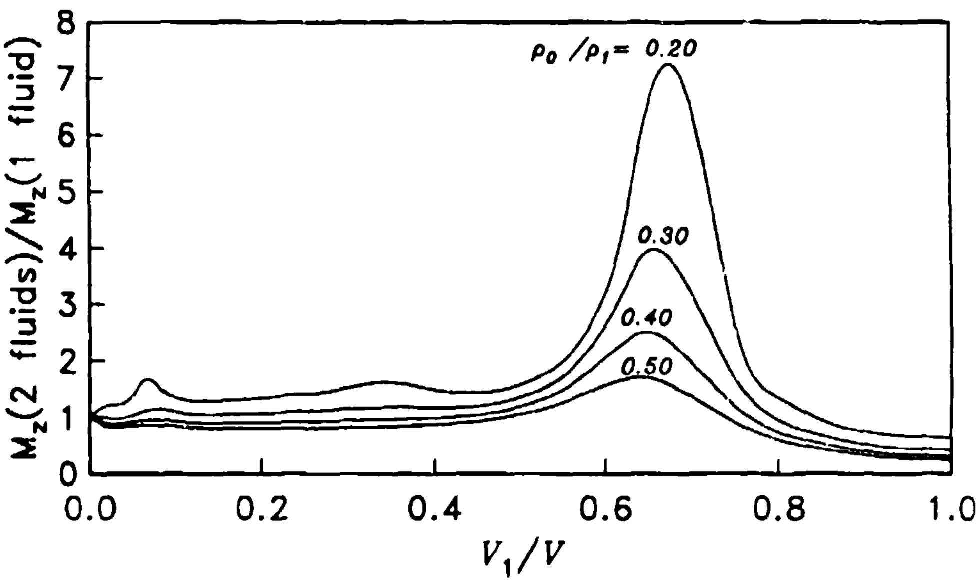

Two Fluids: Roll moment vs. Fill ratio

$\eta = 4.5, \ \theta = 1, \ \tau = 0.008$

$Re_0 = 25, \ Re_1 = 10^4$

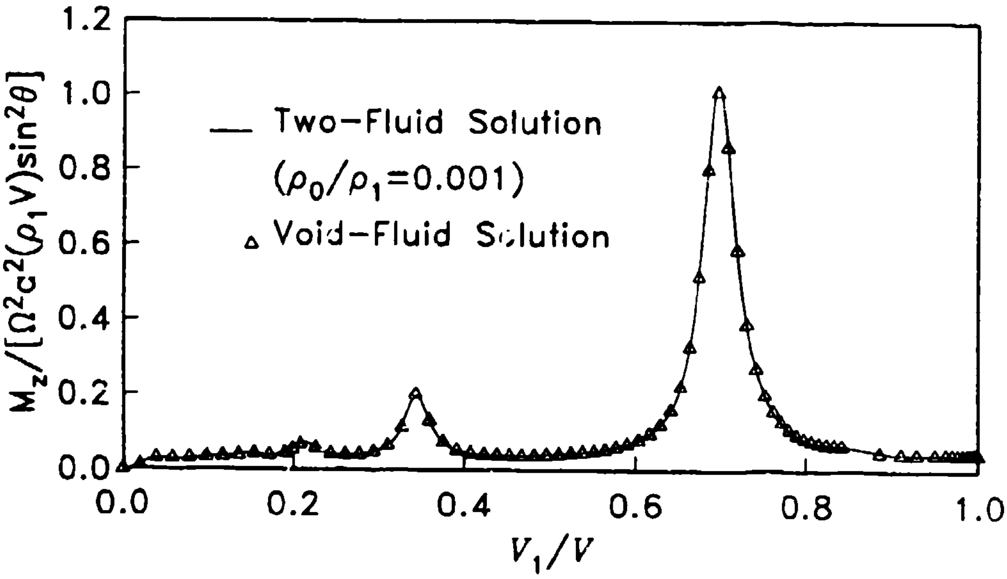

Two Fluids: Roll moment ratio vs. Fill ratio

$\eta = 4.5,\ \theta = 1,\ \tau = 0.008$

$Re_0 = 25,\ Re_1 = 10^4,\ \rho_0/\rho_1 = 0.98$

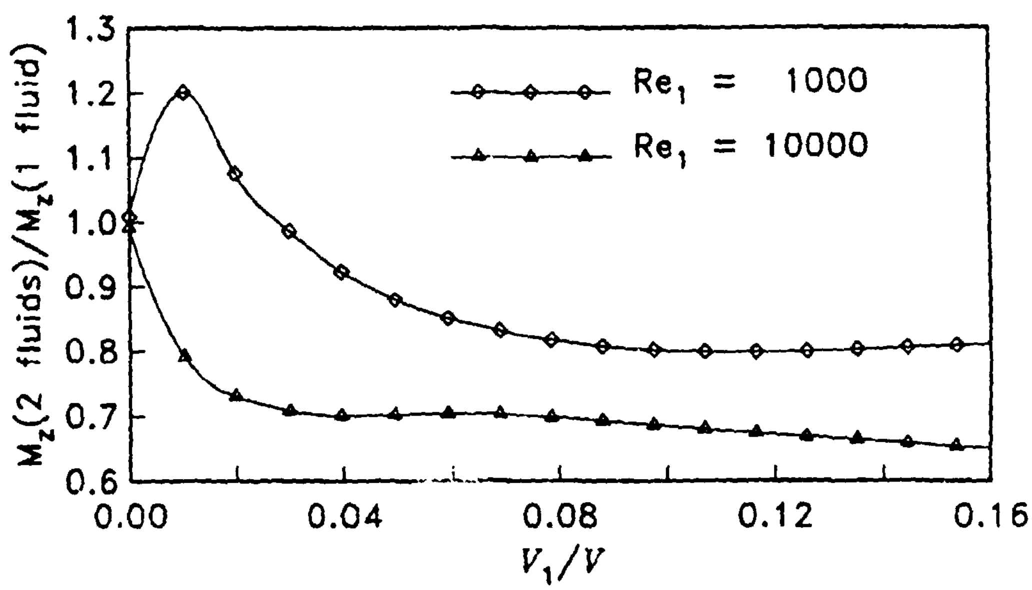

Complete Fill: Roll moment vs. Reynolds Number

$\eta = 4.5,\ \theta = 20,\ \tau = 0.16667$

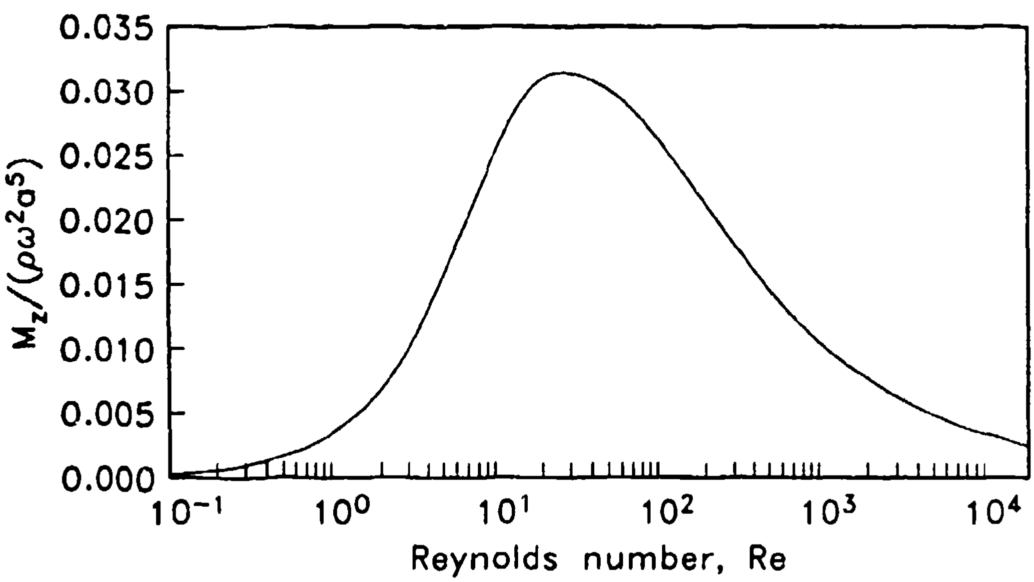

Two Fluids: Roll moment vs. Inner-fluid Reynolds Number

$\eta = 4.5,\ \theta = 20,\ \tau = 0.16667,\ Re_1 = 19250$

$\rho_0/\rho_1 = 0.98$

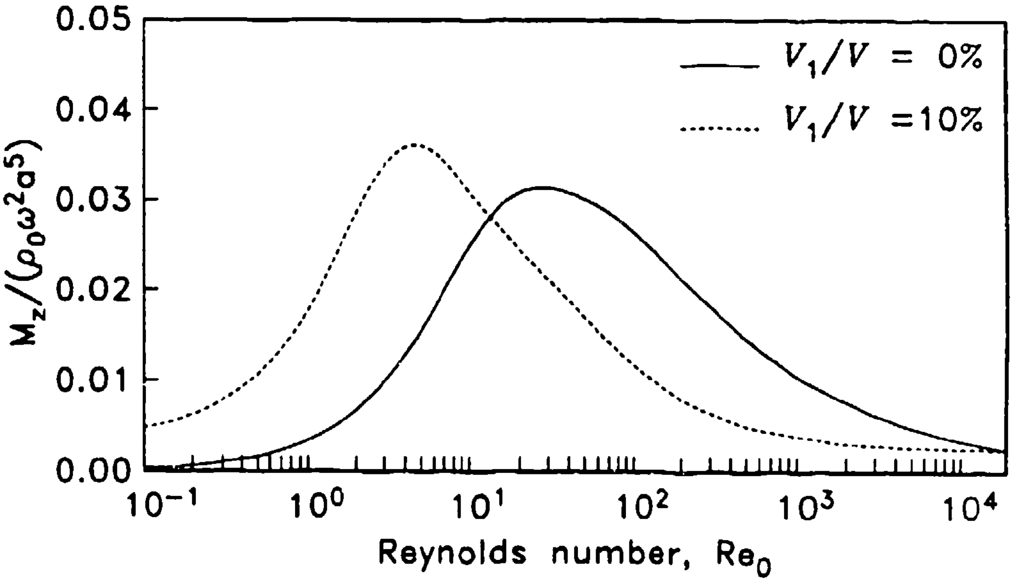

Two Fluids: Pitch moment vs. Inner-fluid Reynolds Number

$\eta = 4.5$, $\theta = 20$, $\tau = 0.16667$, $Re_1 = 19250$

$\rho_0/\rho_1 = 0.98$

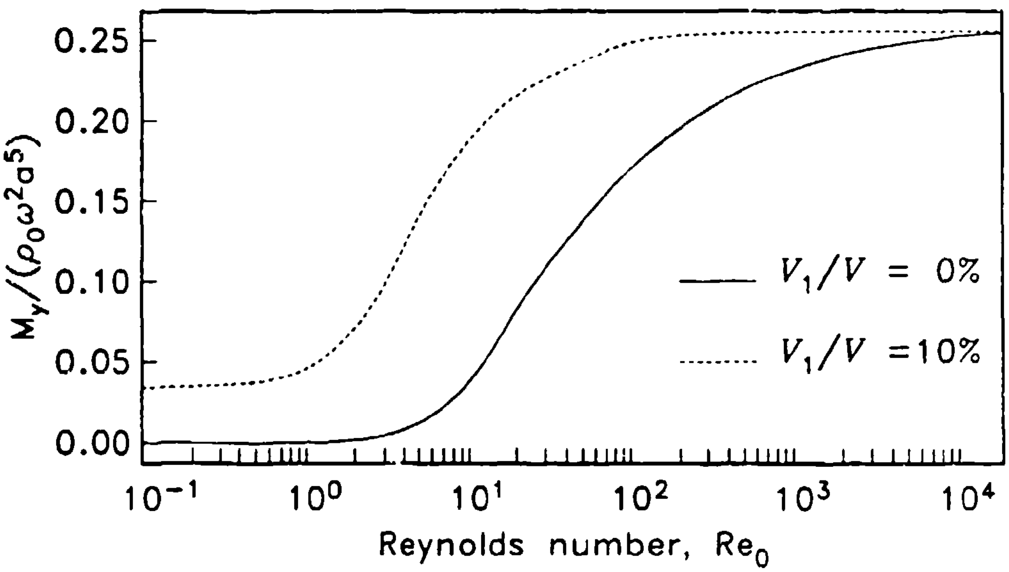

Partial Fill: Roll moment vs. Fill radius

$\eta = 4.5,\ \theta = 20,\ \tau = 0.08674$

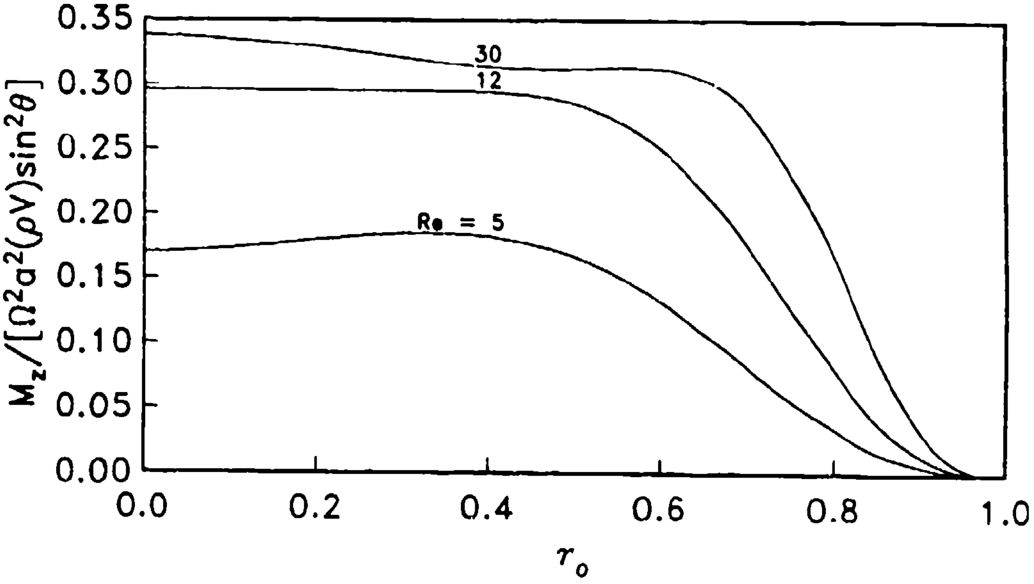

Partial Fill: Roll moment vs. Fill radius

$\eta = 4.5, \ \theta = 20, \ \tau = 0.08674$

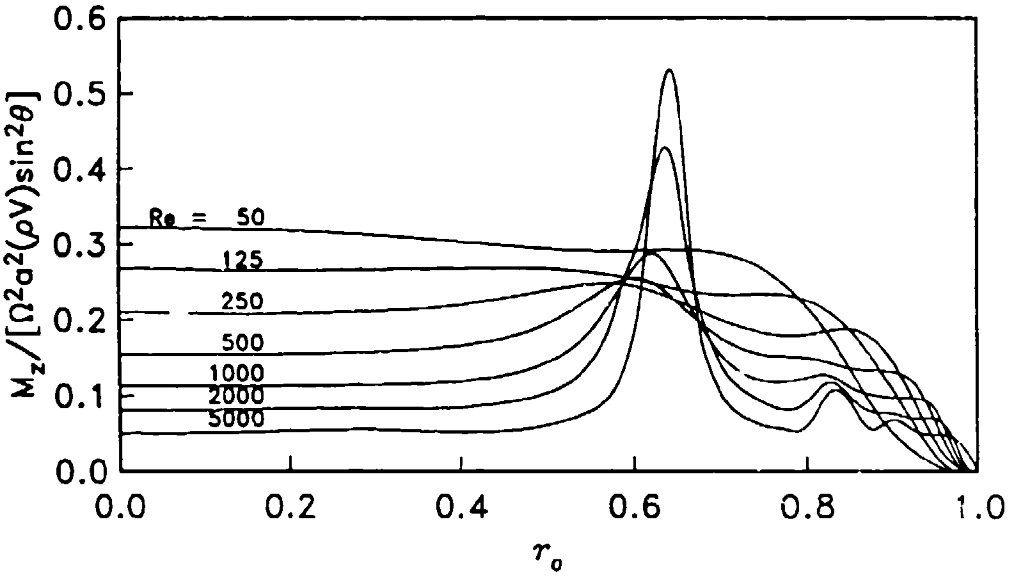

Central Rod: Roll moment vs. Fill radius

$\eta = 4.5, \ \theta = 20, \ \tau = 0.08674$

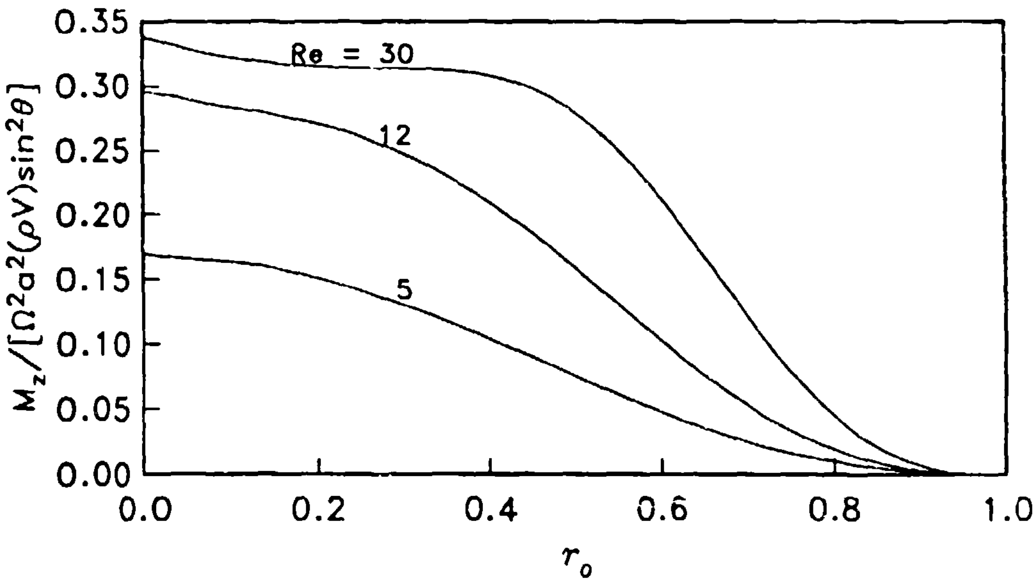

Central Rod: Roll moment vs. Fill radius

$\eta = 4.5, \ \theta = 20, \ \tau = 0.08674$

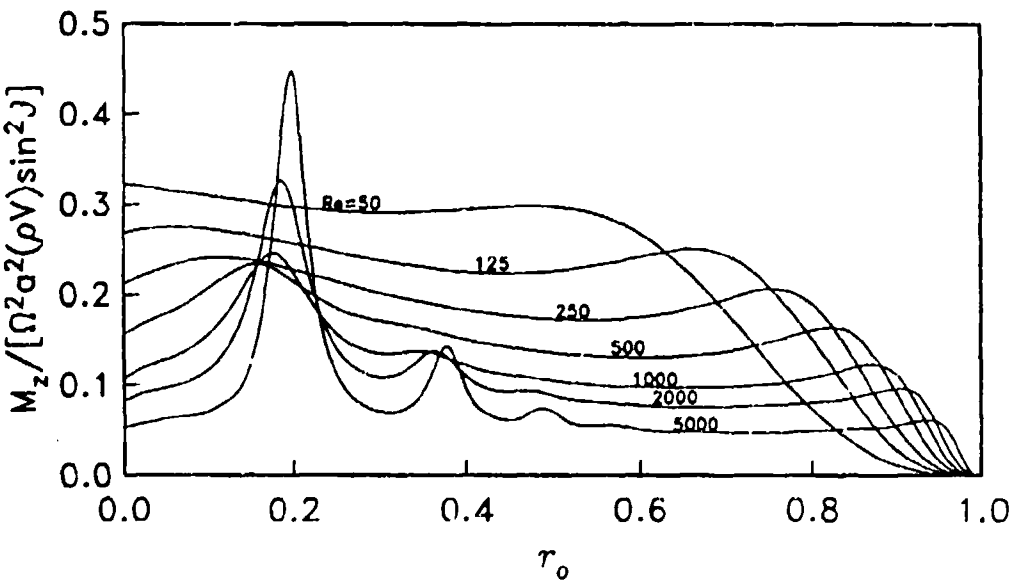

Roll moment vs. Fill radius

Re = 10^4, η = 2, θ = 2, τ = 0.1111

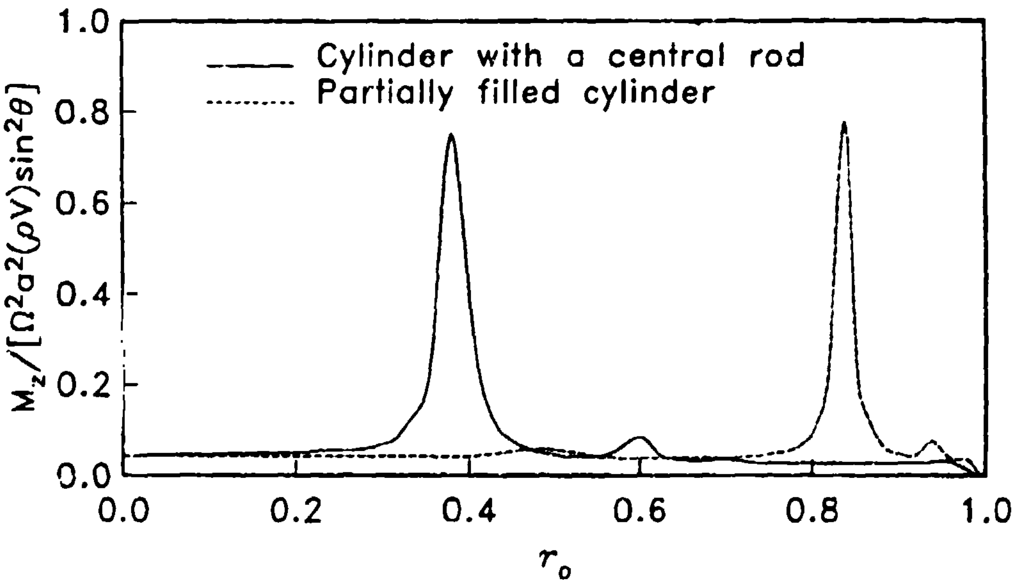

Roll moment vs. Fill radius

$Re = 10^4$, $\eta = 1.5$, $\theta = 2$, $\tau = 0.1111$

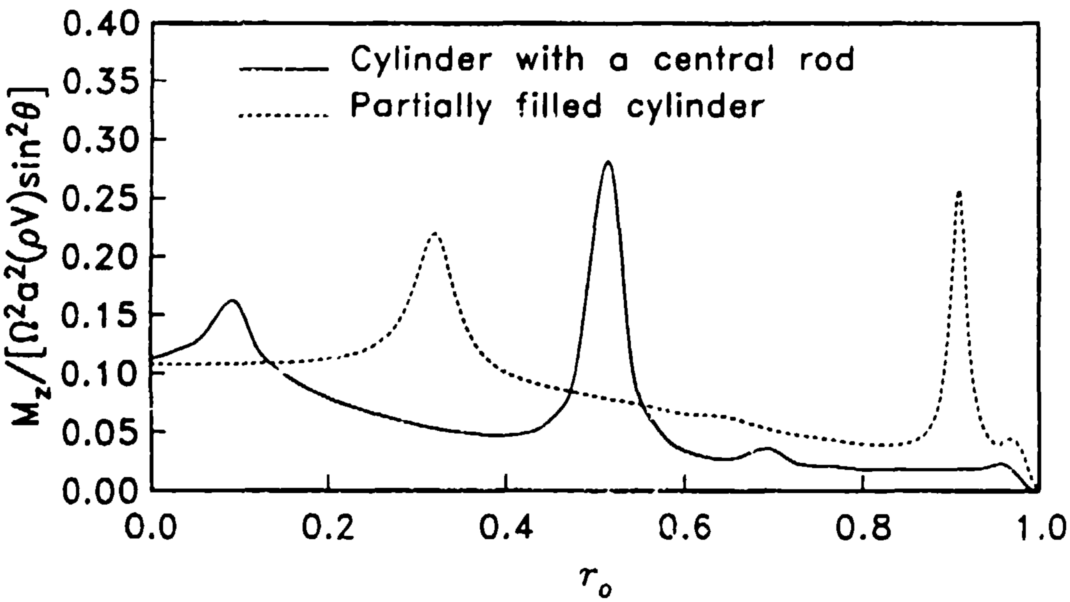

INVISCID ANALYSIS (PARTIAL FILL)

$$w = i \sum_{k=0}^{\infty} [A_k J_1(\beta_k r) + B_k Y_1(\beta_k r)] \gamma_k \cos(\gamma_k z)$$

$$\gamma_k = (2k+1)\frac{\pi}{2\eta}, \quad \beta_k = \gamma_k \sqrt{t^2 - 1}$$

$$\left[t J_1(\beta_k) + J_1{}'(\beta_k)\right] A_k + \left[t Y_1(\beta_k) + Y_1{}'(\beta_k)\right] B_k = 2(1+t)\frac{(-1)^{k+1}}{\eta \gamma_k^2}$$

$$\left[(1 - t^2 + \frac{t^3}{4}) J_1(\beta_k r_0) + \frac{t^2}{4} r_0 J_1{}'(\beta_k r_0)\right] A_k \; +$$

$$\left[(1 - t^2 + \frac{t^3}{4}) Y_1(\beta_k r_0) + \frac{t^2}{4} r_0 Y_1{}'(\beta_k r_0)\right] B_k = (1 + \frac{t}{2} + \frac{t^2}{2}) r_0 \frac{(-1)^{k+1}}{\eta \gamma_k^2}$$

$$\left[(1 - t^2 + \frac{t^3}{4}) Y_1(\beta_k r_0) + \frac{t^2}{4} r_0 Y_1{}'(\beta_k r_0)\right] \left[t J_1(\beta_k) + J_1{}'(\beta_k)\right] \; -$$

$$\left[(1 - t^2 + \frac{t^3}{4}) J_1(\beta_k r_0) + \frac{t^2}{4} r_0 J_1{}'(\beta_k r_0)\right] \left[t Y_1(\beta_k) + Y_1{}'(\beta_k)\right] = 0$$

CENTRAL ROD: Critical fill radius vs. aspect ratio

Coning frequency: τ=0.08674

Nutation angle: θ=20.

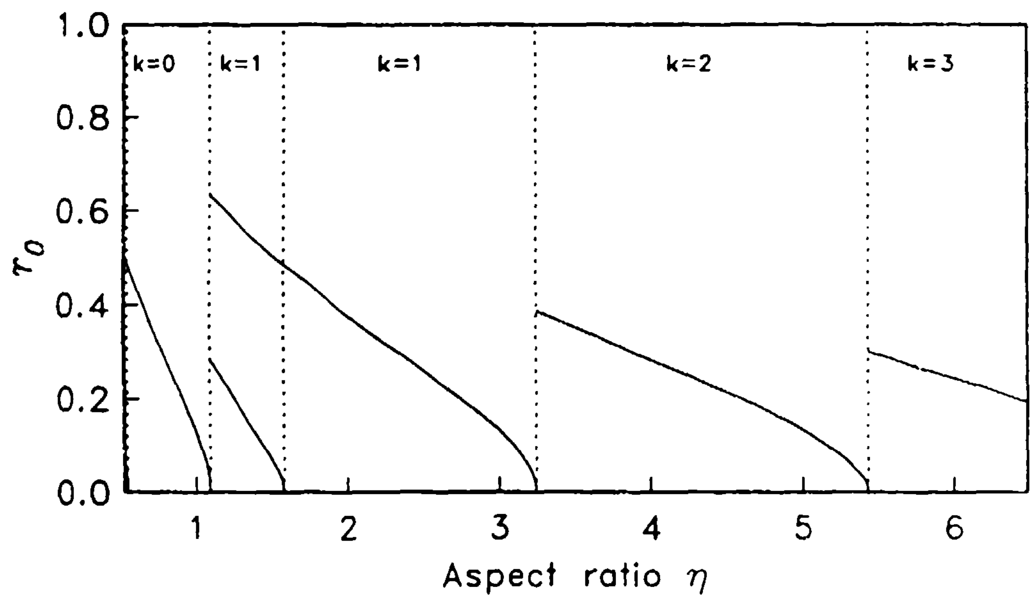

PARTIAL FILL: Critical fill radius vs. aspect ratio

Coning frequency: τ=0.08674

Nutation angle: θ=20.

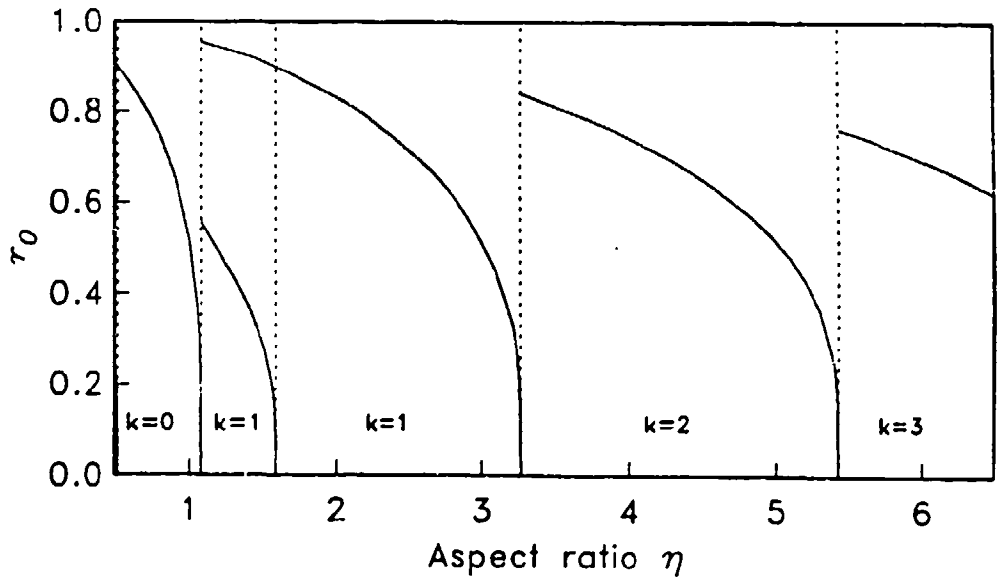

PARTIAL FILL: Interface shape (r_0=0.2,0.8, ϕ=0)
Re = 10000, τ = 0.08333, η = 3, θ = 20

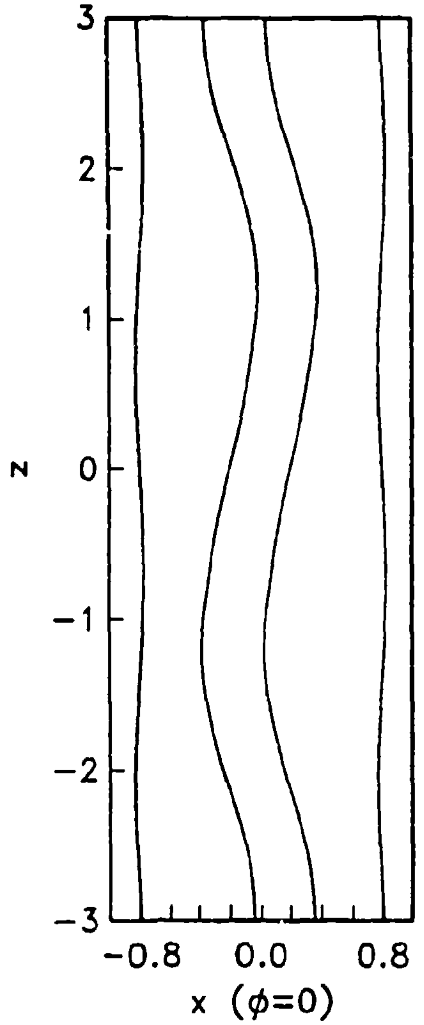

PARTIAL FILL: Interface shape (τ_0=0.2,0.8, ϕ=0)

Re = 10000, τ = 0.08333, η = 3, θ = 2

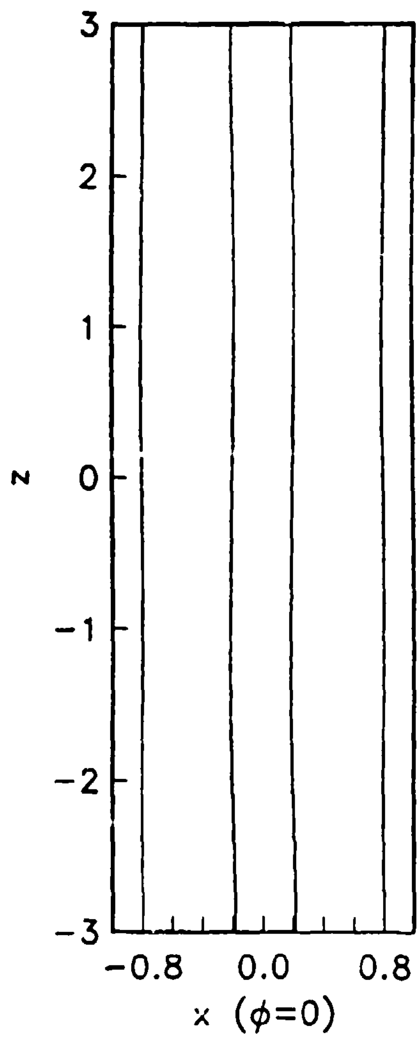

TWO FLUIDS: Interface shape (r_0 = 0.84, ϕ = 90)
Re_0 = 30, Re_1 = 10000, τ = 0.1, η = 4.5, θ = 20
ρ_0/ρ_1 = 0.01

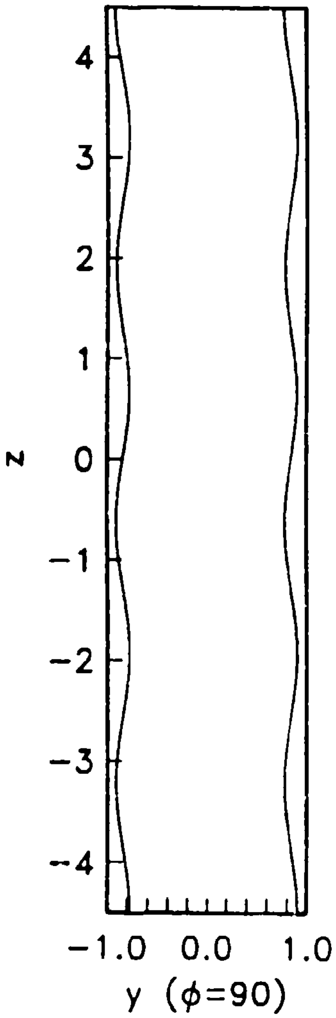

TWO FLUIDS: Interface shape (r_0 = 0.66, ϕ = 90)
Re_0 = 30, Re_1 = 10000, τ = 0.1, η = 4.5, θ = 20
ρ_0/ρ_1 = 0.001

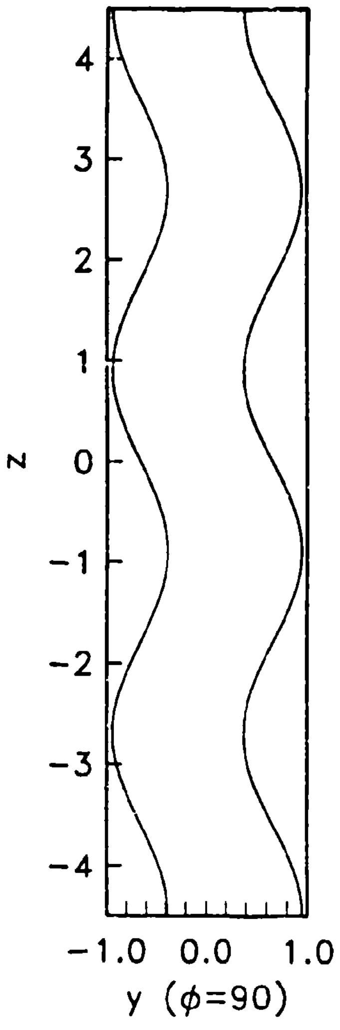

TWO FLUIDS: Interface shape (r_0 = 0.66, ϕ = 90)
Re_0 = 30, Re_1 = 10000, τ = 0.1, η = 4.5, θ = 2
ρ_0/ρ_1 = 0.001

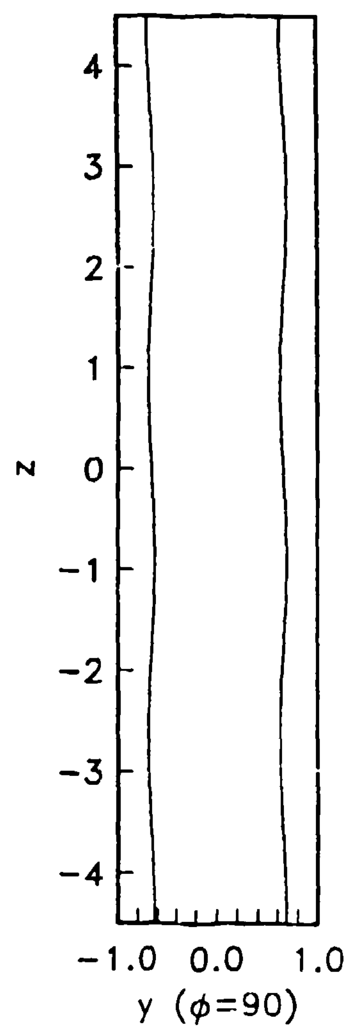

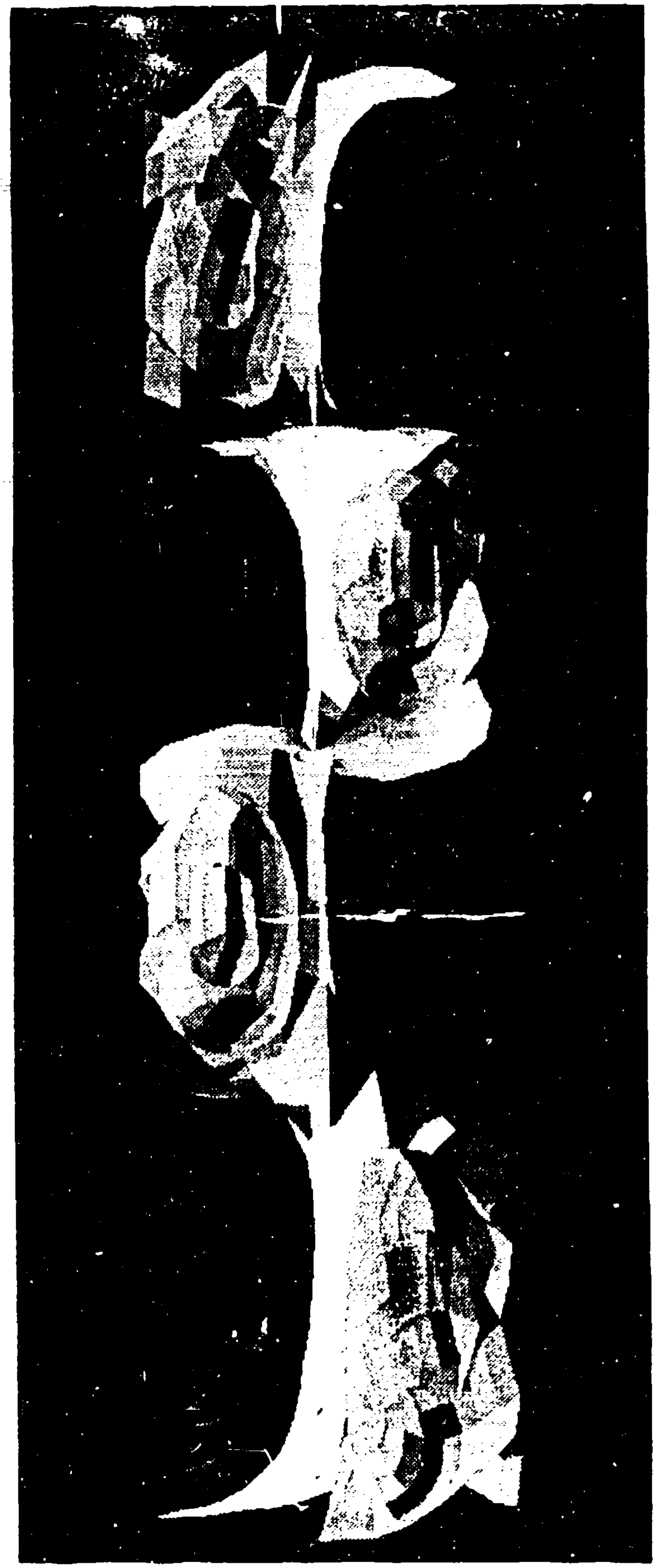

Blank

BALLISTIC RESEARCH LABORATORY

US ARMY
LABORATORY COMMAND

Direct Measurement of Liquid Effects Using a Moment Balance

David Hepner
Charles Mitchell

BRL-LFD-FFAB

Outline

- Moment Magnitude Measurement Techniques
- Flight Simulator and Moment Balance Hardware
- Parameter Definition and Experiment Selection
- Data and Error Sources
- Conclusion and Recommendations

Liquid Moment Magnitude History

- Flight data - short range, yawsonde data, cut and try hardware
- Scaled free gyro - amplitude growth - epsilon - Clsm* - compare - Clsm.
- Scaled forced gyro - pressure - Cp - compare & integrate theory - Clsm.
- Full-scale despin fixture - roll moment - Clrm - Clsm .
- Full-scale flight simulator - moment - Clsm.

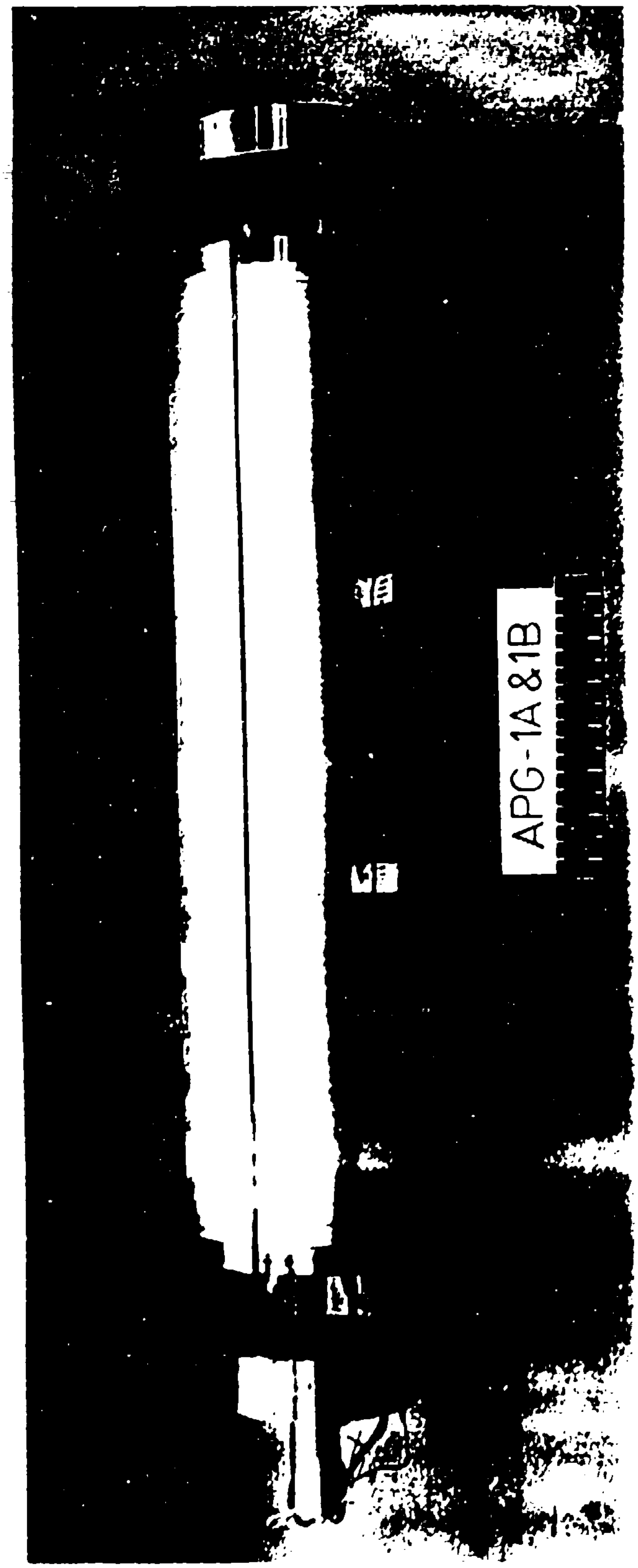

NASA
L-87-1791

NASA
L-87-1779

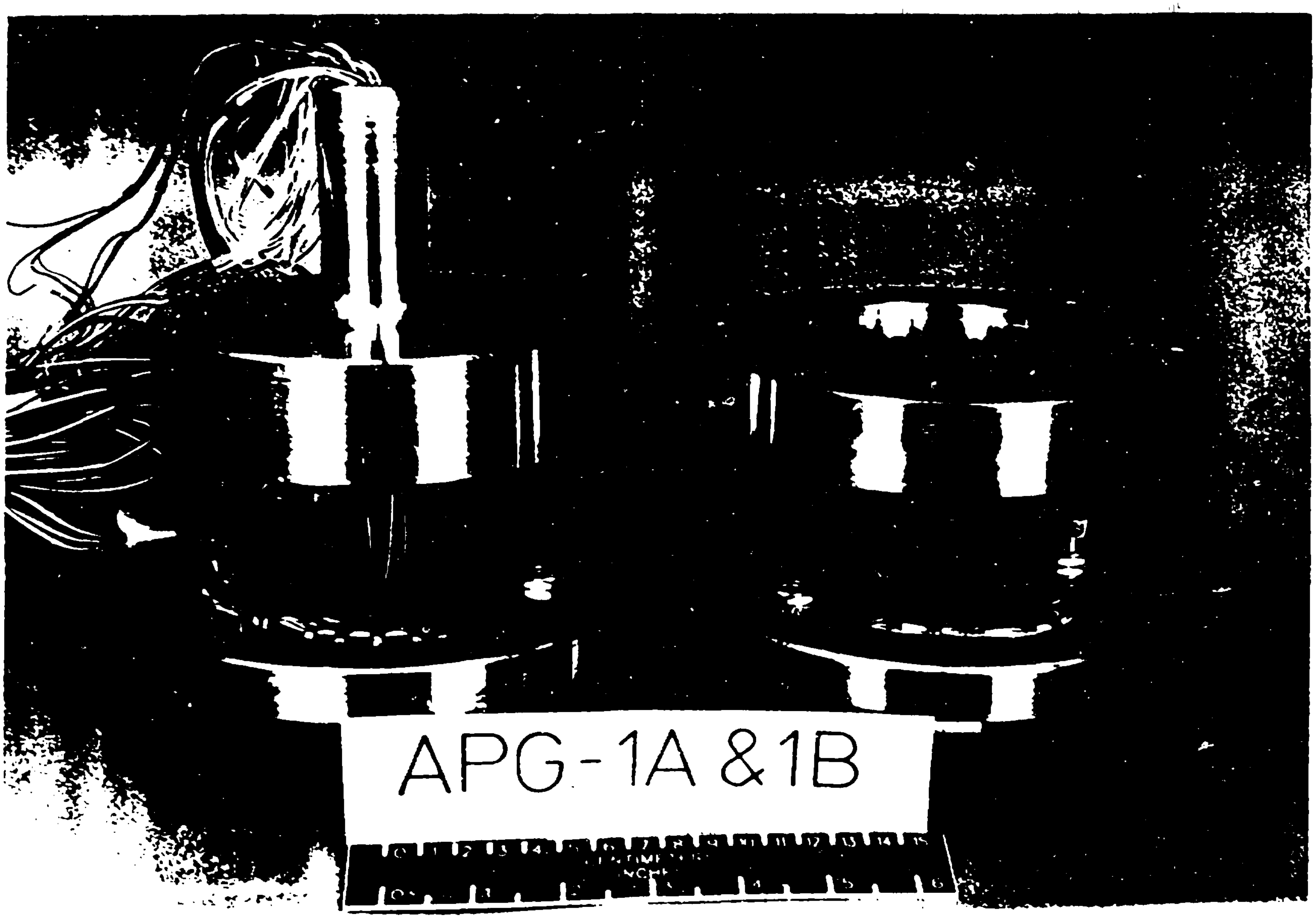

Balance Calibration

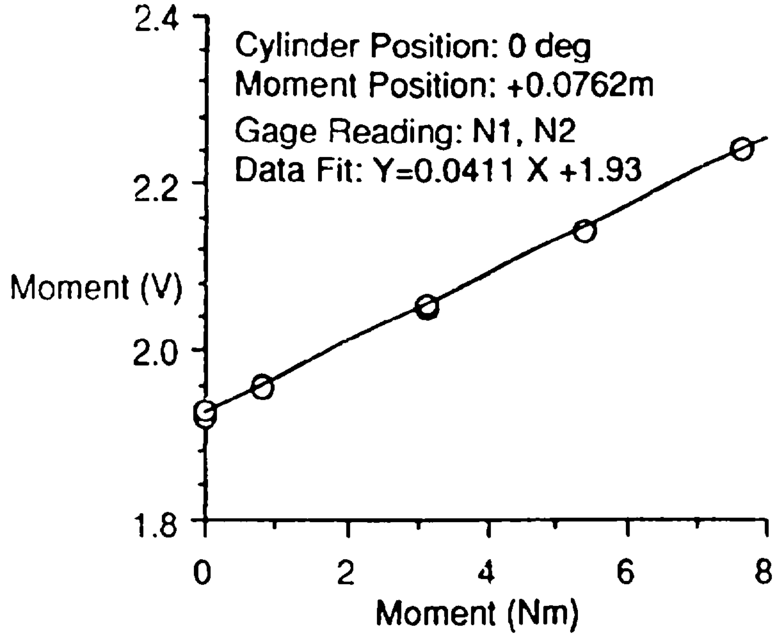

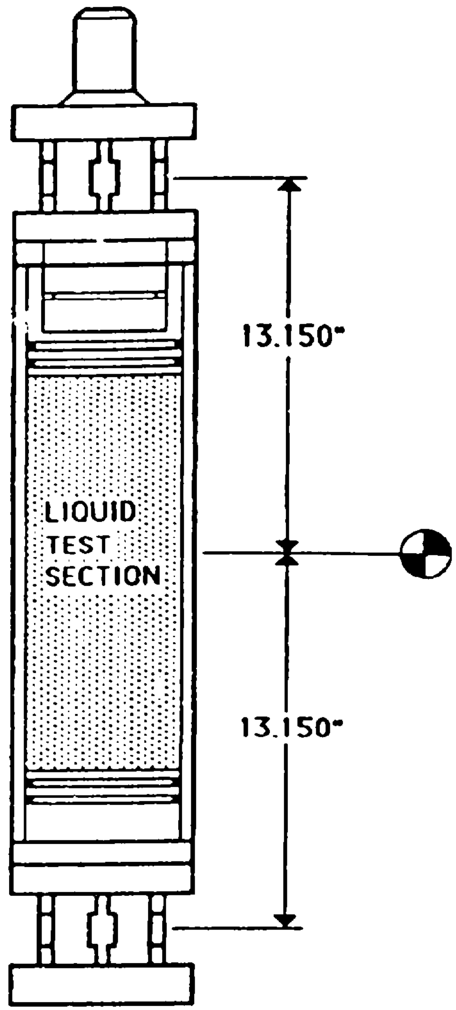

Simplified Data Aquisition Schematic

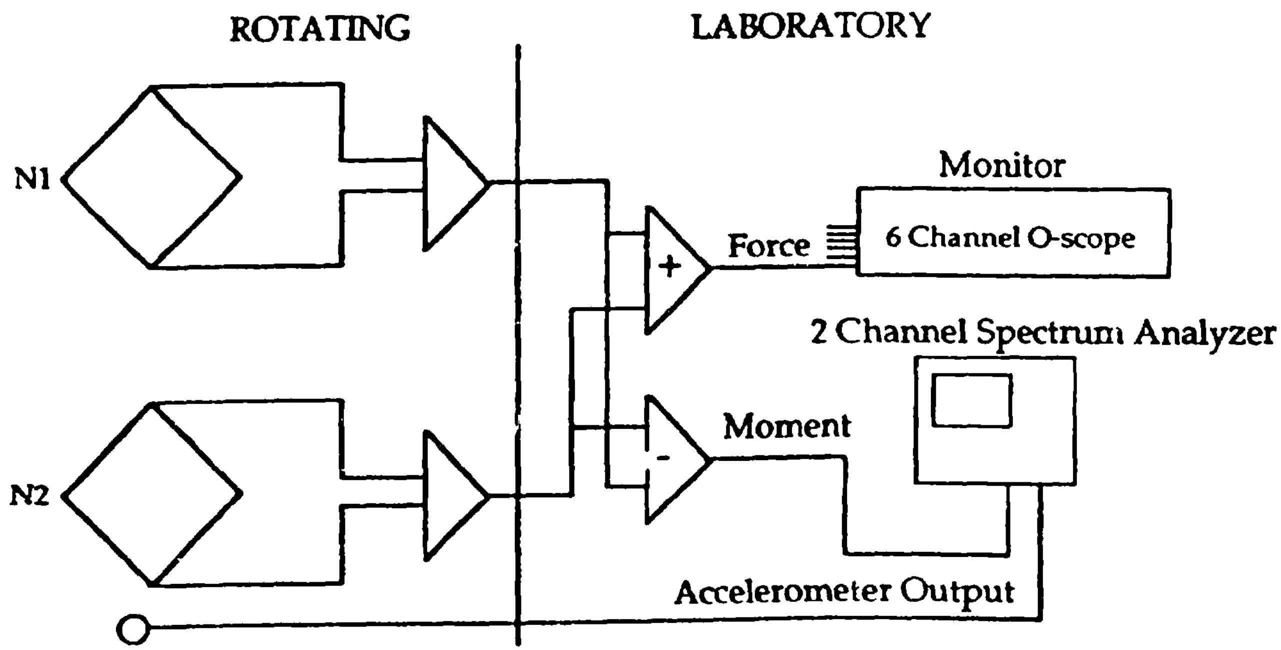

Measurements: Power spectrum (amp)of total moment magnitude (M)
Frequency response (phase) moment w/r Accel (β)

Monitor: Roll gage sets 1&2
Force (N1+N2)
Moment (N1-N2)
Accelerometer Out

Definitions and Symbols

- Reynolds number and cavity parameters

$Re = \frac{a^2 p}{\mu}$

a = cylinder radius
p = cylinder inertial spin rate
μ = kinematic viscosity
c/a = aspect ratio
c = cylinder length
h/a = offset ratio
h = axial offset

- Tau - nondimensional coning frequency

$\tau = \frac{\dot{\phi}}{p}$

$\dot{\phi}$ = cylinder inertial coning rate

- Side and in-plane moment

$M_{lsp} = M \cos(\beta)$

$M_{lip} = M \sin(\beta) - M_{sip}$

M = measured moment magnitude
β = measured phase angle
M_{sip} = solid in-plane moment

- Liquid moment coefficient

$C_{lsm} = \frac{M_{lsp}}{m_l a^2 p \dot{\phi} K}$

$C_{lim} = \frac{M_{lip}}{m_l a^2 p \dot{\phi} K}$

m_l = mass of liquid in a completely filled cavity
$K = \sin(\alpha)$
α = cylinder coning angle

Experiment Selection Criteria

- Hardware - c/a, Ix & Iy, moment sensitivity, offset single-mode motion, spin rate, coning rate and amplitude

- Liquid - Re, Fill

  High Re yields high moment magnitude, narrow bandwidth, with nonlinear effects occuring at small angles, and long settling times.

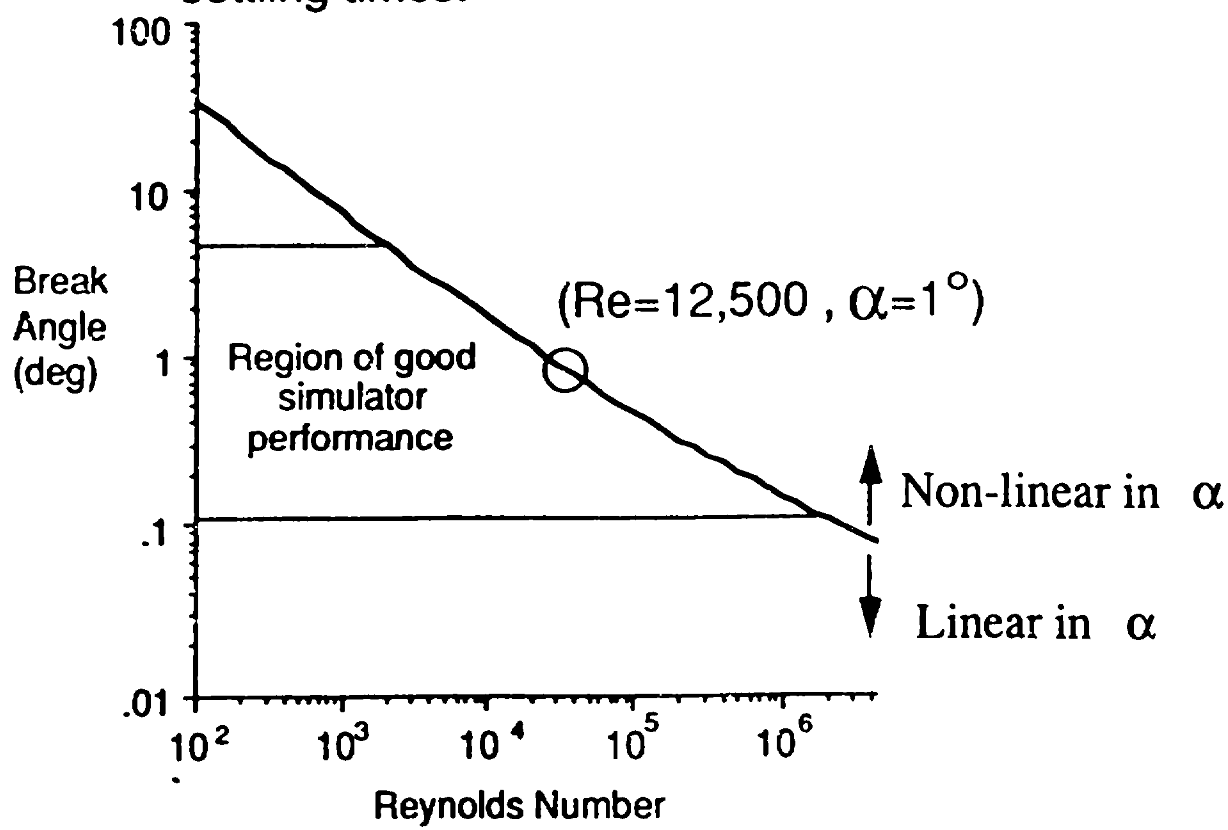

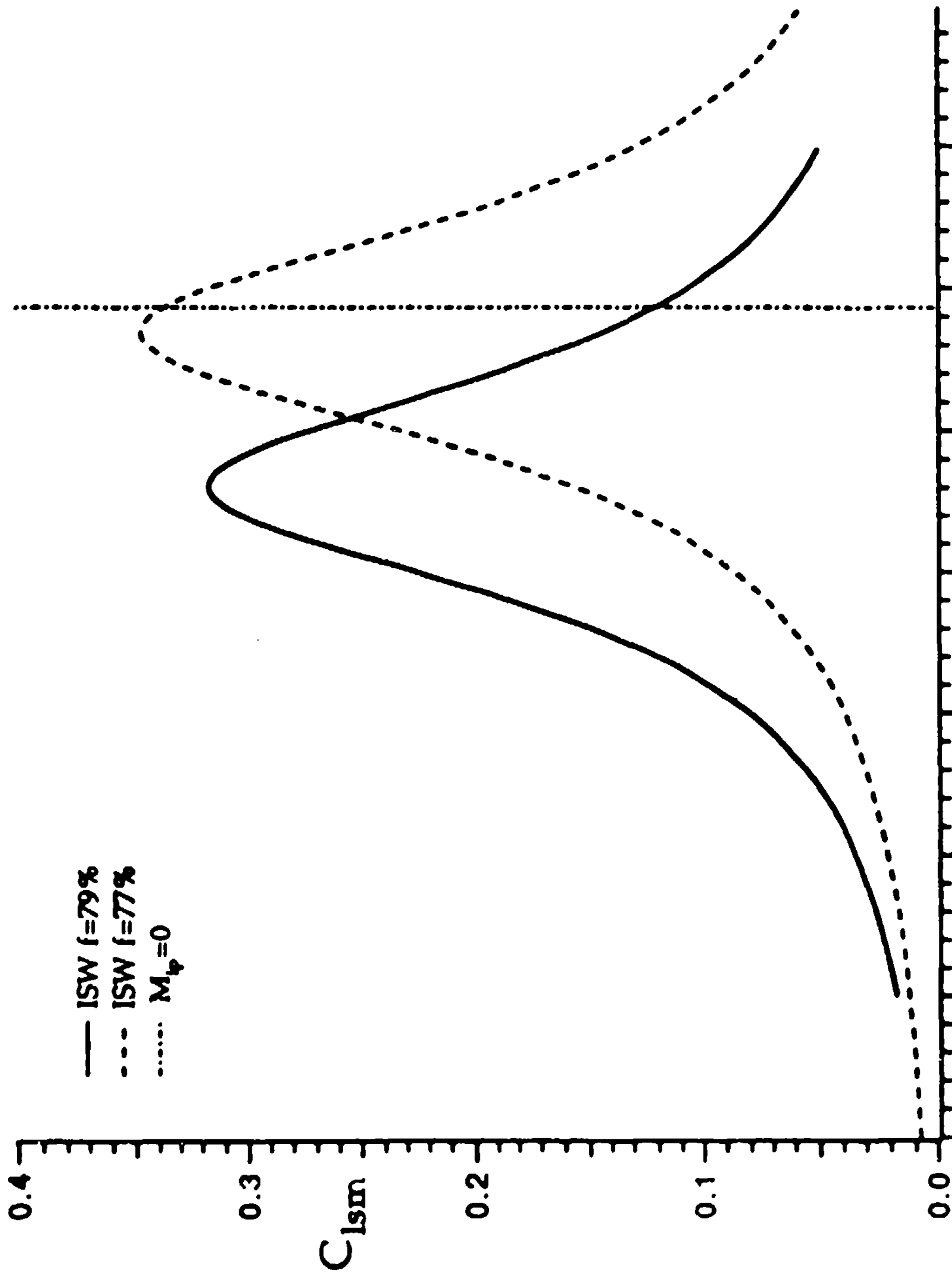

ISW f=79%
ISW f=77%
M_{tp}=0
C_{lsm}
0.0
0.1
0.2
0.3
0.4
0.04
0.06
0.08
0.10
τ

Liquid Moment Magnitude

0.0987

- Liquid Side Moment for Re=12,624, f=77.03%, c/a=3.126, tau=~~0.987~~

Spin(Hz)	Angle (deg)	Coning rate (Hz)	Liquid Side Moment (Nm)
45	1.0	4.44	0.936
90	1.0	8.88	3.744
135	1.0	13.33	8.424
90	5.0	8.88	18.720

- Liquid Side Moment for Re=126, f=80%, c/a=3.126, tau=0.987

Spin(Hz)	Angle (deg)	Coning rate (Hz)	Liquid Side Moment (Nm)
45	1.0	4.44	0.09
90	1.0	8.88	0.36
135	1.0	13.33	0.81
90	5.0	8.88	1.80

Sample Output Data

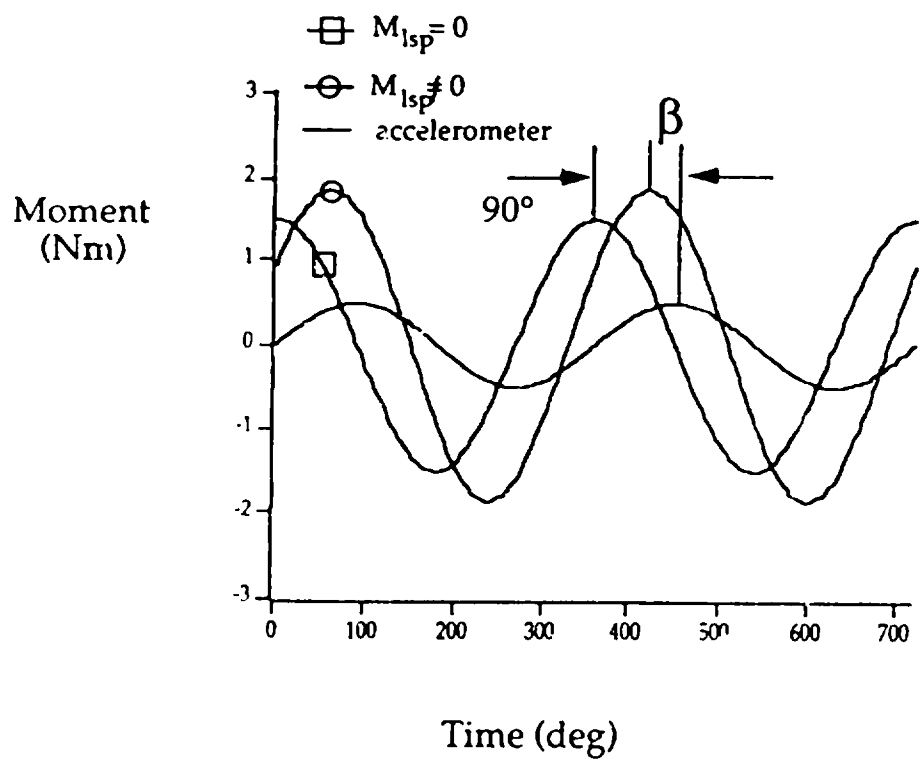

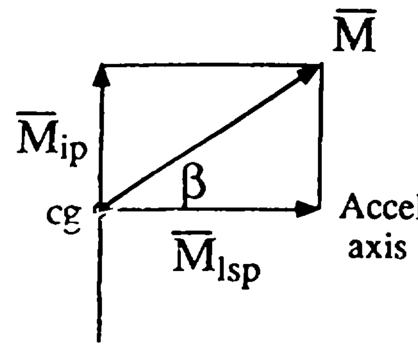

Moment Diagram

Solid In-Plane Moment

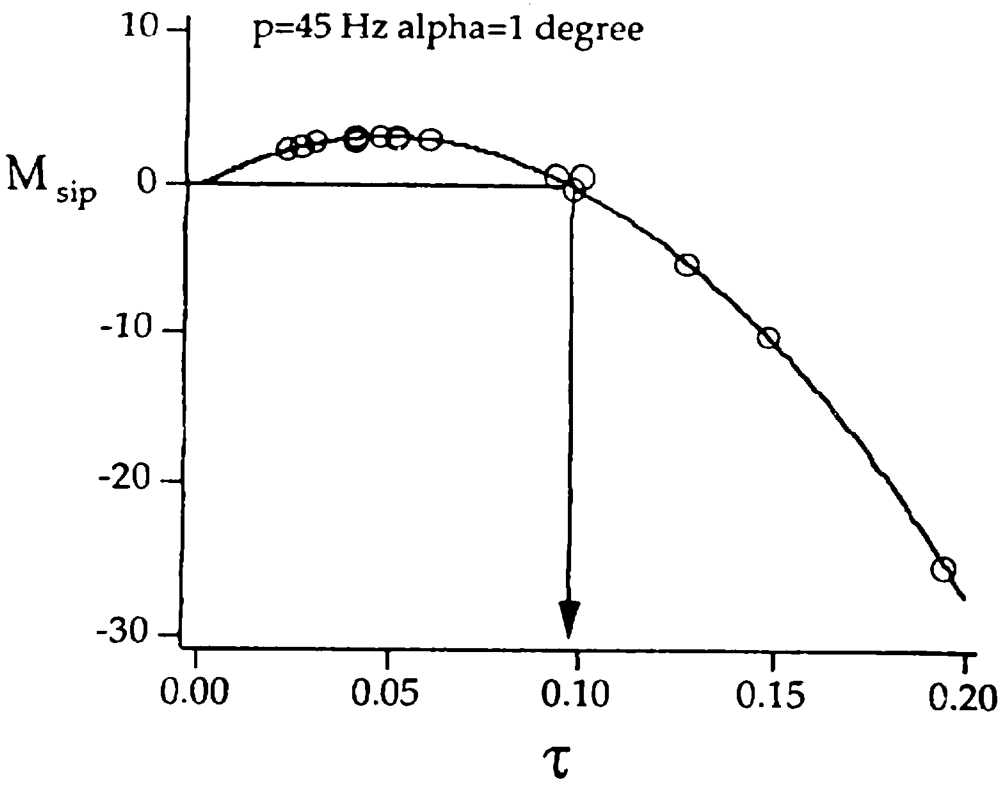

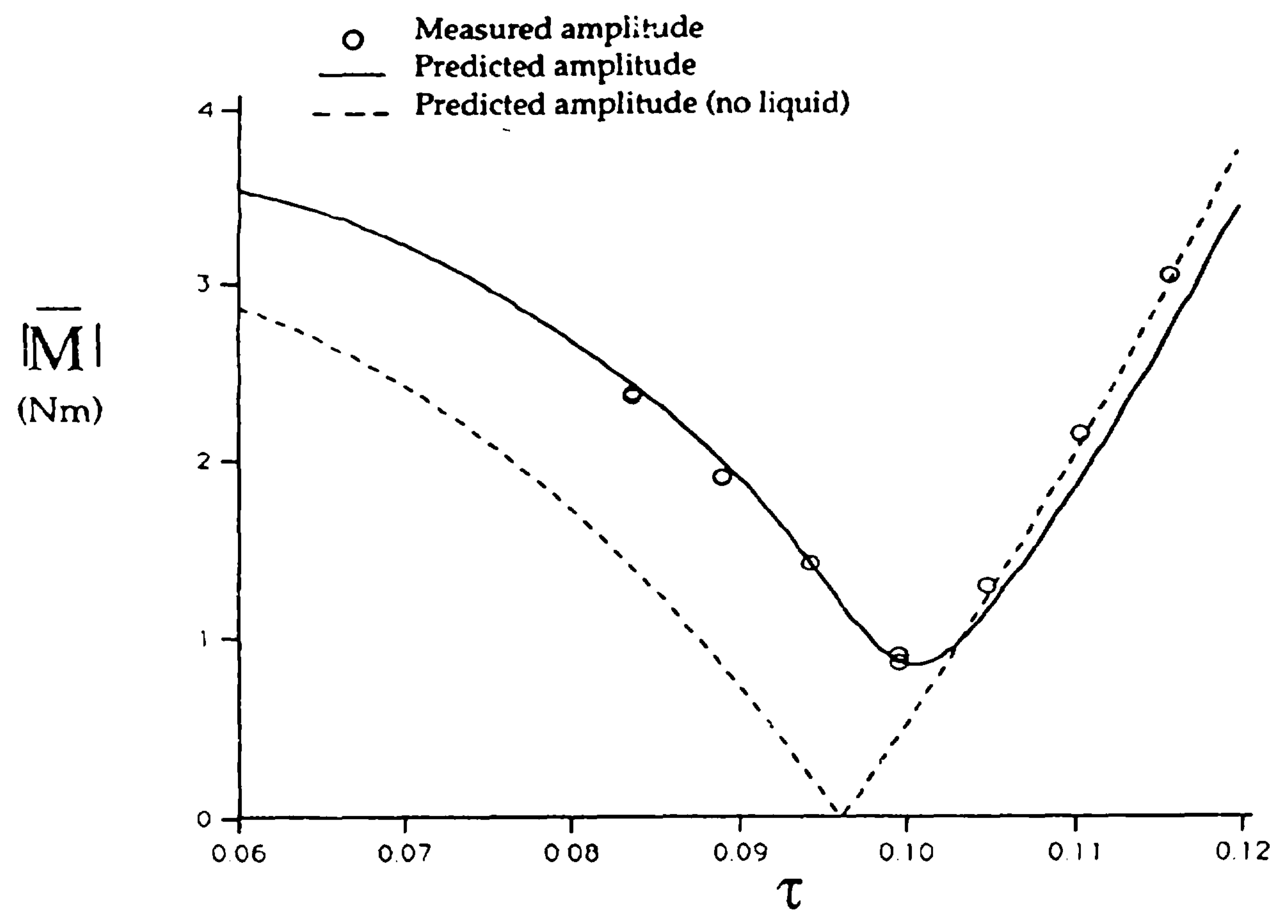

Power spectrum response plot of amplitude for liquid filled cavity.

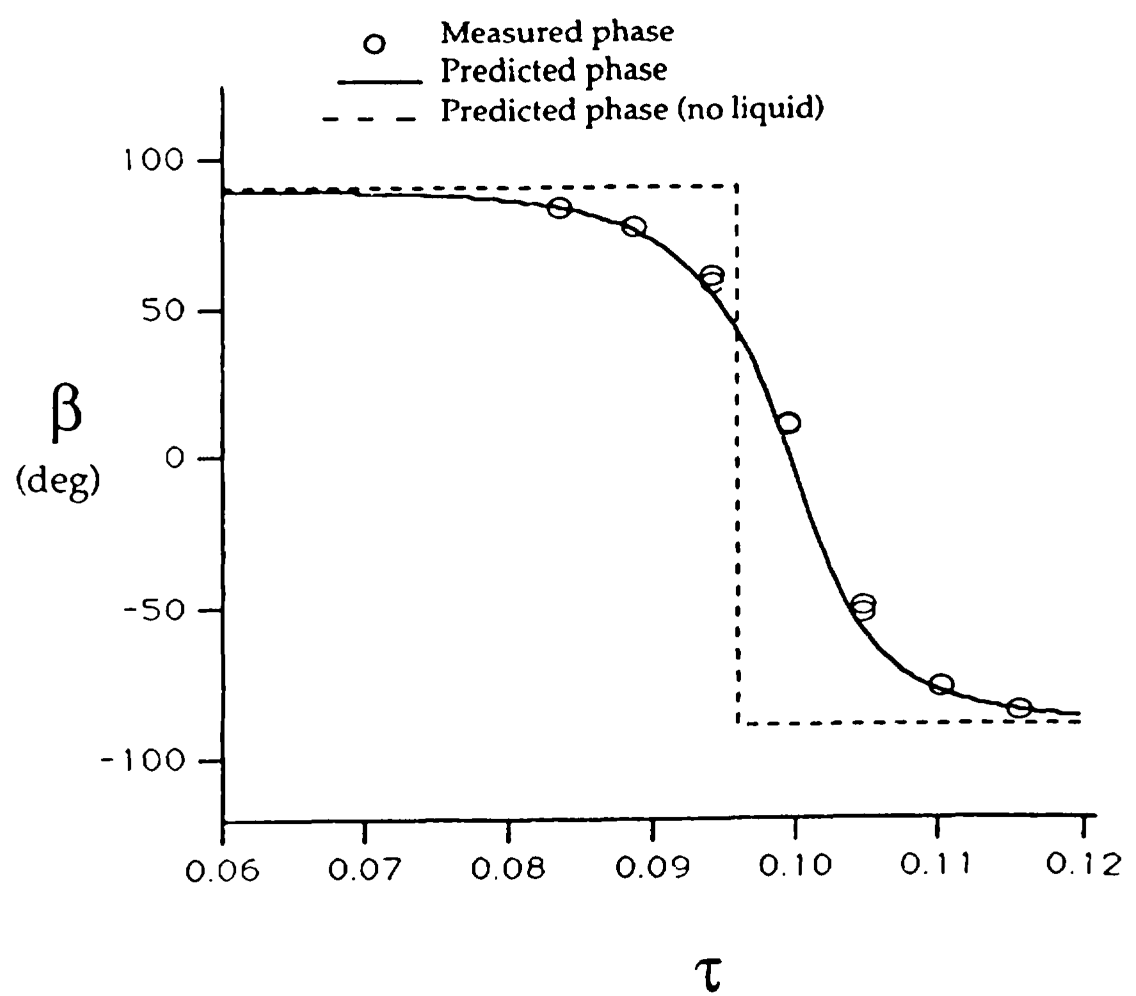

Frequency response plot of phase for liquid filled cavity.

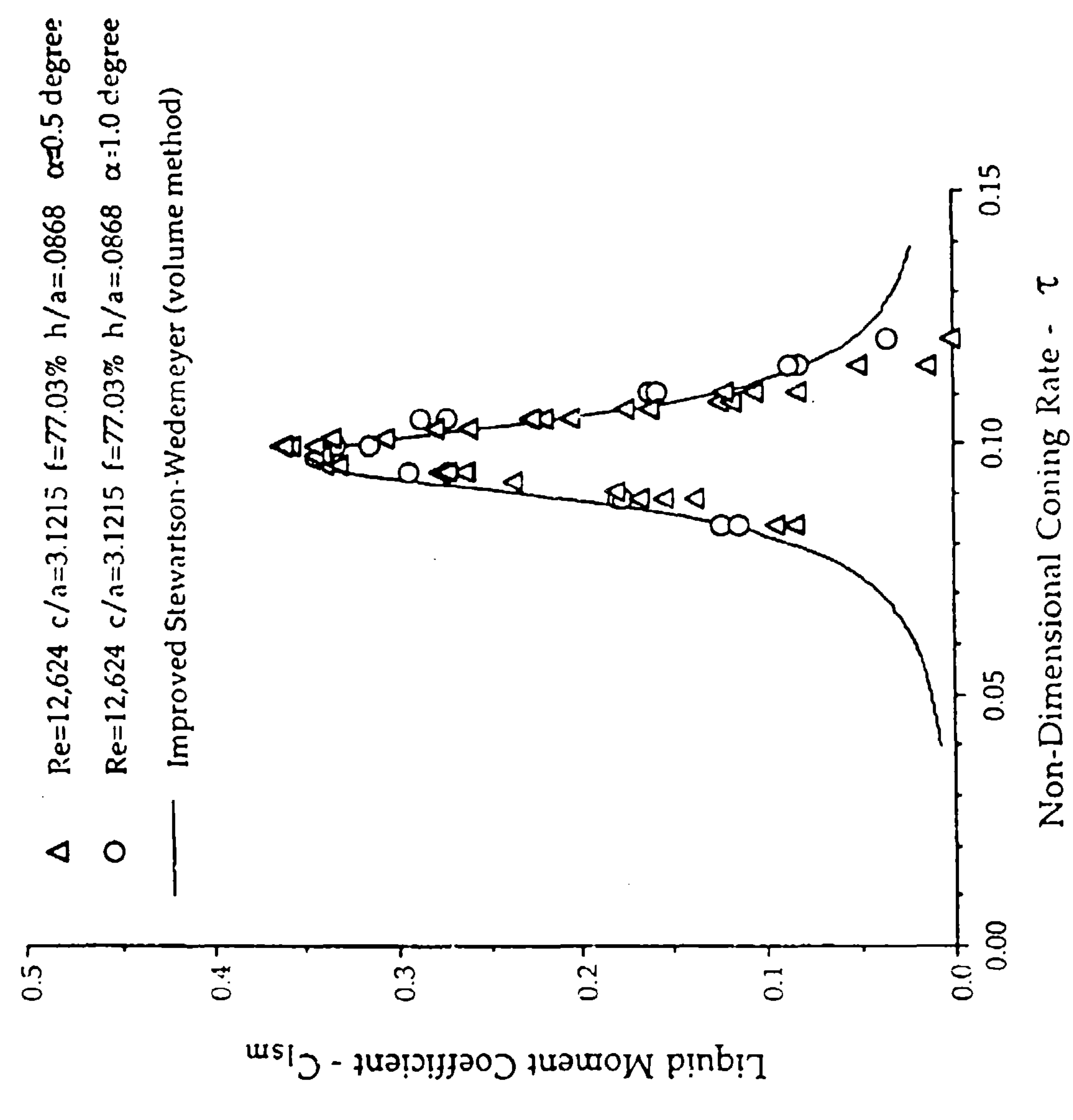

Re=12,624 c/a=3.1215 f=77.03% h/a=.0868 α=0.5 degree
Re=12,624 c/a=3.1215 f=77.03% h/a=.0868 α=1.0 degree
Improved Stewartson-Wedemeyer (volume method)
Liquid Moment Coefficient - C_{lsm}
Non-Dimensional Coning Rate - τ
0.0
0.1
0.2
0.3
0.4
0.5
0.00
0.05
0.10
0.15

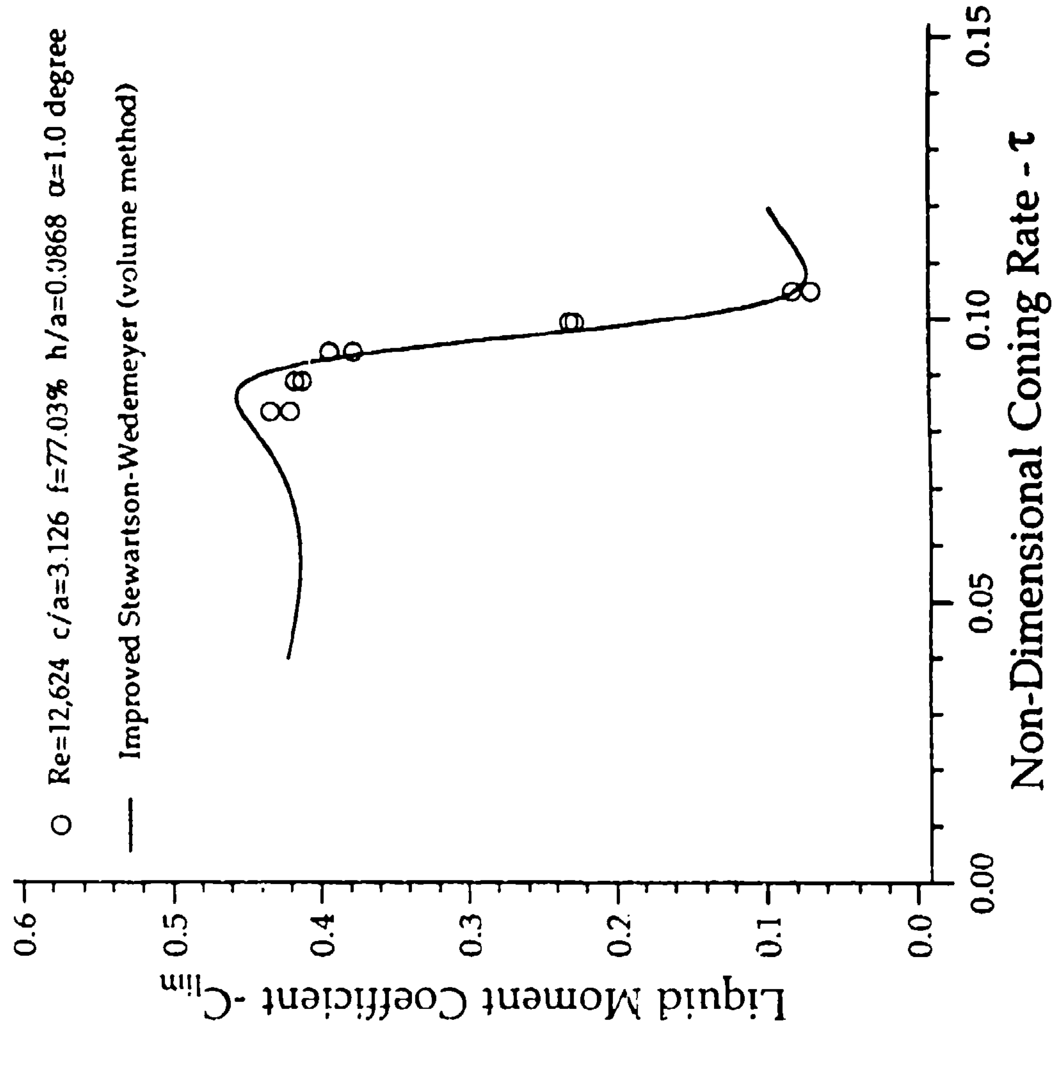

O Re=12,624 c/a=3.126 f=77.03% h/a=0.0868 α=1.0 degree
— Improved Stewartson-Wedemeyer (volume method)
Liquid Moment Coefficient -C$_{lim}$
Non-Dimensional Coning Rate - τ
0.0
0.1
0.2
0.3
0.4
0.5
0.6
0.00
0.05
0.10
0.15

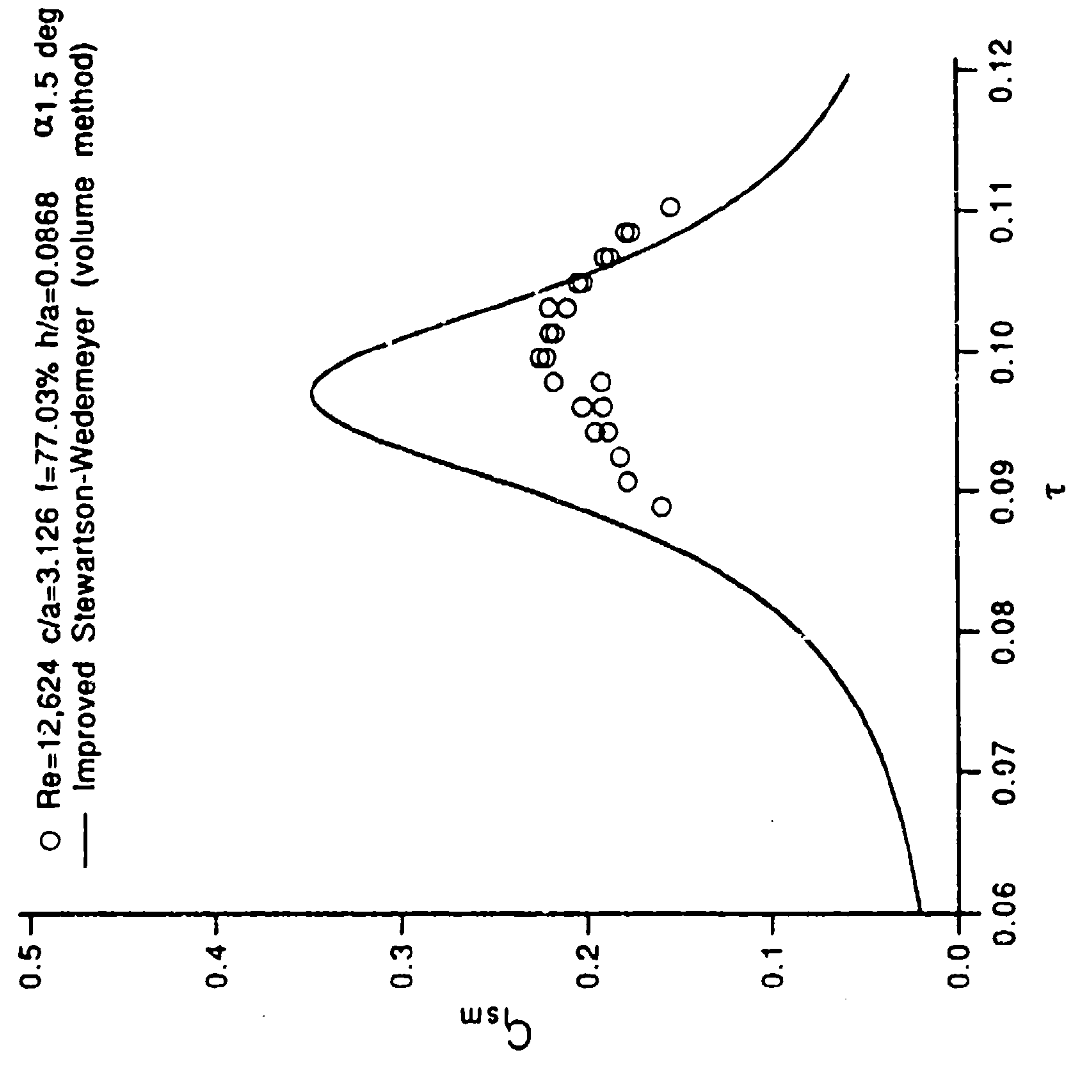

Re=12,624 c/a=3.126 f=77.03% h/a=0.0868 α1.5 deg
Improved Stewartson-Wedemeyer (volume method)
0.0
0.1
0.2
0.3
0.4
0.5
C_{sm}
0.06
0.07
0.08
0.09
0.10
0.11
0.12
τ

Error Sources

- Re = f (viscosity, a, spin).
- Measurement of fluid volume .
- Aspect ratio = f (c, a, deformation).
- Fluid temperature change during test (work dependent).
- Quality of motion at large coning angles (non-circular effects).
- Accelerometer cross axis sensitivity, circuitry, measurement.
- Relative magnitude of in-plane moment to side moment.
- Moment balance sensitivity, circuitry, measurement.
- Dynamic frequency response of moment balance.

Conclusions

- Measurements for liquid moments at Re=12,624.
- Established resolution and operating range of balance.
- Methodology for arbitrary payload configuration.
- Recommendations for arbitrary payload:
  - Excellent modeling of solid parts is required.
  - Good simulation of balance reactions including external forces.
  - Reduction of component errors through testing.
  - Second generation balance system improvements.

ROTATING FLUIDS WORKSHOP

LABORATORY FLIGHT STABILITY EVALUATION OF PRODUCTION M825A1 PAYLOAD CANISTERS

John W. Molnar

U.S. Army, Chemical Research, Development and Engineering Center
Research Dir, Physics Div, Aerodynamics Research
and Concepts Assistance Branch

22-23 April 1991

Army High Performance Computing Research Center
University of Minnesota

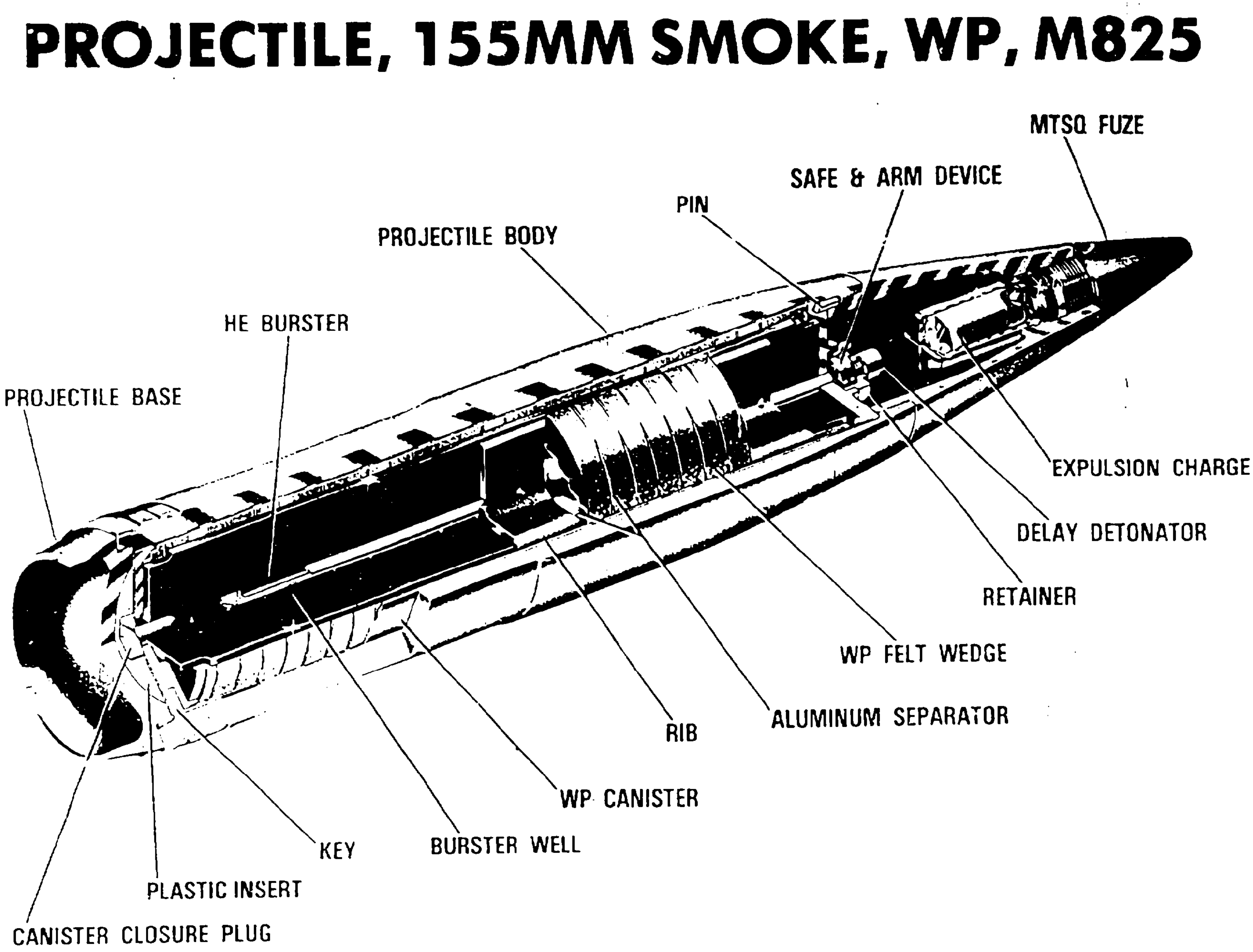

FIGURE 2. Internal Arrangement of M825 WP Smoke, 155mm Artillery Projectile

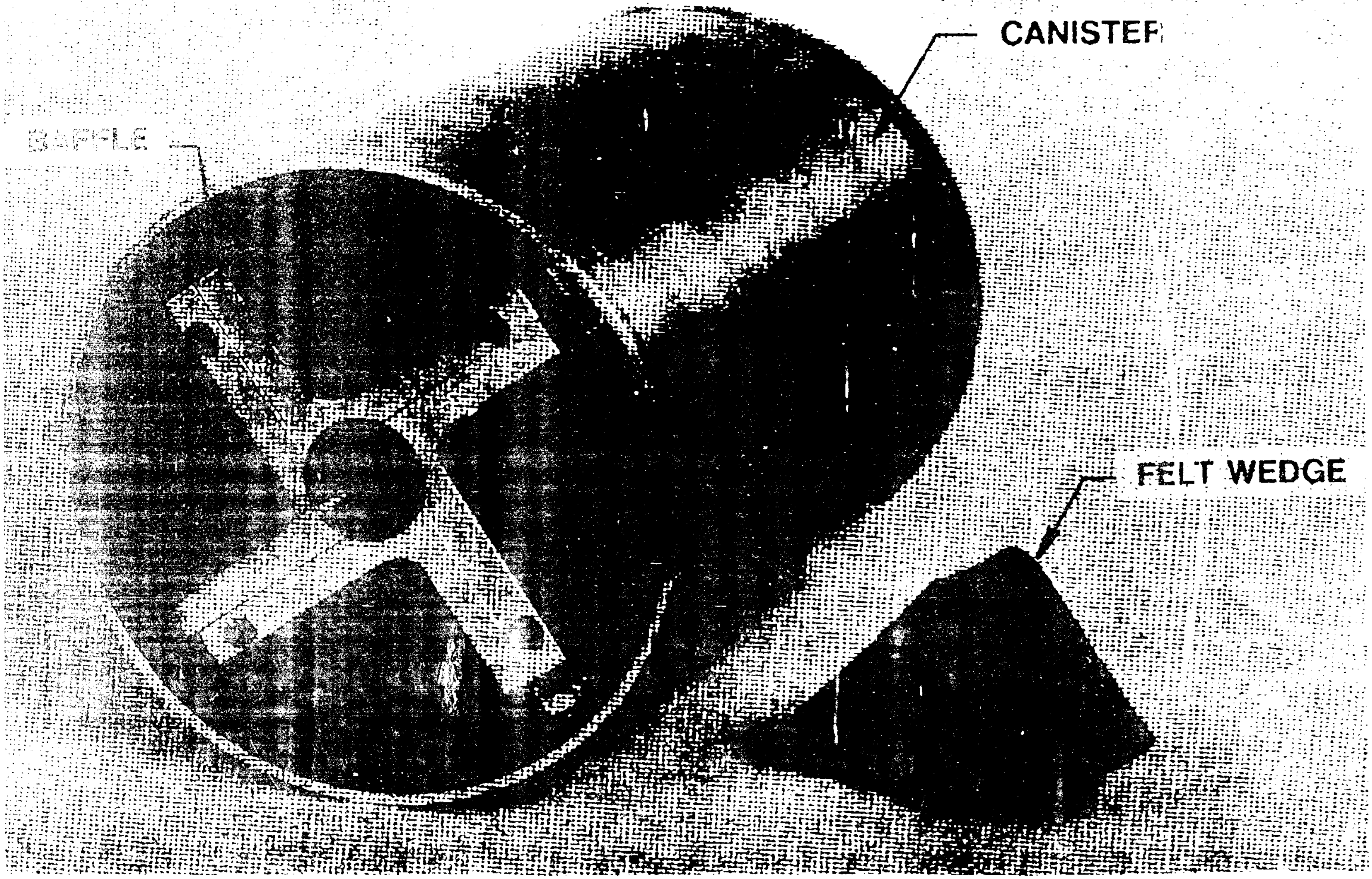

Canister, Baffle and Felt Wedge Components

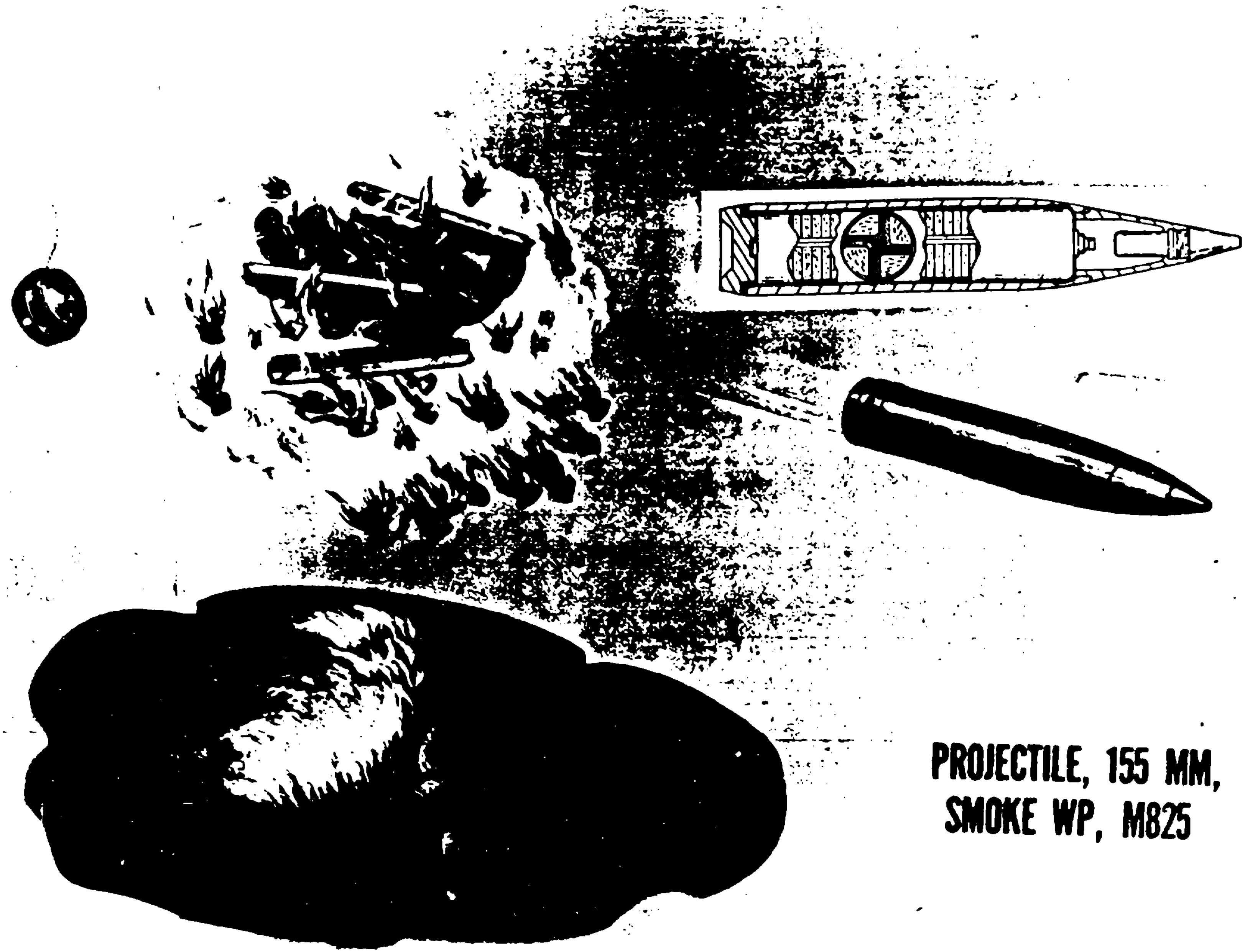

PROJECTILE, 155 MM,
SMOKE WP, M825

RELATION OF PAYLOAD INDUCED DESTABILIZING YAWING MOMENT AND DESPIN MOMENT TERMINOLOGY

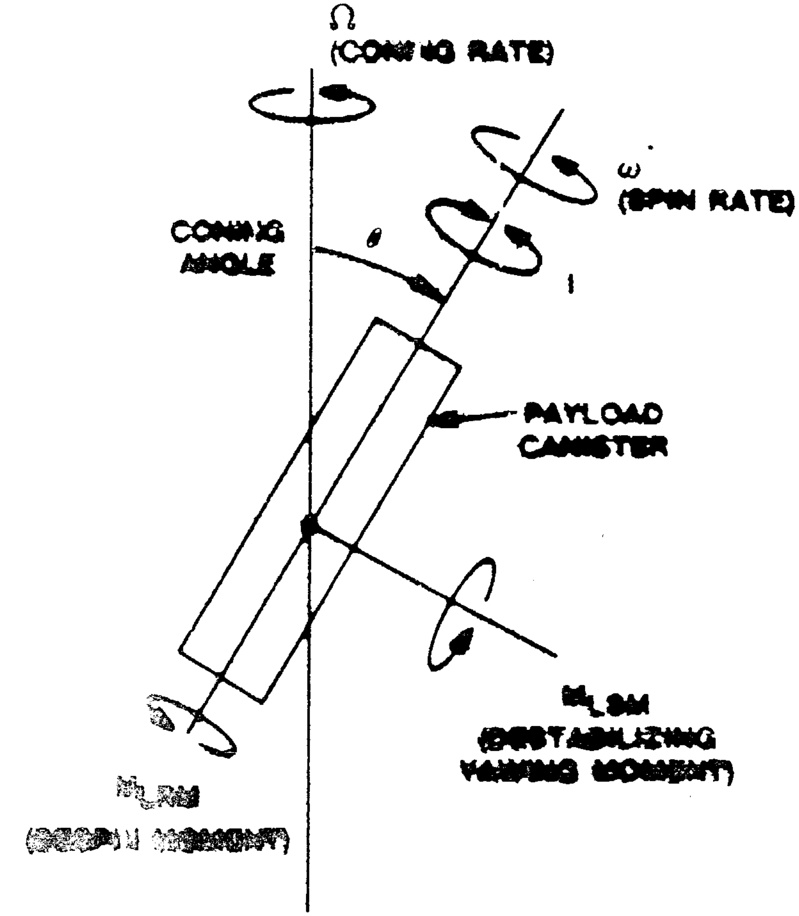

$$M_{LSM} = \frac{M_{LRM}}{\tan \theta}$$

A0332-9010-A1 1146-02

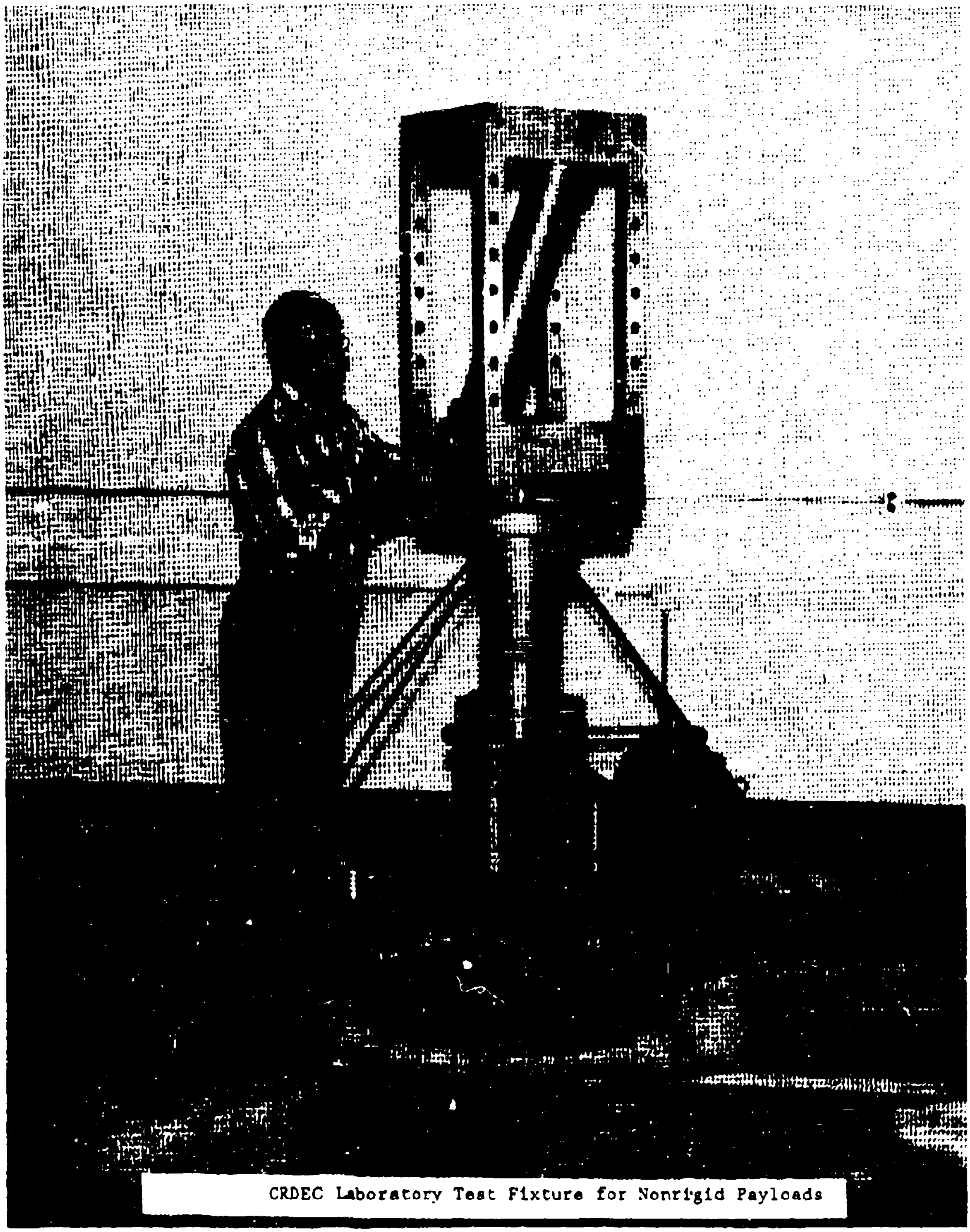

CRDEC Laboratory Test Fixture for Nonrigid Payloads

RELATION OF FLIGHT AND TEST FIXTURE MOTION

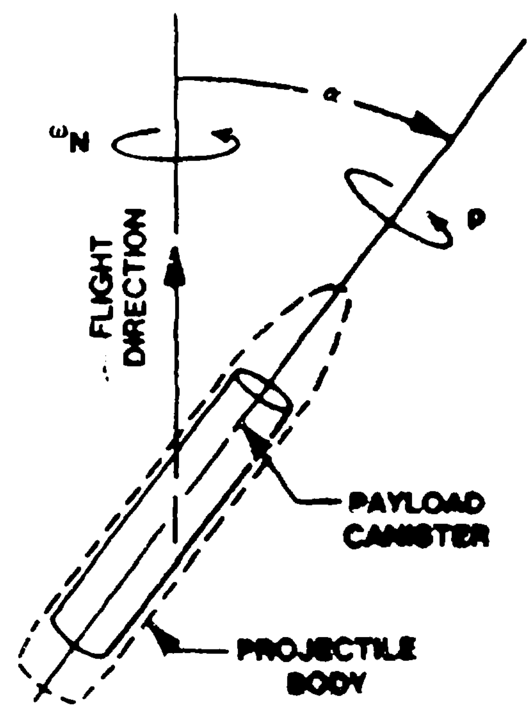

PAYLOAD IN FLIGHT

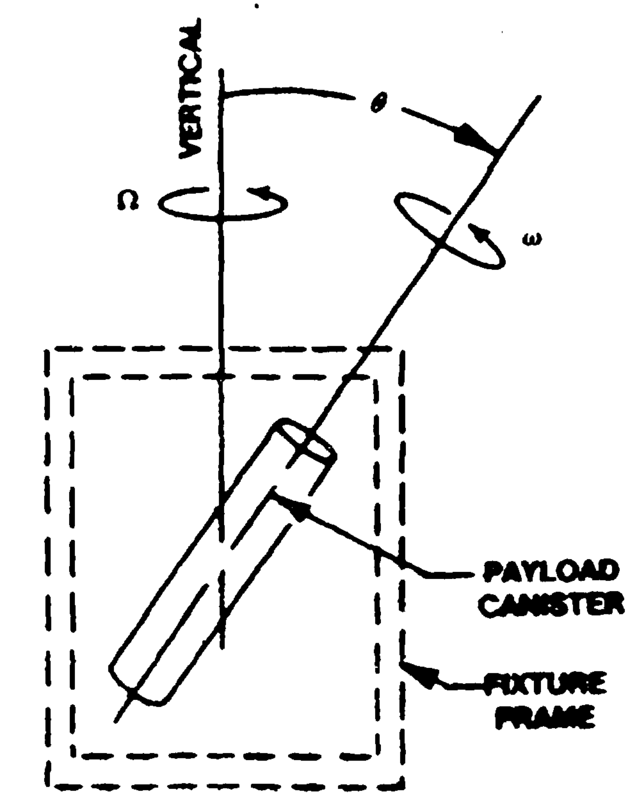

PAYLOAD ON TEST FIXTURE

M825A1 Payloads Tested

A total of 12 different M825A1 payload canisters were evaluated during this study as listed below:

CONFIG. No.	DESCRIPTION	CRDEC No.	EMPTY Wt.* lbs.	FILLED Wt.** lbs.	SIMULANT Wt. lbs.	I (EMPTY)* Slug-Ft.	I (FILLED)** Slug-Ft.
1	STD L A	#6	23.88	37.01	13.13	.055000	.064838
2	STD H A	#38	24.26	37.33	13.07	.055317	.065125
3	STD L B	#45	24.06	37.17	13.11	.055128	.064895
4	STD H B	#51	24.16	37.23	13.07	.055200	.065000
5	FAT L A	#18	24.24	37.36	13.12	.055211	.065046
6	FAT H A	#12	24.32	37.37	13.05	.055291	.064968
7	FAT L B	#57	23.83	36.93	13.10	.054930	.064753
8	FAT H B	#78	24.10	37.12	13.02	.055139	.064858
9	FAT P A	SHEET #1	24.81	37.35	12.54	.055863	.065095
10	FAT P A	SHEET #2	24.83	37.30	12.47	.055846	.065089
11	FAT P A	ROLL #1	24.56	37.23	12.67	.055683	.065133
12	FAT P A	ROLL #2	24.41	37.23	12.82	.055540	.065030

Where:

STD = Standard radius felt wedges, R=2.46"
FAT = Enlarged radius felt wedges, R=2.56"
L = Light weight felt wedges, Thickness 0.725"-0.780"
H = Heavy weight felt wedges, Thickness 0.781"-0.850"
A = Manufacturer A
B = Manufacturer B
P = Production felt wedges
A SHEET = Manufacturer A felt supplied in sheets
A ROLL = Manufacturer A felt supplied in rolls

* Canister contains all payload components except WP simulant.
** Canister contains all payload components including liquid WP simulant.

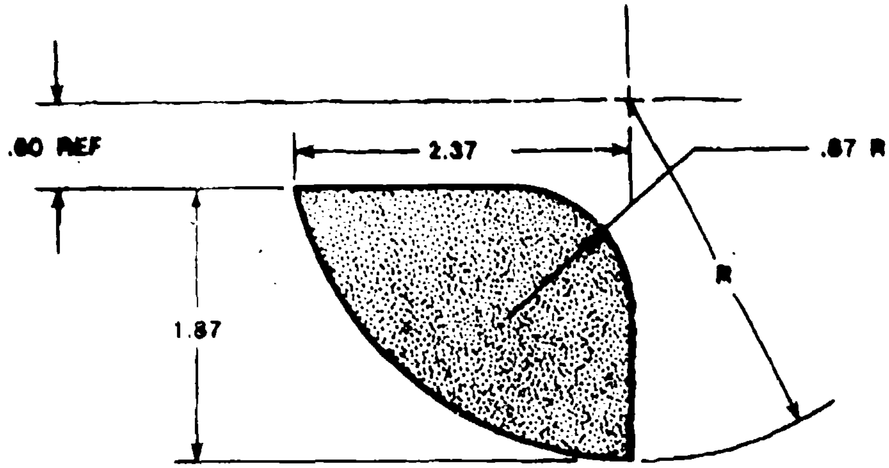

DESIGNATION	R
SPEC	2.46
ENLARGED	2.56

FELT SHEET: CLOTH, FELT, WOOL, PRESSED, TYPE I
CLASS 12R3, .75 THICK
SPEC C-F-206

NOTE: ALL DIMENSIONS ARE IN INCHES

TABLE 1

Properties of Fluorinert (Physical Simulant for Liquid White Phosphorus)		
	Fluorinert* (25 ° C)	White Phosphorus (43.3 ° C)
Density	1.73 gm/ml	1.73 gm/ml
Viscosity	1.50 CS	1.50 CS
Surface Tension	15.4 dynes/cm	71.6 dynes/cm

NOTE: Blend of Fluorinert FC40 and FC72, 1 Part FC40 to 0.129 Part 0.129 Part FC72 by volume. Fluorinert is an electronic fluid manufactured by: Commercial Chemical Division/3M, 223-65-04 3M Center, St. Paul, MN 55144-1000.

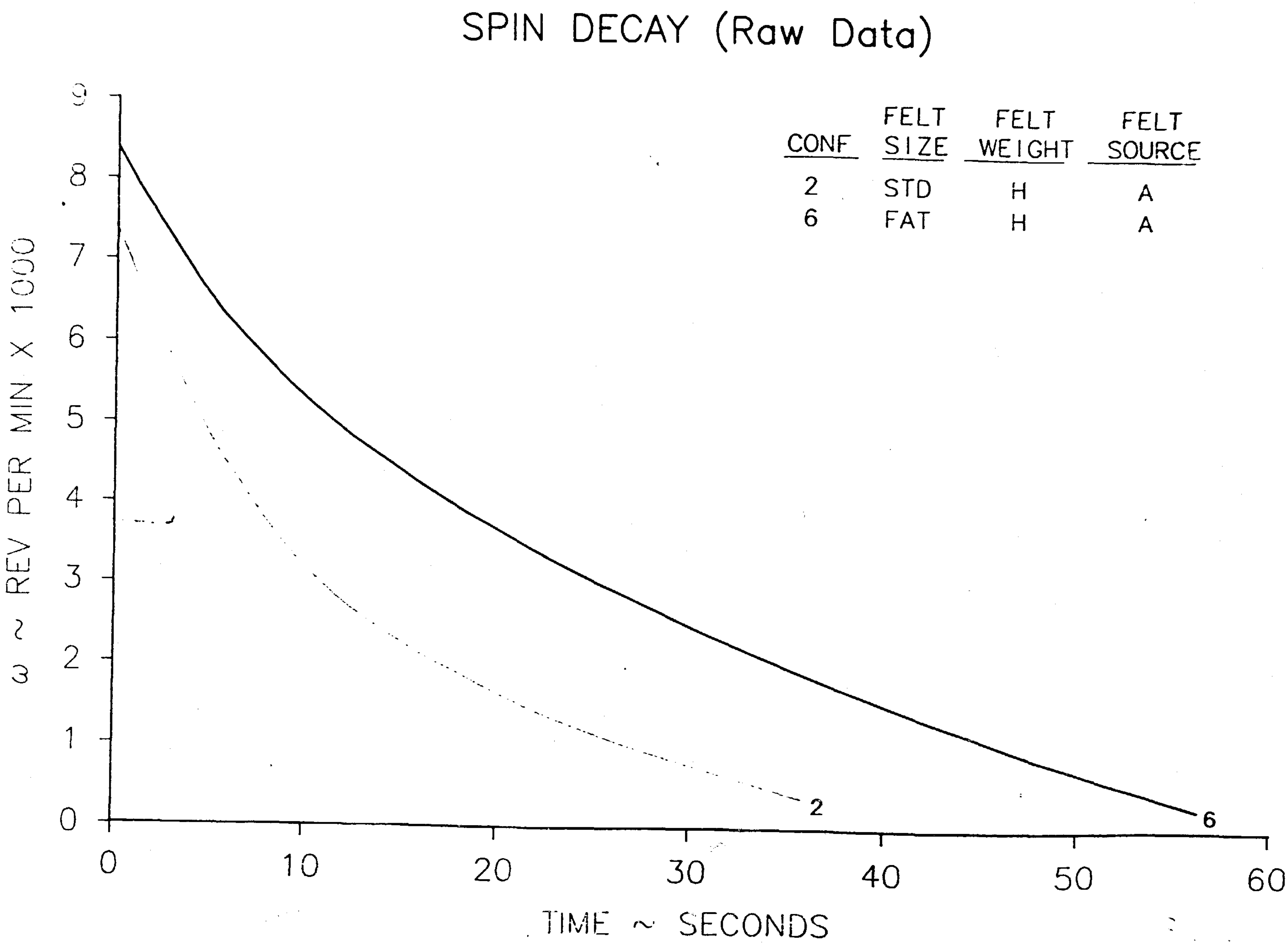
SPIN DECAY (Raw Data)
CONF FELT SIZE FELT WEIGHT FELT SOURCE
2 STD H A
6 FAT H A
ω ~ REV PER MIN X 1000
TIME ~ SECONDS
0
1
2
3
4
5
6
7
8
9
10
20
30
40
50
60

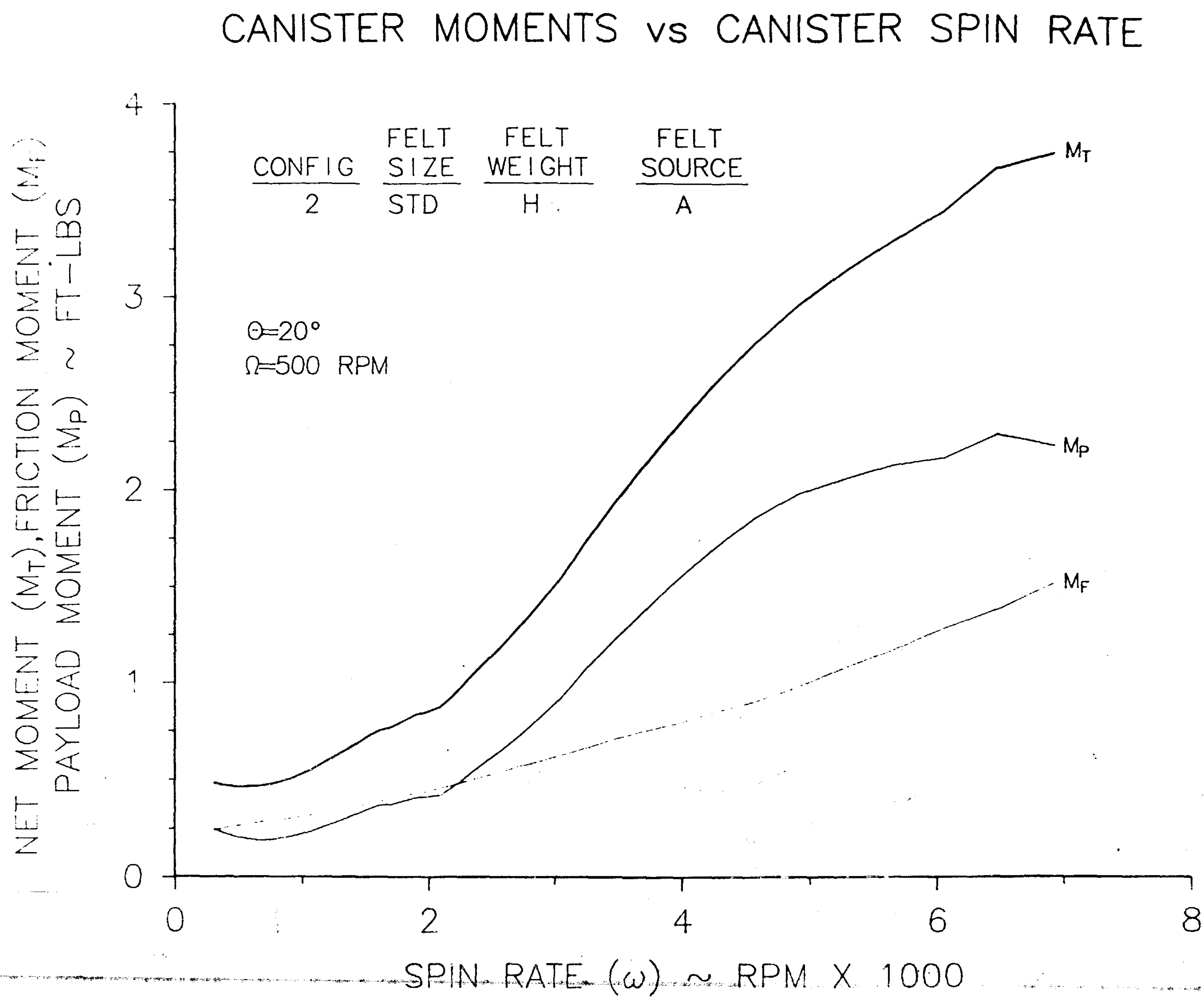
CANISTER MOMENTS vs CANISTER SPIN RATE
CONFIG 2
FELT SIZE STD
FELT WEIGHT H
FELT SOURCE A
Θ=20°
Ω=500 RPM
M_T
M_P
M_F
NET MOMENT (M_T), FRICTION MOMENT (M_F)
PAYLOAD MOMENT (M_P) ~ FT-LBS
SPIN RATE (ω) ~ RPM X 1000
0
1
2
3
4
0
2
4
6
8

PAYLOAD MOMENTS vs CANISTER SPIN RATE

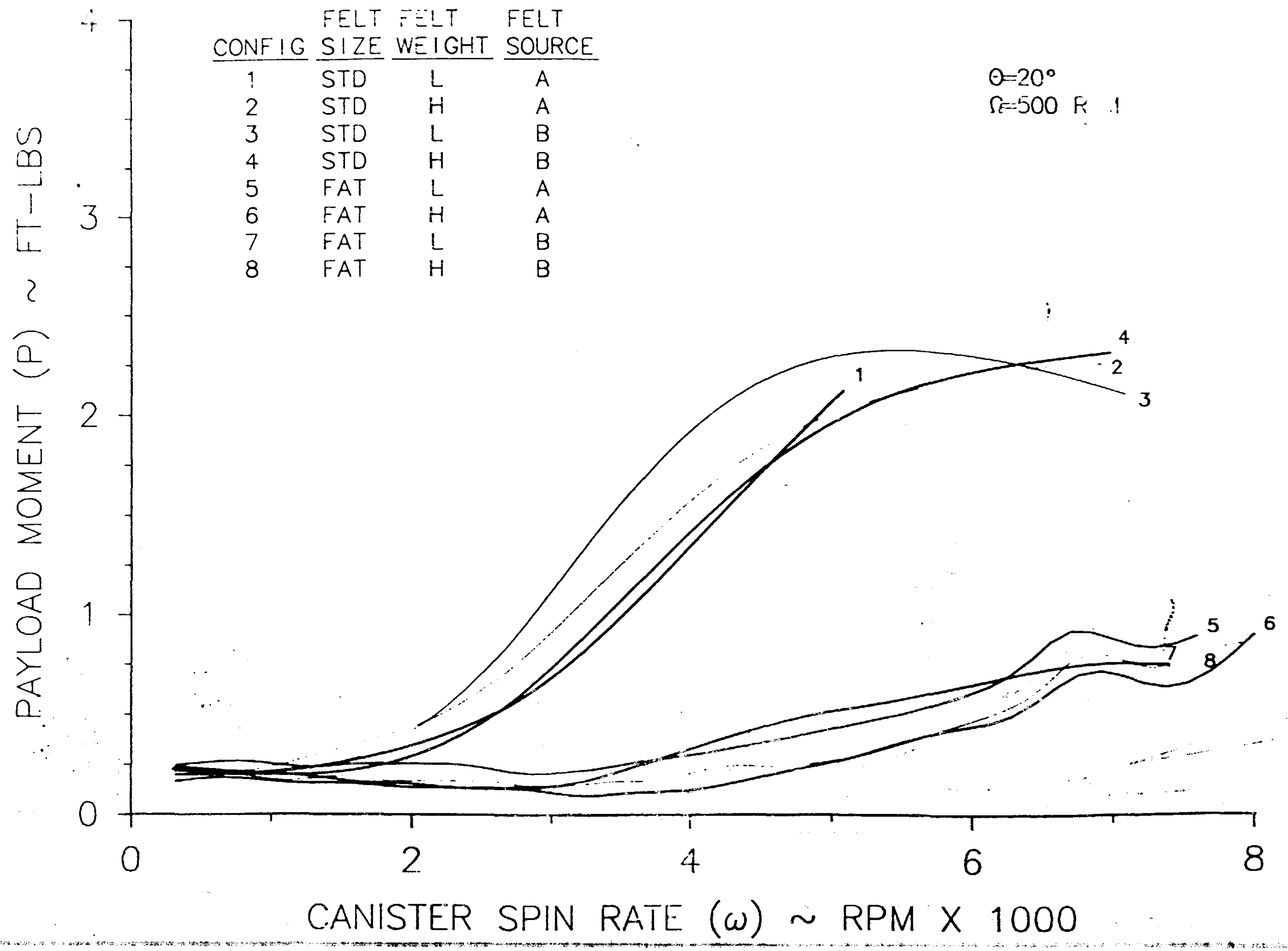

PAYLOAD MOMENTS vs CANISTER SPIN RATE

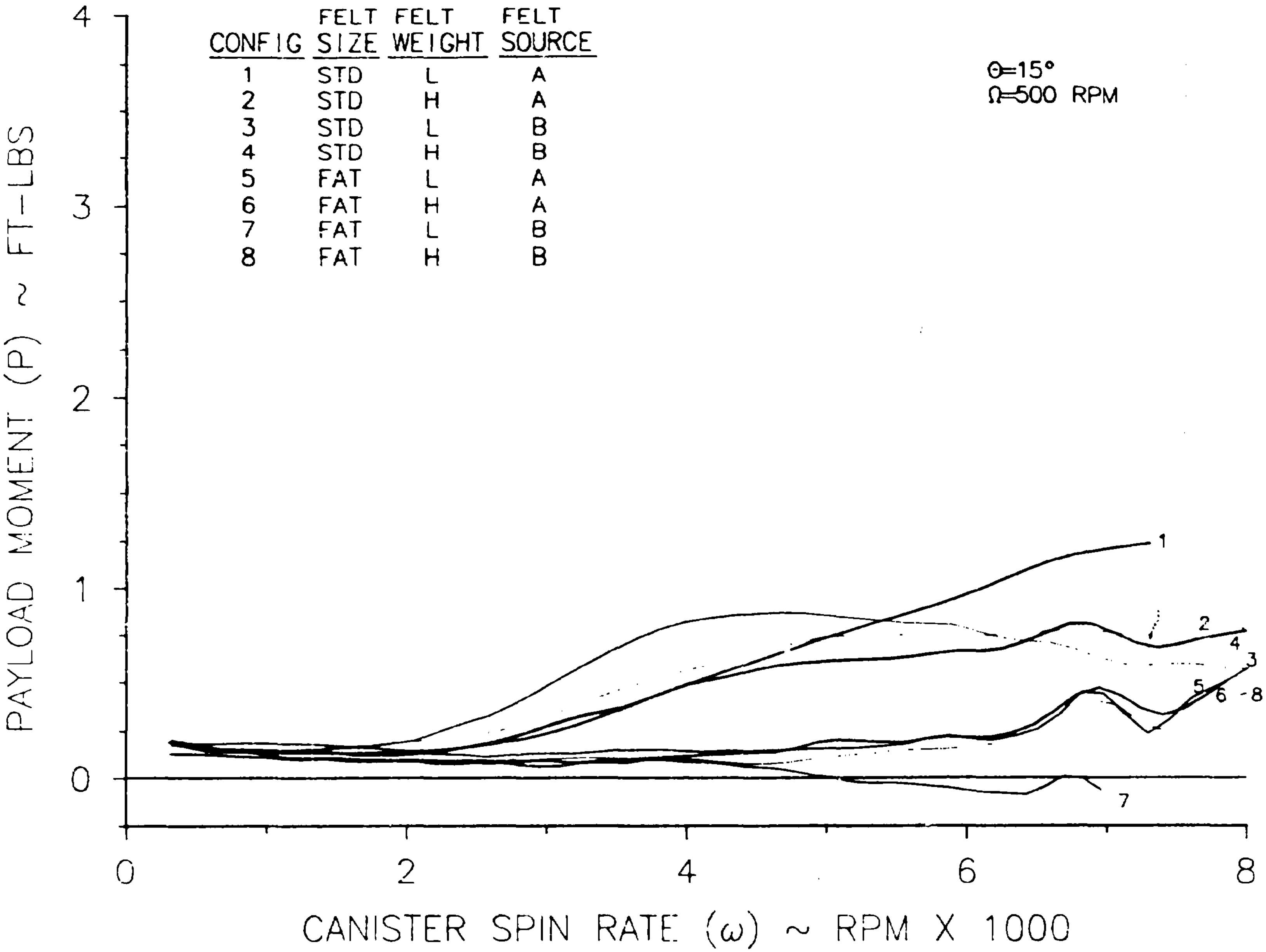

PAYLOAD MOMENTS vs CANISTER SPIN RATE

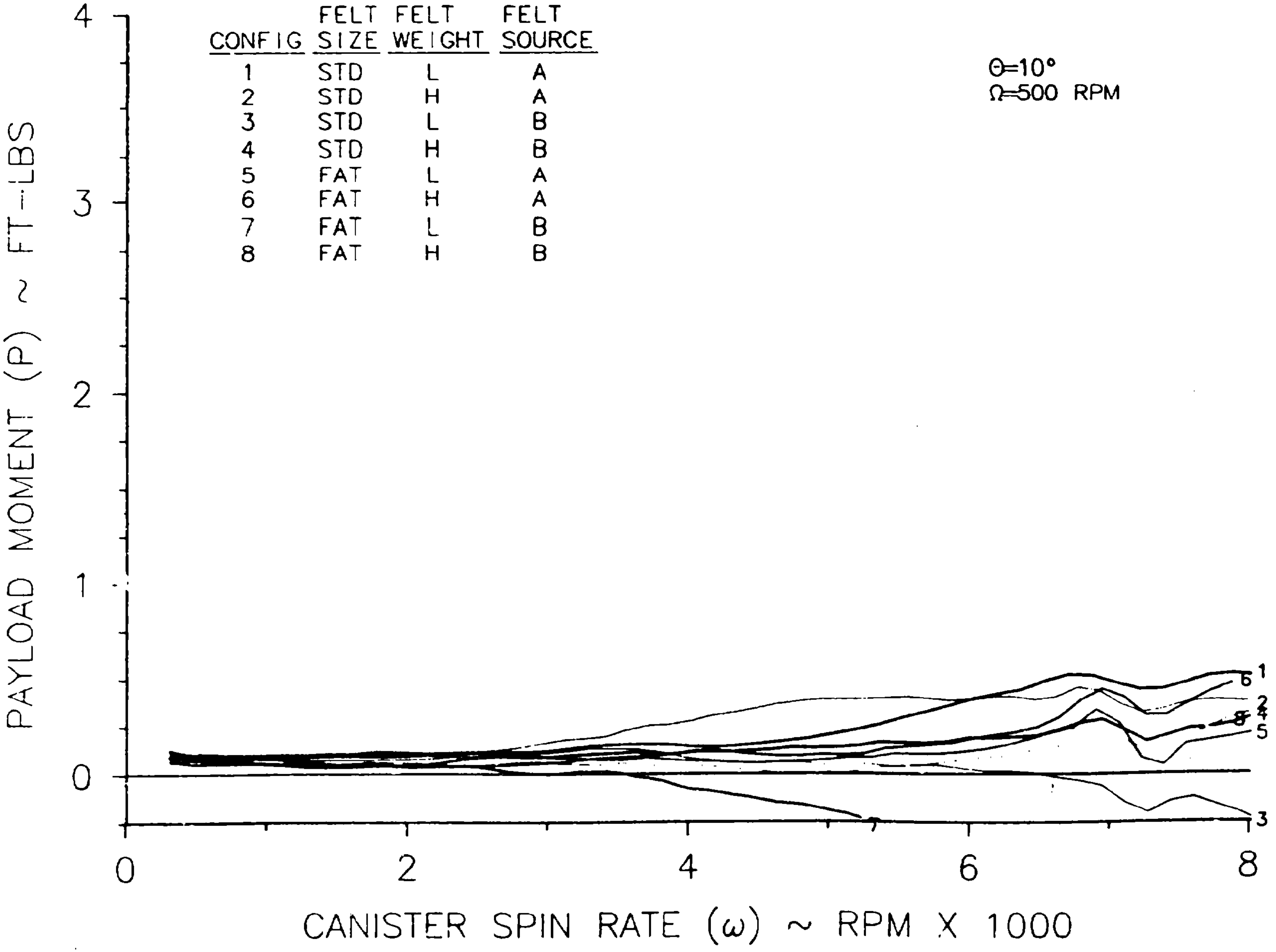

CONFIG	FELT SIZE	FELT WEIGHT	FELT SOURCE
1	STD	L	A
2	STD	H	A
3	STD	L	B
4	STD	H	B
5	FAT	L	A
6	FAT	H	A
7	FAT	L	B
8	FAT	H	B

TABLE 2

ZONE	V_o	P_o, ω (RPM)	ω_N, Ω (RPM)	α, θ (DEG)
4	Transonic	6,000	500	0 through 20

PAYLOAD MOMENTS vs CONING ANGLE

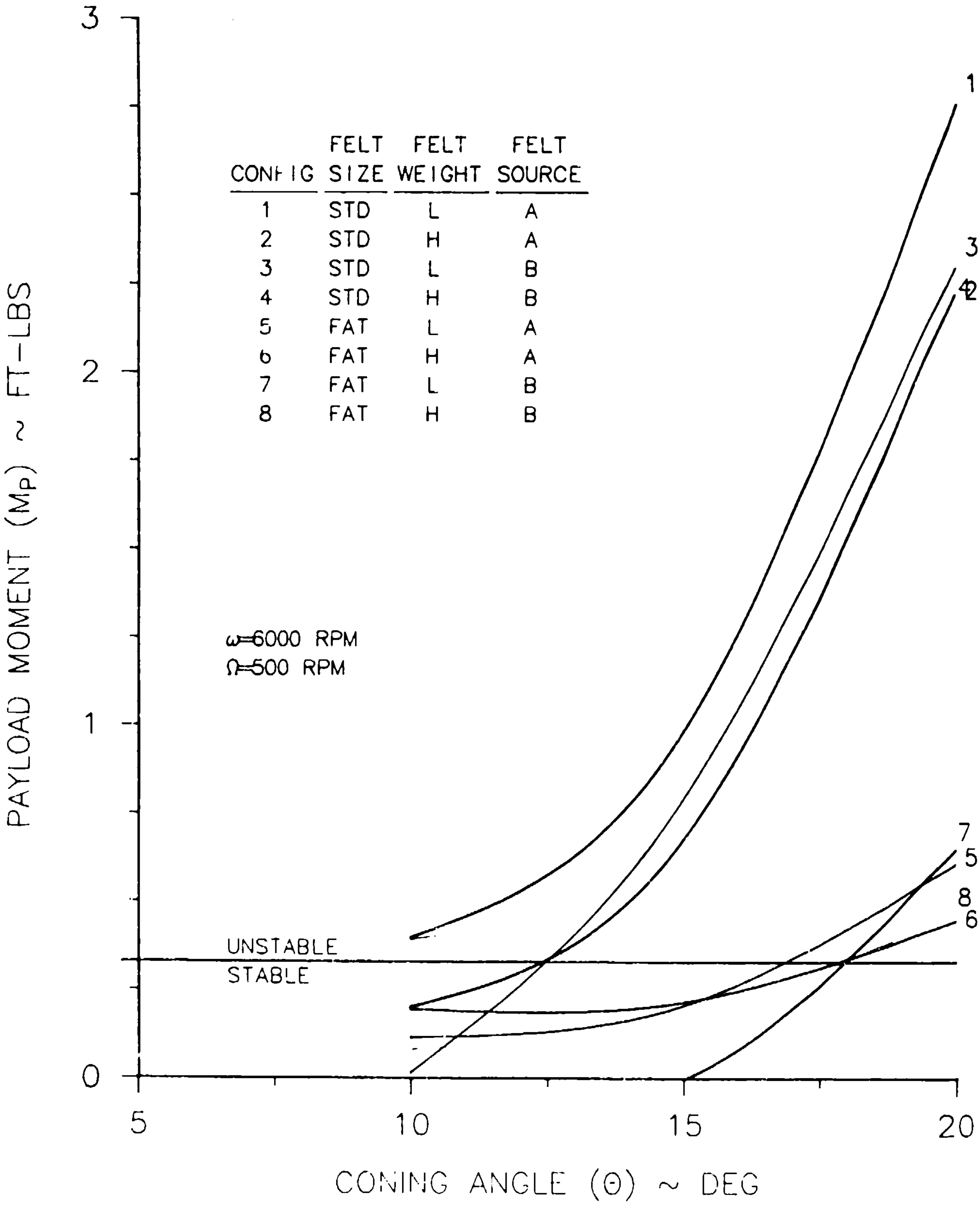

PAYLOAD MOMENTS vs CANISTER SPIN RATE

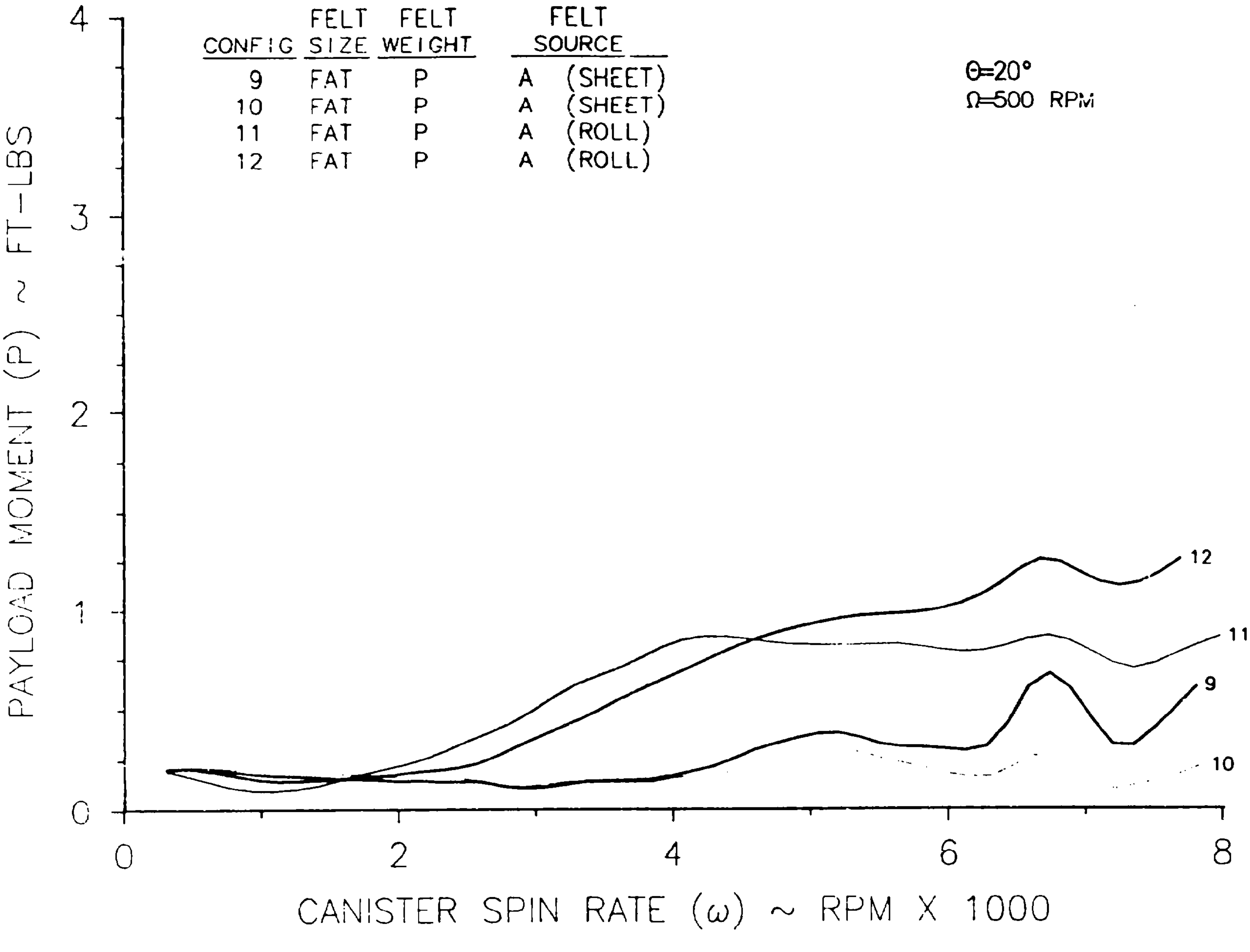

PAYLOAD MOMENTS vs CONING ANGLE

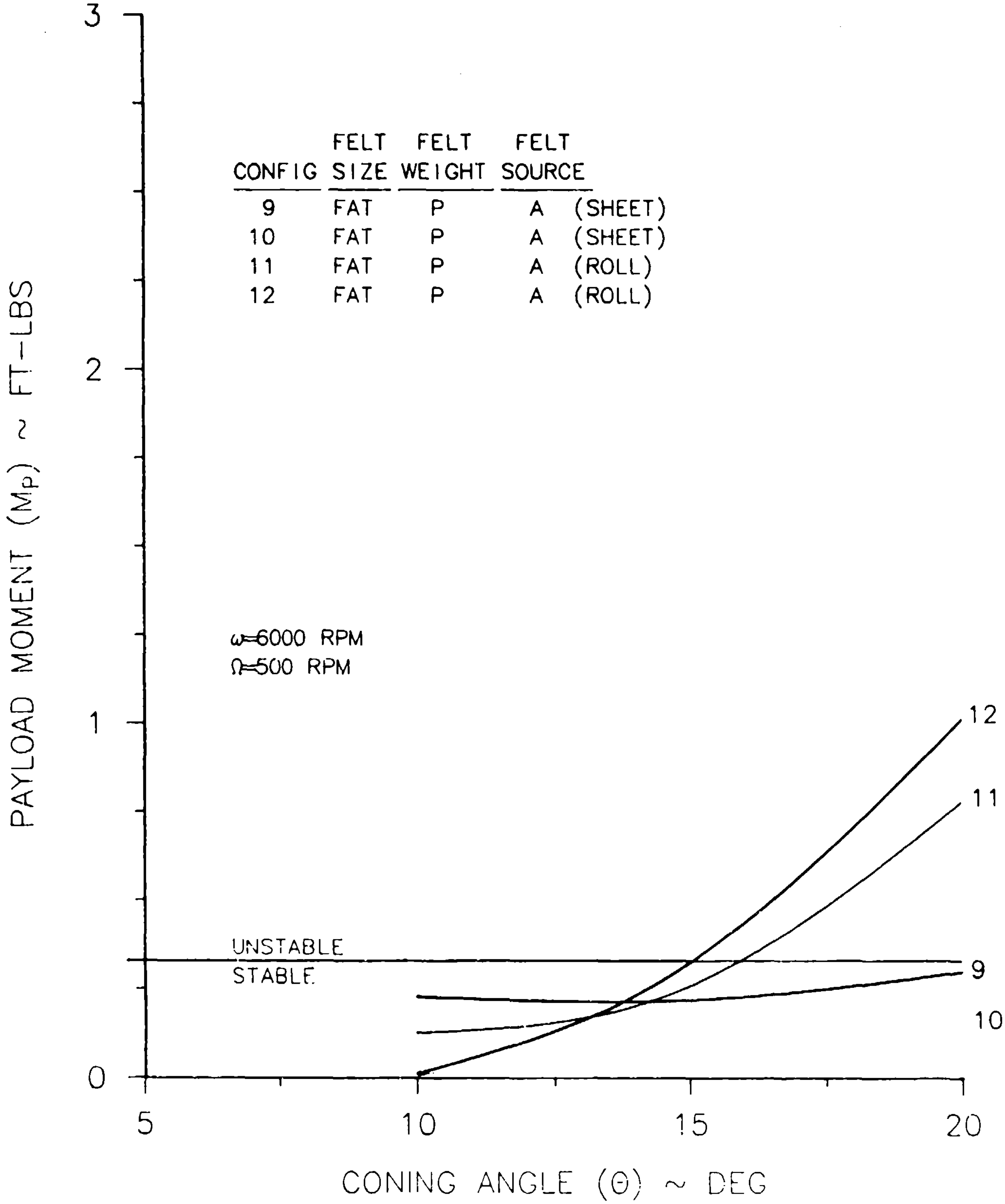

Conclusion:

This was the latest in an ongoing test series supporting the M825 Smoke Round Program. The Projectile Flight Simulator or "Spin Fixture" has been used in the development of the M825 Smoke Round and in evaluating sample units from production runs for consistency in materials and manufacturing process. It has been a valuable tool for both practical and research programs.

Theory and Experiments for Rotating Porous Media Flow

Gene Cooper
T. Gordon Brown
W. P. D'Amico

Ballistic Research Laboratory

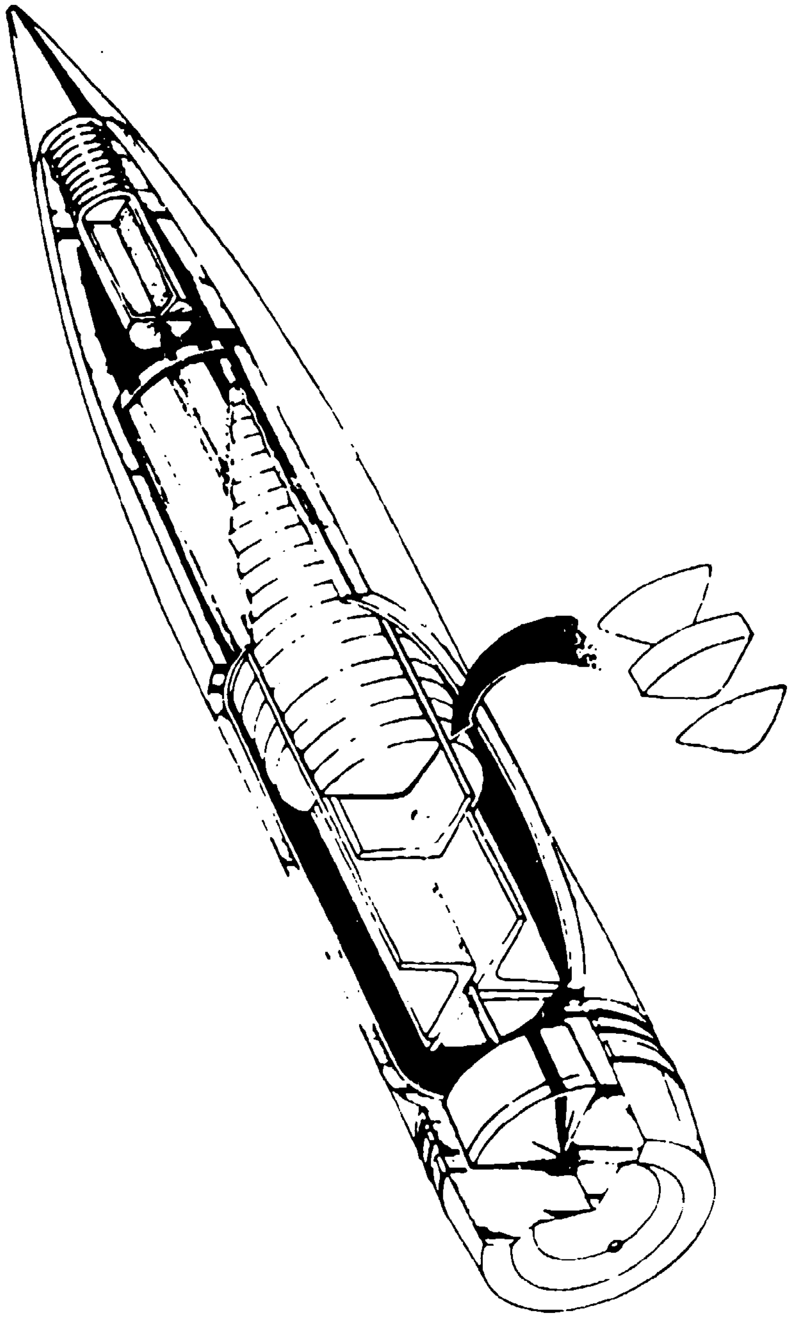

Simplified Representation of M825

Begin with a standard porous flow model

Conduct permeability tests

Conduct tests for yaw moment at small amplitudes

Consider improvements

Darcy's Law

$$\vec{D}_r = -\frac{\mu}{\kappa}\left(\vec{V}_R\right) = -\rho_L a\dot{\phi}^2 C_r \left(\frac{\vec{V}_R}{a\dot{\phi}}\right)$$

μ is the dynamic viscosity

κ is the porosity

$\vec{V}_R$ is the velocity of liquid relative to the porous medium

ρ_L is liquid density

$C_r = \frac{\mu}{\rho_L \kappa \phi}$

$\vec{D}_r$ is a pressure gradient induced by the porous media

Moment Equations

- Homogeneous Isentropic Felt
- N Spacers

$$M_Y + M_Z = C_{LM}$$

$$C_{LM} = C_{LSM}(\tau, \epsilon, C_r, f) + C_{LIM}(\tau, \epsilon, C_r, f)$$

Velocity Transformation

$$V = Radial = V_H - \frac{(s-i)xC_r}{(\gamma+2i)}$$
$$W = Theta = W_H - \frac{(s-i)xC_r}{(\gamma+2i)}$$
$$U = Axial = U_H - \frac{(s-i)xC_r}{(\gamma+2i)}$$

- Stewartson Equation

$$\frac{\partial^2 p}{\partial r^2} + \frac{1}{r}\frac{\partial p}{\partial r} - \frac{p}{r^2} = -\frac{(\gamma^2+4)}{\gamma^2}\frac{\partial^2 p}{\partial x^2}$$
$$\gamma = (\epsilon + i)\tau - i + C_r$$
$$\tau = Frequency, \epsilon = DampingFactor$$

$p = pressure$ and V_H, W_H, U_H are functions of p

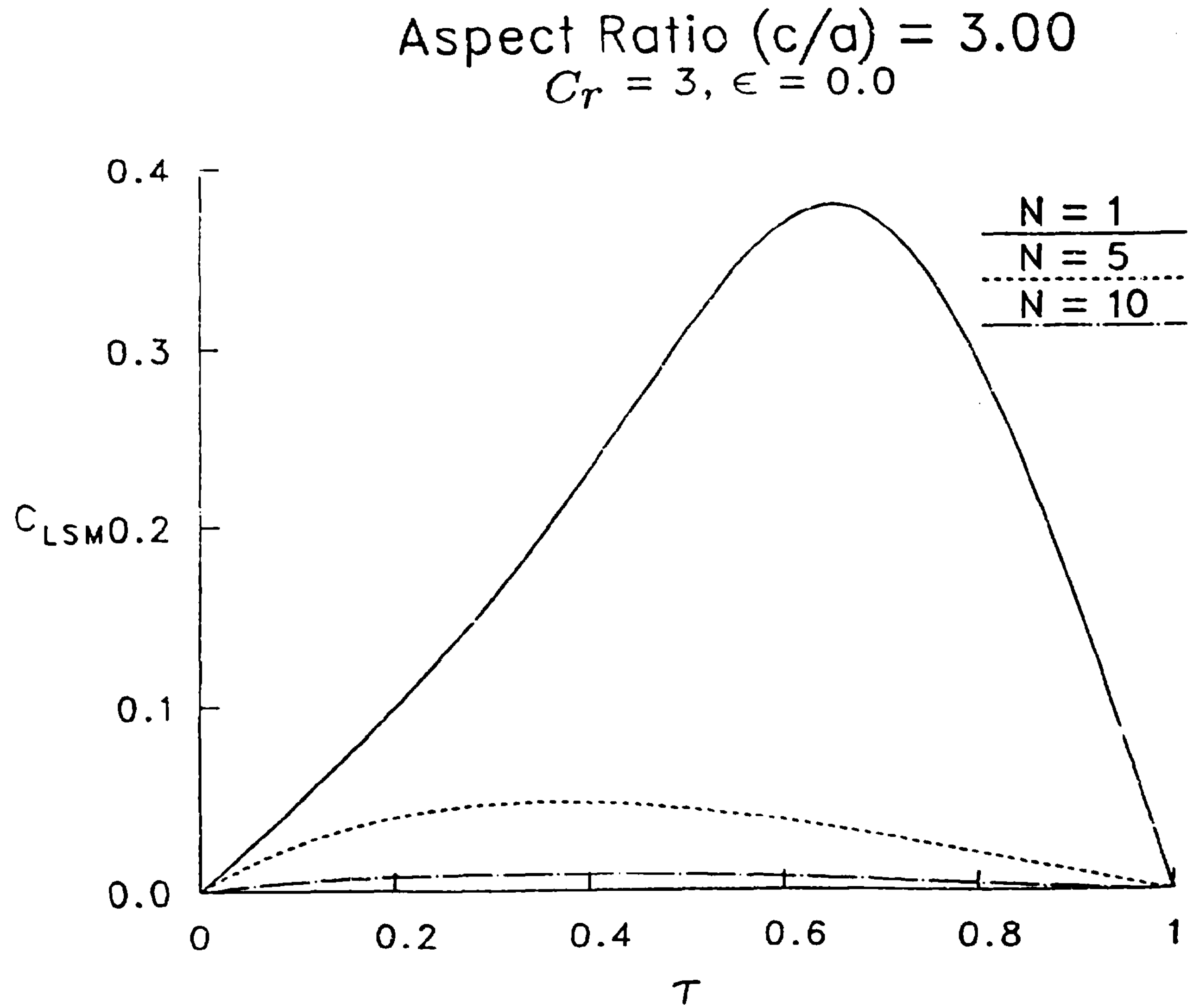

Comparison of C_{LSM} versus τ for f = 3, $C_r = 3$, $\epsilon = 0.$,N =1, 5, 10 and C_{LSM} frozen

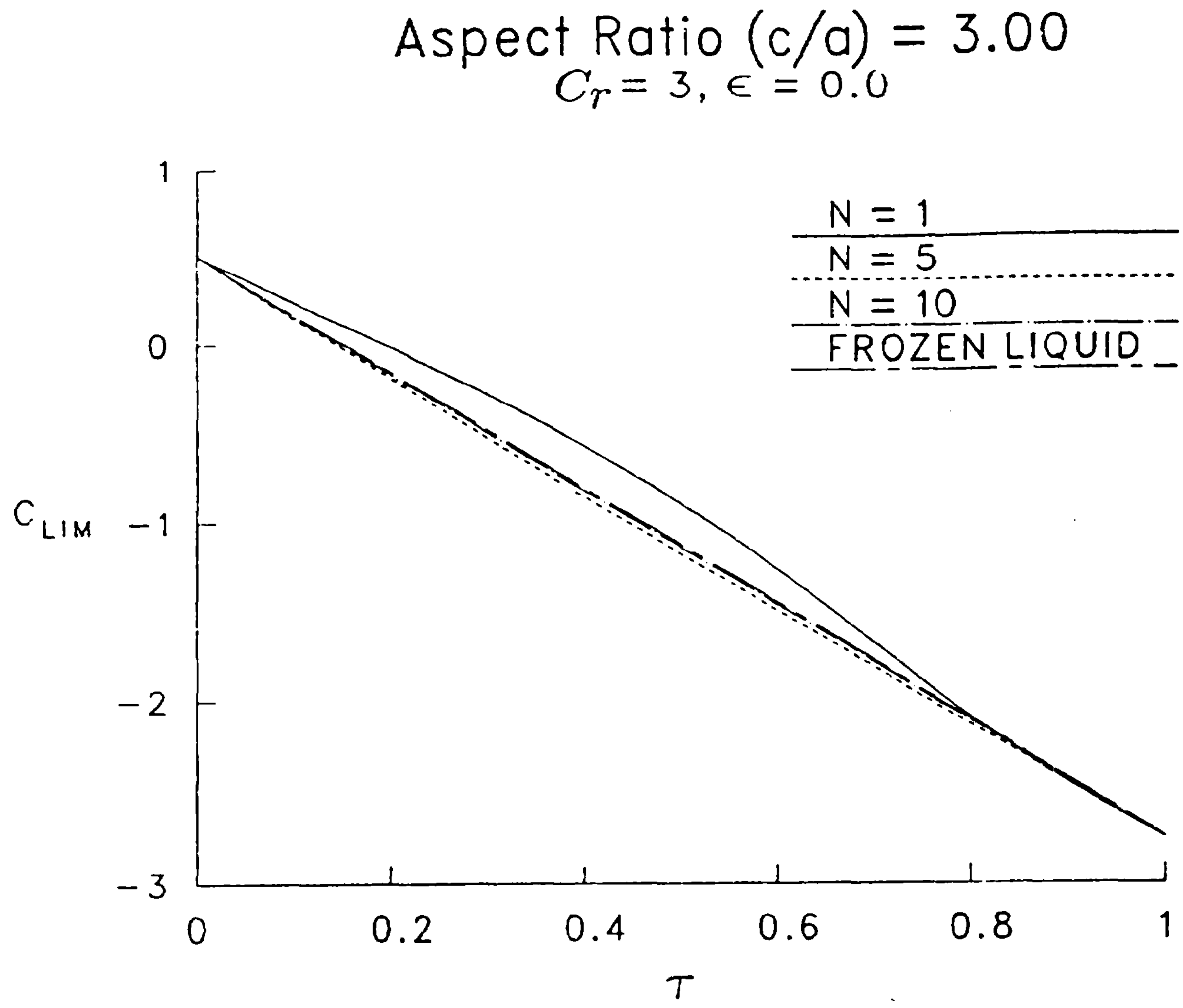

Comparison of C_{LIM} versus τ for f = 3, $C_r = 3$, $\epsilon = 0.$,N =1, 5, 10 and C_{LIM} frozen

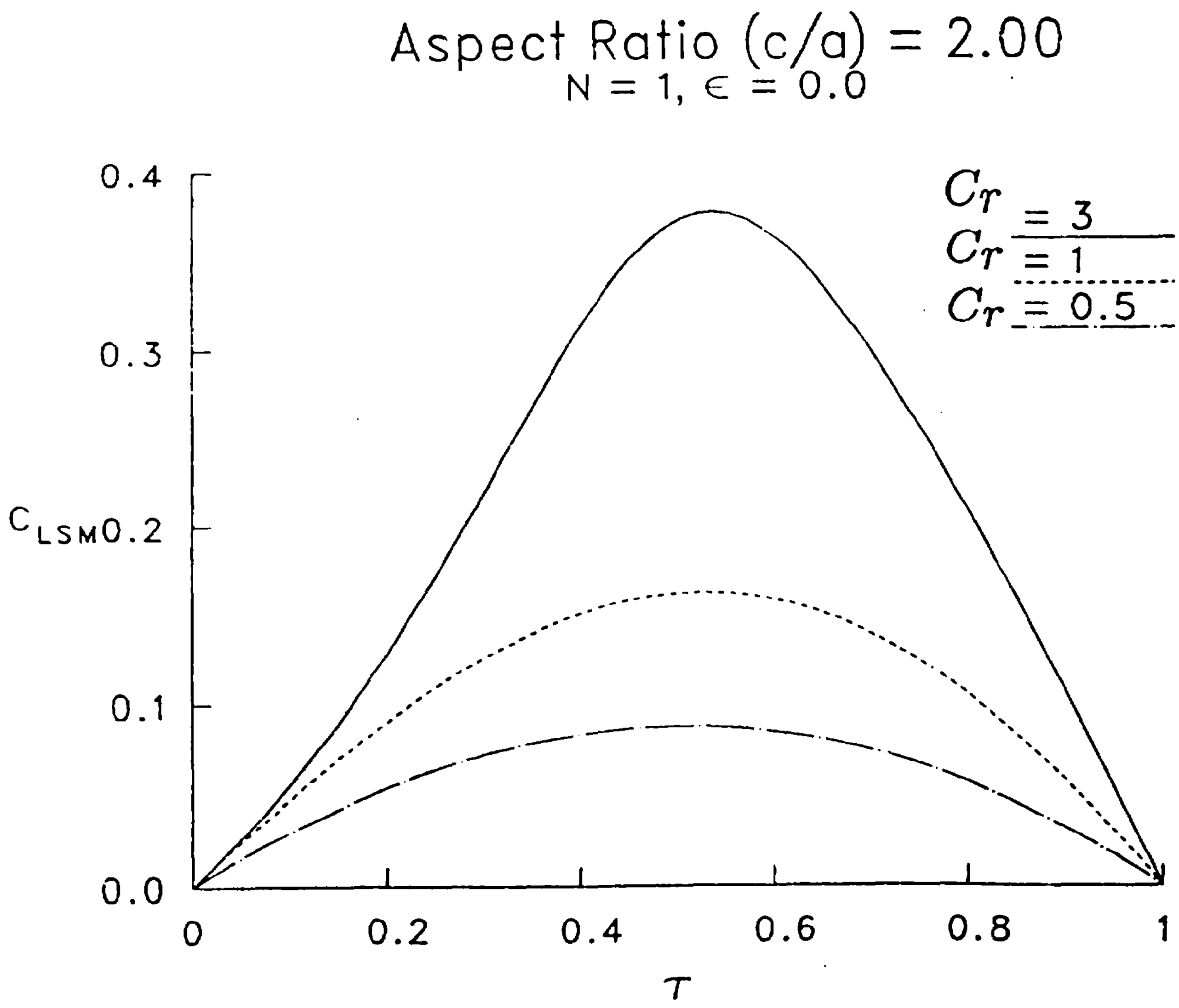

Comparison of C_{LSM} versus τ for f = 2, N =1, ϵ = 0., C_r = 3, 1, 0.5

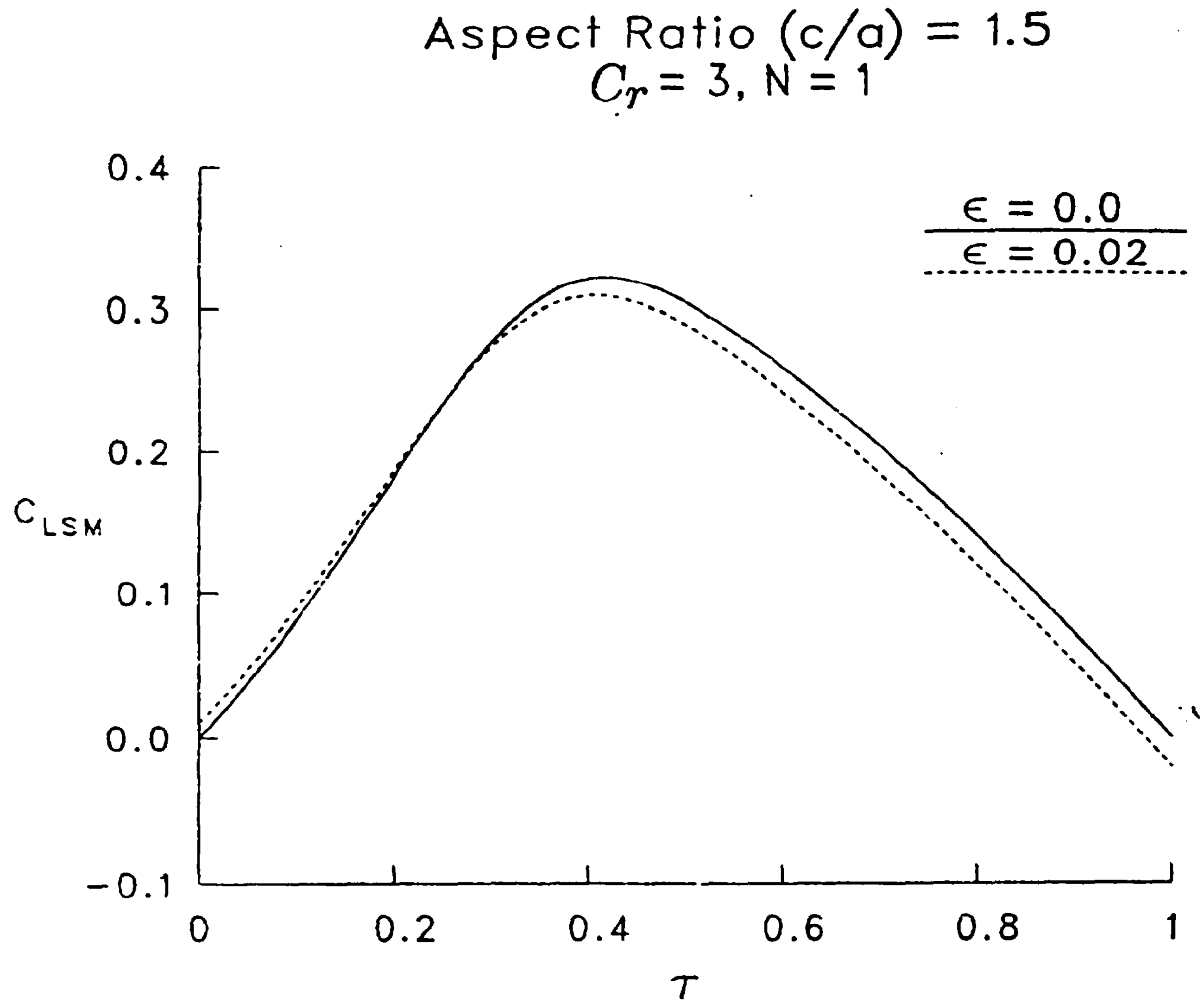

C_{LSM} versus τ for f = 1.5, $C_r = 3$, $\epsilon = 0.0, 0.02$

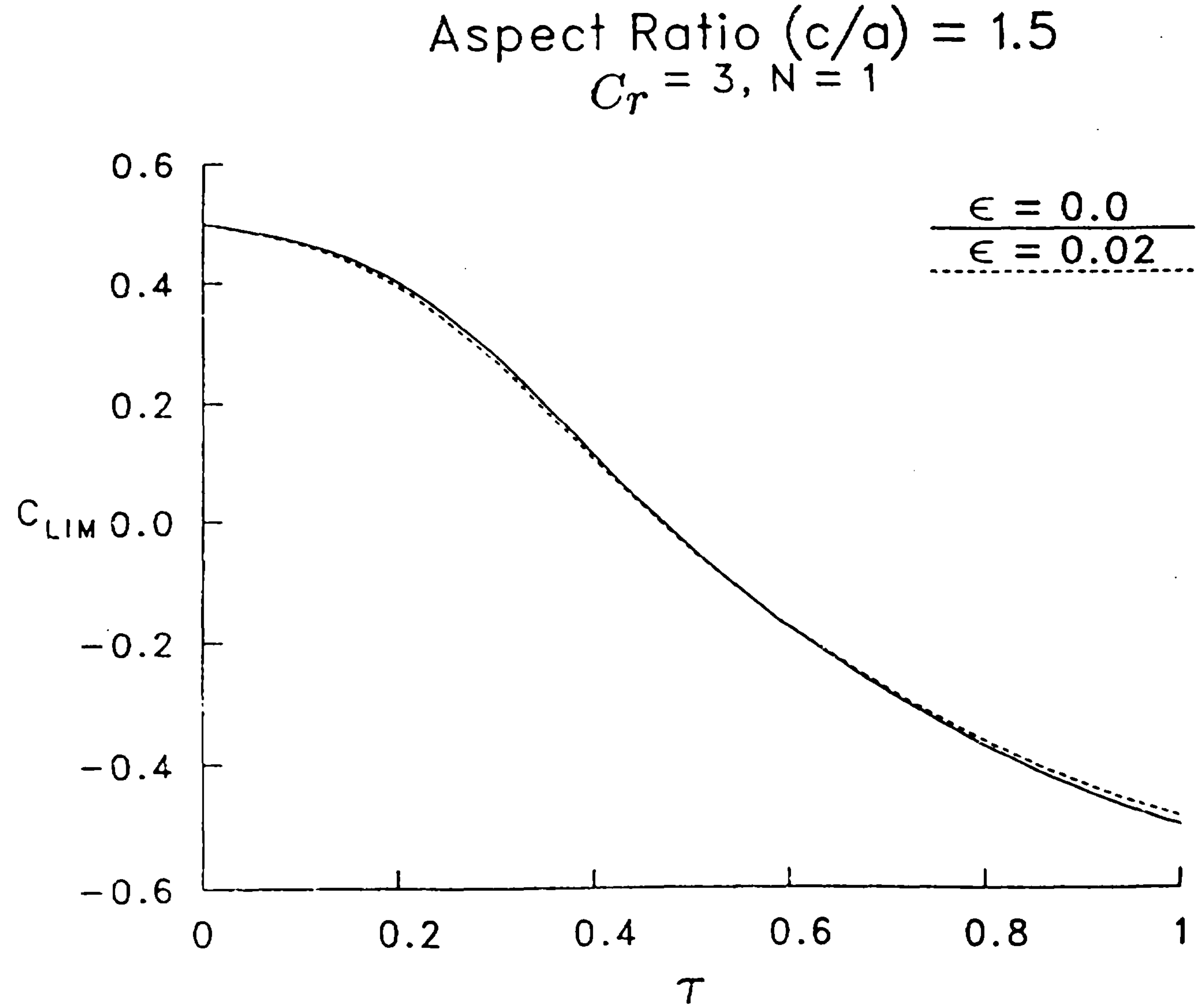

C_{LIM} versus τ for f = 1.5, $C_r = 3$, $\epsilon = 0.0, 0.02$

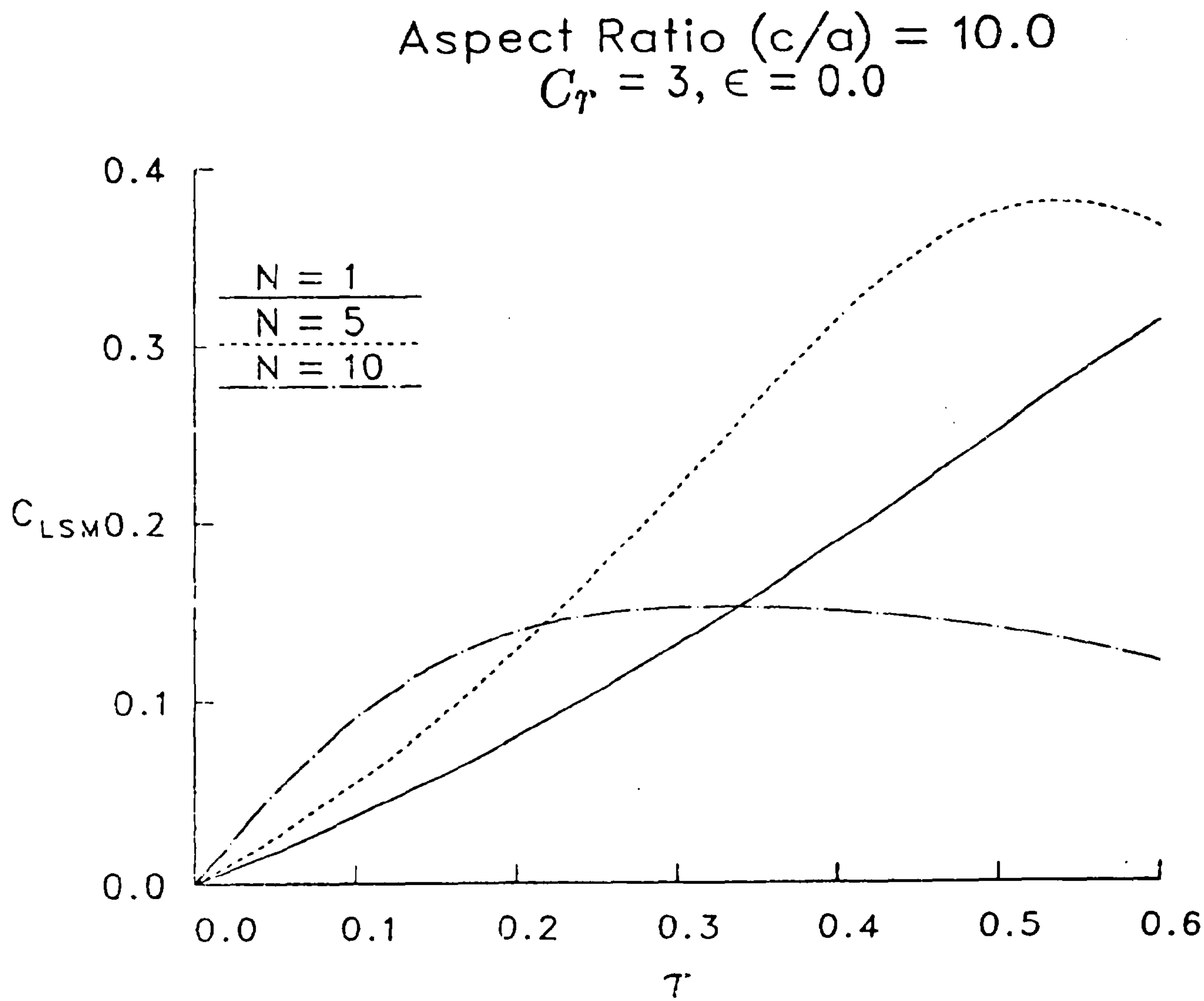

Comparison of C_{LSM} versus τ for $f = 10, C_r = 3, \epsilon = 0.0, N = 1, 5, 10$

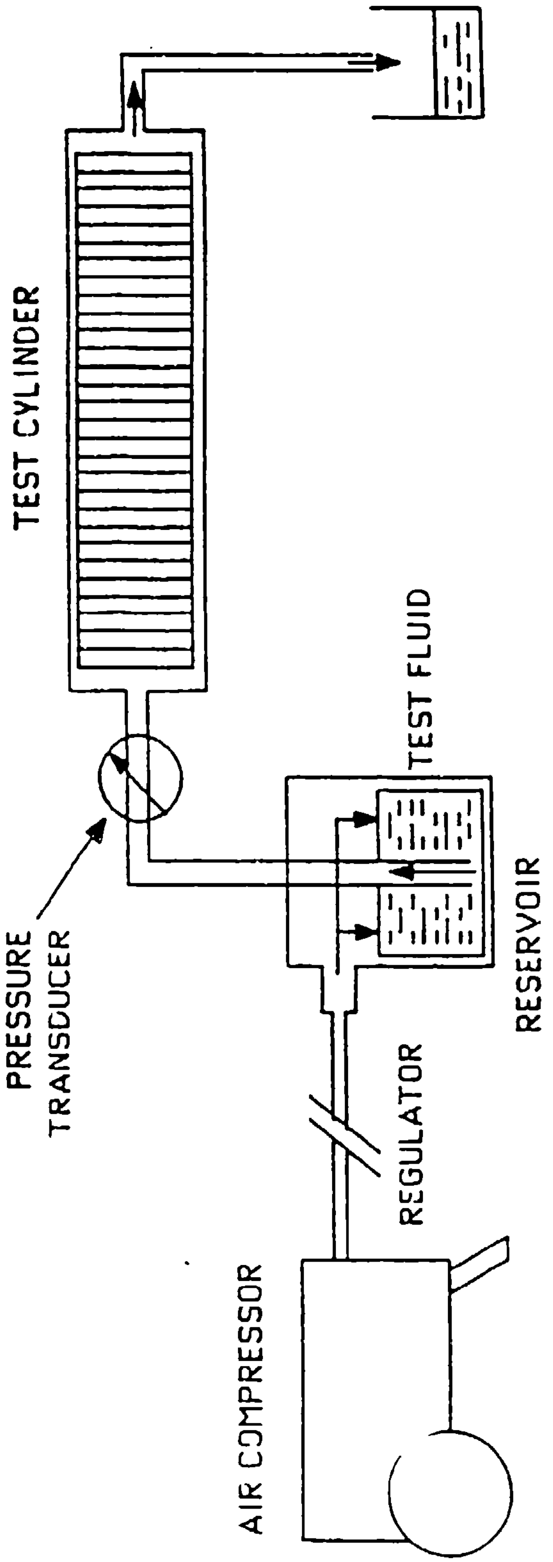
TEST CYLINDER
TEST FLUID
PRESSURE TRANSDUCER
RESERVOIR
REGULATOR
AIR COMPRESSOR

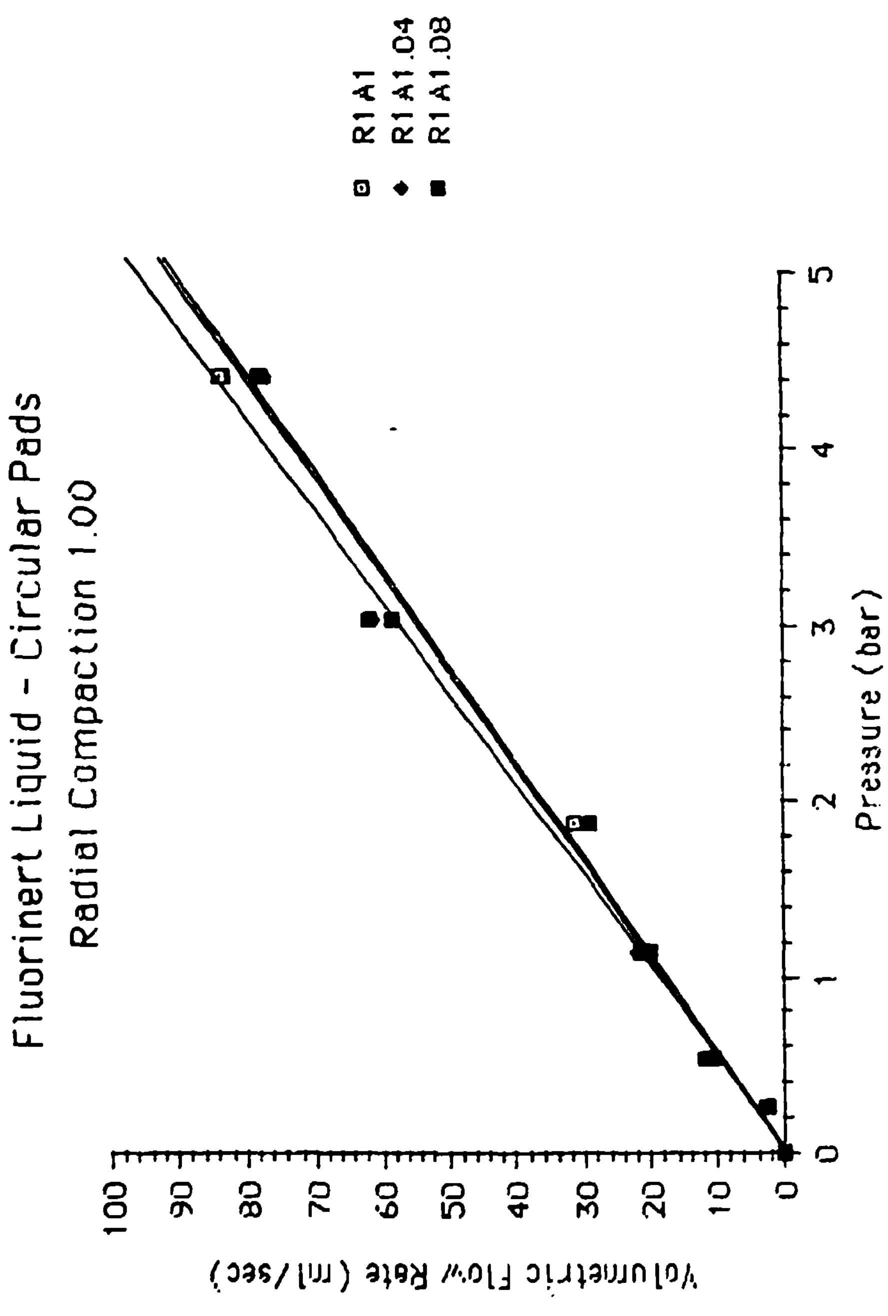

Fluorinert Liquid - Circular Pads
Radial Compaction 1.00
R1A1
R1A1.04
R1A1.08
Pressure (bar)
Volumetric Flow Rate (ml/sec)
0
1
2
3
4
5
0
10
20
30
40
50
60
70
80
90
100

Fluorinert Liquid - Circular Pads

Axial Compaction 1.00

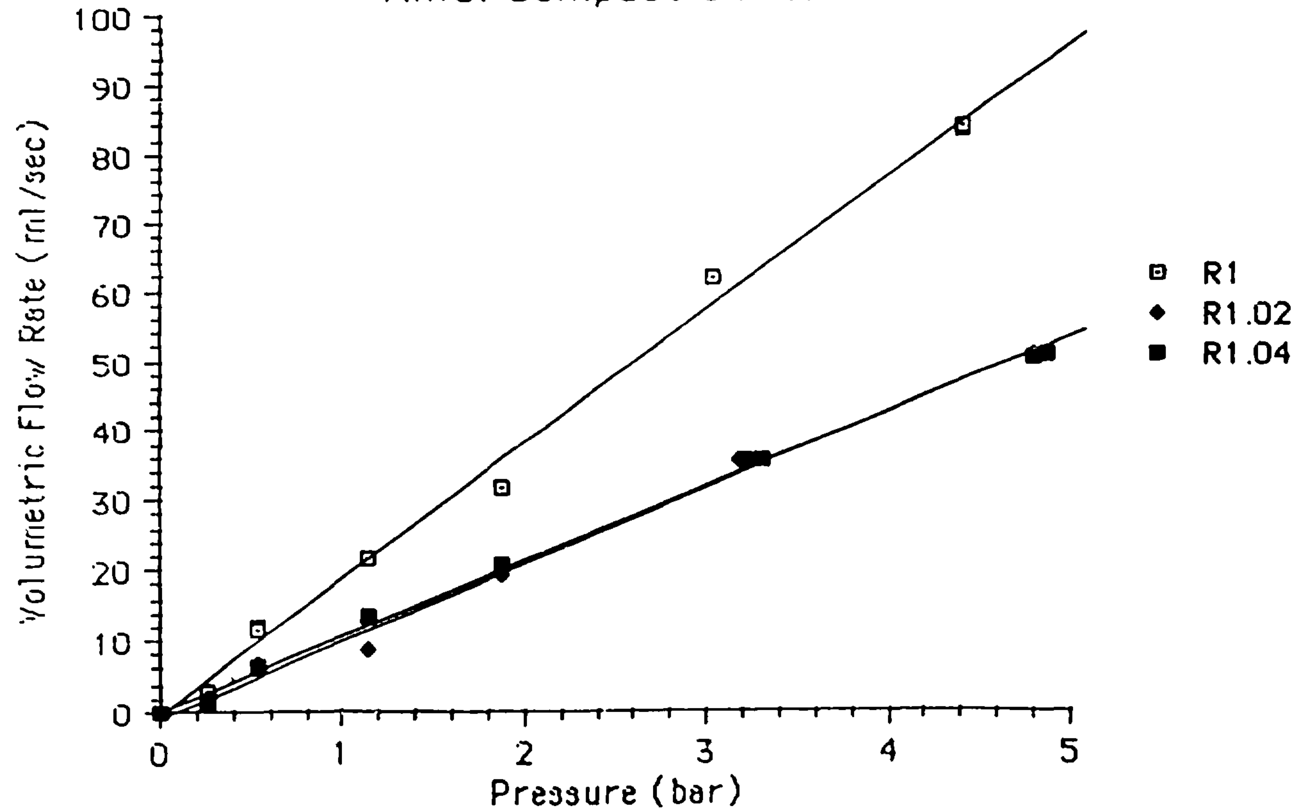

Permeability Results

Compaction		Permeability
Radial	Axial	($cm^2 \times 10^7$)
1.00	1.00	2.33
1.00	1.04	2.20
1.00	1.08	2.19
1.02	1.00	1.31
1.04	1.00	1.28

Radial compaction is more efficient

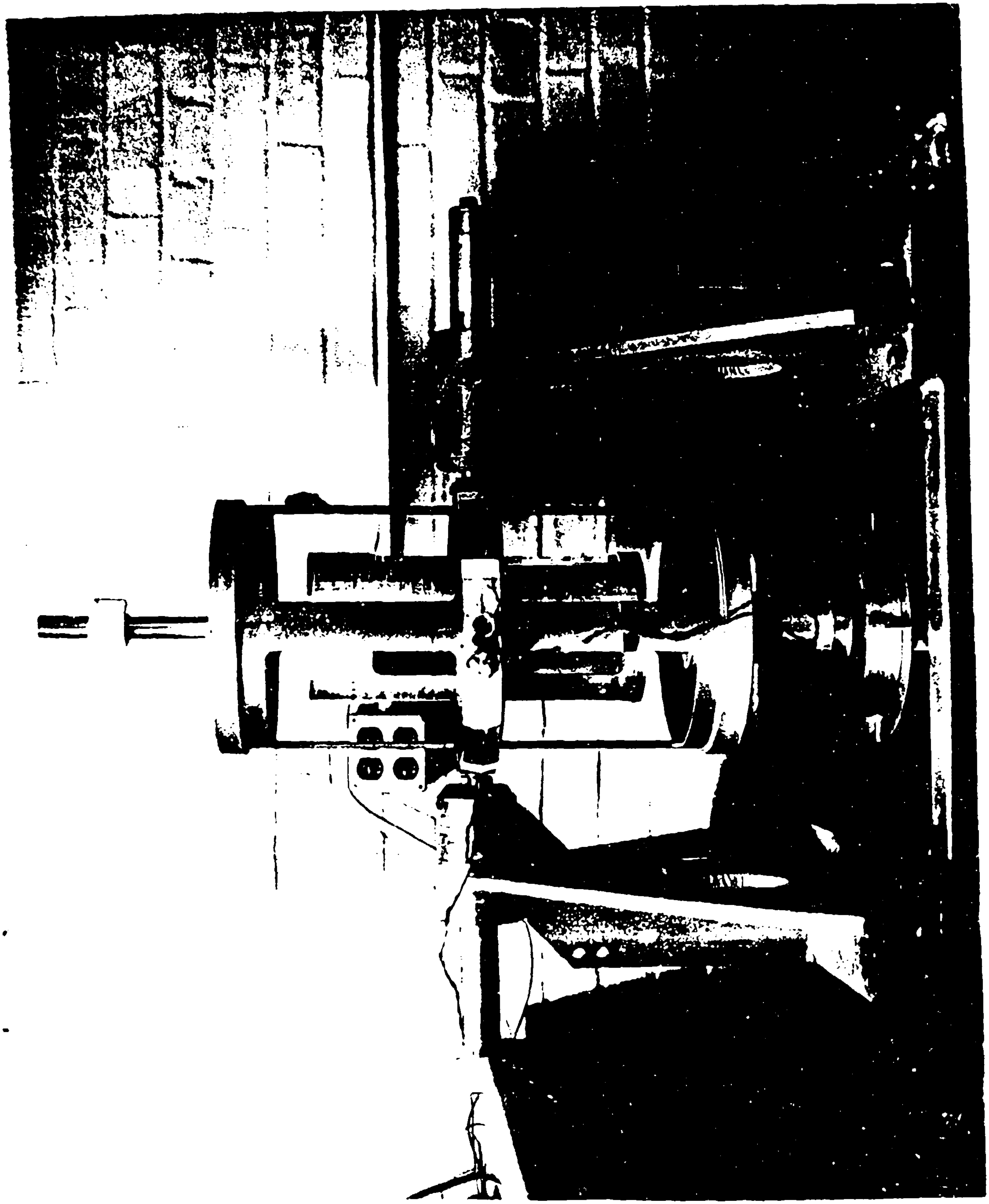

CROSS SECTION OF EXPERIMENTAL FELT CANISTER

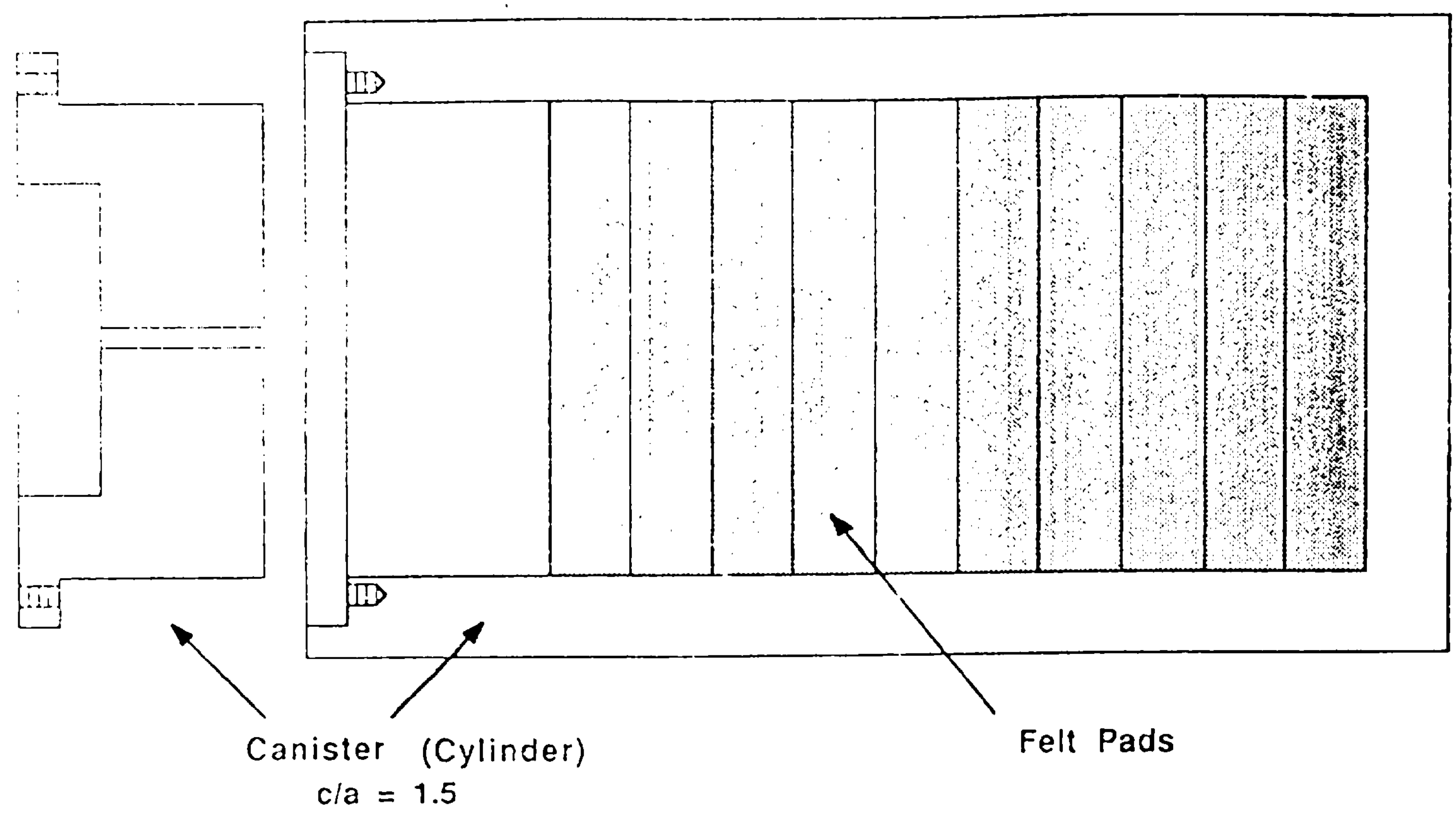

AXIAL - 1.00 , RADIAL - 1.00

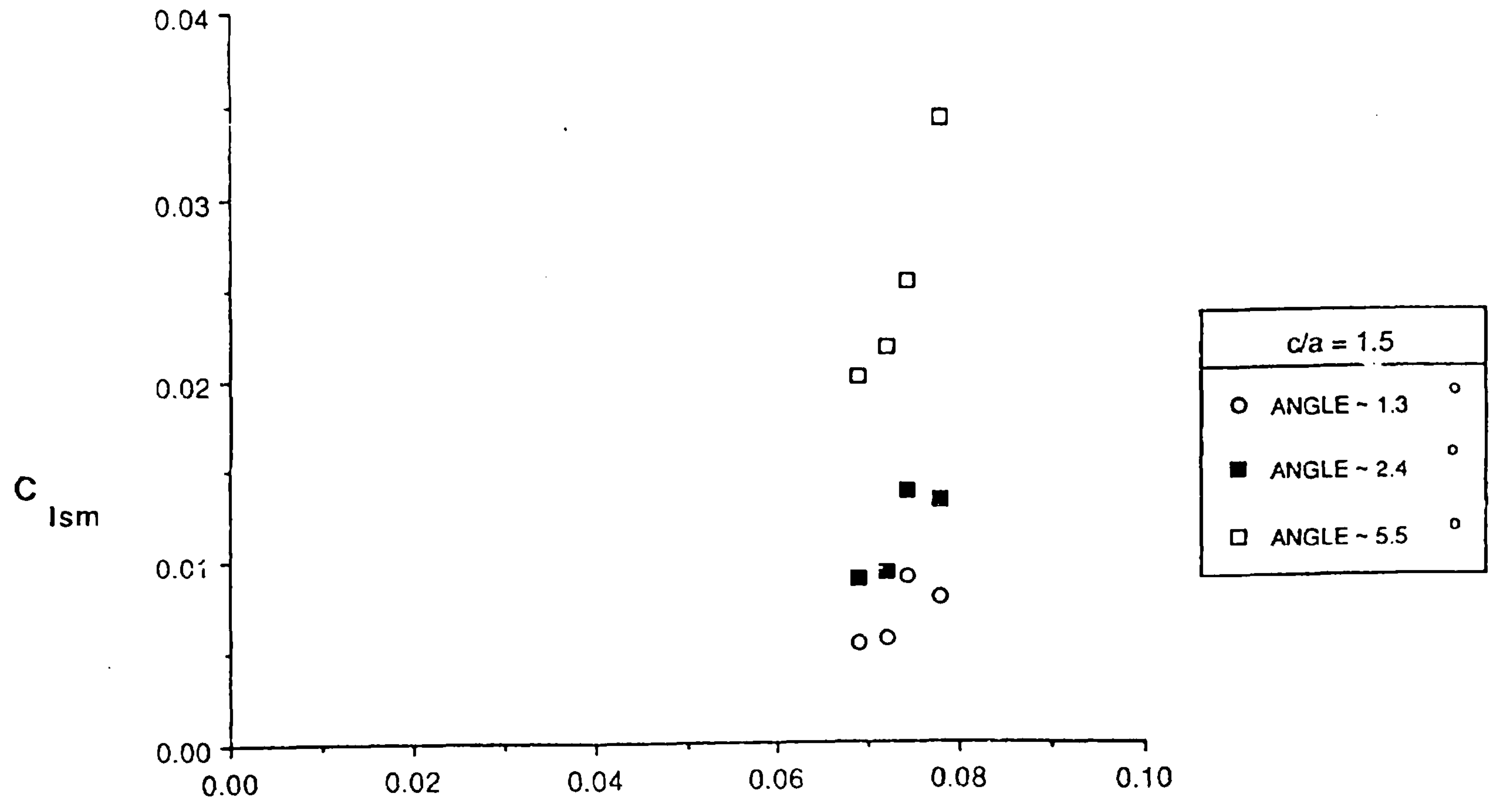

NON-DIMENSIONAL CONING FREQUENCY

COMPARISON OF AXIAL AND RADIAL COMPACTION

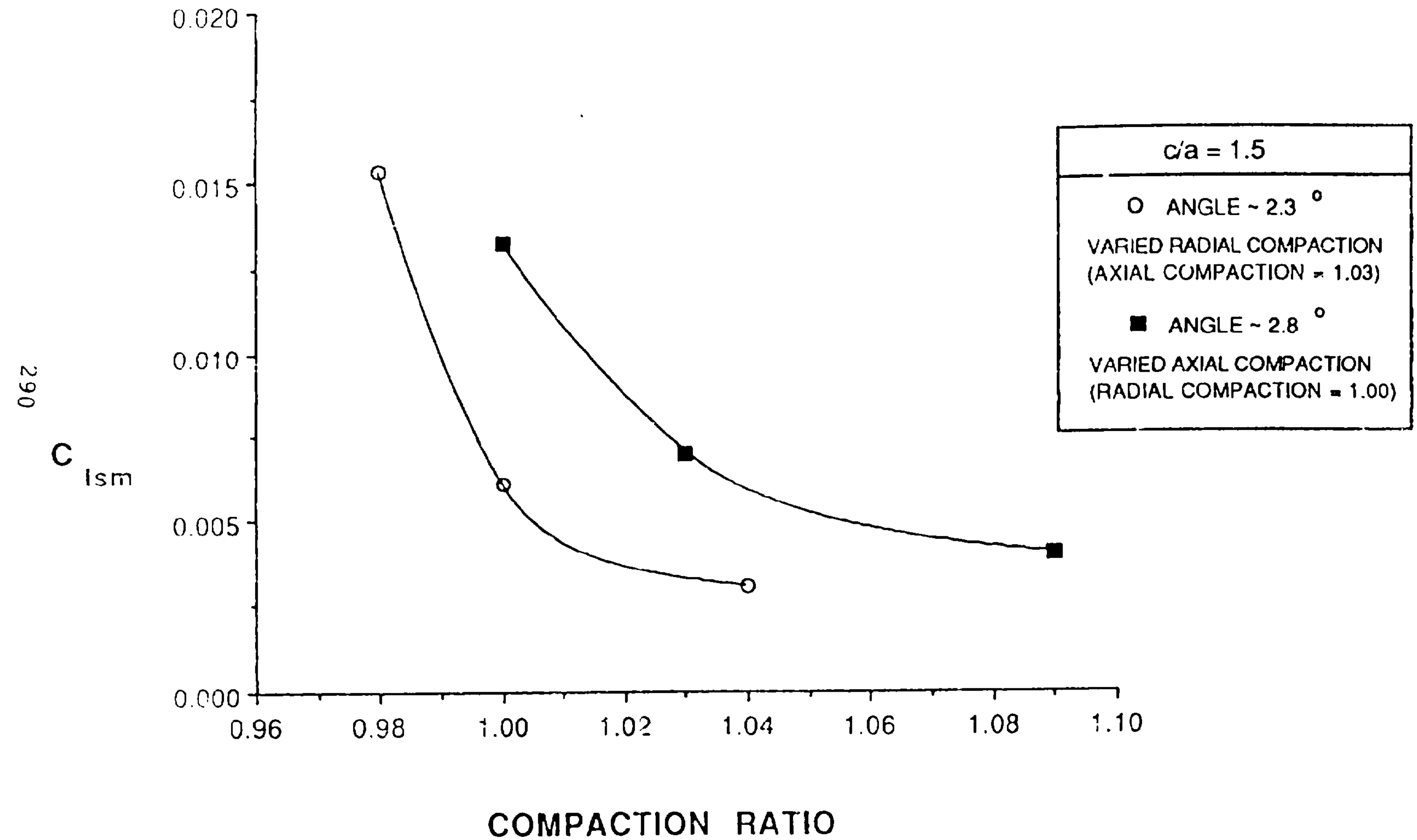

Comparison of BRL-Free Gyro and CRDEC-Test Fixture Felt Experiment

Compaction Ratio - Axial = 1.00
Radial = 1.00

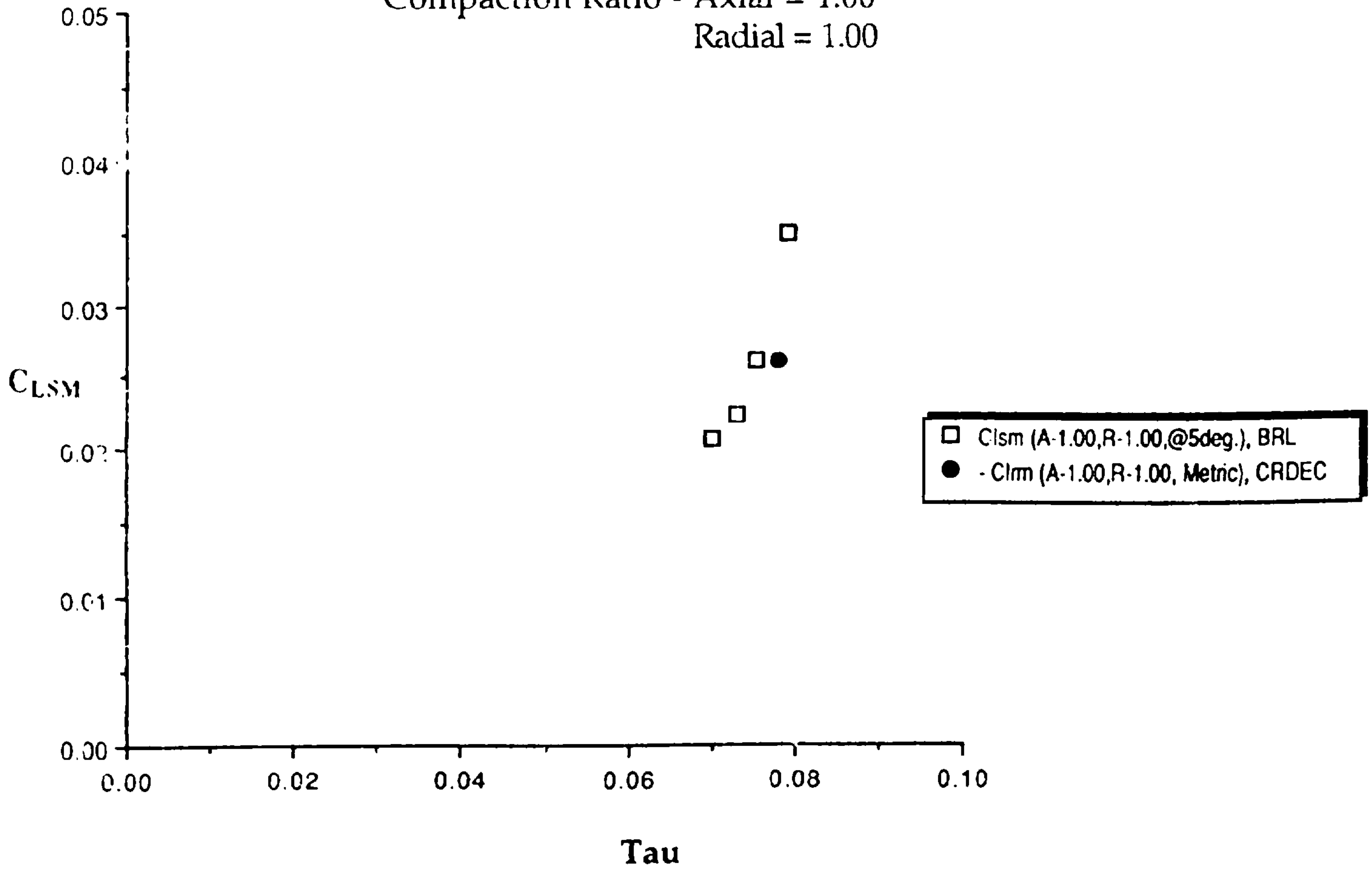

Comparison of BRL-Free Gyro and CRDEC-Test Fixture Felt Experiment

Compaction Ratio: Axial = 1.0
Radial = 1.04

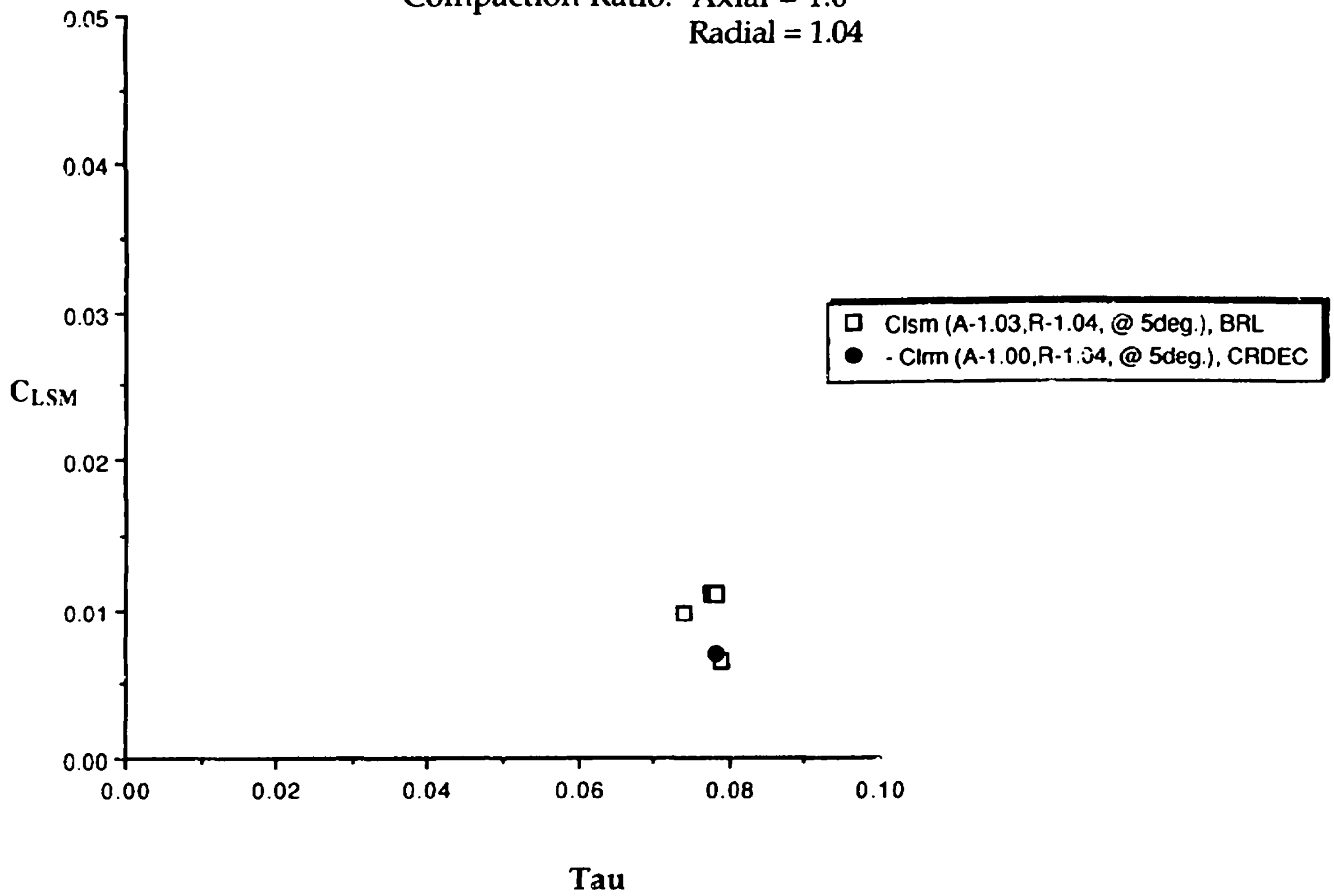

Conclusions

Linear theory has proper basis

Poor agreement between theory and experiment

Radial permeability measurements needed

Agreement between M825 canister and disk pad tests

Reformulate based upon current interests

Blank

ROTATING FLUIDS WORKSHOP

EFFECTS OF INTERIOR CANISTER WALL ROUGHNESS ON LIQUID DESPIN MOMENTS

Daniel J. Weber

U.S. Army, Chemical Research, Development and Engineering Center
Research Dir, Physics Div, Aerodynamics Research
and Concepts Assistance Branch

22-23 April 1991

Army High Performance Computing Research Center
University of Minnesota

INTRODUCTION

- Highly viscous liquid fills (e.g. 100K CS) can cause flight instabilities.
- Small amounts of low viscosity fluids (e.g. 5% water) added to the high viscosity liquid can eliminate instabilities.
- Drawbacks to additive appı ach:
    - Two fluids must be immiscible.
    - Low viscosity additives must have a greater density than high viscosity fluid.
- Smooth canister wall may reduce surface shear stresses.
    - Achieve results similar to additive approach.
    - Eliminates drawbacks of additive approach.

CANISTER CONFIGURATIONS TESTED

- Standard canister c/a = 4.5, (roughness ≈ 125 to 250 micro inch finish)
- Smooth canister c/a = 4.5, (roughness ≈ 9 to 17 micro inch finish)
- Smooth canister coated with silicone based marine wax.
- Smooth canister coated with teflon based marine wax.
- Rough wall canister c/a = 4.57, standard canister painted with grit filled safety paint. (roughness ≈ 50,000 micro inch finish)

TEST CONDITIONS

Fluids

- 10,000 CS Silicone
- 100,000 CS Silicone
- 10,000 CS Silicone + 5% water (Standard canister only)
- 100,000 CS Silicone + 5% water (Standard canister only)

Coning Rates

- 300 rpm
- 400 rpm
- 500 rpm

Coning Angle

- 20 °

Terminology

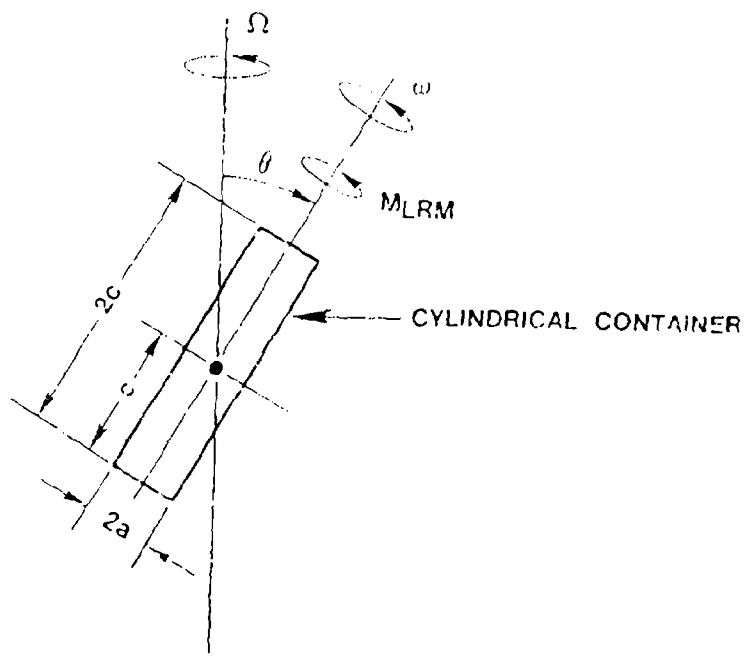

TEST PROCEDURE

For a specific coning angle and coning rate:

- The canister is spun up to $\approx$ 10,000 rpm as the coning rate is established at the predetermined rate.
- With the coning rate held constant, the canister is allowed to spin down.
- Canister despin is recorded versus time.
- From the despin data, the Total Moment (M_T) is calculated, $M_T = I\dot{\omega}$, where I is the axial moment of inertia of the empty canister.
- The liquid moment is found from $M_L = M_T - M_F$, where M_F, friction moment, is determined using the same procedure described above but with no fluid in the canister, $M_L = 0$.

Effects of Canister Wall Roughness

ν = 10,000 CS Silicone Fluid

Ω = 300 rpm, Θ = 20 °

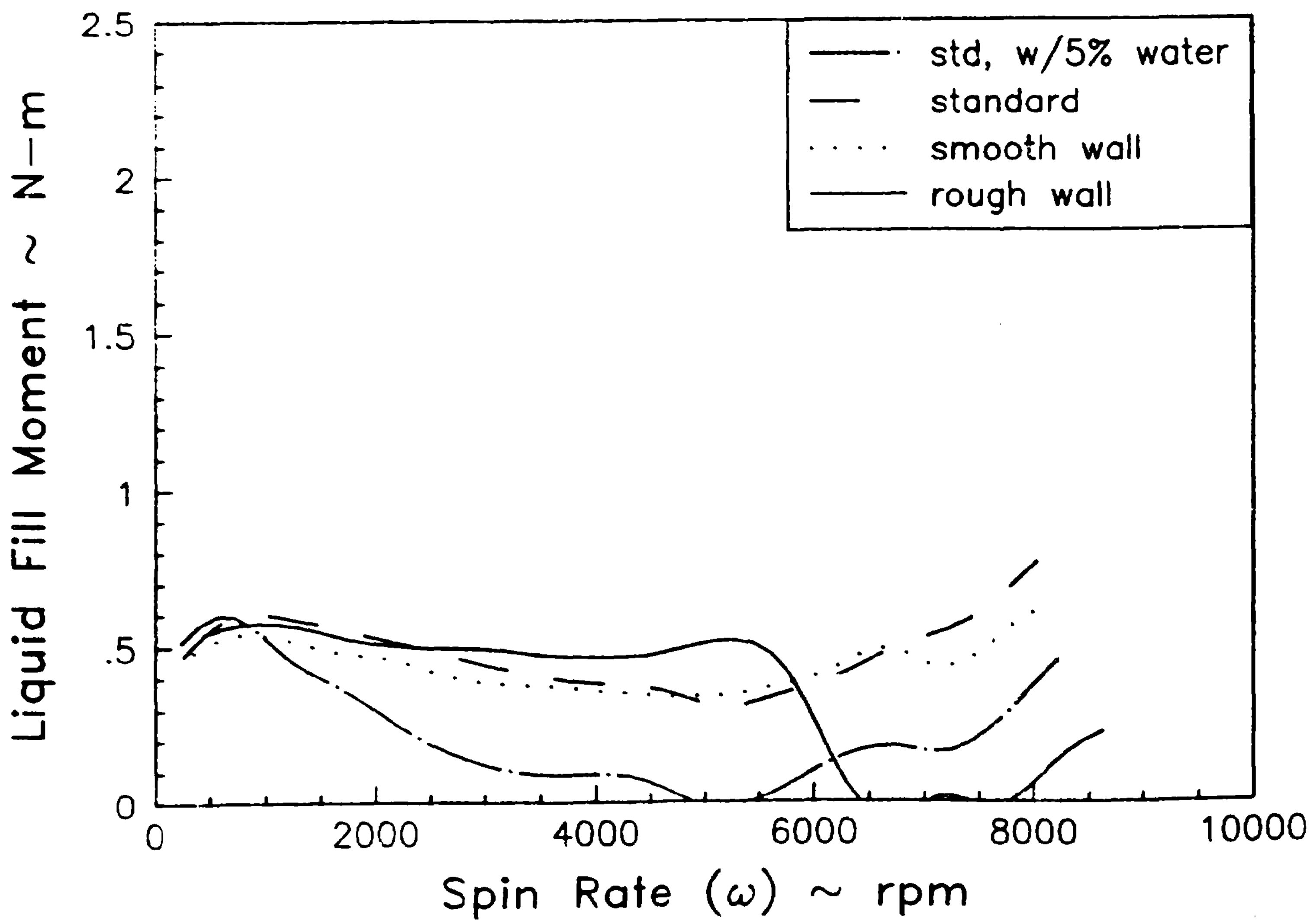

Effects of Canister Wall Roughness

ν = 10,000 CS Silicone Fluid

Ω = 400 rpm, Θ = 20 °

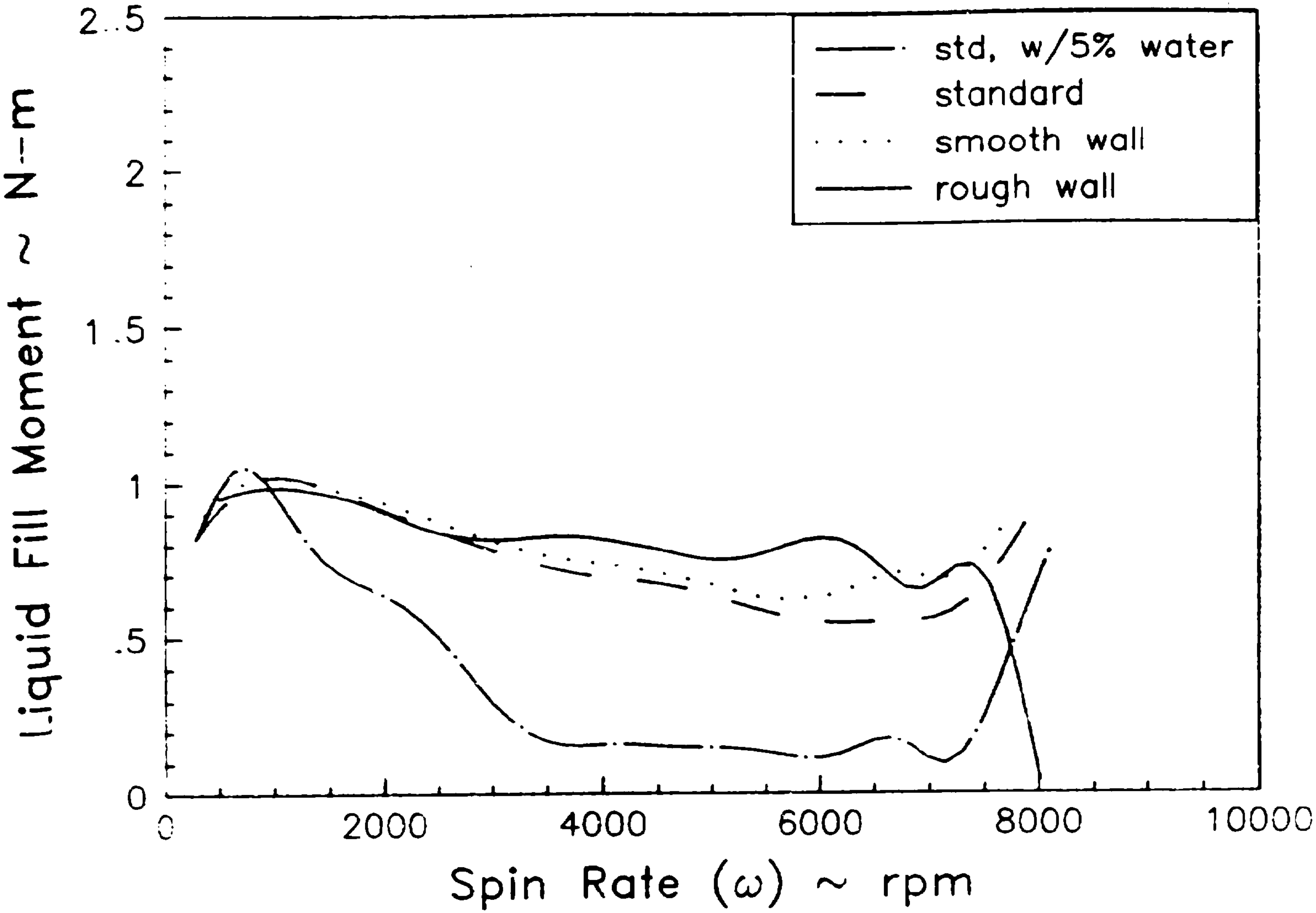

Effects of Canister Wall Roughness

ν = 10,000 CS Silicone Fluid

Ω = 500 rpm, Θ = 20 °

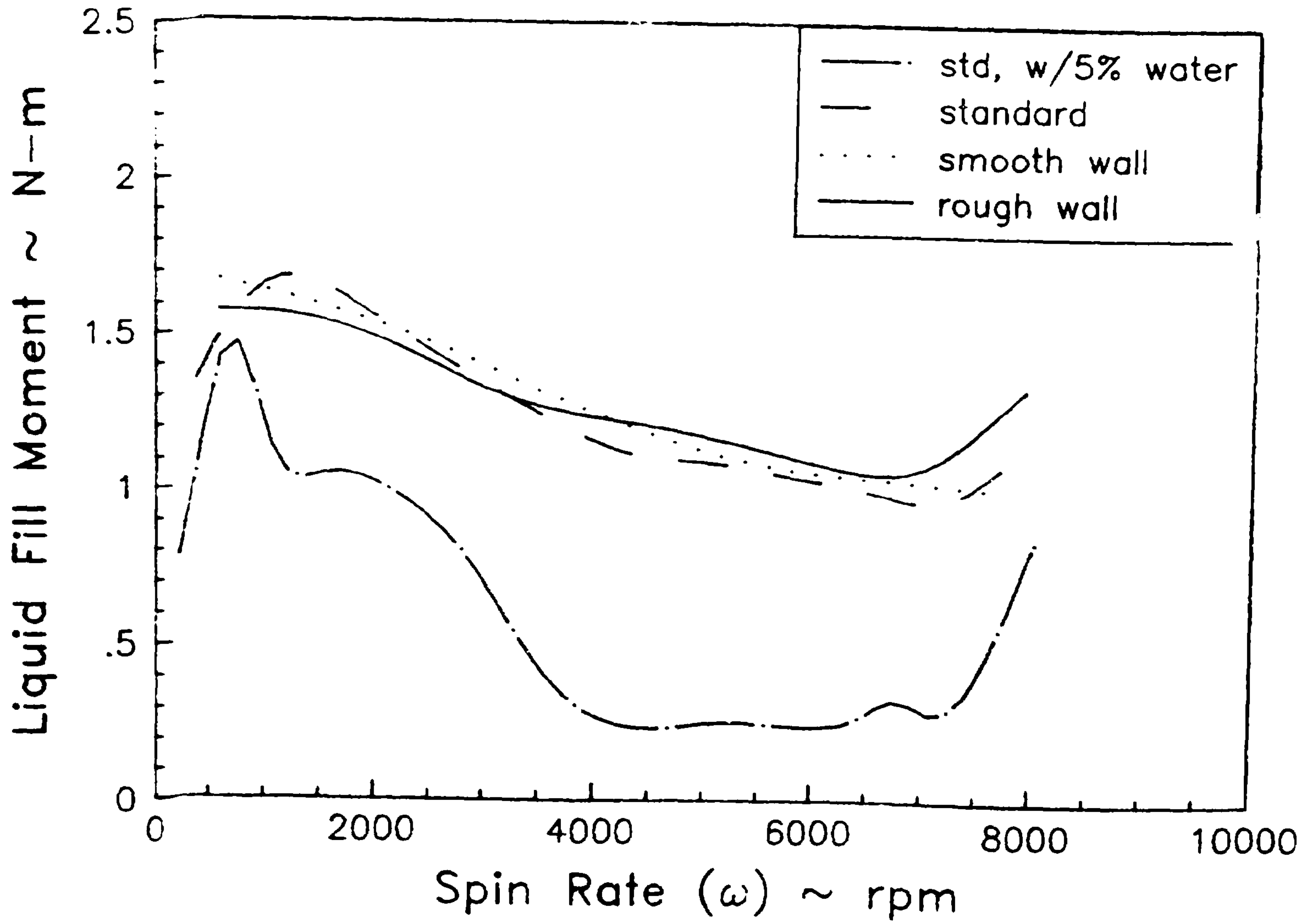

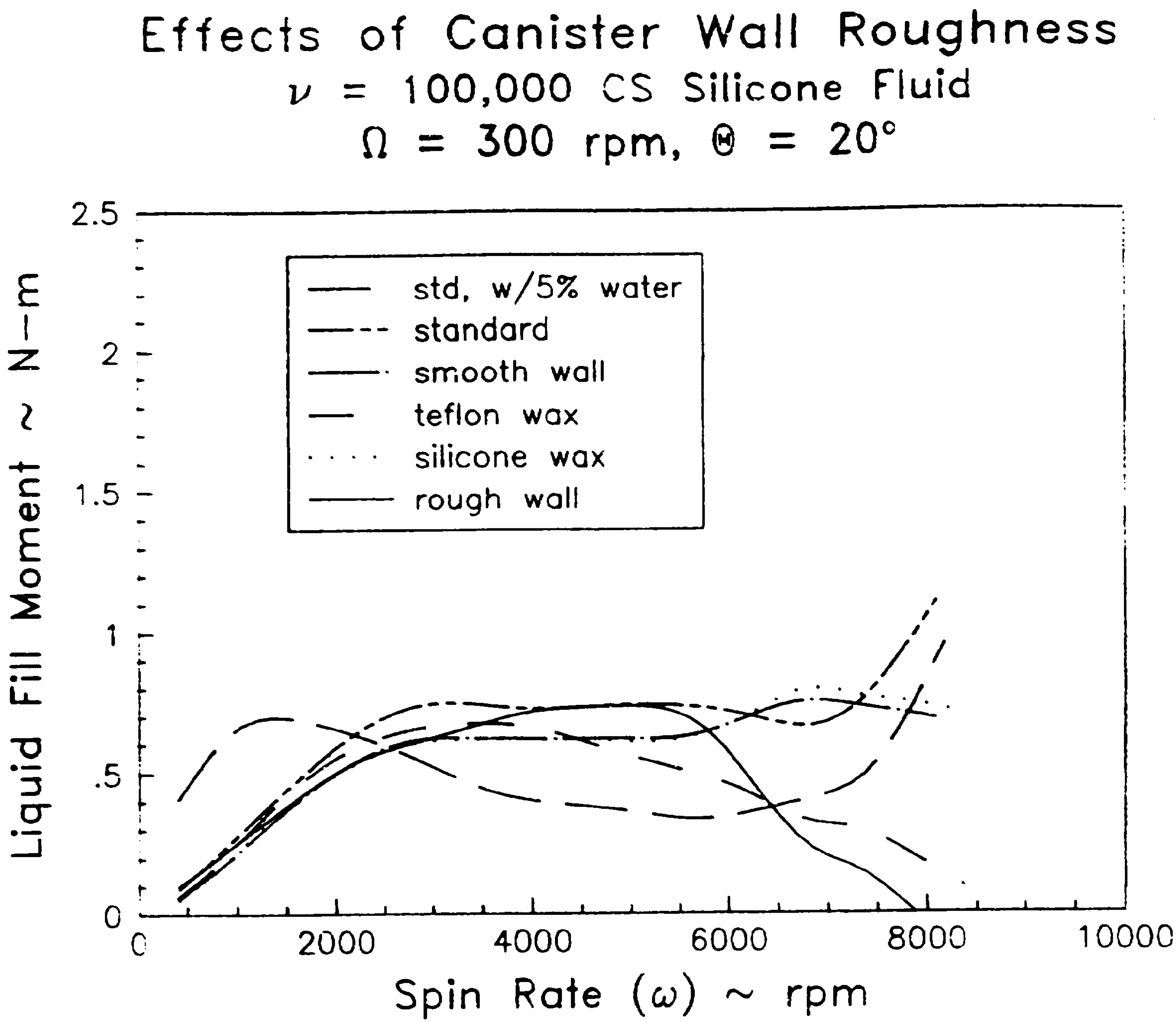

Effects of Canister Wall Roughness
ν = 100,000 CS Silicone Fluid
Ω = 300 rpm, Θ = 20°
std, w/5% water
standard
smooth wall
teflon wax
silicone wax
rough wall
Liquid Fill Moment ~ N–m
Spin Rate (ω) ~ rpm
0
.5
1
1.5
2
2.5
0
2000
4000
6000
8000
10000

Effects of Canister Wall Roughness
ν = 100,000 CS Silicone Fluid
Ω = 400 rpm, Θ = 20°

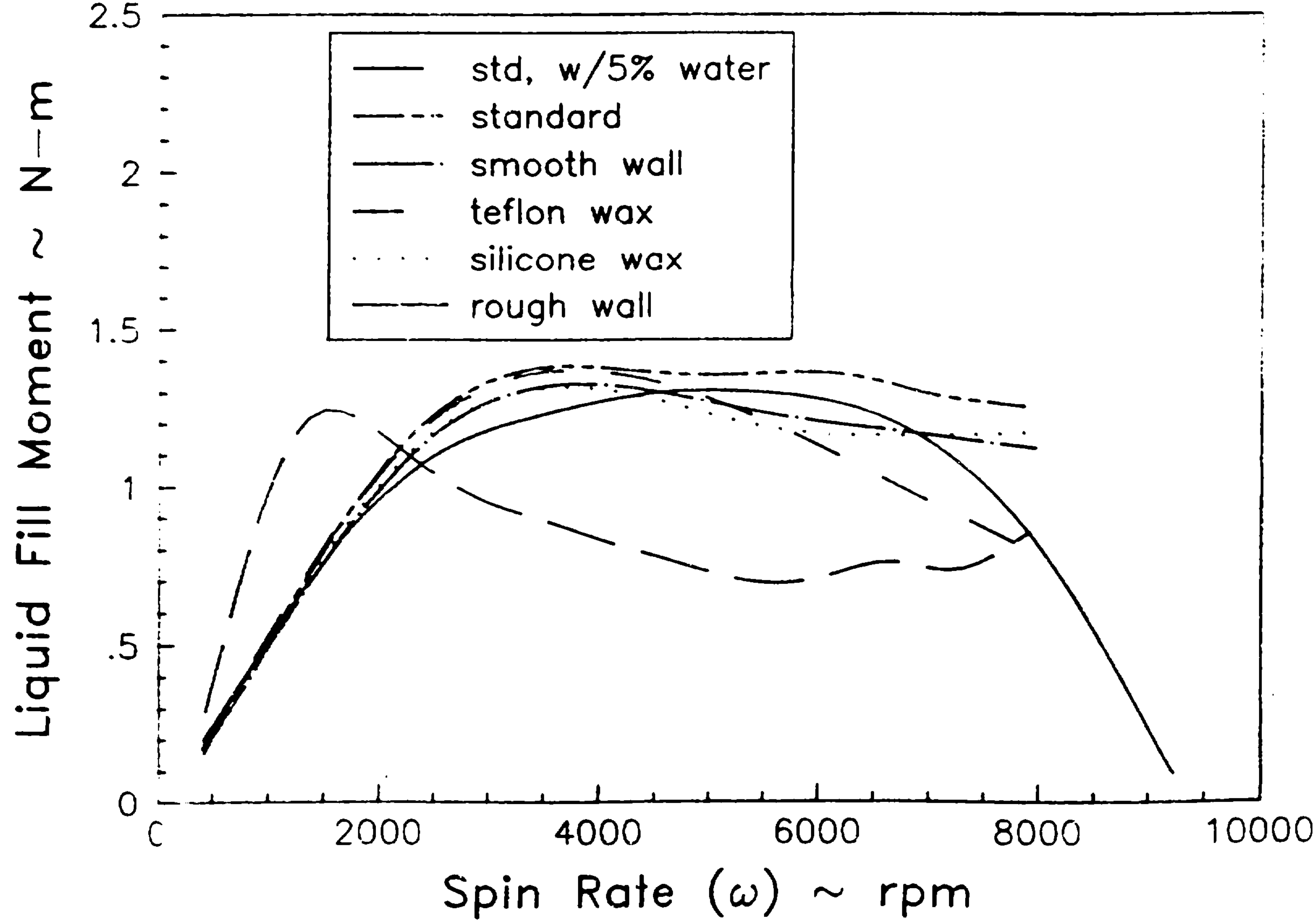

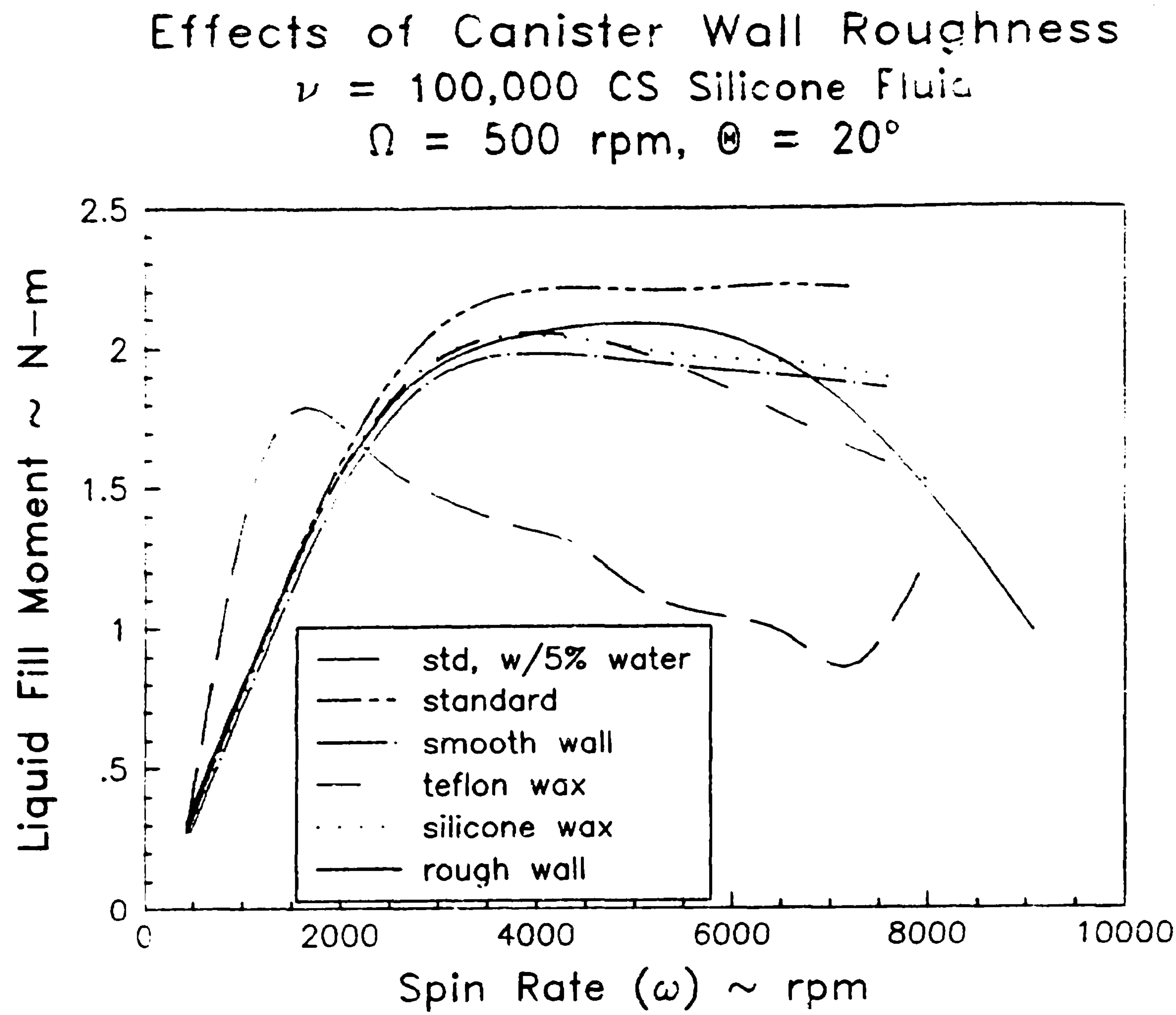
Effects of Canister Wall Roughness
ν = 100,000 CS Silicone Fluid
Ω = 500 rpm, Θ = 20°
2.5
2
1.5
1
.5
0
0
2000
4000
6000
8000
10000
Liquid Fill Moment ~ N-m
Spin Rate (ω) ~ rpm
std, w/5% water
standard
smooth wall
teflon wax
silicone wax
rough wall

Effects of Canister Wall Roughness
$\Theta = 20°$

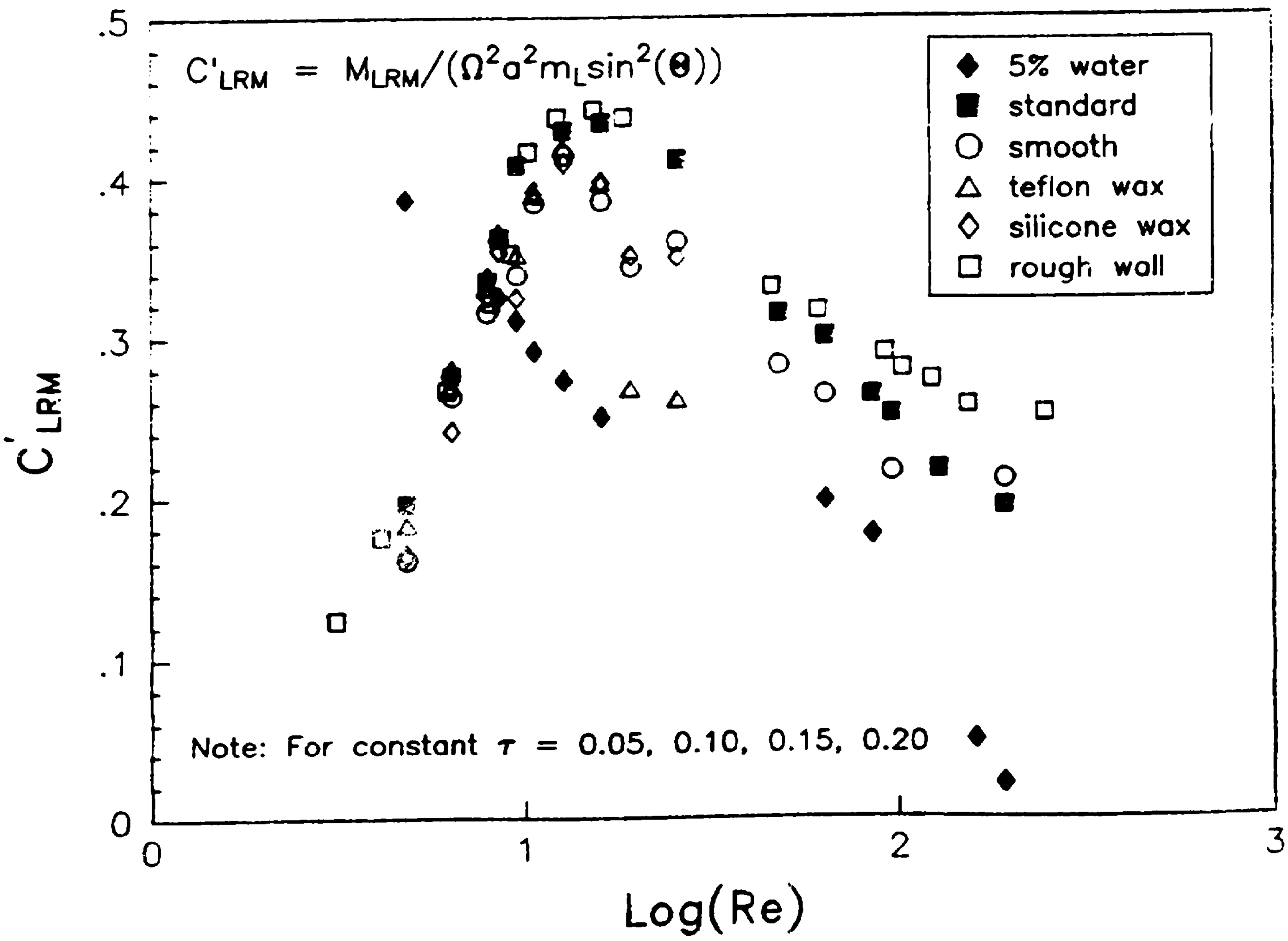

CONCLUSIONS

- For typical artillery shell flight conditions (Ω = 500 rpm, ω = 6000 rpm) the additive approach yielded the best results, reducing the despin moment by ≈ 50% (ref. Standard Canister).

- 10,000 cs Silicone Fluid
  For typical artillery shell flight conditions the canister wall roughness had little or no effect on the despin moment.

- 100,000 cs Silicone Fluid
  For typical artillery shell flight conditions the despin moments (ref. Standard Canister) for the smooth and rough canister configurations were decreased ≈ 10%.

- Log(Re′) versus Liquid Payload Coefficient
  Re′ > 10: 5% water produced smallest coefficients, standard and rough canister produced the largest coefficients and the smooth canisters produced results in-between.

- Above 6000 rpm, the rough and smooth teflon waxed canisters produced a significant decrease in despin moment.

ROTATING FLUIDS WORKSHOP

INSTRUMENTED FLIGHT TESTS ARTILLERY PROJECTILES WITH SELECTED LIQUID-FILLS

Miles C. Miller

U.S. Army, Chemical Research, Development and Engineering Center
Research Dir, Physics Div, Aerodynamics Research
and Concepts Assistance Branch

22-23 April 1991

Army High Performance Computing Research Center
University of Minnesota

INSTRUMENTED FLIGHT TESTS

OBJECTIVE: To confirm theoretical and laboratory results through flight tests of liquid-filled artillery projectiles

TEST ITEMS: 155mm Artillery Projectiles having the following fills:

# ROUNDS	LIQUID-FILL	ADDITIVE	PREDICTED RESULTS
2	100K CS	None	Unstable
2	100K CS	5% Water	Stable
2	10K CS	None	Unstable
2	10K CS	5% Water	Stable
2	30K CS	None	Unstable
2	30K CS	5% Water	Stable
2	100K CS (Viscoelastic)	None	Stable
2	100K CS (50% Fill)	None	Unstable

FIRING CONDITIONS: Zone 4 (Transonic) with induced yaw

INSTRUMENTATION: Yaw Sondes and radar

LOCATION: Dugway Proving Ground

A0332-9103-L91 1-13324

DESTABILIZING MOMENT DUE TO PARTIAL-FILL

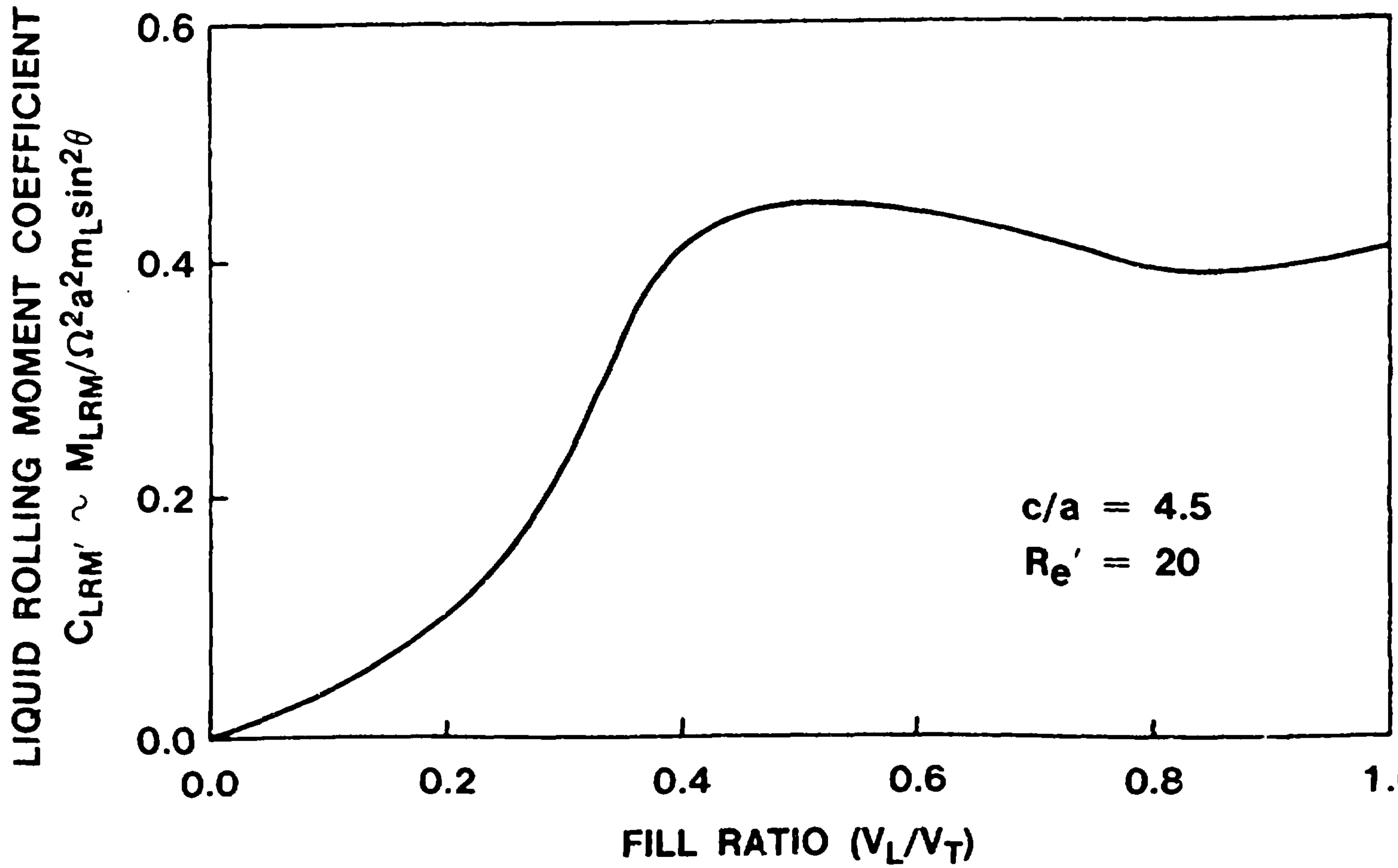

AO332-9005-P90 1-13319

EFFECT OF PARTIAL-FILL INDUCED YAW LAUNCH

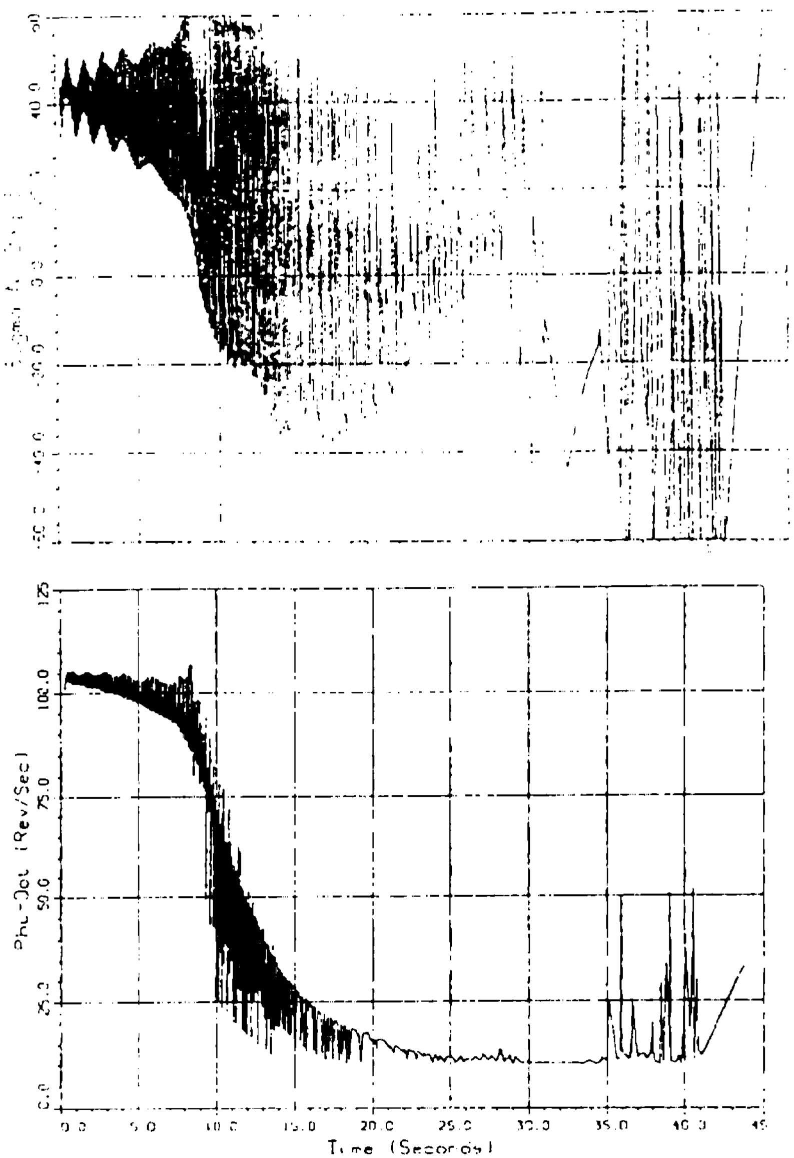

100K CS

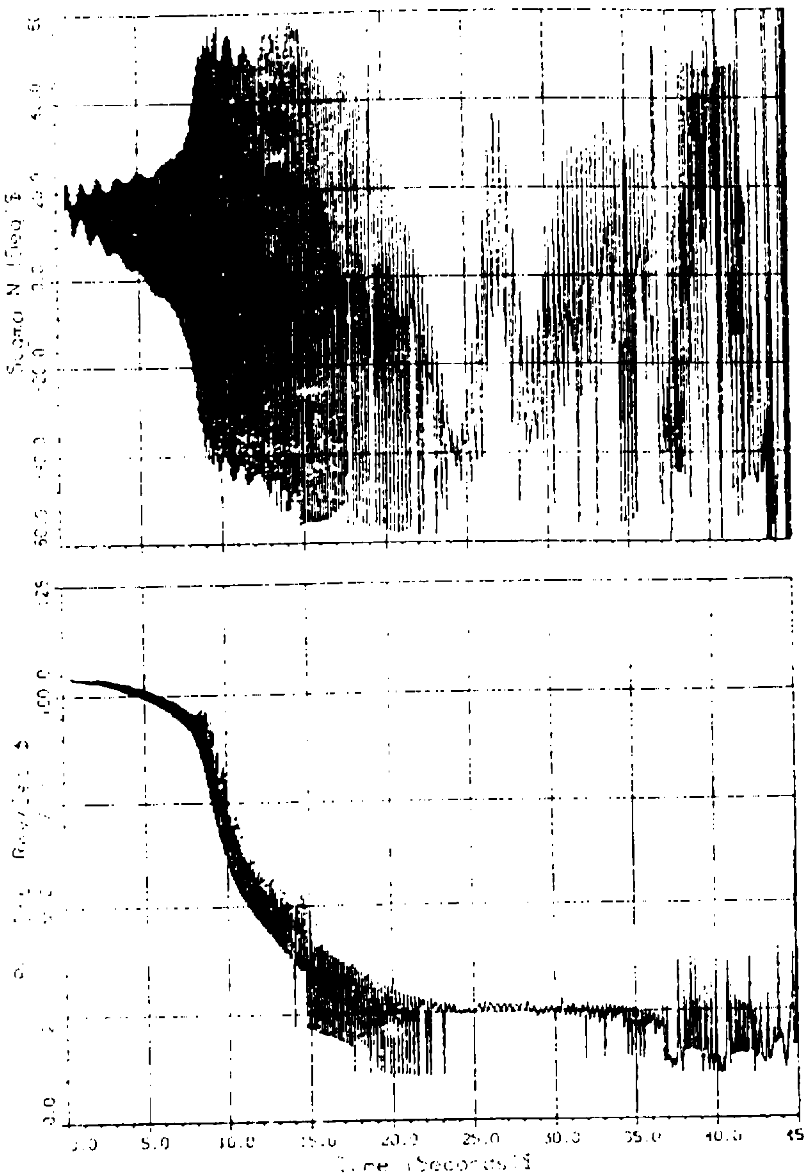

100K CS (50 % FULL)

EFFECT OF PARTIAL FILL

NORMAL LAUNCH

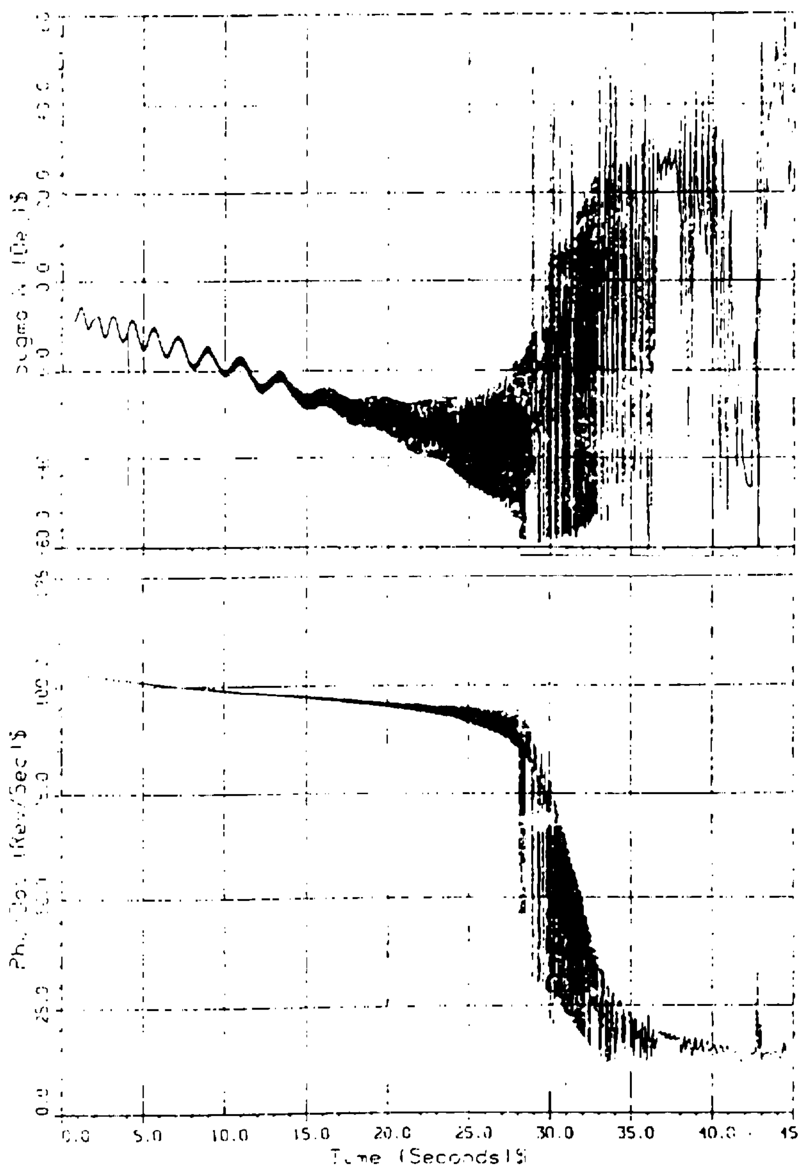

100 KCS

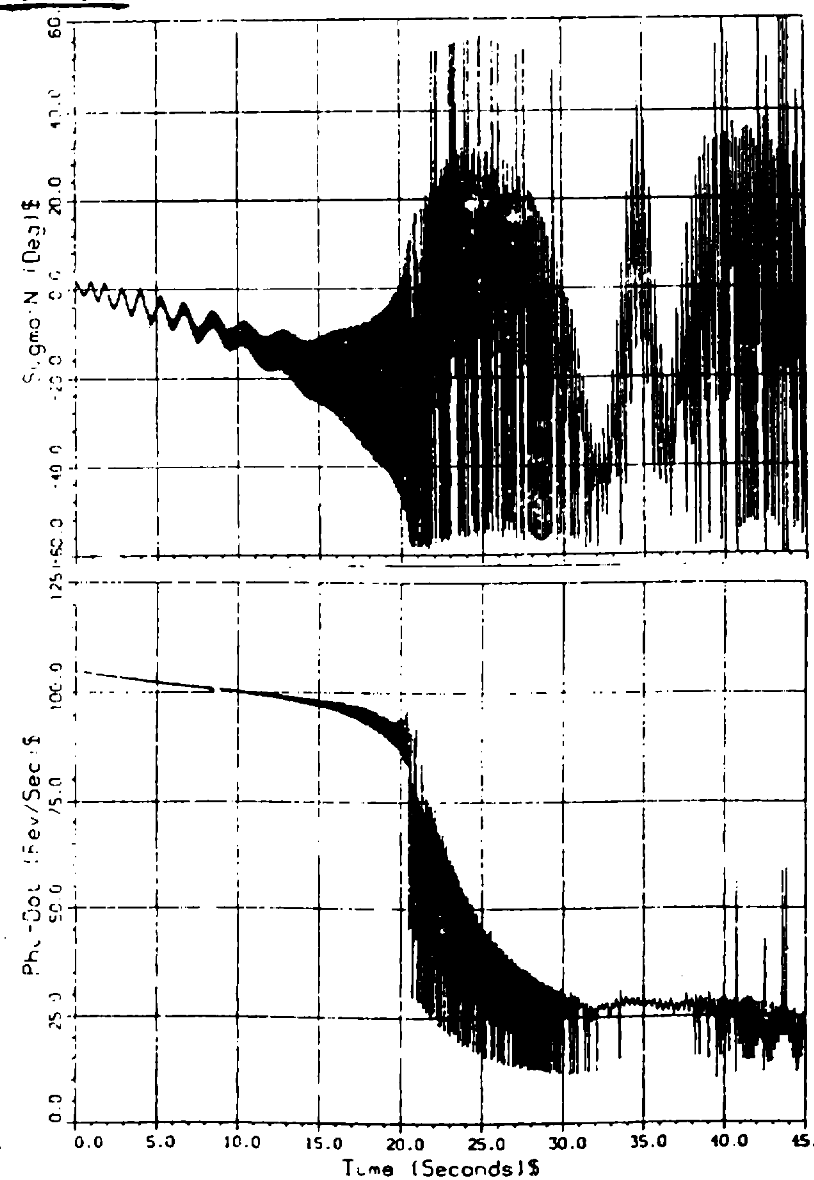

100 KCS (50% FULL)

VISCOELASTIC PROPERTIES FOR
NON-NEWTONIAN FLUID (DEM WITH 12.1% K-125)

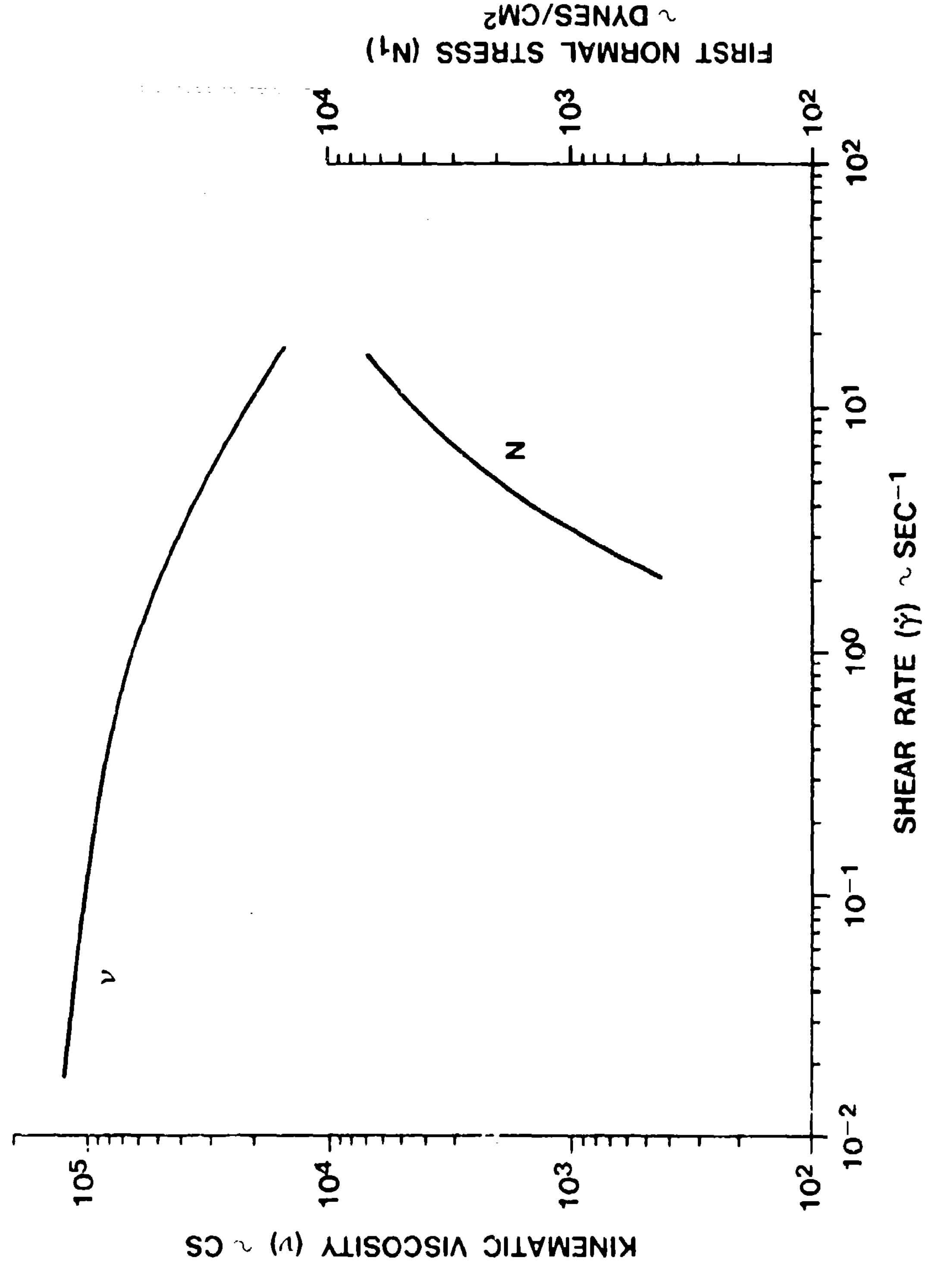

COMPARISON OF LIQUID FILL DESPIN MOMENTS FOR NON-NEWTONIAN AND NEWTONIAN FLUIDS

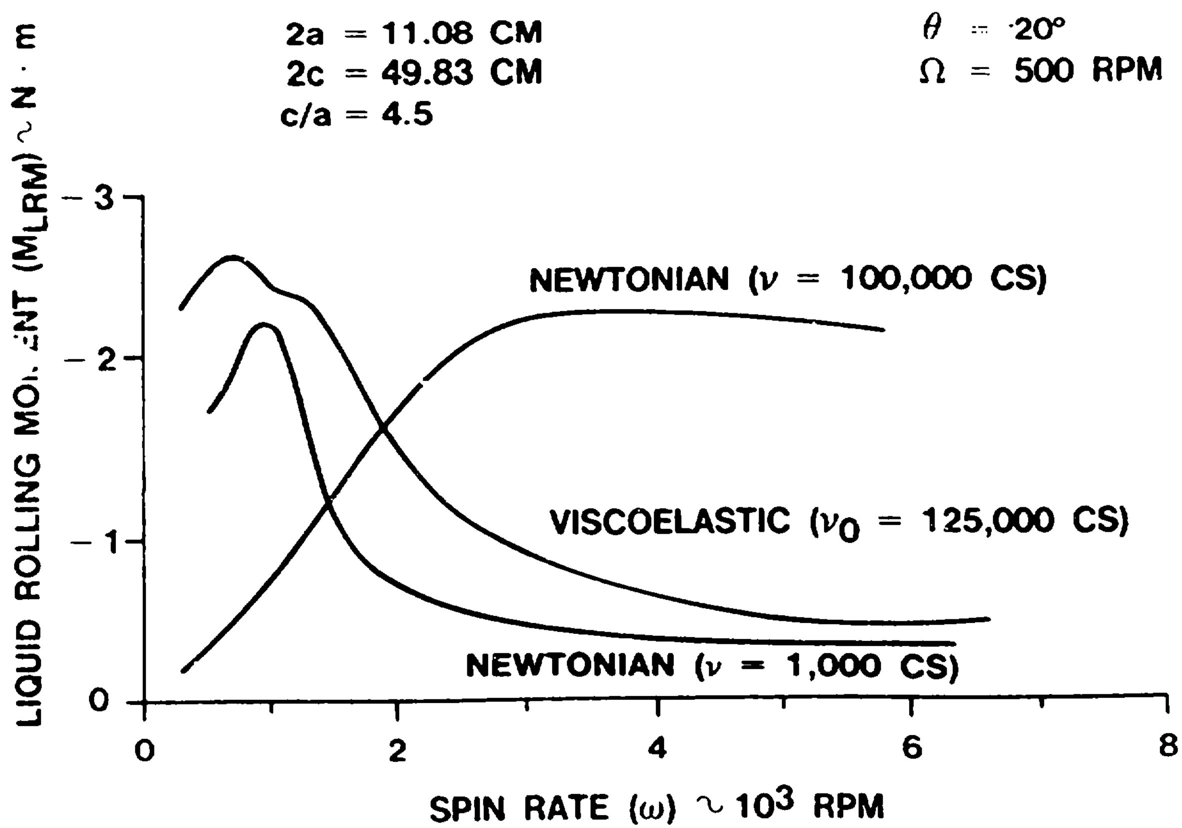

A0332-Q9 1589-02

EFFECT OF VISCOELASTICITY

NORMAL LAUNCH

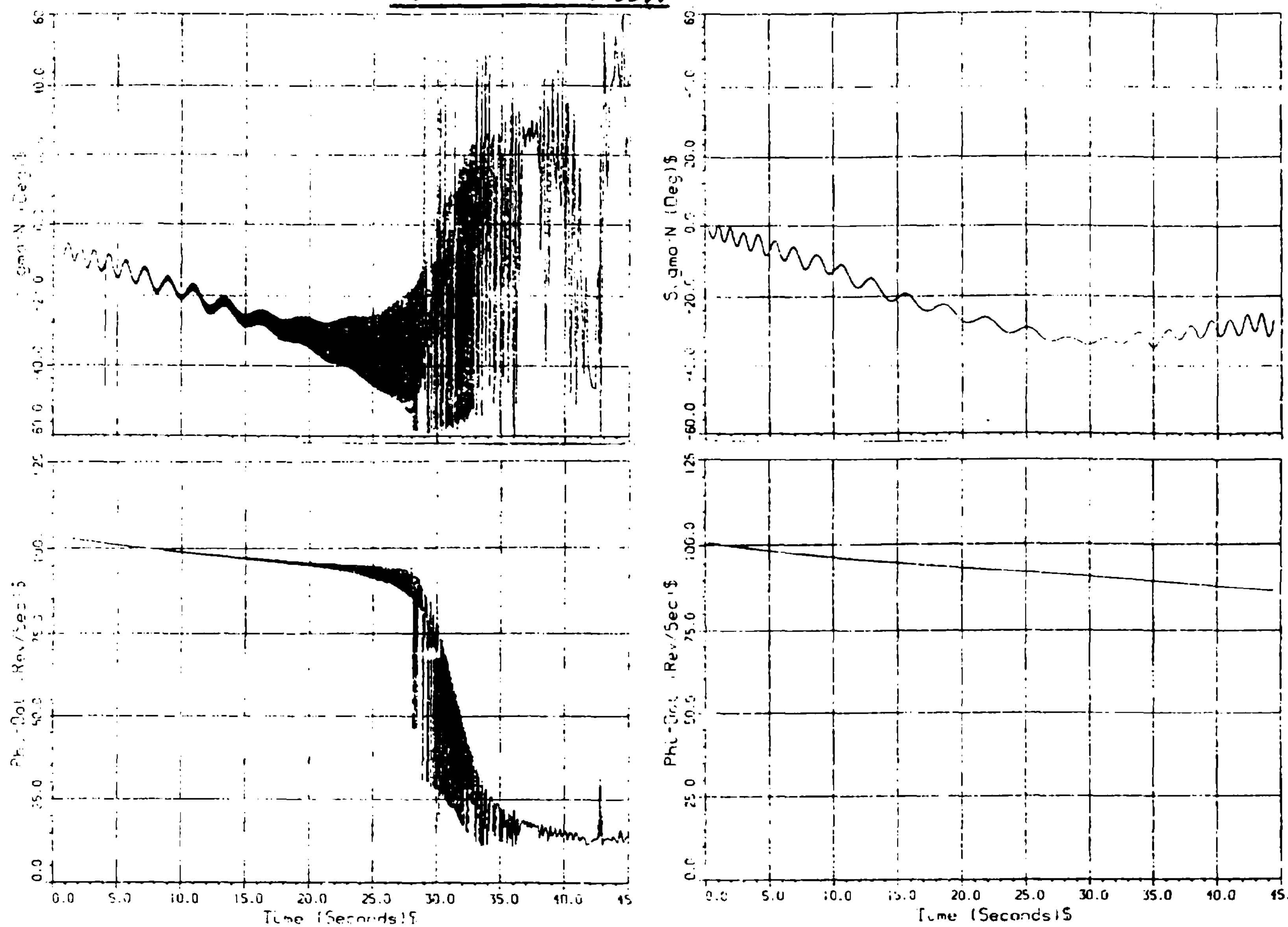

100K CS

100K CS VISCOELASTIC

EFFECT OF VISCOELASTICITY

INDUCED YAW LAUNCH

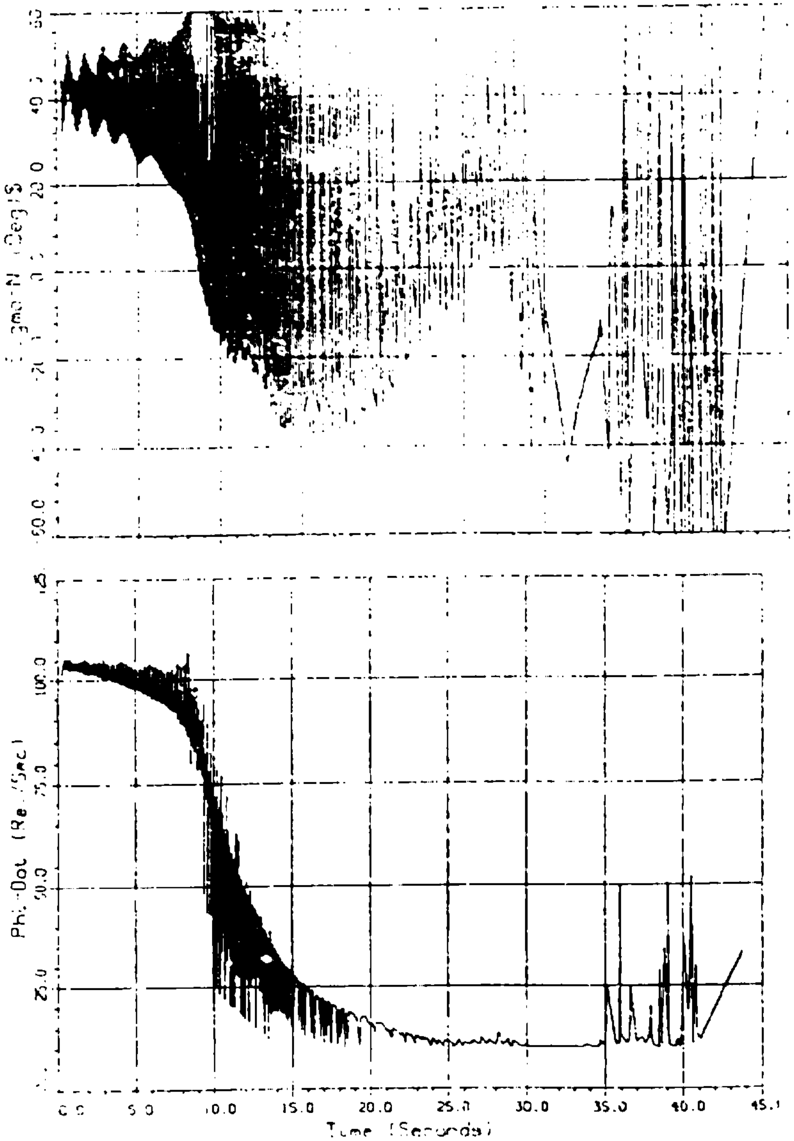

100K CS

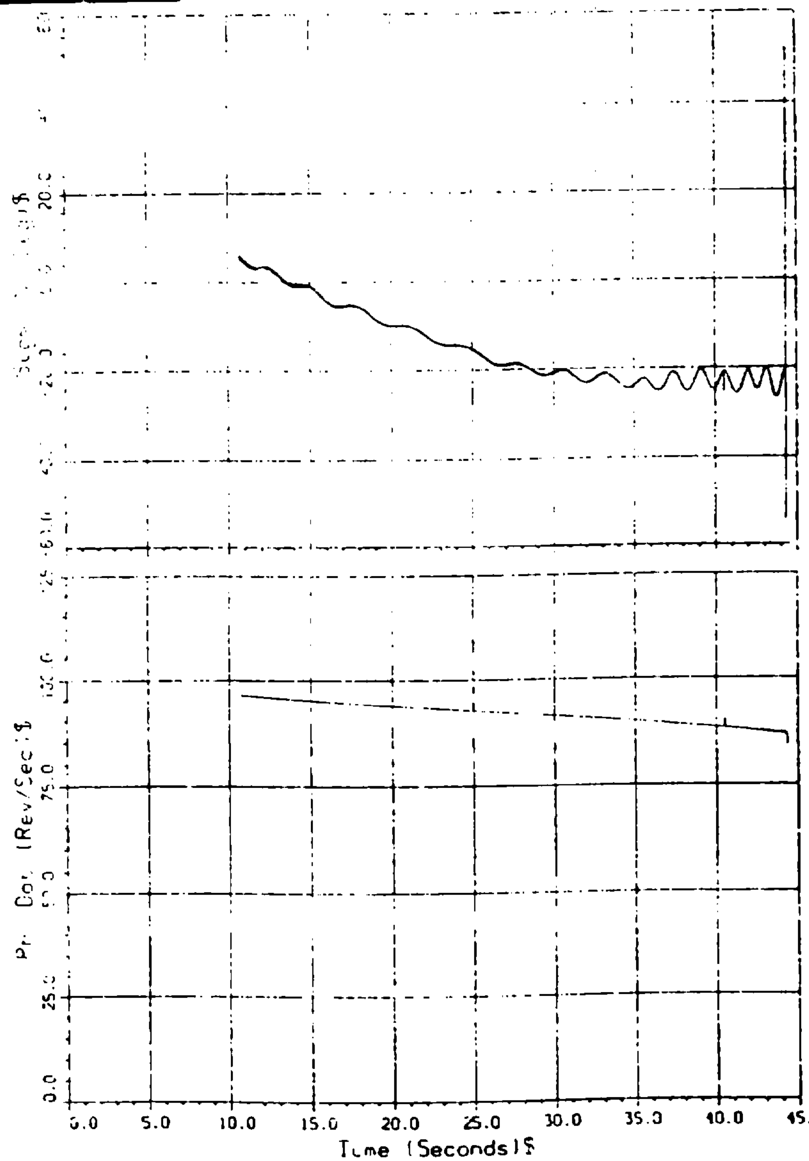

100K CS VISCOELASTIC

DAN JOSEPH'S EXPERIMENT
UNIVERSITY OF MINNESOTA, 1985

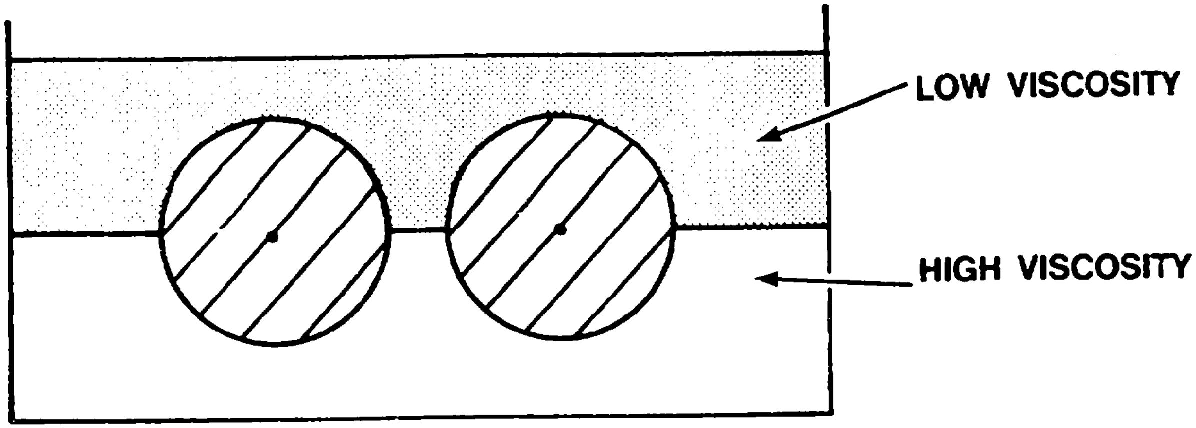

ROLLERS STATIONARY

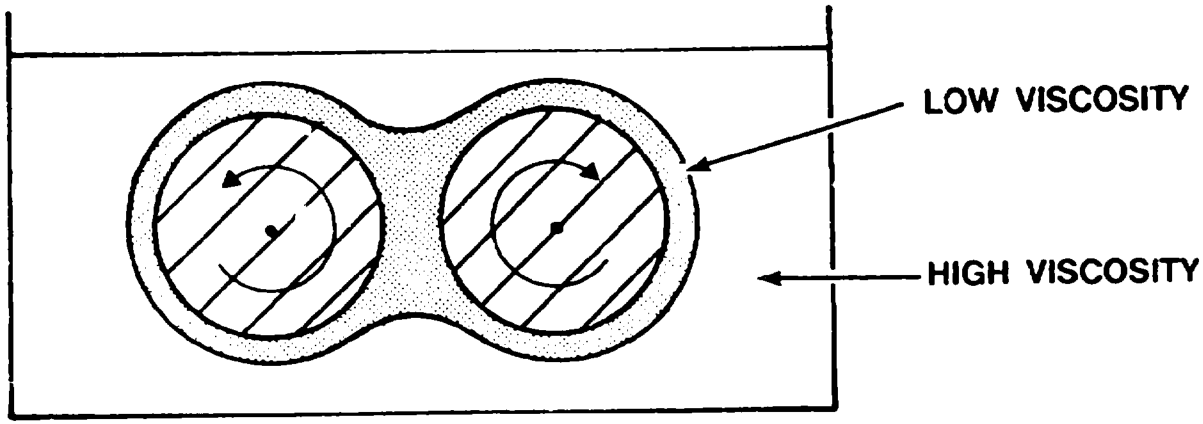

ROLLERS ROTATING

NOTE: 1) EQUAL DENSITIES
2) IMMISCIBLE
3) REDUCED TORQUE

A0332-9011-D1 0308-29

LIQUID-ROLLING MOMENT FOR 100K CS LIQUID-FILL WITH WATER ADDITIVE

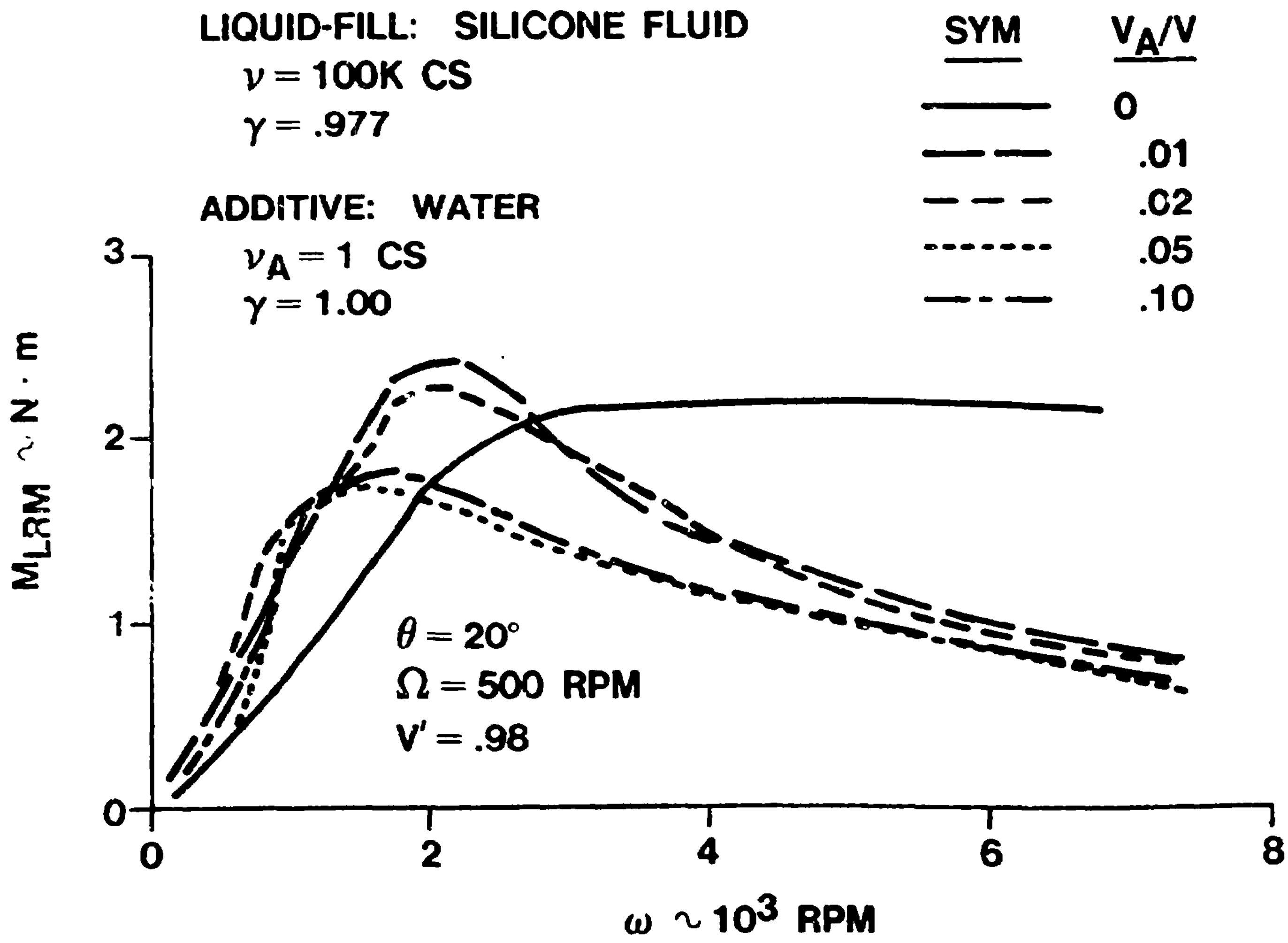

A0332-9010-A1 0187-06

EFFECT OF ADDITIVE VOLUME WITH 100K CS LIQUID-FILL

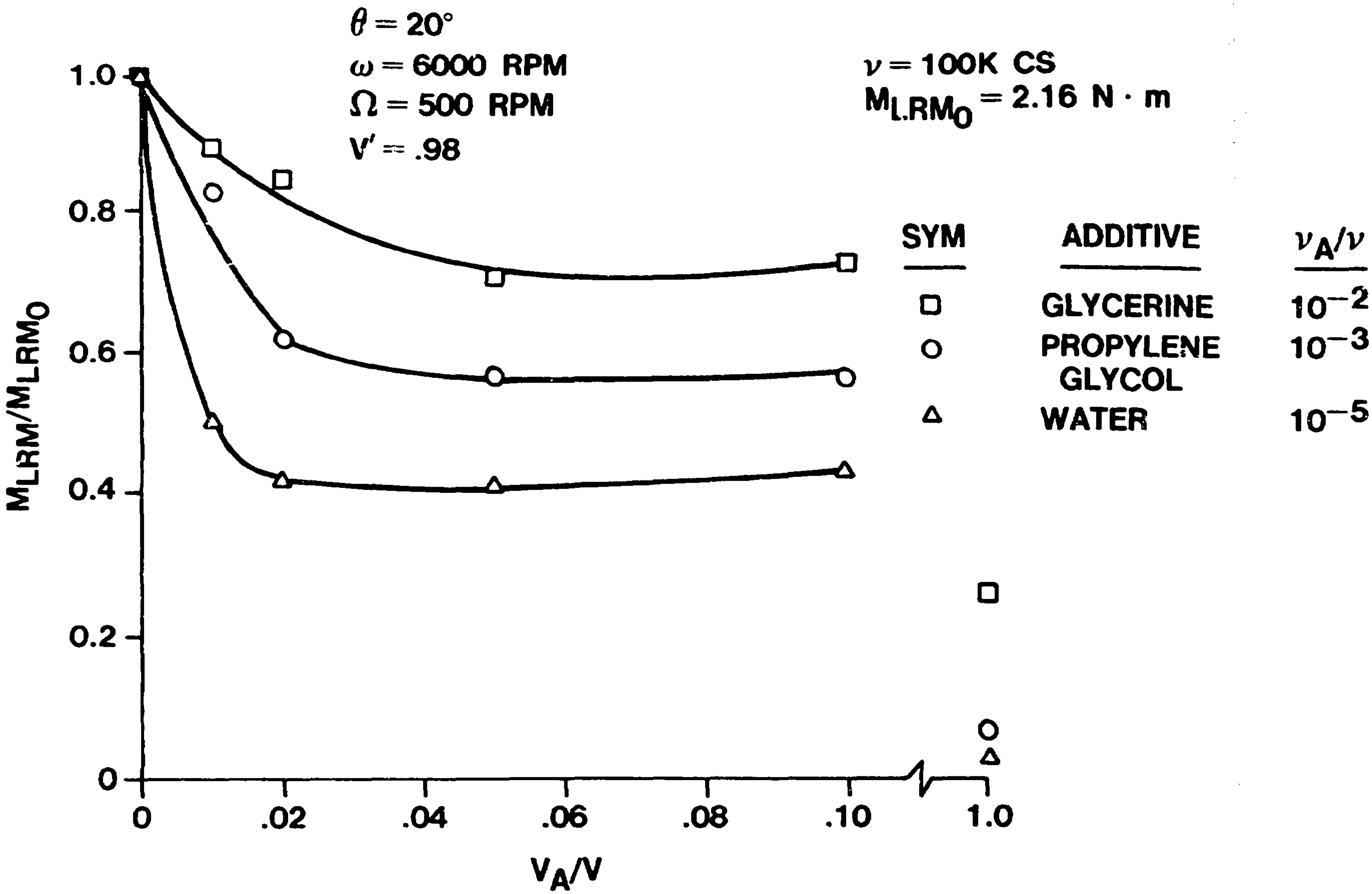

A0332-9010-A1 0187-09

EFFECT OF VARIOUS ADDITIVES WITH 100K CS LIQUID-FILL

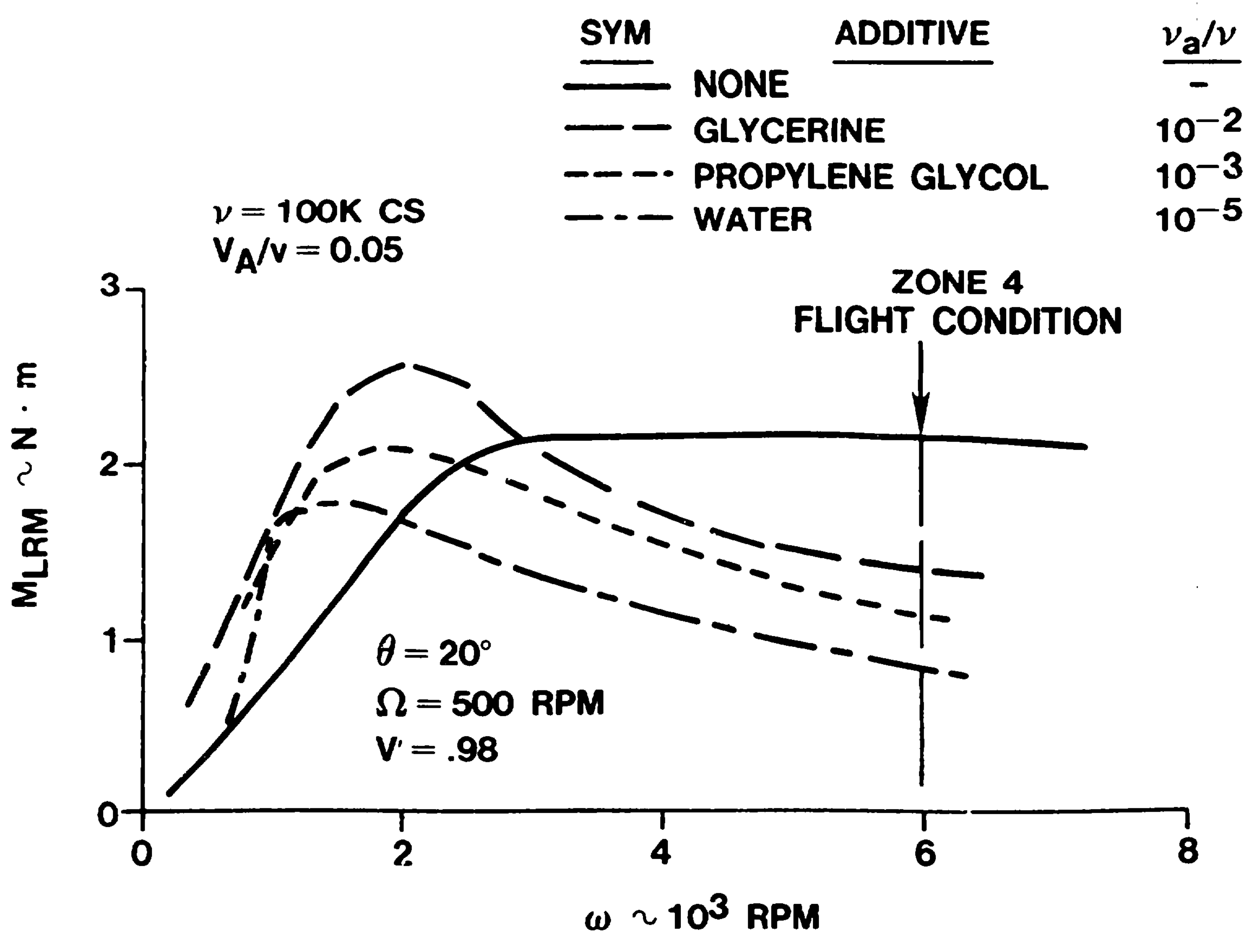

A0332-9010-A1 0187-10

LIQUID ROLLING MOMENT FOR 100K CS LIQUID-FILL WITH WATER ADDITIVE HAVING 1000 PPM POLYOX

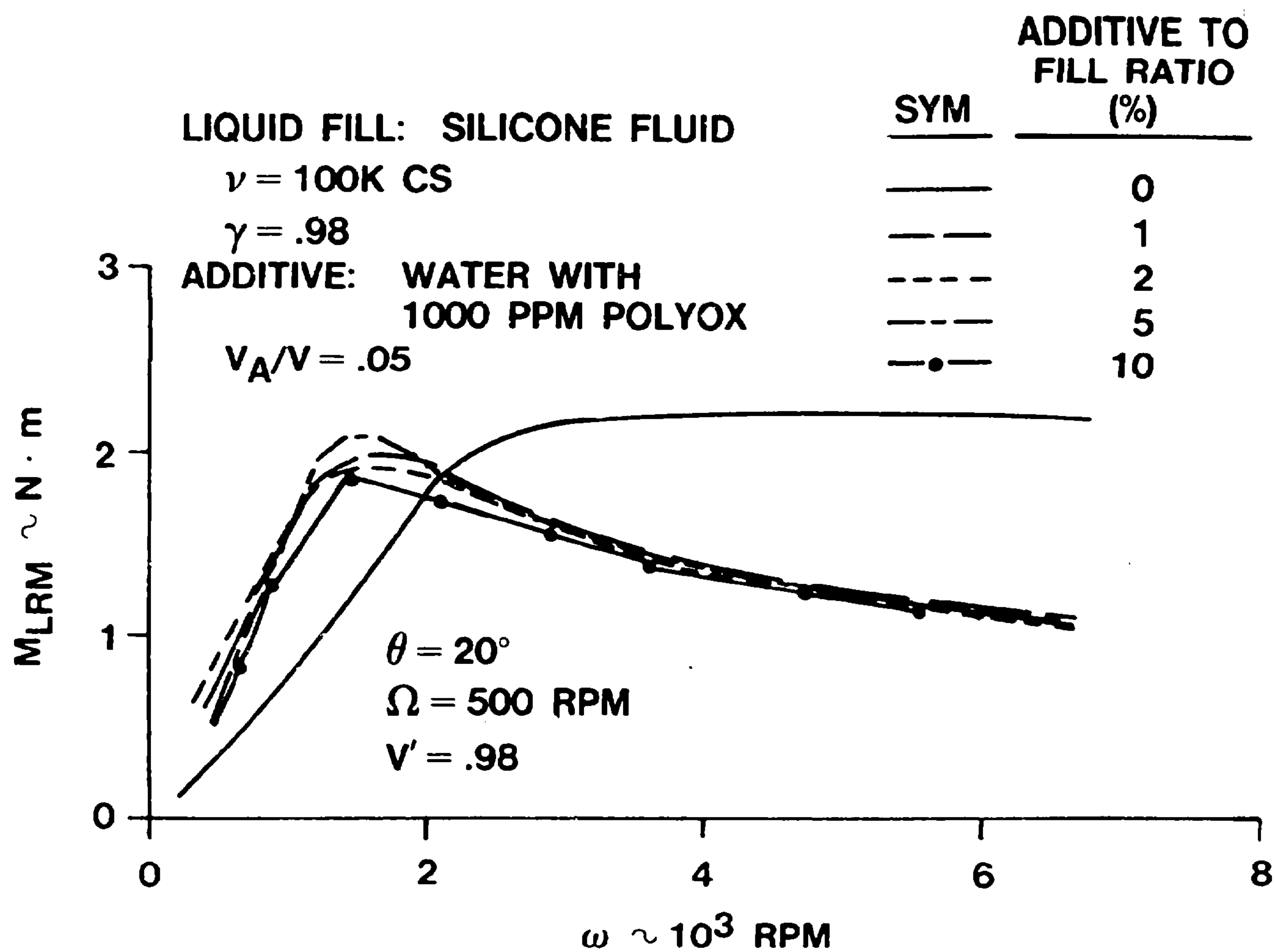

A0332-9011-D1 0306-26

LIQUID-ROLLING MOMENT COEFFICIENT VERSUS REYNOLDS NUMBER

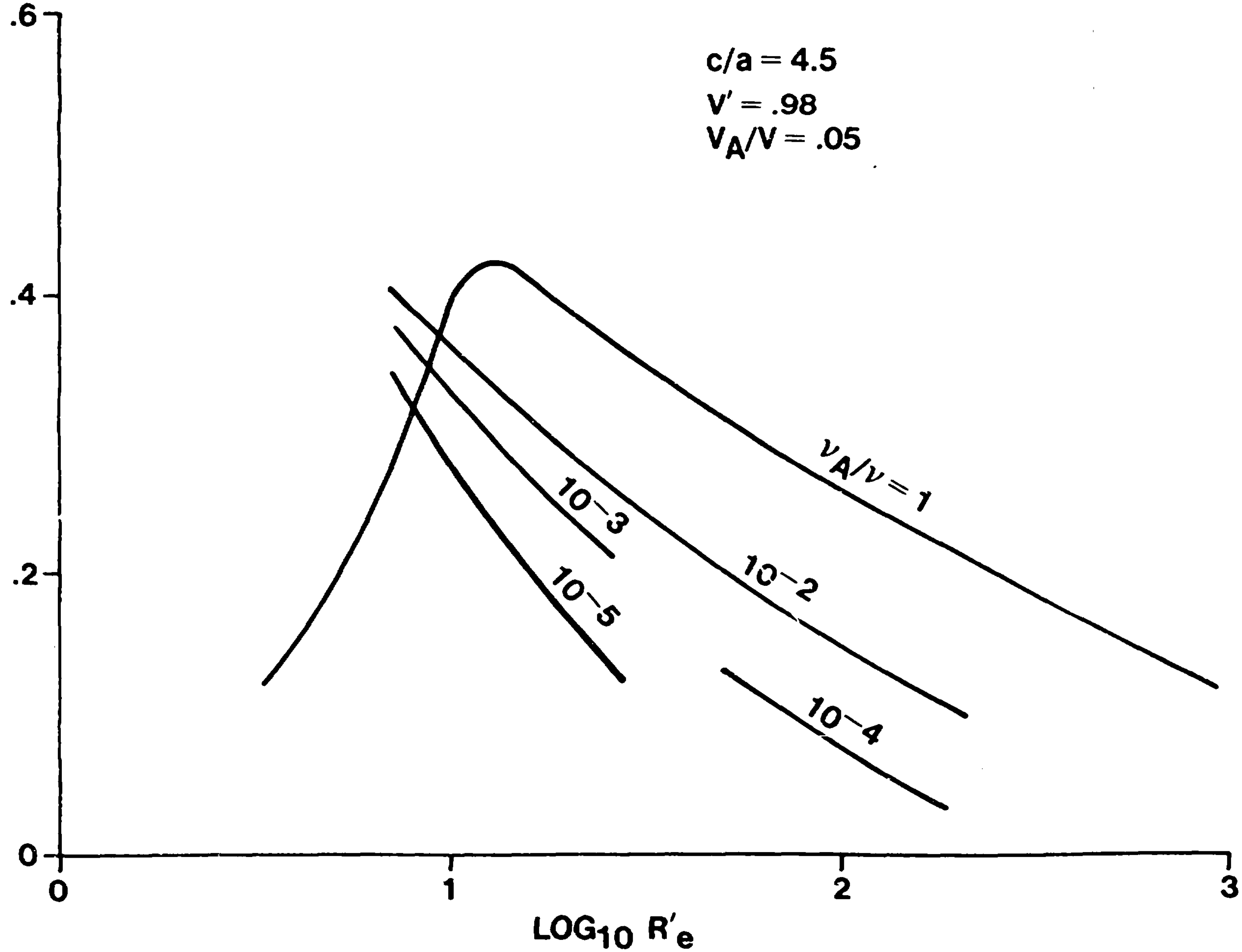

A0332-9010-81 0187-22

COMPARISON OF NEWTONIAN LIQUID-FILLS WITH ADDITIVE AND VISCOELASTIC FLUID

SYM	FLUID-FILL	ADDITIVE
	NEWTONIAN, 100K CS	NONE
	NEWTONIAN, 10K CS	NONE
	NEWTONIAN, 1K CS	NONE
	VISCOELASTIC, 125K CS*	NONE
	NEWTONIAN, 100K CS	WATER**, 1 CS

* SHEAR THINNING (ZERO SHEAR RATE VISCOSITY)

** $V_A/V = .05$

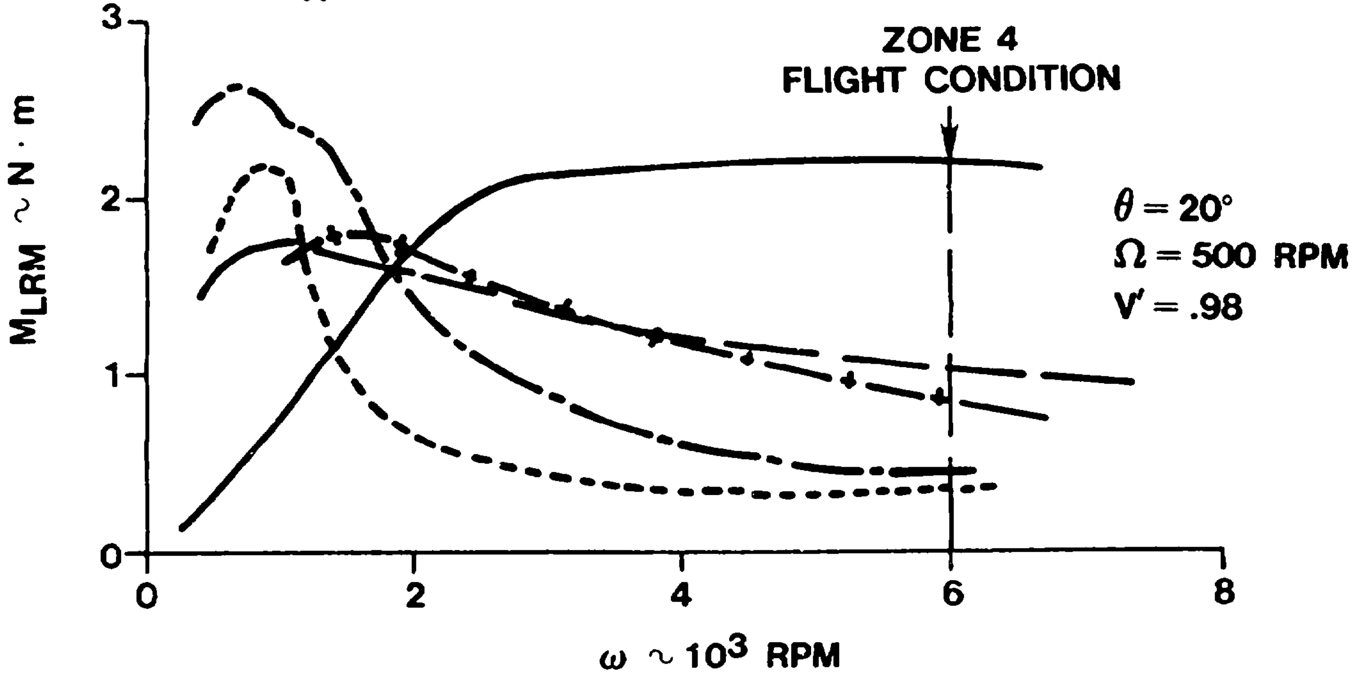

A0332-9010-A1 0187-17

EFFECT OF ADDITIVE

NORMAL LAUNCH

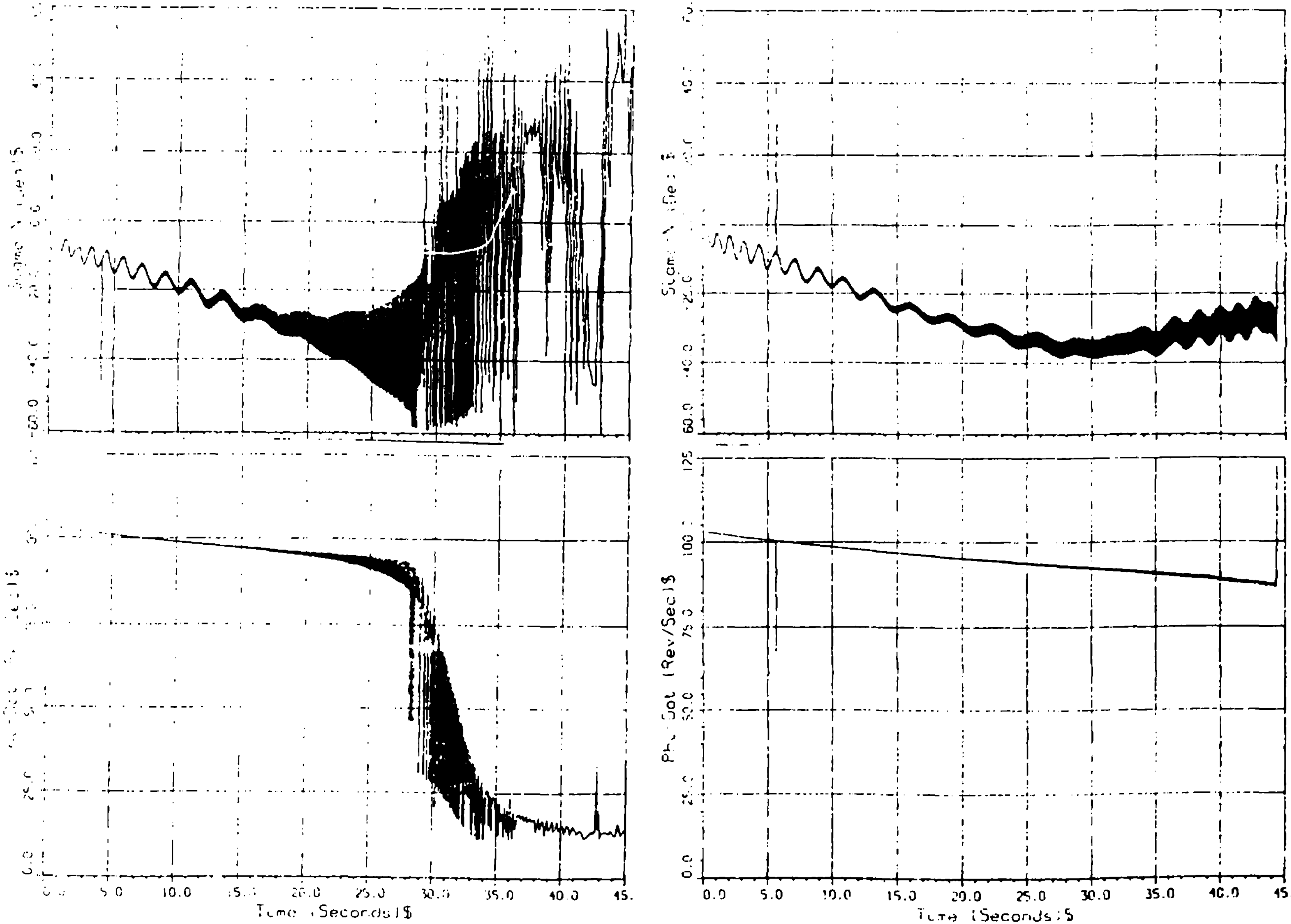

100K CS

100K CS W/ADDITIVE

EFFECT OF ADDITIVE

NORMAL LAUNCH

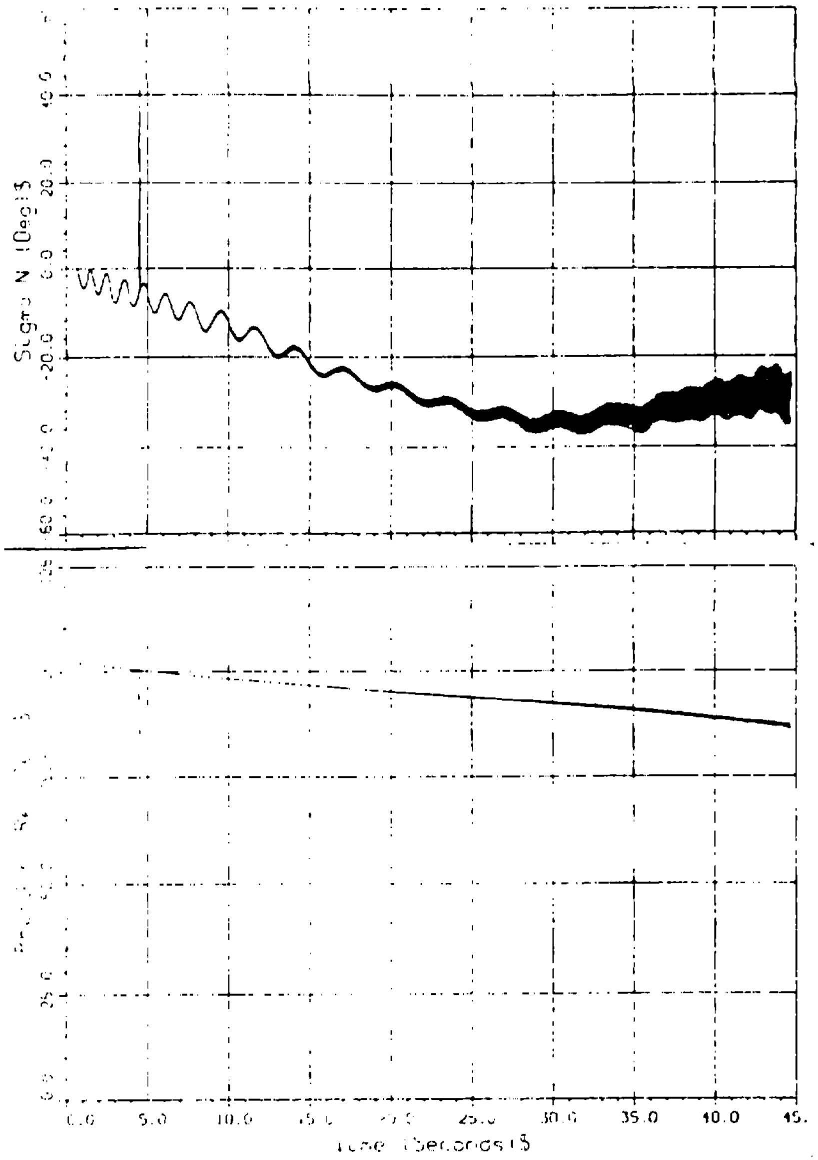

35K CS

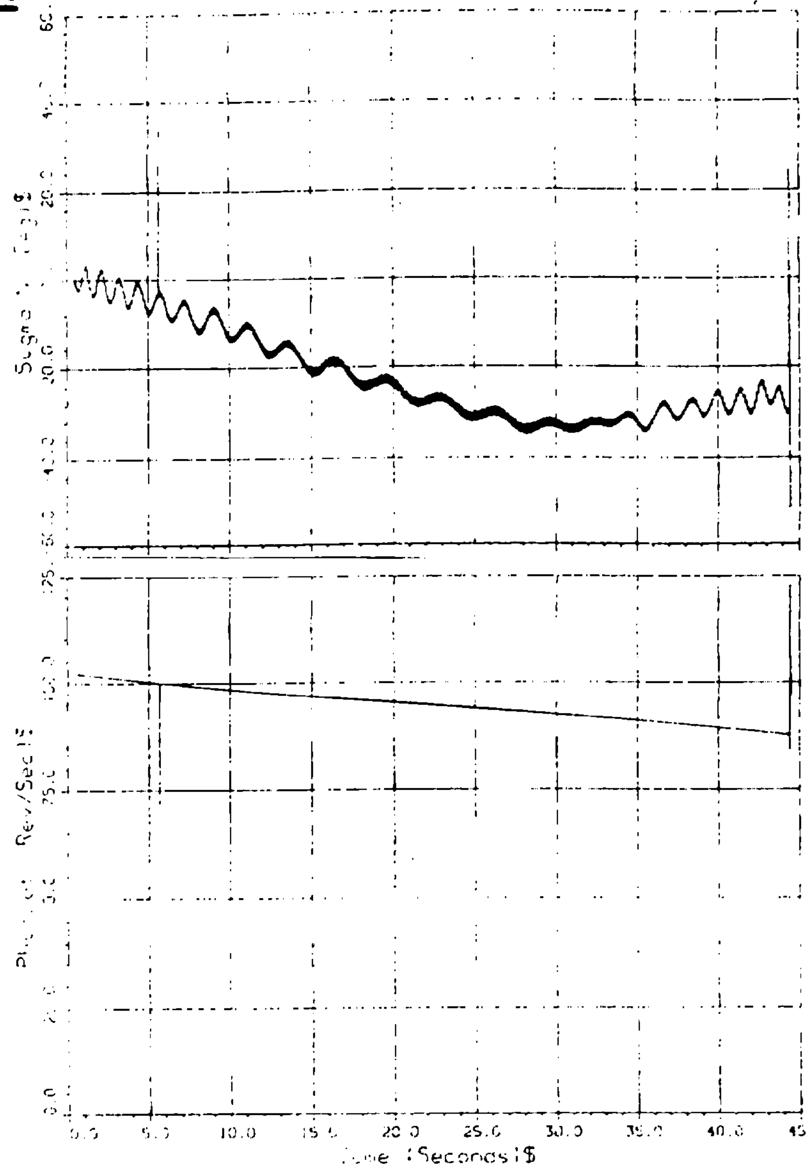

35K CS W/ADDITIVE

EFFECT OF ADDITIVE

NORMAL LAUNCH

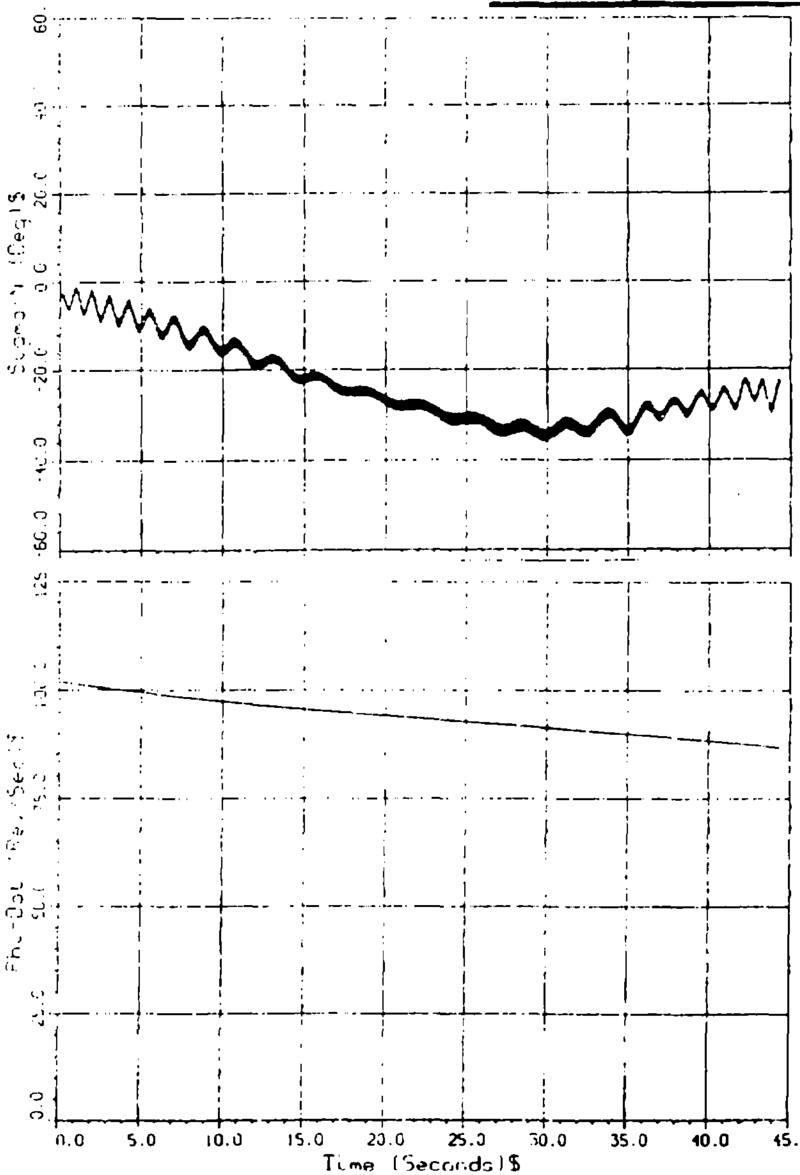

10K CS

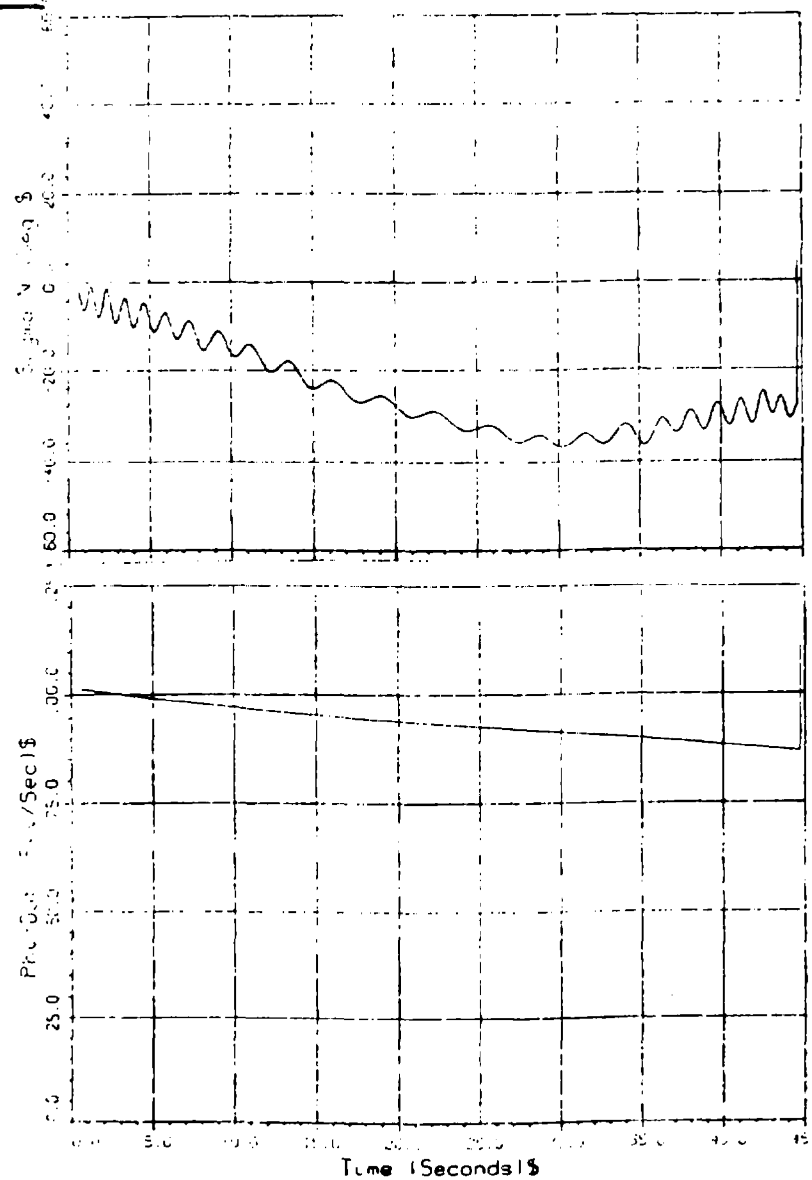

10K CS W/ADDITIVE

EFFECT OF ADDITIVE INDUCED YAW LAUNCH

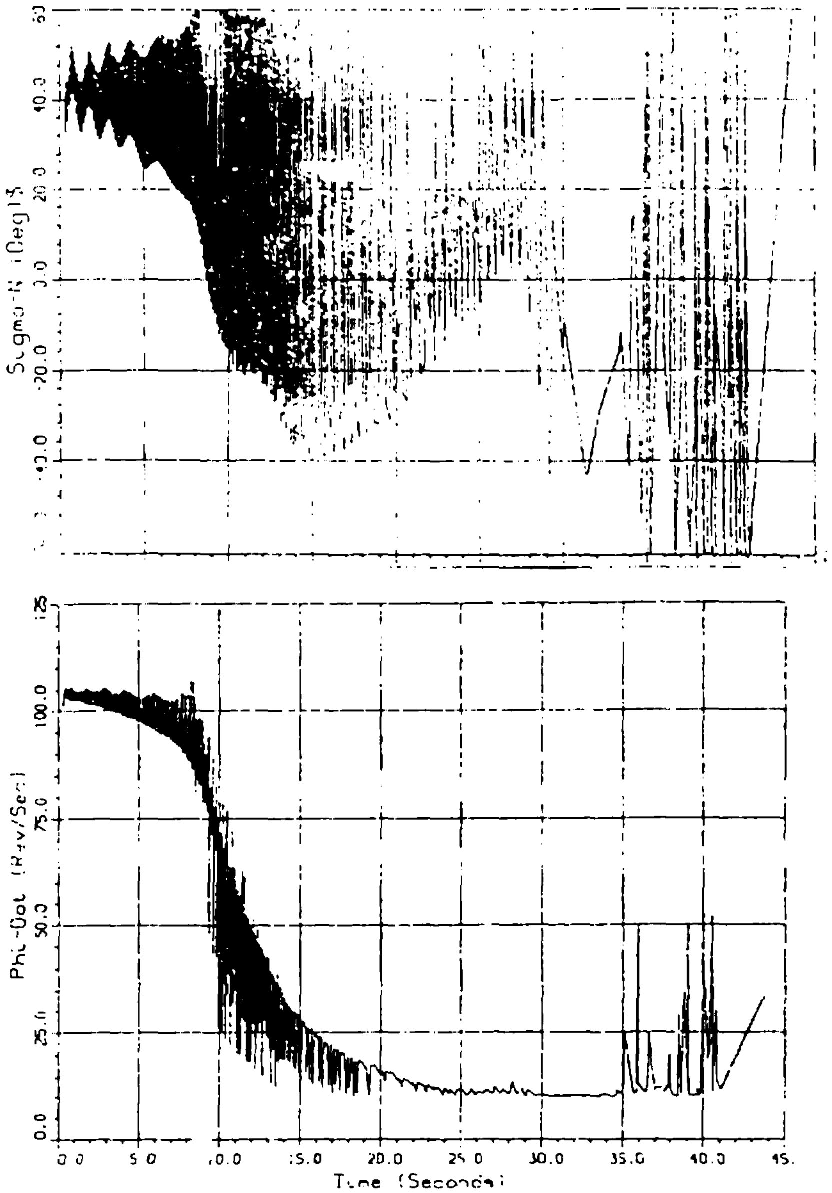

100K CS

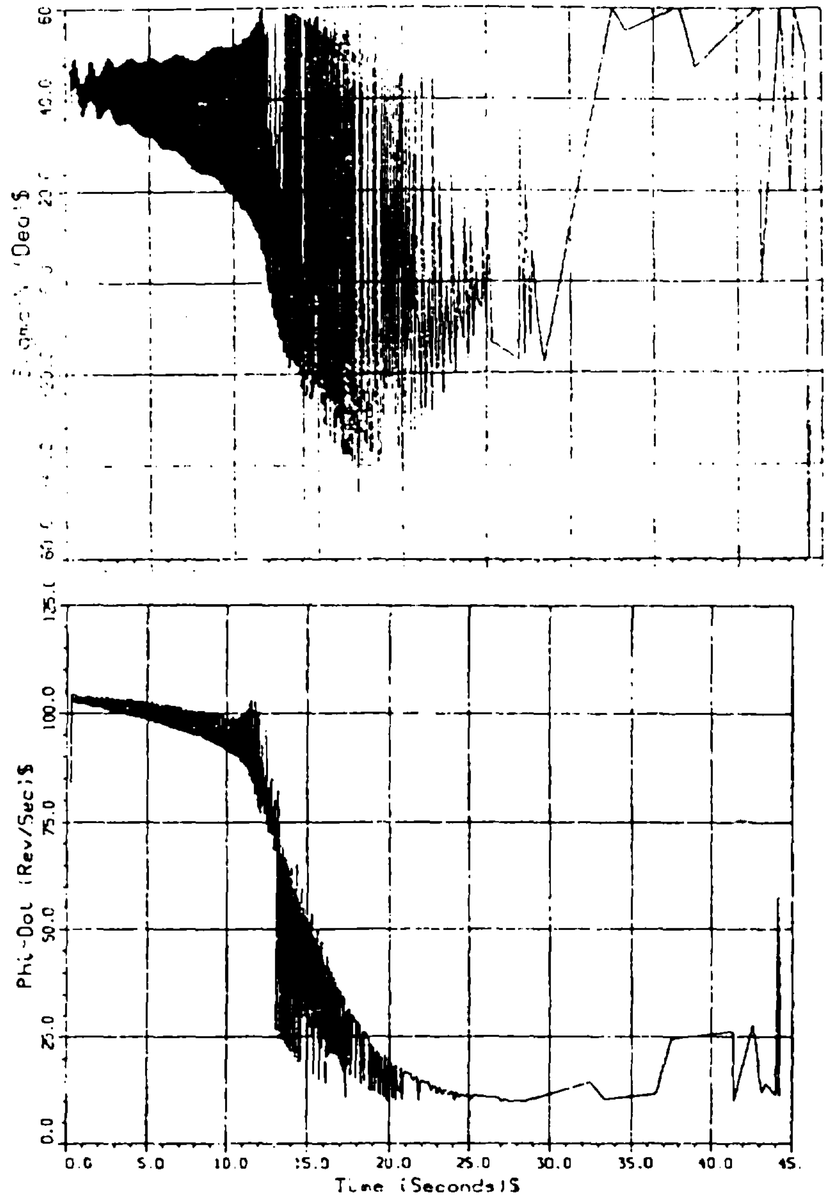

100K CS W/ADDITIVE

EFFECT OF ADDITIVE

INDUCED YAW LAUNCH

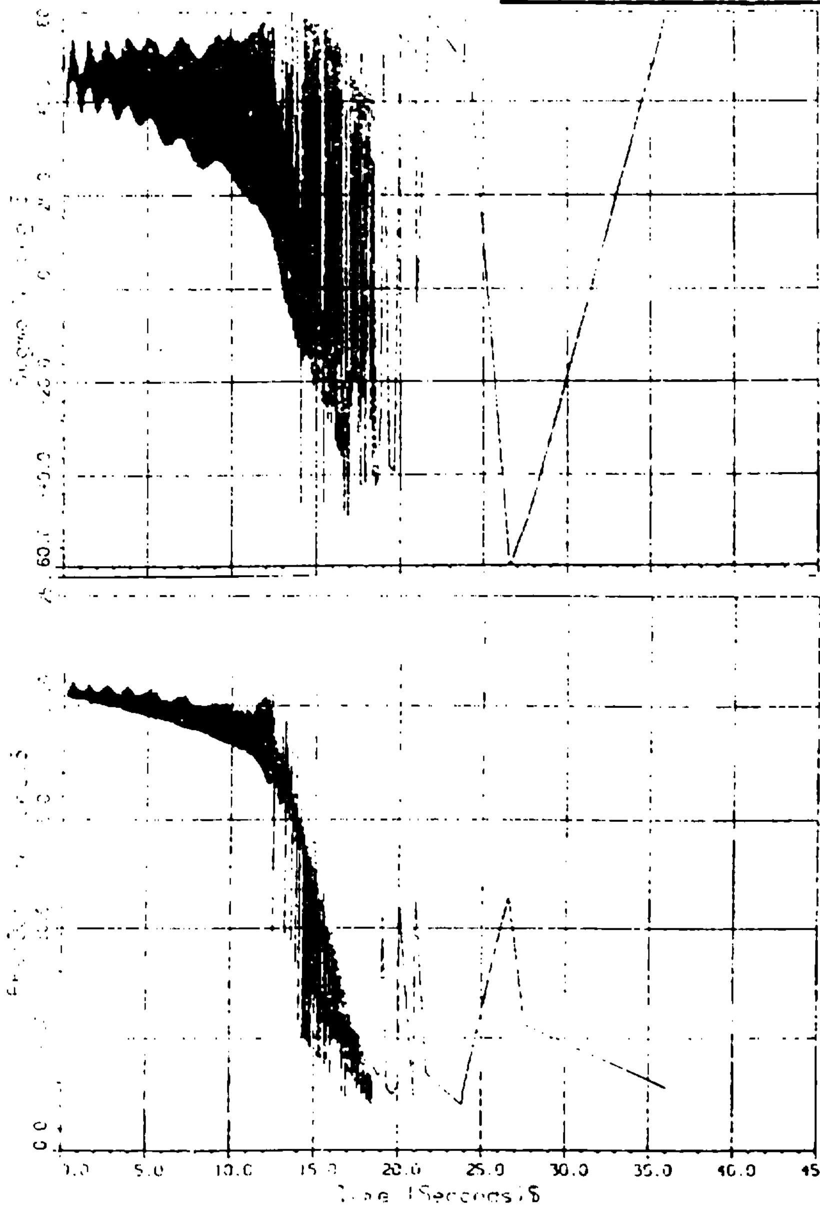

35K CS

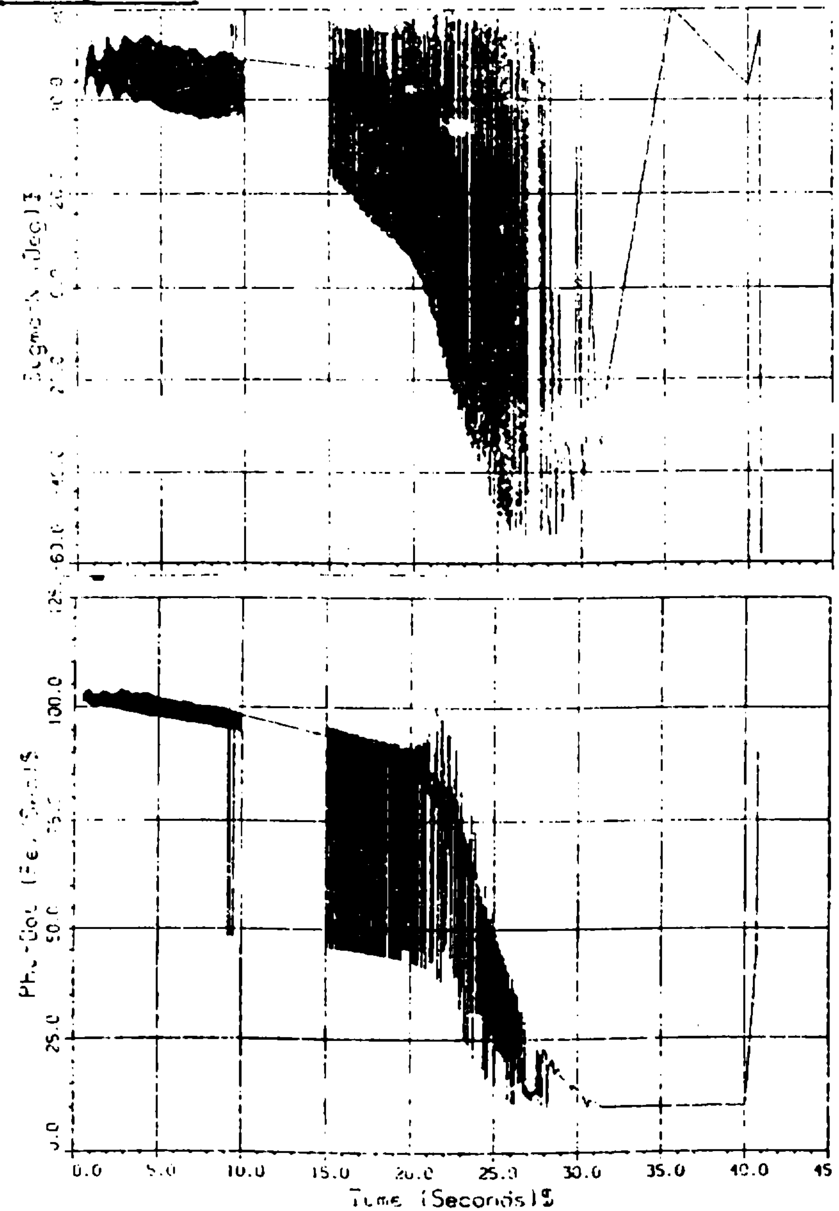

35K CS WITH 5% WATER

EFFECT OF ADDITIVE

INDUCED YAW LAUNCH

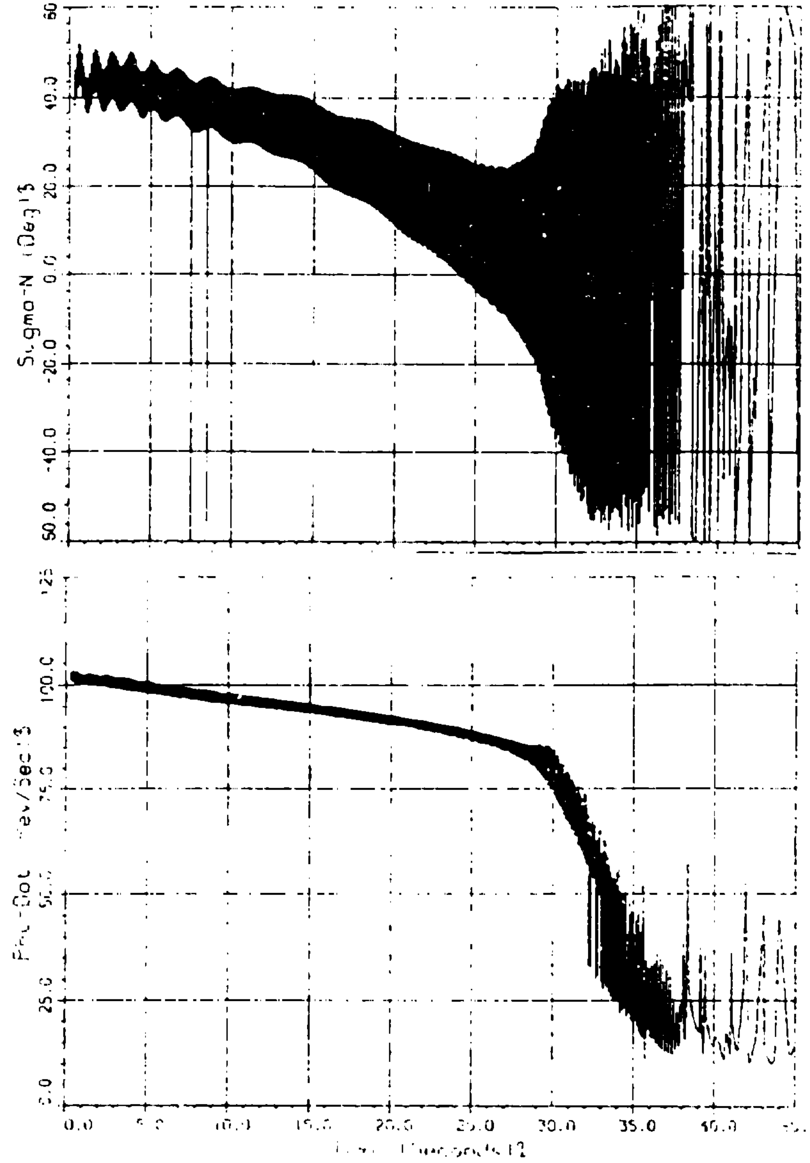

10K CS

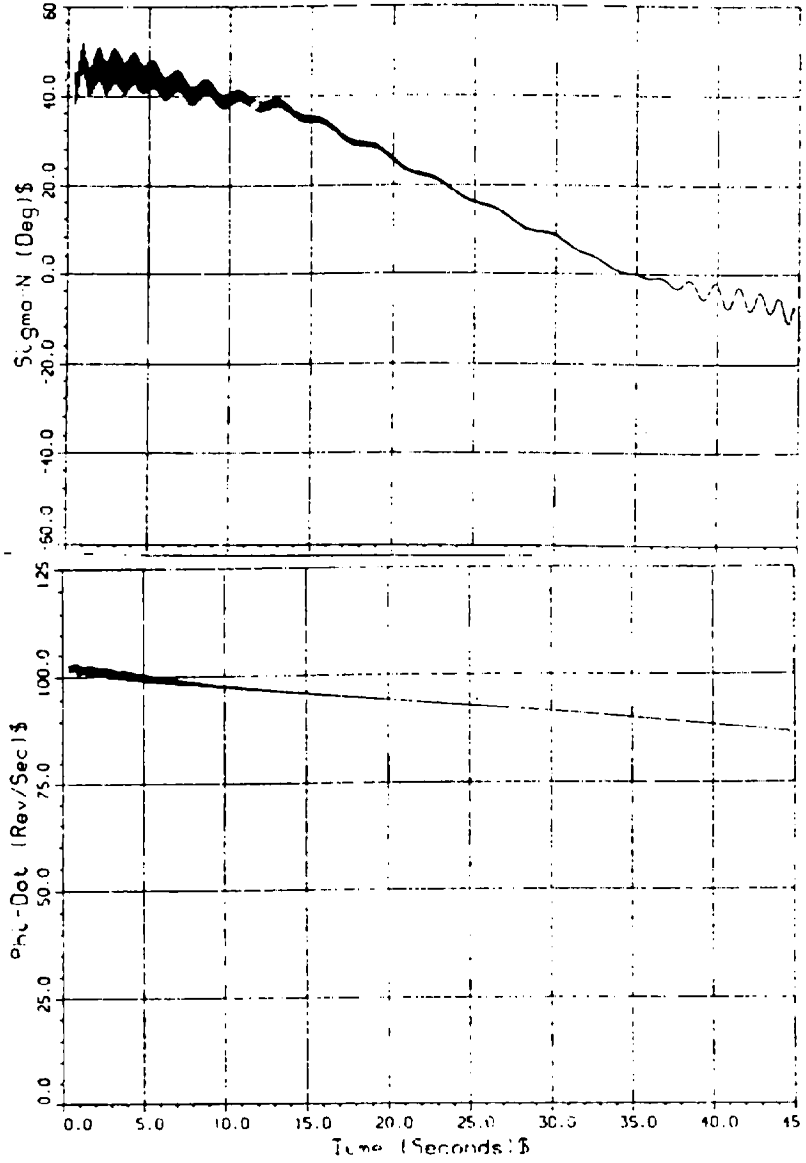

10K CS W/ADDITIVE

SUMMARY OF ADDITIVE FLIGHT TEST RESULTS

Fill	Additive	Initial Yaw	Flight Stability
100K CS	No	Large	Catastrophic @ 8 Sec
"	Yes	"	" @ 12 Sec
35K CS	No	"	" @ 13 Sec
"	Yes	"	" @ 22 Sec
10K CS	No	"	" @ 29 Sec
"	Yes	"	Stable Flight
100K CS	No	Small	Catastrophic @ 28 Sec
"	Yes	"	Stable Flight (Limit at end)
35K CS	No	"	Stable Flight (Limit at end)
"	Yes	"	Stable Flight
10K CS	No	"	Stable Flight (Limit at end)
"	Yes	"	Stable Flight
100K CS (50% Full)	No	Large	Catastrophic @ 8 Sec
"	No	Small	Catastrophic @ 21 Sec
100K CS (Viscoelastic)	No	Large	Stable Flight
"	No	Small	Stable Flight

Note: Zone 4 Charge, 850 mils (47.5 deg.) QE, 5000 ft ground elevation, M825 projectiles with standard, two piece base, large yaw = 10-12 deg., small yaw = 2 deg.

CONCLUSIONS

* GOOD AGREEMENT BETWEEN THEORY, LABORATORY EXPERIMENTS AND FLIGHT TESTS FOR VISCOELASTIC LIQUID-FILL.

* GOOD AGREEMENT BETWEEN THEORY, LABORATORY EXPERIMENTS AND FLIGHT TESTS FOR PARTIAL-FILL CONDITION.

* LOW VISCOSITY, IMMISCIBLE LIQUID ADDITIVE ALWAYS REDUCES DESTABILIZING LIQUID MOMENT.

* ADDITIVE PRODUCED STABLE FLIGHTS FOR ALL LIQUID-FILL VISCOSITIES TESTED UNDER NORMAL LAUNCH CONDITIONS.

* ADDITIVE PRODUCED STABLE FLIGHTS FOR ONLY THE LOWEST LIQUID-FILL VISCOSITY TESTED UNDER INDUCED YAW LAUNCH CONDITIONS.

* POSSIBLE REASON FOR DIFFERENCES BETWEEN LABORATORY PREDICTIONS AND FLIGHT FOR ADDITIVE.

  - Transient effects during firing may have delayed distribution of additive to side wall of container.

  - May require increased amount of additive (10%-15%) rather than 5% used in these tests.

Summary of New Directions for
Liquid-Filled Projectile Studies

*NOTE: The following items were suggested and agreed upon by those in attendance at the Workshop. They have not been put under any specific category nor have they been prioritized.

Coordinate efforts between ARO, BRL and CRDEC concerning data, terms and comparison of results.

Concerned about achieving better agreement between experimental and theoretical results.

Investigate heavier immiscible, low viscosity additives (i.e., salt water) to improve transient distribution for reducing viscous liquid-fill instabilities.

Explain linear and non-linear effects.

Conduct bifurcation studies.

Determine density of felt wedges when saturated with white phosphorus.

Conduct additional yaw sonde instrumented flight tests of liquid-filled projectiles.

Perform internal flow visualization studies in laboratory.

Investigate experimentally, the effect of non-cylindrical containers (i.e., cylinders with endcaps that are ellipsoidal, conical, etc.) for highly viscous liquids.

Evaluate longitudinal baffles to reduce destabilizing moment due to highly viscous liquid-fills.

Analyze transient effects of immiscible, low viscosity additives in reducing instabilities (yaw sonde, spin-up experiments, theoretical, etc.).

Investigate large despin moment at low spin rates for viscoelastic fluids.

Unsteady and gravity effects at low Reynolds numbers.

Non-linear, unsteady and shape effects at high Reynolds numbers.

Determine Reynolds number limits for existing codes.

Establish single analytical method for liquid-filled projectiles that handles entire Reynolds number range (i.e., one stop method).

"WORKSHOP" RECOMMENDATIONS
(Not Prioritized)

1. Obtain more detailed effects of immiscible additives in preventing flight instabilities.

2. Study effect of unconventional geometry (i.e., baffles, internal payload shape, etc) in creating and preventing flight instabilities.

3. Determine influence of porous media in reducing flight instabilities.

4. Investigate larger range of visco-elastic fluids related to flight instabilities.

5. Understand transient effects during launch and flight.

6. Include effect of chemical reactions during flight.

7. Analyze in-flight, mixing phenomena.

8. Evaluate non-linear dynamic factors.

9. Evaluate in-flight thermal effects.

10. Obtain additional laboratory and flight test data to provide experimental validation of theoretical results.

11. Determine influence of combined internal and external flow effects on flight stability.

Blank

LIST OF REGISTRANTS

Workshop on Rotating Fluids held at the Army High Performance Computing Research Center April 22-23, 1991

Eugene R. Cooper
U.S. Army Ballistic Research Laboratory
ATTN: SLCBR-LF
Aberdeen Proving Ground, MD 21005-5066
(301) 278-3109

William P. D'Amico
U.S. Army Ballistic Research Laboratory
ATTN: SLCBR-LF
Aberdeen Proving Ground, MD 21005-5066
(301) 278-3109

Nathan Gerber
U.S. Army Ballistic Research Laboratory
ATTN: SLCBR-LF
Aberdeen Proving Ground, MD 21005-5066
(301) 278-3109

Harvey Greenspan
Department of Mathematics
Massachusetts Institute of Technology
Cambridge, MA 02139
(617) 253-4381

David J. Hepner
U.S. Army Ballistic Research Laboratory
ATTN: SLCBR-LF
Aberdeen Proving Ground, MD 21005-5066
(301) 278-3109

Thorwald Herbert
Department of Mechanical Engineering
Ohio State University
Columbus, OH 43210
(614) 292-4975

Dan Joseph
Department of Aerospace Engineering & Mechanics
University of Minnesota
Minneapolis, MN 55455
(612) 625-8000

Rihua Li
Department of Mechanical Engineering
Ohio State University
Columbus, OH 43210
(614) 292-4975

Miles C. Miller
U.S. Army Chemical Research, Development & Engineering Center
ATTN: SMCCR-RSP-A
Aberdeen Proving Ground, MD 21010-5423
(301) 671-2186

John Molnar
U.S. Army Chemical Research, Development & Engineering Center
ATTN: SMCCR-RSP-A
Aberdeen Proving Ground, MD 21010-5423
(301) 671-2186

Charles Murphy
U.S. Army Ballistic Research Laboratory
ATTN: SLCBR-LF
Aberdeen Proving Ground, MD 21005-5066
(301) 278-3109

Michael J. Nusca
U.S. Army Ballistic Research Laboratory
ATTN: SLCBR-LF
Aberdeen Proving Ground, MD 21005-5066
(301) 278-3109

Mohamed Selmi
Department of Mechanical Engineering
Ohio State University
Columbus, OH 43210
(614) 292-4975

John Strikwerda
Computer Science Department
University of Wisconsin
Madison, WI 53706
(608) 262-0822

Daniel Weber
U.S. Army Chemical Research, Development & Engineering Center
ATTN: SMCCR-RSP-A
Aberdeen Proving Ground, MD 21010-5423
(301) 671-2186

Julian Wu
Army Research Office
P.O. Box 12211
Research Triangle Park, NC 27709-2211
(919) 549-4321

Left to right: Thorwald Herbert, Mike Nusca, Julian Wu, Charlie Murphy
Harvey Greenspan, Daniel Weber, Jack Molnar, Bill D'Amico, Dan Joseph,
John Strikwerda, Rihua Li, Miles Miller, Mohamed Selmi, Howard Hu

WORKSHOP ON PROBLEMS OF ROTATING FLUIDS
Program Agenda

Monday, April 22, 1991

8:30 am	Welcome	Dr. Donald Austin Executive Director, AHPCRC
8:45	Opening Remarks	Dr. Daniel Joseph Aerospace Engineering & Mechanics, U of MN
9:00	Overview of CRDEC Research Program for Liquid-Filled Projectiles	Mr. Miles Miller Chemical Research Development & Engineering Center
9:30	Analysis and Visualization of the flow in a Spinning and Nutating Container (Computer Demonstration)	Dr. Thorwald Herbert Ohio State University
10:30	Tour of Army High Performance Computing Research Center	Dr. George Sell Director, AHPCRC
11:30	LUNCH	
1:00 pm	Tour of Fluid Dynamics Laboratory	Dr. Daniel Joseph Aerospace Engineering & Mechanics, U of MN
2:30	A Centrifugal Spectrometer	Dr. Harvey Greenspan Massachusetts Institute of Technology
3:00	Moment Exerted by a Viscous Liquid in a Spinning, Coning Container	Dr. Charles Murphy Ballistics Research Laboratory

Tuesday, April 23, 1991

8:30 am	Computational Study of the Unsteady Flow in a Spinning and Nutating Cylinder	Dr. Rihua Li Ohio State University
9:00	Numerical Simulations of Non-Cylindrical Liquid-Filled Containers	Mr. Michael Nusca Ballistics Research Laboratory
9:30	Motion of Two Immiscible Fluids in a Spinning and Coning Cylinder	Mr. Mohamed Selmi Ohio State University
10:00	Direct Measurement of Liquid Effects Using a Moment Balance	Mr. David Hepner Ballistics Research Laboratory
10:30	Laboratory Flight Stability Evaluation of Production M825A1 Payload Canisters	Mr. John Molnar Chemical Research Development & Engineering Center
11:00	LUNCH	

(OVER)

1:00 pm	Theory and Experiments for Rotating Porous Media Flow	Dr. Gene Cooper Ballistics Research Laboratory
1:30	Effect of Interior Canister Wall Roughness on Liquid Despin Moment	Mr. Daniel Weber Chemical Research Development & Engineering Center
2:00	Instrumented Flight Tests Artillery Projectiles with Selected Liquid-Fills	Mr. Miles Miller Chemical Research Development & Engineering Center
2:30	Wrap-up and Final Remarks	All
3:30	Adjourn	